ISTANBUL TECHNICAL UNIVERSITY ★ GRADUATE SCHOOL OF SCIENCE ENGINEERING AND TECHNOLOGY

EXPERIMENTAL AND NUMERICAL MODELLING STUDIES FOR INTERPRETING AND ESTIMATING THE p-δ BEHAVIOR OF SINGLE PILES IN UNSATURATED SOILS

Ph.D. THESIS

Z. Nil TAYLAN KUTLU

Department of Civil Engineering

Soil Mechanics and Geotechnical Engineering Programme

MAY 2013

ISTANBUL TECHNICAL UNIVERSITY ★ GRADUATE SCHOOL OF SCIENCE ENGINEERING AND TECHNOLOGY

EXPERIMENTAL AND NUMERICAL MODELLING STUDIES FOR INTERPRETING AND ESTIMATING THE p-δ BEHAVIOR OF SINGLE PILES IN UNSATURATED SOILS

Ph.D. THESIS

Z. Nil TAYLAN KUTLU
(501062303)

Department of Civil Engineering

Soil Mechanics and Geotechnical Engineering Programme

Thesis Advisor: Assoc. Prof. Aykut ŞENOL
Co-Advisor : Prof. Dr. Sai K. VANAPALLI

MAY 2013

İSTANBUL TEKNİK ÜNİVERSİTESİ ★ FEN BİLİMLERİ ENSTİTÜSÜ

SUYA DOYGUN OLMAYAN ZEMİNLERDE TEKİL KAZIK p-δ DAVRANIŞININ TAHMİNİ VE YORUMLANMASINA DAYALI DENEYSEL VE SAYISAL MODELLEME

DOKTORA TEZİ

Z. Nil TAYLAN KUTLU
(501062303)

İnşaat Mühendisliği Anabilim Dalı

Zemin Mekaniği ve Geoteknik Mühendisliği Programı

Tez Danışmanı: Doç. Dr. Aykut ŞENOL
Tez Eş Danışmanı : Prof. Dr. Sai K. VANAPALLI

MAYIS 2013

Zehra Nil Taylan Kutlu, **a Ph.D.** student of **ITU Graduate School of Science Engineering and Technology** student ID 501062303, successfully defended the **thesis** entitled "Experimental and Numerical Modeling Studies for Interpreting and Estimating the p-δ Behavior of Single Piles in Unsaturated Soils", which she prepared after fulfilling the requirements specified in the associated legislations, before the jury whose signatures are below.

Co-advisor :	**Prof.Dr. Sai K. VANAPALLI** University of Ottawa	.....
Jury Members :	**Assoc. Prof. Dr. Recep İYİSAN** Istanbul Technical University	.....
	Prof. Dr. Kutay ÖZAYDIN Yıldız Technical University	.....
	Prof. Dr. Mete İNCECİK Istanbul Technical University	.....
	Assoc. Prof. Dr. Mehmet BERİLGEN Yıldız Technical University	.....
	Assoc. Prof. Dr. Huriye BİLSEL Eastern Mediterranean University	.....

Date of Submission : 28 December 2012
Date of Defense : 13 May 2013

To my dear father & mother

and

To my loving spouse & my lovely son Mert Ali

FOREWORD

I am very grateful to my supervisors Assoc. Prof. Dr A. Senol and Prof. Dr. S.K. Vanapalli for their guidance, support and assistance throughout the period of the presented research work and made my path possible as a doctoral student. I remain forever indebted to my supervisors.

I would like to present my special thanks to Assoc. Prof. Dr A. Senol as he always believes in my success. I appreciate all his helps not only for my thesis but also for my academic achievements.

I would like to express my sincere appreciation to Prof. Dr. Sai K. Vanapalli for his continuous support from the very first day I met him in 2007 in Ottawa. He gave me the opportunity of a lifetime by including me in his *'unsaturated soils'* research team. Dr. Vanapalli; you made a great difference and contribution to my life. I appreciate everything you did for me. The completion of this thesis would not have been possible without your encouragement, mentorship and your invaluable suggestions that I will remember all through my life.

I would also like to express my gratitude to Dr W. T. Oh for his assistance, support and discussions on issues presented in this thesis. Thanks are also extended to the technical officer, Jean Claude Celestin and my colleagues, Lu Lu, Fathi Mohamed, Joseph Areghan, Mudasser Noor, Nick, Hana Adem, Afshin Khoshand and Farzad Mo at the University of Ottawa Geotechnical lab for their time, help, assistances, and good company. A most special thanks is given to my best friend Volkan Ezcan, for his patience and friendship during my studies. I would also like to extend my appreciation to Loretto Beninger for all her great friendship and support when I was in Canada. She played a very important role for my success to complete my studies there. I am grateful to all of you.

The Scientific and Technological Research Council of Turkey (TUBITAK) for the financial support provided during this research is gratefully acknowledged.

I would also like to thank my parents for their valuable support. With all my heart I dedicate my thesis to my father for the strength he gave me, to accomplish anything. He is the greatest inspiration in my life. I would like to express my gratitude first to my father and then to my mother for all their support, encouragement and understanding without which I would not have managed to complete this thesis.

Finally, special appreciation goes to my dear husband Yavuz Kutlu for his patience, continuous support and encouragement during this long journey and to my baby boy Mert who has joined this journey in the last one year and cheered me up. I love you both.

May 2013

Zehra Nil TAYLAN KUTLU
(M.Sc. Engineer)

TABLE OF CONTENTS

Page

ABBREVIATIONS

AEV	**:** Air Entry Value
API	**:** American Petroleum Institute
ASCOMPAC	**:** As Compacted
ASTM	**:** American Standart for Testing of Materials
ATT	**:** Axis Translation Technique
avg	**:** average value
C	**:** Compression
cal	: calculated value
CNL	**:** Constant Normal Load
CPT	**:** Cone Penetration Test
CSM	**:** Critical State Model
D	**:** Drained
DAS	**:** Data Acquisition System
ESA	**:** Effective Stress Approach
est	: estimated value
f	: value at failure
FEA	**:** Finite Element Analysis
GWT	**:** Groundwater Table
HAE	**:** High Air Entry
ICFEP	**:** Imperial College Finite Element Program
IHT	**:** Indian Head till
initial	: initial value
LS	**:** Loam soil
LC	**:** Lower Cromer till
LVDT	**:** Linearly Variable Displacement Transducer
meas	: experimentally measured value
OCR	**:** Overconsolidation Ratio
OMC	**:** Optimum Moisture Content
SAT	**:** Saturated
sat	: saturated condition
SWCC	**:** Soil Water Characteristic Curve
T	**:** Tension
TSA	**:** Total Stress Approach
UD	**:** Undrained
UNSAT	**:** Unsaturated
unsat	: unsaturated condition
USC	**:** Ultimate Shaft Capacity

LIST OF TABLES

Page

LIST OF FIGURES

Page

LIST OF SYMBOLS

α, β : fitting parameters for elastic modulus
$\alpha\,(^{o})$: wetting contact angle
α : adhesion factor for the alpha method
β : Bjerrum – Burland coefficient for the beta method
γ_d : dry unit weight of soil
γ_t : total unit weight of soil
δ : displacement of model pile or in-situ single pile
$\Delta\sigma'_h, \Delta\sigma'_r$: change in horizontal (radial, lateral) effective stress
Δt : radial displacement
$\Delta\Psi_t$: total potential change
$\Delta\Psi_c$: the change due to capillary potential
$\Delta\Psi_o$: the change due to osmotic potential
$\Delta\Psi_e$: the change due to electric fields
$\Delta\Psi_f$: the change due to van der Waals fields
θ : volumetric water content
θ_r : residual volumetric water content
θ_s : volumetric water content at saturation
Θ : the normalized water content
κ : fitting parameter for shear strength
λ : frictional capacity coefficient for the lambda method
κ : slope of the swelling line (for Chapter 8)
λ : slope of the the critical state line in $ln\ p'$-v space (in Chapter 8)
υ, μ : fitting parameters for shear strength of unsaturated fine-grained soils
μ : Poisson's ratio
π : osmotic suction
ρ_d : dry density of the soil
σ : applied stress in shear strength tests
σ_1 : major principal stress (total)
σ_3 : minor principal stress (total)
$(\sigma_1 - \sigma_3)$: deviator stress
σ'_1 : major principal stress (effective)
σ'_3 : minor principal stress (effective)
σ'_h : horizontal (radial, lateral) effective stress
τ : shear strength of soil
τ_{unsat} : shear strength of soil unsaturated soils
$\tau_{suction}$: shear strength ofdue to contribution of matric suction
ν : Poisson’s ratio
ϕ' : effective internal friction angle for saturated condition

ϕ_b : contribution of suction towards the shear strength of unsaturated soil
χ : effective stress parameter
Ψ : soil suction
Ψ_{total} : total potential – total suction
Ψ_{matric} : matric suction
$\Psi_{osmotic}$: osmotic suction
Ψ_r : residual suction value
$\Psi(^o)$: dilatancy angle
$(\sigma_n - u_a)$:net normal stress
$(u_a - u_w)$:matric suction
$(u_a - u_w)_{avg}$: average matric suction value
$(u_a - u_w)_b$: air-entry value
A_s : the area of the pile shaft
A_b : the area of the pile tip
B : width of the foundation
C_s : Swelling index
C_c : Compression index
c : total cohesion
c' : effective cohesion for saturated condition
c_a : adhesion between the pile and soil
$c_u, c_{u(sat)}$: undrained shear strength for saturated soils
$c_{u(unsat)}$: undrained shear strength for unsaturated soils
c_u/σ'_v : undrained shear strength ratio ($\psi = c_u/\sigma'_v$)
D, d : pile diameter
$d\tau_{unsat}$: incremental shear strength contribution due to suction
e : void ratio
E_{sat} : elasticity modulus for saturated condition
E_{unsat} : elasticity modulus for unsaturated condition
f_s : pile shaft resistance
G : shear modulus
I_p : plasticity index
k : cohesion increase parameter
K_o : lateral earth pressure coefficient at rest
L : pile length
L/D : pile slenderness ratio
M : the slope of the critical state line projected into p'- q stress space,
M_{ring} : mass of the specimen ring
M_{soil} : mass of the soil specimen
N_q : bearing capacity factor
n :porosity
p' : effective mean stress,
P_a : atmospheric pressure
q_u : unconfined compressive strength
q : deviator stress
Q_{ult} : ultimate bearing capacity
Q_f : Ultimate pile shaft bearing capacity
$Q_{f(us)}$: ultimate shaft bearing capacity of piles in unsaturated soils
Q_p : pile end bearing capacity
$Q_{(u_a - u_w)}$: ultimate shaft capacity due to matric suction

R	**:** air-water interface curvature
r	**:** pile radius
S	**:** degree of saturation
S_r	**:** residual degree of saturation
T_s	**:** surface tension
t	**:** pile-soil interface zone thickness
u_a	**:** pore-air pressure
u_w	**:** pore-water pressure
v	**:** specific volume = (1+ e),
v_o	**:** the specific volume at critical state,
w	**:** water content
$w_{initial}$	**:** initial compaction water content
w_L	**:** liquid limit
w_P	**:** plastic limit

EXPERIMENTAL AND NUMERICAL MODELLING STUDIES FOR INTERPRETING AND ESTIMATING THE p-δ BEHAVIOR OF SINGLE PILES IN UNSATURATED SOILS

SUMMARY

In geotechnical engineering practice, conventional soil mechanics principles are used for the design of shallow and deep foundations assuming the soil is in a state of saturated condition. However, such an assumption may not be representative of the actual field conditions in most situations as soils are typically found in a state of unsaturated condition. This is particularly true for soils in arid and semi-arid regions, where the ground water table is at a greater depth. Due to this reason, the loads that are transmitted from the superstructure to the shallow and deep foundations are distributed within the unsaturated soil zone above the ground water table. Several recent studies have shown that the bearing capacities of both coarse and fine-grained soils are significantly influenced due to the contribution of suction.

There are some studies reported in the literature that are useful for the design of shallow foundations in unsaturated soils. However, there are limited studies reported in the literature that discuss the design of pile foundations taking account of the influence of suction in unsaturated soils. The key objective of the research studies presented in this thesis is directed towards developing simple and reliable techniques or semi-emprical models including numerical modelling studies that can be used in geotechnical engineering practice to estimate the bearing capacity of single piles in coarse and fine-grained unsaturated soils.

Several single model pile tests were performed in a laboratory environment to study the influence of suction on the pile shaft resistance placed in a statically compacted unsaturated fine-grained soil (i.e. glacial till) at different constant initial water content conditions. A constant initial water content assures uniform matric suction value in the compacted soil over the entire depth. Stainless solid steel cylindrical rods with different diameters and circular high strength plastic tank were used as model piles and as testing chamber, respectively. Model pile tests were conducted under both saturated and unsaturated conditions under different drainage conditions.

These test results were interpreted using the coventional methods such as the α, β and λ methods introducing modifications. In addition, semi-empircal models were also proposed for estimating the carrying capacity of single piles using the soil water characteristic curve *(SWCC)* data and the conventional saturated shear strength parameters. The proposed semi-empirical models are useful for estimating the variation of total shaft resistance of piles with respect to suction. There is a good comparison between the predicted bearing capacity values using the proposed semi-emprical models and the measured values from the model pile test results.

A separate testing program was undertaken to evaluate the shaft resistance of jacked mild steel open end pipe test piles in two different sandy soils (i.e. Soil #1: silty sand

and Soil #2: clean concrete sand) under saturated and unsaturated conditions. The contribution of matric suction on the shaft bearing capacity of single piles placed in non-plastic compacted coarse grained soils was evaluated by introducing modifications to the conventional β-method.

Within the scope of this thesis, load-displacement (i.e. p-δ) behavior of a single pile in a glacial till is also modeled using an elastic-plastic Mohr-Coulomb model. Different scenarios of saturated and unsaturated soil conditions were considered to estimate the influence of suction towards the load carrying capacity of single piles. The commercially available finite element analysis software program (SIGMA/W) is used to perform the numerical modeling analyses. The theoretical background and the numerical modeling technique associated with this approach are presented in detail. This approach is simple and requires only the conventional shear strength parameters and the *SWCC*. The numerical modeling studies were performed both on in-situ single pile under saturated and unsaturated soil conditions. Conventional empirical methods were also used for estimating the ultimate shaft capacity. Comparisons are provided between both these approaches to highlight how conservative the presently used conventional approaches are in geotechnical practice.

The studies presented in the thesis are consistent with the approaches and methods that are used in conventional engineering practice. In other words, they are simple to follow and hence they are promising and encouraging for implementing the mechanics of unsaturated soils in to engineering practice.

SUYA DOYGUN OLMAYAN ZEMİNLERDE TEKİL KAZIK p-δ DAVRANIŞININ TAHMİNİ VE YORUMLANMASINA DAYALI DENEYSEL VE SAYISAL MODELLEME

ÖZET

Zemin mekaniği, mühendislik mekaniği ve zemin özelliklerinin bir birleşimi olarak ortaya çıkmaktadır. Bu tanımlama birçok zemin türünü kapsamaktadır. Klasik zemin mekaniği temel prensipleri, doymuş zeminlerin davranışlarının incelenmesi temeline dayanarak gelişmiştir. En genel tanımlama ile zeminler bu kapsamda doymuş kum, silt ve kil zeminler olarak sınıflandırılmışlardır. Geoteknik mühendisliği uygulamalarında temel tasarım hesapları geleneksel doygun zemin mekaniği prensiplerine dayandırılarak yapılmaktadır. Ancak doğada klasik zemin mekaniğinin öngördüğü prensip ve yaklaşımlara uymayan ve farklı davranış gösteren birçok zemin malzemesi bulunmaktadır. Bu durum, mevcut basitleştirilmiş kabullerin yanı sıra; mühendislik alanında daha gerçekçi sonuçların elde edilebilmesi için; zeminlerin doğal hallerine en yakın olan çözümlerin yaratılmasının ve bu haldeki davranışlarının da incelenmesinin gerekliliğini ortaya koymaktadır.

Bu bakış açısı ile, temel zemin mekaniği, çalışma alanları bakımından en genel hatları ile suya doygun ve doygun olmayan zeminler şeklinde iki ana başlık altında incelenebilmektedir. Doymuş zeminlerin iki fazlı sistemler olması mühendislik uygulamalarındaki kullanımlarını ve kabullerini yaygın hale getirmiştir. Suya doygun olmayan zeminler: dane, su, hava olmak üzere başlıca üç fazdan oluşmaktadır. Dördüncü bir faz olarak ise hava-su temas yüzeyi de dikkate alınmaktadır. Her iki durum da gerek mevcut fiziksel yapıları gerekse mühendislik davranışları açısından farklılıklar göstermektedirler. Mühendislik uygulamarında sıkça karşılaştığımız kazı, örseleme, kompaksiyon gibi işlemler suya tam doygun olmayan zeminleri ortaya çıkartmaktadır. Sıkıştırılmış (kompakte) zeminler, yüksek plastisiteli şişen zeminler, su muhtevasındaki artışa bağlı olarak yüklemeler altında çöken gevşek siltli zeminler ve negatif boşluk suyu basıncı etkisi altındaki zeminlerin tümü suya doygun olmayan zemin davranışına en temel örnekleri teşkil etmektedirler. Özellikle yeraltı su seviyesinin derinde bulunduğu durumlarda, mevcut sığ ve derin temel yapılarından doğan gerilme dağılımları, yeraltı su seviyesinin üzerinde kalan, suya doygun olmayan bölgelerde etkili olmaktadır. Son yıllarda temel sistemlerinin taşıma gücü kapasitelerine ilişkin yapılan bir çok bilimsel çalışmada, kaba ve ince daneli zeminlerde, emme basıncının kayma mukavemetine olan katkısı ile taşıma gücü üzerine olan etkisinin kayda değer ölçülere ulaştığı raporlanmıştır

İnşaat mühendisliğinde, dünya genelinde son on yıl içerisinde özellikle altyapı inşaatları önemli ölçüde hız kazanarak artmaktadır. Karayolları, havaalanları, dolgular, barajlar gibi birçok geoteknik mühendislik projeleri doygun olmayan zeminlere örnek teşkil eden sıkıştırılmış (kompakte) zeminler üzerine inşaa edilmektedirler. Bu anlamda, sıkıştırılmış zeminler üzerine inşaa edilecek

mühendislik yapılarının tasarımında, suya doygun olmayan zemin mekaniği prensiplerinden faydalanmak daha uygun olmaktadır.

Literatürde son on yıl içerisinde yapılan çalışmalarda, suya doygun olmayan kaba ve ince daneli zeminlerde sığ temel sistemlerinin tasarımı ile ilgili araştırmalar büyük ölçüde yer almaktadir. Bu çalışmalarda, negatif boşluk suyu basıncının (emme basıncı) kayma mukavemeti ve temel taşıma gücü kapasitesine olan önemli etkisi deneysel veriler ve sayısal analizler ile raporlanmıştır. Ancak, suya doygun olmayan zeminlerde negatif boşluk suyu basıncı etkisi altında benzer mühendislik davranış özellikleri göstermesi beklenen kazıklı temeller ile ilgili yapılmış, az sayıda çalışmaya rastlanmaktadır.

Sunulan tez çalışması kapsamında temel amaç, geoteknik mühendislik uygulamalarında kullanılmak üzere, sayısal modellemeleri de içerek şekilde basit teknik ve yarı ampirik modeller geliştirerek, suya doygun olmayan kaba ve ince daneli zeminlerde bulunan kazıklı temel sistemlerinin taşıma gücünün hesaplanarak belirlenmesidir.

Bu amaçla, laboratuvar ortamında kurulan deney düzeneği kullanılarak, farklı su muhtevalarında hazırlanan ve statik kompaksiyon ile sıkıştırılmış ince daneli zeminlerde (Indian Head buzul tili ve killi kum-Loam zemin) emme basıncının kazık çevre sürtünmesine etkisi kazık yükleme model deneyleri ile araştırılmıştır. Yapılan deneylerde, farklı su muhtevalarında ve dolayısıyla farklı emme basıncı değerlerinde hazırlanan numuneler ile zemin doygunluk derecesenin kazık çevre sürtünmesine olan etkisi araştırılmıştır. Oluşan emme basıncının kazık uç direncine olan etkisi bu çalışma dahilinde dikkate alınmamıştır

Deneyler, 300^{mm}x300^{mm} boyutlarında dairesel yüksek dayanımlı plastik test tankında gerçekleştirilmiştir. Model kazıklar, farklı çaplardaki paslanmaz çelik içi dolu dairesel kesit boru çubuklardan yapılmıştır Numuneler, optimum su muhtevasında ve optimumdan daha düşük değerde seçilen üç farklı su muhtevasında hazırlanarak, 50kPa ila 200kPa değerlerinde değişen emme basınçları elde edilmiştir. Zemin numunesi, tank içerisine 350kPa değerine kadar statik kompaksiyon ile sıkıştırılarak yerleştirilmiştir. Model kazık deneyleri, suya doygun ve suya doygun olmayan durumlar için, drenajlı ve drenajsız yükleme durumlarında gerçekleştirilmiştir. Zeminin sabit bir su muhtevası değerinde hazırlanması, deneyde kullanılan zeminin derinlik boyunca sabit emme basıncı değerine sahip olmasına imkan sağlamaktadır.

Eksenel yük altındaki tekil kazıkların taşıma gücü hesabında çok yaygın olarak kullanılan klasik α-alfa (Skempton 1959), β- beta (Burland 1973) ve $\lambda-$ lamda yöntemleri (Vijayvergiya ve Focht 1972) suya doygun olmayan zeminler için değiştirilip genişletilerek deney sonuçlarının yorumlanmasında ve aynı zamanda emme basıncına bağlı taşıma gücü kapasitesinin değişim fonksiyonunun elde edilmesinde kullanılmıştır.

Negatif boşluk suyu (emme) basıncı ölçümleri, zemin-su karakteristik eğrilerinin belirlenmesi ve kayma mukavemeti test sonuçları sunulmuştur. Önerilen modifiye yarı ampirik modeller ile (genişletilmiş α-alpha, β- beta ve $\lambda-$ lambda), zemin su karakteristik eğrileri ve suya doygun kayma mukavemeti parametreleri (c',ϕ') kullanılarak, suya doygun olmayan zeminlerde tekil kazıkların çevre sürtünmesinden doğan taşıma gücü değerlerinin tahmin hesapları gerçekleştirilmiştir. Deney sonucunda elde edilen ve önerilen yöntemlerin kullanılması ile hesaplanan taşıma gücü değerleri karşılaştırmalı olarak sunulmaktadır.

Yapılan, deney sonucunda, suya doygun olmayan durumda model kazık çevre sürtünmesinin suya doygun duruma kıyasla 5-6 kat fazla olduğu gösterilmiştir. Deneysel sonuçlar, klasik hesap yöntemlerinin suya doygun olmayan zeminler için kullanılması durumunda çok güvenli sonuçlar verdiğini göstermektedir.

Kaba daneli zeminlerde negatif boşluk suyu basıncının tekil kazık çevre taşıma kapasitesine etkisi ise, ayrı bir deney programı ile iki farklı kum zemin (siltli kum ve kum)içerisine yerleştirilen çelik boru model kazık üzerinde suya doygun ve doygun olmayan durumlar için incelenmiştir. Elde edilen sonuçlar sırasıyla suya doygun ve doygun olmayan zemin koşulları için klasik ve modifiye β-yöntemi kullanılarak değerlendirilmiştir. Analiz ve değerlendirme sonuçlarından, siltli kum zeminlerde mevcut negatif boşluk suyu basıncının nihai çevre taşıma kapasitesine katkısının %40-%50 mertebelerinde olduğu ancak kum zemin için bu katkının ihmal edilebilecek kadar az olduğu ortaya konulmuştur.

Sunulan tez çalışması kapsamında, deneysel çalışmalara ek olarak, tekil kazık yük-deplasman davranışları elastik-plastik Mohr-Coulomb modeli kullanılarak sayısal analiz teknikleri ile modellenmiştir. Negatif boşluk suyu basıncının kazık taşıma gücüne olan etkisi farklı boşluk suyu basınç profilleri için incelenerek modellenmiştir. Sayısal modellemeler, *SIGMA/W* sonlu elemanlar analiz programı kullanılarak ve suya doygun olmayan zemin davranışını tanımlamaya uygun yaklaşımların da model içerisine dahil edilmesiyle yapılmıştır. Oluşturulan sayısal analiz modeli, arazi koşullarını temsilen yerinde dökme betonarme kazık için doygun ve doygun olmayan zemin koşullarında gerçekleştirilmiştir. Nihai kazık çevre taşıma kapasitesi bilinen ampirik metodlar ile de hesaplanarak, sayısal analiz sonuçları ile karşılaştırılmıştır. Karşılaştırma sonuçları bilinen hesap yaklaşımlarının doygun olmayan zeminler için kullanılması durumunda aşırı güvenli yaklaşımlar ortaya koyduğunu göstermektedir.

Tez kapsamında yapılan çalışmalarda, ölçüm ve hesaplamalardan elde edilen taşıma gücü değerleri arasındaki uyum ve önerilen modifiye; α-alpha, β- beta ve $\lambda-$ lambda; yöntemlerinin bilinen yaklaşımlar ile tutarlılık ve paralellik göstermeleri, suya doygun olmayan zemin mekaniği prensiplerinin pratik mühendislik alanında uygulanabilirliğini desteklemektedir.

1. INTRODUCTION

1.1 Statement of the Problem

Both the shallow and deep foundations in many situations are placed in soils that are typically in a state of unsaturated condition. However, in conventional engineering practice, the influence of capillary stresses (i.e. matric suction) in the unsaturated zone (i.e. capillary zone) above the groundwater table is ignored. The soil profile is generally assumed to be either fully saturated in practice as it is simple for analysis and also it is a conservative approach. Experimental and theoretical difficulties associated with the controlling and measuring suction and rationally interpretating the influence of suction on the bearing capacity and settlement behavior have discouraged the practitioners in implementing use the mechanics of unsaturated soils in the design of both shallow and deep (i.e. pile) fundations.

The design of pile foundations in practice are conventionally based on the principles of saturated soil mechanics or empirical procedures or based on in-situ test results. Typically, pile foundations are designed assuming saturated, dry or submerged conditions. The influence of unsaturated soil conditions above the ground water table level and the possible water table fluctuation effects on a single pile are not typically analyzed extending the mechanics of unsaturated soils. There are no studies that are reported in the literature to estimate the shaft resistance of piles due to the contribution of capillary stresses or specifically the matric suction to the best of the knowledge of the author.

1.2 Research Objectives

The key objective of the thesis is to develop simple and reliable techniques and models that can be easily used in geotechnical engineering practice for the implementation of the mechanics of unsaturated soils to estimate the shaft bearing capacity of a single pile. The research program focus was directed towards

developing a theoretical framework based on laboratory studies performed on model piles. This framework has been also extended for numerical modelling to estimate the load-displacement behaviour of piles.

The key objectives of the presented research are:

- To study the influence of matric suction on the bearing capacity behavior of single piles in unsaturated coarse and fine-grained soils by performing model pile load tests.
- To estimate the shaft bearing capacity of single pile by modifying the conventional α, β and λ methods and to estimate the contribution of matric suction.
- To propose semi-empirical models to predict the variation of shaft capacity of piles in unsaturated coarse and fine-grained soils with respect to matric suction using the saturated soil parameters and the Soil Water Characteristic Curve (*SWCC)* as a tool.
- To propose numerical models to simulate the load versus displacement behavior of piles in-situ and as well as model poles.
- To demonstrate how conservative the conventional calculation methods are when they are extended for unsaturated soils.

1.3 Scope of the Study

1.3.1 Litreature review

Significant advances were made during the last 50 years towards better understanding the engineering behavior of unsaturated soils. These studies have contributed to develop theoretical frameworks, experimental methods and constitutive models including the numerical techniques. The focus of the research presented in this thesis is directed towards proposing tools for interpreting and estimating bearing capacity of single pile foundations. The carrying capacity of piles in unsaturated soils is signficantly influened by the shear strength behavior. Due to this reason, literature review focus has been directed towards providing more background on shear strength of unsaturated soils both under drained and undrained loading conditions.

1.3.2 Theoretical background

In recent years, empirical or semi-empirical models have been proposed in the litreature for the estimation or prediction of the shear strength of unsaturated soils (Vanapalli et al., 1996; Fredlund et al., 1996). The *SWCC* is used as a tool for the prediction of the shear strength of unsaturated soils. The present understanding related to the shear strength of unsaturated soils has been extended for interpretation of the behavior of single piles and also for estimation of the shaft bearing capacity of single piles in unsaturated soils.

The most commonly used conventional semi-empirical methods in geotechnical engineering practice as the α, Skempton (1959), the β, Burland (1973), Meyerhof (1976) and the λ, Vijayvergiya and Focht (1972) methods were modified to estimate the shaft bearing capacity of single pile in both saturated and unsaturated coarse and fine-grained soils.

1.3.3 A study for estimating shaft bearing capacity of test piles in non-plastic unsaturated soils based on previous experimental work

A testing program was undertaken at the Lakehead University was used to evaluate the shaft resistance of jacked steel open end pipe piles embedded in two different sandy soils (i.e. Soil #1: silty sand and Soil #2: clean concrete sand) both under saturated and unsaturated conditions. Two different types of sand were placed in a test tank at different compaction water contents and initial dry density values. The matric suction value were measured using commercially available tensiometers, which were embedded at different depths, immediately after compaction, while raising the water table to the ground surface and subsequently while lowering the water level to the base of the test pit. Based on the results of the study, a technique for estimating the shaft resistance of test piles under unsaturated conditions is presented taking account influence of matric suction extending an effective stress analysis approach of the conventional β method which is the modified β method. This method is applied to the results to estimate the the shaft bearing capacity of a single pile by using the *SWCC* and the saturated shear strength parameters.

1.3.4 Shaft bearing capacity of test piles in fine grained unsaturated soils

The experimental studies to address the research objectives were undertaken at the Geotechnical Laboratory of the University of Ottawa. A comprehensive experimental program was undertaken using a fine grained compacted soil (i.e. Indian Head till and Loam soil) to determine the shaft bearing capacity of a single pile in saturated and unsaturated conditions. The shear strength parameters and the interface strength parameters between the pile material and soil determined by conventional direct shear test apparatus. Other soil properties for the tested soils were also determined in the laboratory including the *SWCC* using the pressure plate apparatus. The shear strength parameters, and other soil properties with the model pile dimensions were used for calculating the shaft bearing capacity of a single pile under staurated soil condition using the effective stress analysis and total stress analysis conventional empirical methods for drained and undrained loadings respectively. Based on the experimental results of the tested soil and other conventional soil properties, the shaft bearing capacity of a single pile in unsaturated soil were interpreted using the modified α, β and λ methods.

1.3.5 Modelling the load versus displacement behaviors of a single pile in unsaturated fine grained soils

A numerical model is developed using the elastic-plastic Mohr-Coulomb model to simulate load versus displacement behavior of a single pile placed in unsaturated soil condition. This model is extended to reanalyze the load-displacement results of an in-situ single pile in an unsaturated glacial till of Lower Cromer till obtained by the critical state concept model (Georgiadis, 2003).

The finite element analysis is undertaken using the commercial finite element analysis program SIGMA/W (Geostudio 2007) software which is a product of GEO-SLOPE (Krahn, 2007). These analyses were carried out using the elastic – perfectly plastic model extending the Mohr - Coulomb yield criterion. The conventional shear strength parameters (i.e. c' and ϕ') and the SWCC are required for performing the analyses. In addition, the theoreotical background associated with this approach and numerical modeling procedures are succinctly summarized. The SIGMA/W analyses were compared with the analysis results of the case study by Georgiadis et al. (2003) to validate the developed numerical model.

The contribution of suction to the bearing capacity behavior of a full-scale single pile of 20 m in length and 1 m in diameter, placed in glacial till, was investigated considering the influence of capillary stresses above the ground water table. Different groundwater table conditions have been assumed to achieve both positive and negative pore water pressure profiles considering different scenarios. The conventional and unsaturated analyses have been performed assuming drained loading conditions.

1.4 Thesis Outline

The presented thesis is organized as nine chapters. Chapter 1 describes the objective of this thesis research and the scopes and the thesis outline.

Chapter 2 provides litreature review to introduce key unsaturated soil mechanics concepts and all relevant background that is necessary for explaining the research presented in this thesis.

Chapter 3 under the title *Theoretical Background* provides a summary of pile foundation design. In addition, key studies on behavior of pile foundations that are based on the mechanics of unsaturated soils are summarized. Finally, semi-empirical models that were proposed for predicting the variation of shaft capacity of single pile with respect to suction are presented.

Chapter 4 entitled, A Study for Estimating Shaft Bearing Capacity of Test Pile in Non-Plastic Unsaturated Compacted Soils Based on the Previous Experimental Work presents the previous experimental studies performed to study the influence of the matric suction effect on shaft bearing capacity of a model single pile placed in unsaturated coarse grained soil. The design detail of the testing set-up is provided including the interpretation of the test results using the proposed semi-empirical methods.

Chapter 5 entitled, Shaft Bearing Capacity of Test Piles in Fine Grained Unsaturated Compacted Soils: Equipment Details and Methodology presents the experimental study performed to measure the matric suction effect on shaft bearing capacity of a model single pile placed in unsaturated fine grained soil with. The methodology followed in collecting all the necessary information related to the experimental study and the design details of the testing set-up is presented in detail.

Chapter 6 entitled, *Laboratory Test Program and Methodology* provides details about the testing program undertaken for the present research program. The experimental research program consists of a series of single model pile tests were performed in a laboratory environment to study the influence of matric suction on the pile shaft resistance in a compacted fine-grained soils. The model piles were loaded to failure under both saturated and unsaturated conditions under different drainage conditions. Step by step procedures of the experimental methodology is summarized in this chapter.

Chapter 7 titled *Presentation and Interpretation of Test Results* consists of two sub-sections. *Section-1* provides the results for matric suction and *SWCC* measurements and the for the model pile load tests. The load-displacement *(p-δ)* curves associated with the controlled suction and water content are given. Finally, the results for the shear strength measurements including the interface direct shear test and unconfined compression tests are provided. *Section -2* discusses the interpretation of the test results by using the proposed semi-empirical modified methods for the prediction of shaft bearing capacity of single piles for drained and undrained loading conditions in unsaturated soils. The comparison between the measured and the predicted shaft bearing capacities are provided.

In Chapter 8 entitled, Modelling the Load versus Displacement Behavior of a Single Pile in Unsaturated Glacial tills, brief theoretical background related to the numerical modeling techniques of critical state model (CSM) and the conventional elastic-plastic Mohr-Coulomb model is discussed. The critical state model (CSM) extended for unsaturated soils and its implementation to the case study by using the Imperial College Finite Element Method (ICFEP) to investigate the influence of suction and GWT fluctuations on the behavior of a single pile is presented in all details. Elastic-plastic Mohr-Coulomb model is also extended for unsaturated soil condition and the defined case study is adopted and re-analysed using Elastic plastic Mohr-Coulomb model in commercially available finite element analysis software program SIGMA/W. The SIGMA/W analysis results were compared with the previous case study results considering unsaturated soil condition with the ICFEP.

Chapter 9 presents the summary and conclusions of the research program and also provides some recommendations for future studies.

2. LITREATURE REVIEW

2.1 Introduction

This chapter provides a brief background of key concepts related to the mechanics of unsaturated soils. The rational approach of interpreting the unsaturated soils behavior in terms of independent stress state variables is summarized. Information related to how the variation of soil-air-water interphase changes and influences the unsaturated soils behavior is detailed. In addition, the use of soil-water characteristic curve *(SWCC)* as a tool in the estimation or prediction of engineering behavior of unsaturated soils is also discussed succinctly.

The focus of the research presented in this thesis is directed towards developing interpretation techniques and also proposing semi-empirical models for predicting the shaft capacity of single piles in both coarse- and fine-grained soils taking account influence of matric suction. To address these objectives, background information related to the shear strength behavior of unsaturated soils is required. Due to this reason, in this chapter, the shear strength behavior of unsaturated soils under both drained and undrained loading conditions is summarized.

2.2 Effective Stress Concept and Stress State Variables

2.2.1 Saturated soils

Terzaghi (1936) introduced the effective stress principle for interpreting the mechanical behavior (i.e. shear strength and volume change) of saturated soils as (2.1):

$$\sigma' = \sigma - u_w \qquad \textbf{(2.1)}$$

where σ' = effective normal stress, σ = total normal stress, u_w = pore-water pressure.

Figure 2.1 provides details of how effective normal stress, $(\sigma - u_w)$ and shear stresses τ_f act on an element *x-y* and *z* directions of soil under dry and saturated conditions. In

addition, the matrix equation consistent with the principles of continuum mechanics is shown.

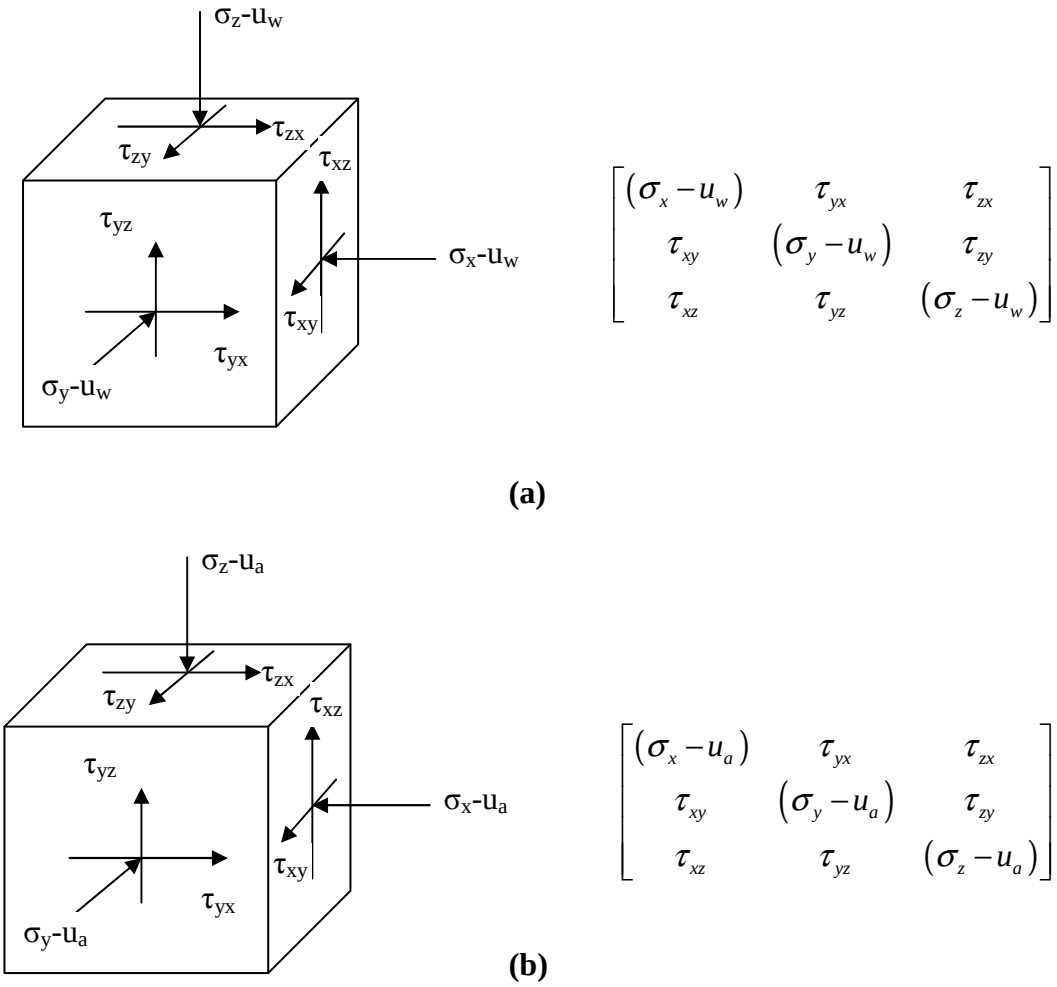

$$\begin{bmatrix} (\sigma_x - u_w) & \tau_{yx} & \tau_{zx} \\ \tau_{xy} & (\sigma_y - u_w) & \tau_{zy} \\ \tau_{xz} & \tau_{yz} & (\sigma_z - u_w) \end{bmatrix}$$

$$\begin{bmatrix} (\sigma_x - u_a) & \tau_{yx} & \tau_{zx} \\ \tau_{xy} & (\sigma_y - u_a) & \tau_{zy} \\ \tau_{xz} & \tau_{yz} & (\sigma_z - u_a) \end{bmatrix}$$

Figure 2.1 : Normal and shear stresses on soil element and corresponding stress tensors: (a) saturated soil, (b) completely dry soil.

Terzaghi effective stress equation, $(\sigma - u_w)$ is a single stress state variable that can be used as a tool to rationally explain the mechanical behavior of both saturated and dry soils, that have only two phases which is soil and water or soil and air, respectively , using constitutive relationships without introducing any empirical parameters that are dependent on other soil properties.

2.2.2 Unsaturated soils

Unlike saturated soils, which are two-phase soil systems, unsaturated soils have multi-phase systems composed of three phases consisting of solid (soil particles), liquid (water) and gas (air). Based on the fundamental definition of a phase, Fredlund

and Morgenstern (1977) introduced the air-water interface, contractile skin as the fourth phase to rationally interpret the engineering behavior of soils that are influenced by the stresses in the soil-water-air interphases. They suggested using the term “unsaturated soils”, instead of “partly saturated soils” or “partially saturated soils” since the inclusion of the smallest amount of free gas into soils renders the system “unsaturated”.

Figure 2.2 shows an unsaturated soil element that can be visualized as a mixture with two phases that come to equilibrium under applied stress gradients (i.e. soil particles, contractile skin) and two phases that flow under applied stress gradients (i.e. air and water). The pore-air, u_a and pore-water, u_w pressures in the soil structure of a soil that is in a state of unsaturated condition influences the engineering behavior of soils (i.e. flow, shear strength and volume change behavior). The changes in pore-pressures in an unsaturated soil are due to moisture fluctuations as precipitation or evaporation, changes in ground water table level or due to other reasons such as excavation of natural soils or compaction.

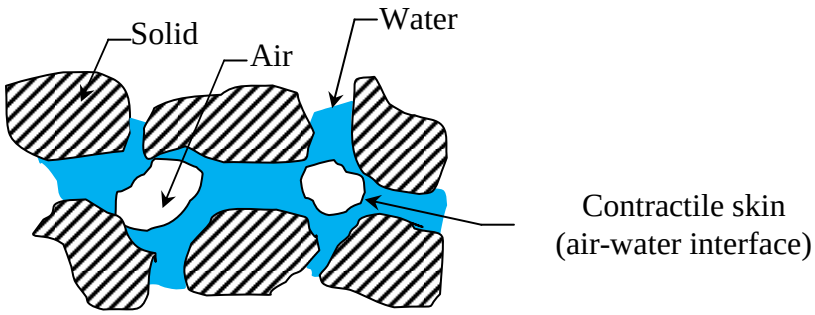

Figure 2.2 : Typical structure in an unsaturated soil.

Bishop (1959) introduced a single-valued factor, χ, into Terzaghi’s effective stress equation for estimating the effective stresses in unsaturated soils as given in (2.2):

$$\sigma' = (\sigma - u_a) + \chi(u_a - u_w) \qquad \textbf{(2.2)}$$

where, σ' = effective stress, σ = total stress, u_a = air pressure in the pore space, u_w = pore-water pressure, $(\sigma - u_a)$ = net normal stress, $(u_a - u_w)$ = matric suction, χ = effective stress parameter which depends on the degree of saturation.

The effective stress parameter χ =1 for saturated soils and χ = 0 for dry soils (Bishop, 1959). In each case (dry or saturated), Bishop’s equation (2.2) shows a

smooth transition to the Terzaghi's effective stress equation (2.1). The parameter χ depends mainly on the degree of saturation *S*.

Bishop and Donald (1961) performed triaxial tests on cohesionless Braehead silt and compacted soils to examine the validity of the effective stress equation proposed by Bishop (1959). The cell pressure (σ_3), the pore-water pressure (u_w), and the pore-air pressure (u_a) were varied keeping the combinations of the stress state variables, $(\sigma_3 - u_a)$ and $(u_a - u_w)$ constant. The test results showed that the measured stress-strain curve was monotonic. These test results indirectly support the validity of the chosen variables $(\sigma_3 - u_a)$ and $(u_a - u_w)$ as stress state variables, for rationally explaining the behavior of unsaturated soils. Other studies however have shown that parameter χ in Bishop's equation is also dependent on the soil structure, wetting and drying cycles or stress changes that contribute to changes in the degree of saturation, *S*. Several investigators experimental studies have shown that there is no unique relationship between the parameter, χ and the degree of saturation (Figure 2.3) (Bishop and Blight, 1963).

Blight (1965), Burland (1964, 1965), Aitchison (1965) and Fredlund and Morgenstern (1977) questioned the validity of using single effective stress equation for unsaturated soils. They suggested that the mechanical behavior of unsaturated soils should be described in terms two independent stress variables. In unsaturated soils, not only the *applied stress* but also the *soil suction* contributes to the deformation of the soil structures; however, their contributions to the deformation are different. In addition, the χ parameter values derived from shear strength are different from the volume change behavior for the same soil. Due to this reason, the use of single effective stress equation cannot rationally explain the mechanical behavior of unsaturated soils. In order to overcome these limitations, it was proposed to use two independent stress state variables to describe the mechanical behavior of unsaturated soils.

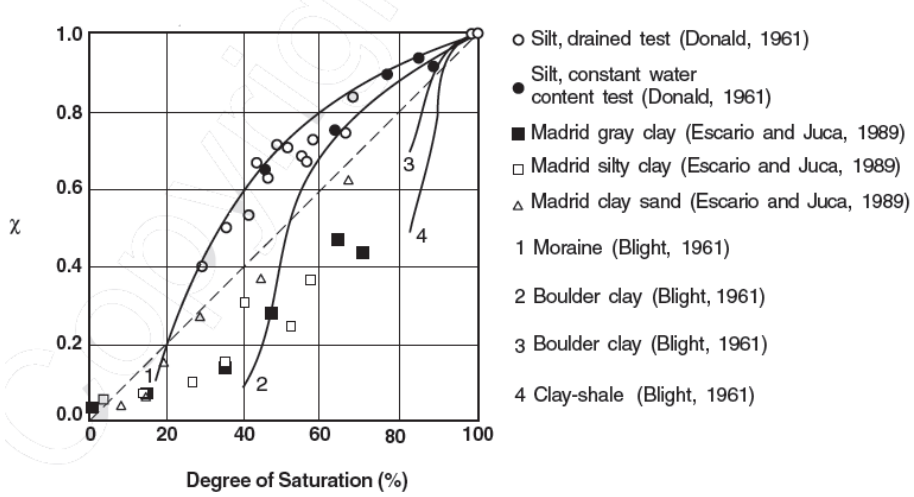

Figure 2.3 : Experimental results showing the relationship between χ parameter and the degree of saturation (Lu and Likos, 2004).

Fredlund and Morgenstern (1977) and Fredlund (1979) provided a theoretical framework for unsaturated soils based on continuum mechanics by experimentally proving that any two of the three possible stress state variables can be used to define the stress state in an unsaturated soil. The three possible combinations which can be used are: i) $(\sigma - u_w)$ and $(u_a - u_w)$ ii) $(\sigma - u_a)$ and $(\sigma - u_w)$ iii) $(\sigma - u_a)$ and $(u_a - u_w)$. The first two stress state variable combinations have the disadvantage that when the pore water pressure changes, both the stress state variables are affected. The advantage of the third combination (i.e. $(\sigma - u_a)$ and $(u_a - u_w)$) is that when the pore-water pressure changes, only one stress variable, $(u_a - u_w)$ is affected. For conventional geotechnical engineering applications, the third combination of the stress state variables is best suited. The pore-air pressure, u_a is typically equal to atmospheric pressure; hence, the stress state $(\sigma - u_a)$ can be easily calculated.

Each of these independent stress variables in three-dimensional space can be represented by a tensor satisfying the continuum mechanics principles. The complete form of the stress state for an unsaturated soil can therefore be written as two sets of independent stress tensors (Figure 2.4).

Using two independent stress-state variables (i.e. $(\sigma - u_a)$ and $(u_a - u_w)$) constitutive relationships can be written for interpreting the engineering behavior of unsaturated soils (Fredlund and Rahardjo, 1993). The use of such a rational framework eliminates the limitations of using single valued effective stress equations that were proposed with parameters that are dependent on other properties of the soil.

$$\begin{bmatrix} (\sigma_x - u_a) & \tau_{yx} & \tau_{zx} \\ \tau_{xy} & (\sigma_y - u_a) & \tau_{zy} \\ \tau_{xz} & \tau_{yz} & (\sigma_z - u_a) \end{bmatrix} \quad \text{and} \quad \begin{bmatrix} (u_a - u_w) & 0 & 0 \\ 0 & (u_a - u_w) & 0 \\ 0 & 0 & (u_a - u_w) \end{bmatrix}$$

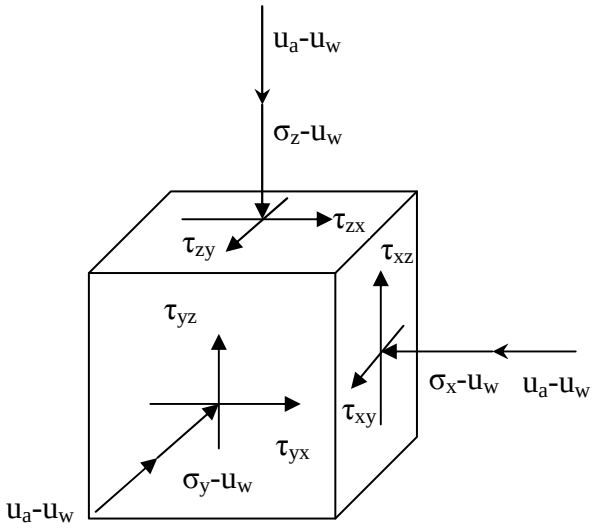

Figure 2.4 : Normal and shear stresses on soil element and corresponding stress tensors for an unsaturated soil.

2.3 Soil Suction

Total soil suction is the thermodynamic potential of soil pore water relative to a reference potential of free water containing no dissolved solutes, having no interactions with other phases that impart curvature to the air-water interface, and having no external forces other than gravity (Lu and Likos, 2004). For a flat air-water interface, the water pressure at equilibrium is equal to the air pressure (i.e. $u_a = u_w$). The physical and physicochemical mechanisms responsible for total soil suction that decrease the potential of pore water relative to this reference state of free water can be written as follows (2.3):

$$\Delta\psi_t = \Delta\psi_c + \Delta\psi_o + \Delta\psi_e + \Delta\psi_f \qquad \textbf{(2.3)}$$

where; $\Delta\psi_t$ = the total potential, $\Delta\psi_c$ = the capillary potential which is change in potential due to curvature at the air-water interface (capillarity), $\Delta\psi_o$ = the osmotic potential which is the change due to dissolved solute effects, $\Delta\psi_e$ = the change due to the presence of electric fields, $\Delta\psi_f$ = the change due to van der Waals fields.

Neglecting temperature, gravity and inertial effects, the primary mechanisms that decrease the potential of soil pore water include capillary and osmotic effects. The algebraic sum of the matric and osmotic components is known as total soil suction and is given in (2.4). The term "matric" reflects earlier usage of the term "matrix", which was intended to describe the component of suction arising from interactions between the pore water and the soil solids, or soil matrix. The capillary potential change is the differential pressure across the meniscus of the air–water interface within the soil which is the unique mechanism to understand unsaturated soil behavior. Suction arising from the influence of dissolved solutes is referred to as osmotic suction, $\psi_{osmotic}$.

$$\psi_{total} = \psi_{matric} + \psi_{osmotic} \qquad \textbf{(2.4)}$$

$$\psi_{total} = (u_a - u_w) + \pi$$

where, ψ_{total} = total potential, $(u_a - u_w)$ = matric suction, π = osmotic suction.

2.3.1 Physical representation of capillary suction

The air-water-solid interface in unsaturated soil within a soil pore can be visualized as equivalent to the air-water interface in a glass tube (i.e. a spherical interface model) which describes the suction component due to capillary effects. The equilibrium of the interface can be maintained by the difference between the air and the pore-water pressures, $(u_a - u_w)$ acting on the pore water which is balanced by the surface tension, T_s, acting at the wetting angle, α, along the air-water contractile skin.

A simple analysis of mechanical equilibrium considering the free-body diagram is shown in Figure 2.5. Vertical force equilibrium considering $(u_a - u_w)$ acting over the area of meniscus and the vertical projection of T_s acting over the circumference of the interface leads to the expression (2.5):

$$u_a(\pi r^2) = u_w(\pi r^2) + T_s \cos\alpha(2\pi r) \qquad \textbf{(2.5)}$$

This relationship (2.5) can be reduced to the form (2.6) as given below:

$$(u_a - u_w) = \frac{2T_s \cos\alpha}{r} \qquad \textbf{(2.6)}$$

where $(u_a - u_w)$ = matric suction, T_s = surface tension, α = the contact angle which varies $0° < \alpha < 90°$ for a partially wetting surface with the air-water interface curvature $R = r/\cos\alpha$.

2.4 Soil Water Characteristic Curve (SWCC)

Soil-water characteristic curve (*SWCC)* is defined as the relationship between the water content, *(w)* or degree of saturation, *(S)* or volumetric water content, (θ) of a soil and the corresponding soil suction. The relationship between the volumetric water content, (θ) degree of saturation, (S) and water content, (w) is given by (2.7) :

$$\theta = S\,n = \rho_d\,w \qquad \textbf{(2.7)}$$

where n = porosity, ρ_d = dry density of the soil.

A typical *SWCC* for a drying soil for the entire range of suction (i.e. from saturated to dry condition) of 0 to 1,000,000 kPa is shown in Figure 2.6a. The curve can be divided into three zones (Figure 2.6a); namely (i) the boundary effect zone also known as the capillary zone, (ii) the transition zone also known as desaturation zone, and (iii) the residual zone.

In the boundary effect zone, the water phase is continuous within the soil pores although desaturation exerts tension on water while matric suction is increasing. As the suction keeps increasing, at a specific suction value, air replaces water from the largest pore in the soil matrix. This specific value of suction is known as the air-entry value *(AEV).*

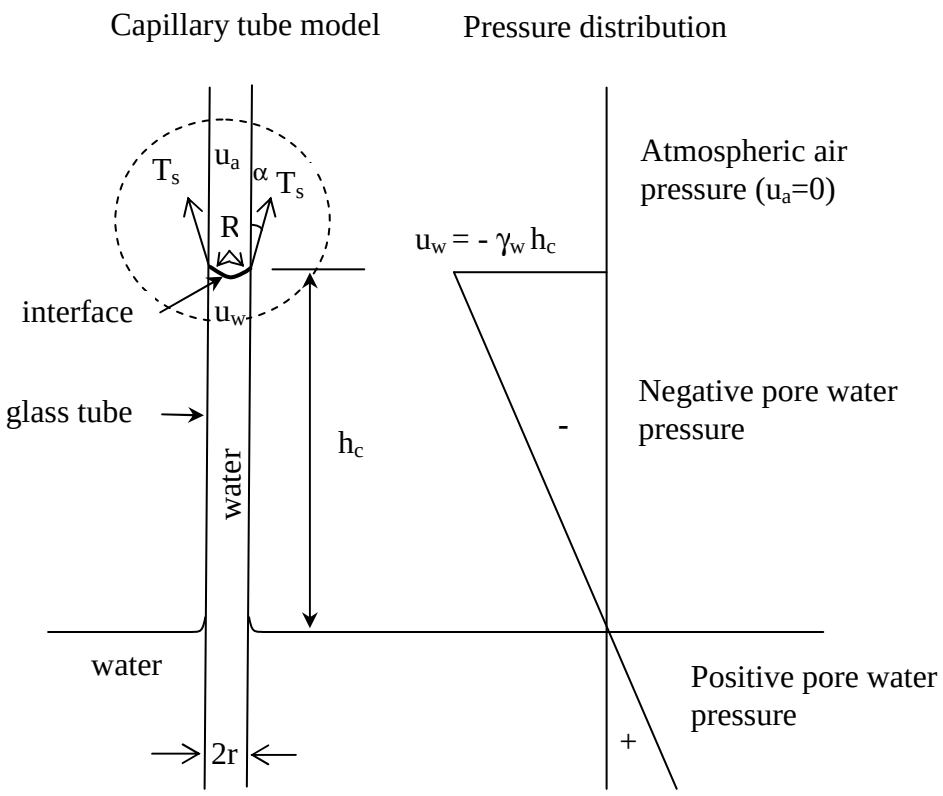

Figure 2.5 : Physical model and phenomenon related to capillarity.

Any increase in matric suction contributes to a significant decrease in water content or degree of saturation beyond the *AEV* (i.e. starting point of the primary transition zone). As desaturation continues in the transition zone (i.e. from primary to secondary transition zone), the area of water in contact with the soil particles decreases and the continuous water paths are blocked with air (Figure 2.6b). Finally, in the residual zone; water content, *w*, degree of saturation, *S* or volumetric water content, θ decreases are small in spite of significant increases in suction values. The amount of water retained within the pore space in this residual state is referred to as the residual water content (w_r), residual volumetric water content (θ_r) or the residual degree of saturation (S_r). The *SWCC* can be used as a conceptual, interpretative, and predictive model for better understanding the unsaturated soil behavior (Barbour, 1998).

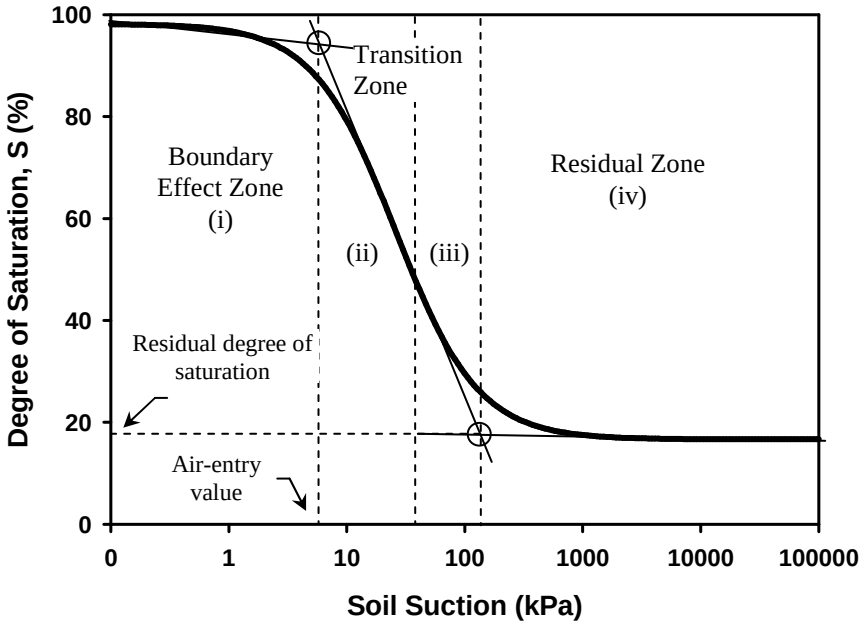

(a)

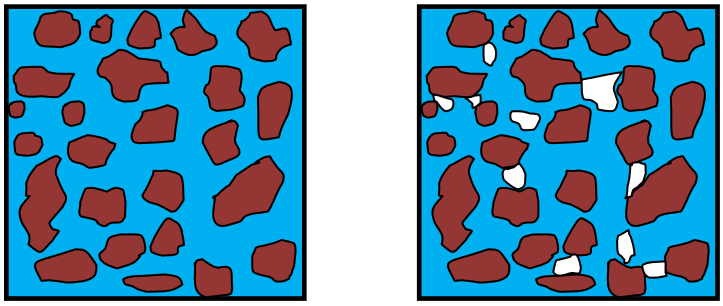

(i) Boundary effect stage (ii) Primary transition stage

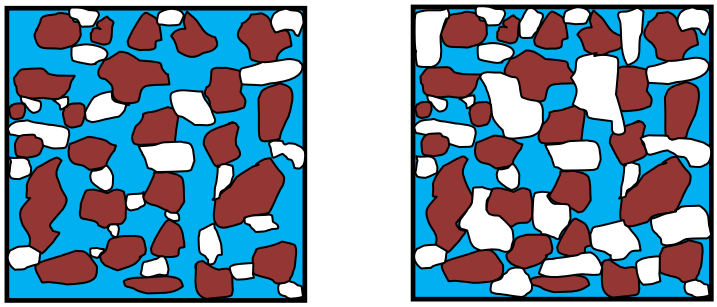

(iii) Secondary transition stage (iv) Residual stage

(b)

Figure 2.6 : (a) Typical soil-water characteristic curve and **(b)** physical representation of air-water-solid interaction in each corresponding desaturation stage (modifed after Vanapalli et al. 1996).

The shape of the *SWCC* is different for different soils (Figure 2.7). Coarse-grained soils such as sands consist of large pore sizes and thus will have a lower *AEV*. Sandy type of soils desaturate rapidly even at low matric suction values. On the other hand, clayey type of soils, gradually desaturate offering resistance to suction as they have smaller pore sizes. These soils typically have larger *AEV*. The rate of desaturation that occurs in the transition zone is related to the distribution of pore sizes. The percentage of fines within the soil and also the soil fabric orientation will affect the shape of the *SWCC*.

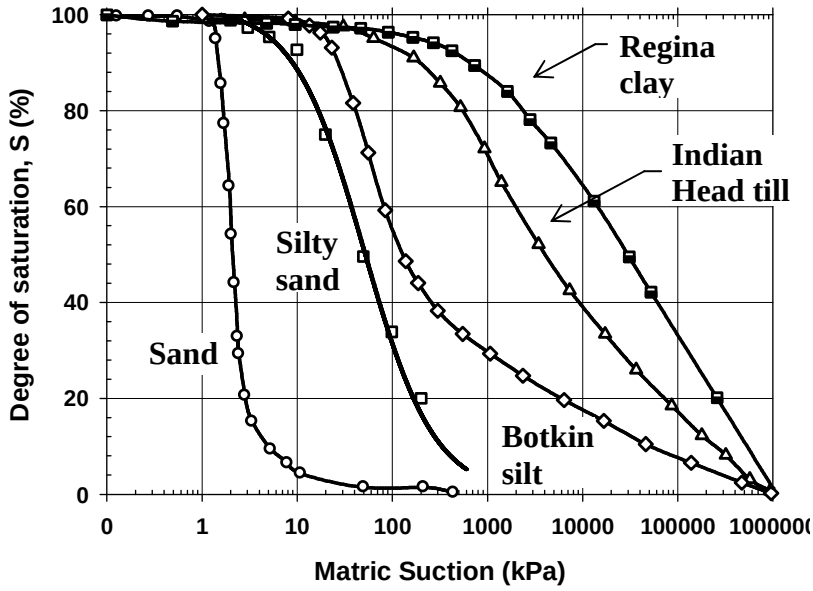

Figure 2.7 : Typical Soil-Water Characteristic Curves (*SWCCs*) for different soil types.

2.5 Shear Strength of Unsaturated Soils

The shear strength of soil is a key property required for several geotechnical applications such as bearing capacity, lateral earth pressures and slope stability. Shear strength of saturated soils can be determined extending the effective stress concept and the Mohr–Coulomb failure criterion as (2.8):

$$\tau = c' + (\sigma - u_w)\tan\phi' \qquad \textbf{(2.8)}$$

where τ = shear stress, c' = effective cohesion, $(\sigma - u_w)$ = effective normal stress, σ = total normal stress, u_w = pore-water pressure, ϕ' = effective angle of internal friction for a saturated soil.

The critical combination of shear and normal stresses (2.8) corresponding to failure condition defines the Mohr-Coulomb failure envelope for saturated soils (Figure 2.8).

2.5.1 Linear or planar failure shear strength envelope approach using two independent stress state variables

Fredlund et al. (1978) proposed an equation for interpretation of shear strength of unsaturated soils in terms of two independent stress state variables as in (2.9):

$$\tau = c' + (\sigma_n - u_a)\tan\phi' + (u_a - u_w)\tan\phi^b \qquad \textbf{(2.9)}$$

where τ = shear strength of an unsaturated soil, c' = intercept of the "extended" Mohr-Coulomb failure envelope on the shear stress axis when the net normal stress and the matric suction at failure are equal to zero; it is also referred to as the "effective cohesion", $(\sigma_n - u_a)$ = net normal stress, ϕ' = friction angle contribution due to net normal stress, $(u_a - u_w)$ = matric suction and ϕ^b = friction angle due to the contribution of matric suction.

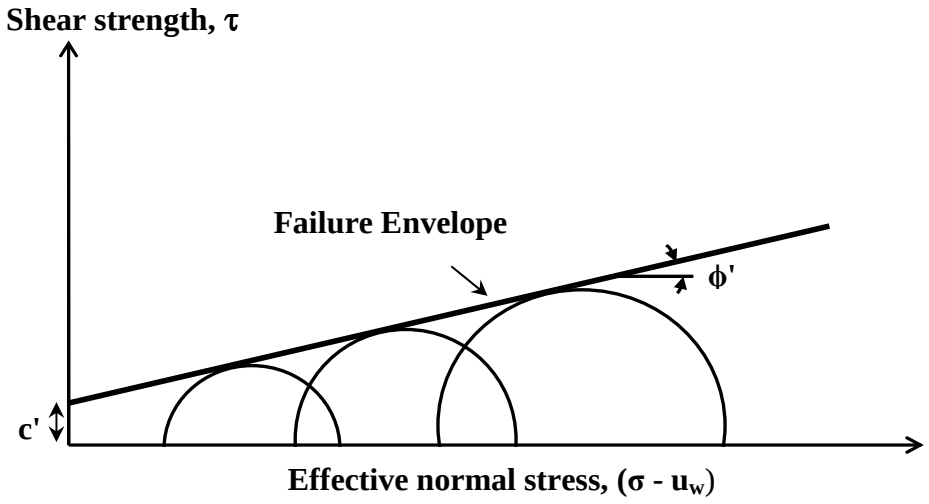

Figure 2.8 : Mohr-Coulomb failure envelope for a saturated soil.

For simplification purposes, the shear strength for unsaturated soil, τ_{unsat} can be visualized as having two components, which constitute the saturated shear strength, τ_{sat} and the shear strength contribution due to suction, $\tau_{suction}$ as given in (2.10).

$$\tau_{unsat} = c' + (\sigma_n - u_a)\tan\phi' + \tau_{suction} \qquad \textbf{(2.10)}$$

The experimental shear strength test data published in Bishop et al. (1960) were reanalyzed by Fredlund et al. (1978) using (2.9). The results are summarized in Figure (2.9a) as τ versus $(u_a - u_w)$ relationship. The resulting planar failure surface is called the extended Mohr-Coulomb failure envelope which is shown as a three dimensional relationship (Figure 2.9b). The failure envelope on τ vs. $(\sigma - u_a)$ plane in Figure 2.9b on which the matric suction is zero, is the same as the Mohr-Coulomb failure envelope for saturated soils.

Ho and Fredlund (1982) performed multistage triaxial shear tests on two different Hong Kong residual soils. The air and water pressures were controlled in the specimen during different stages of testing to achieve different matric suction values. The results were interpreted using Fredlund (1978) equation assuming planar failure surface.

The matric suction can be assumed to contribute to the cohesion of the soil as given below:

$$c = c' + (u_a - u_w)\tan\phi^b \qquad \textbf{(2.11)}$$

where c = total or apparent cohesion of the soil.

Escario (1980) also conducted a series of consolidated drained shear and triaxial tests on unsaturated Madrid gray clay and again reported that an increase in the shear strength with the increasing matric suction supporting the idea of a linear shear strength behavior.

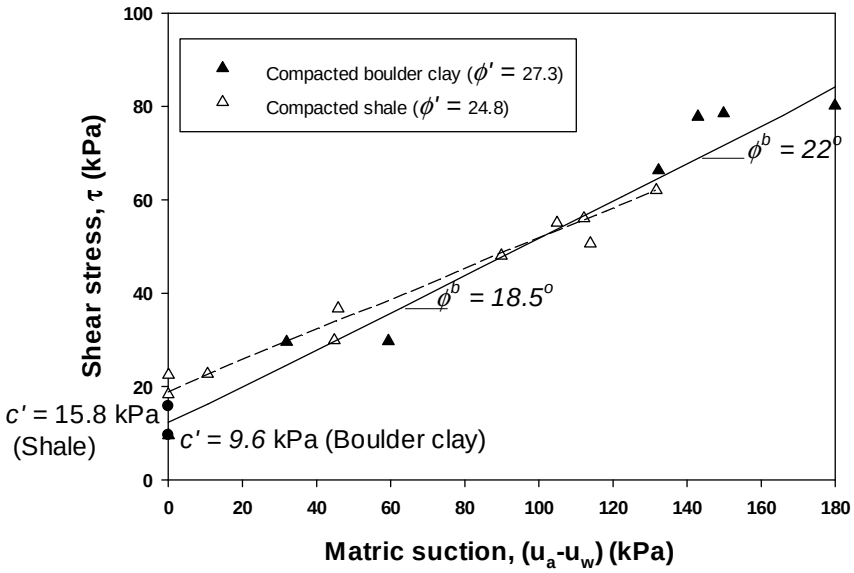

(a)

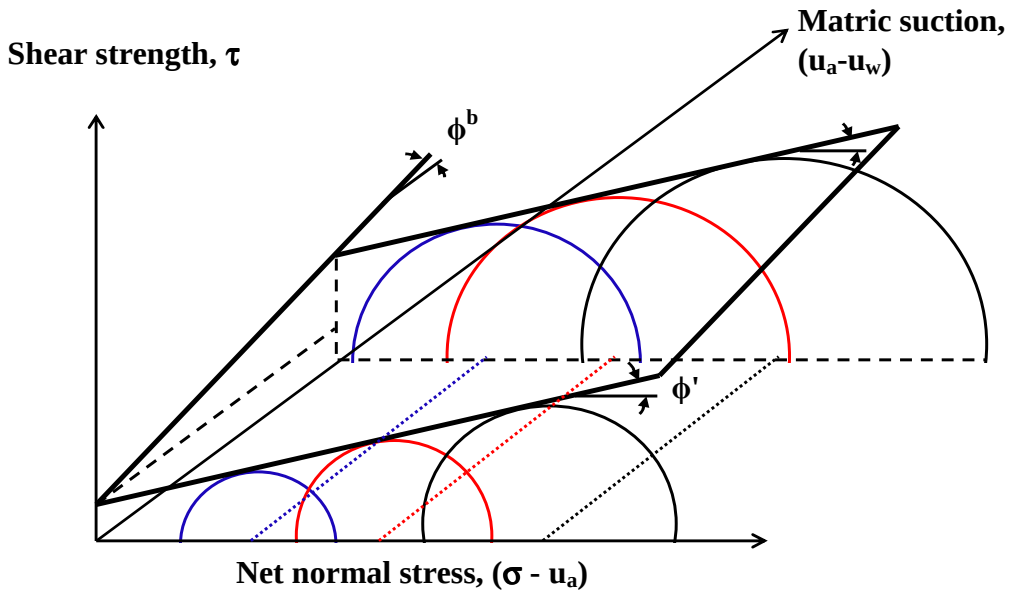

(b)

Figure 2.9 : (a) Planar failure envelopes on the τ versus (u_a-u_w) plane for two compacted soils (figure from Fredlund et al. 1987-data from Bishop et al. 1960), (b) Extended Mohr – Coulomb failure envelope.

2.5.2 Non-linear or curved failure shear strength envelope approach using two independent stress state variables

Later testing by a number of researchers demonstrated that the shear strength behavior is nonlinear (Escario and Saez, 1986; Gan, 1986; Fredlund, 1987; Gan et al., 1988; Gan and Fredlund, 1988). The shear strength contribution due to matric suction, ϕ^b is equal to ϕ' in the low suction range; however ϕ^b decreases with increasing matric suction. Experimental studies of Escario and Saez (1986) multistage direct shear tests on Madrid grey clay shown in Figure 2.10 support the nonlinear relationship when tested over a large suction range.

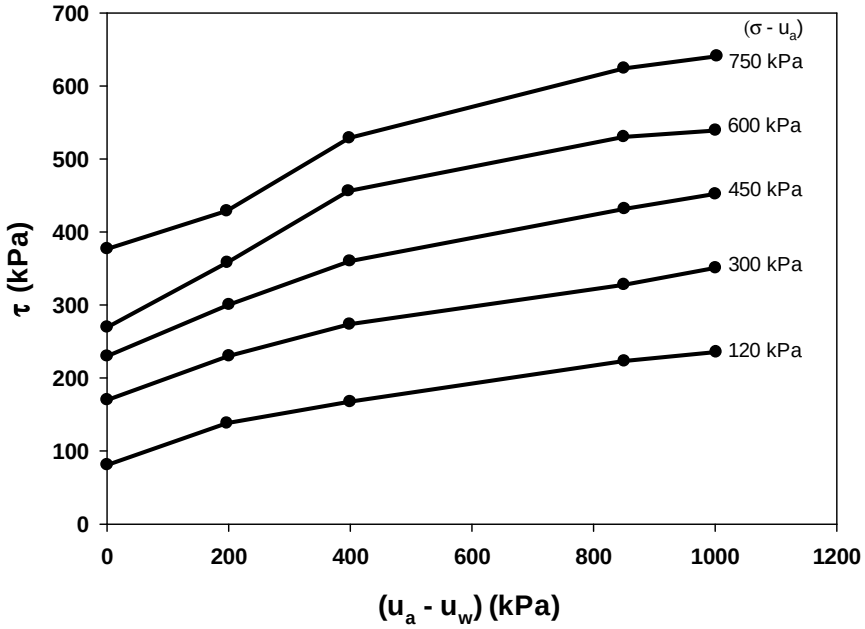

Figure 2.10 : Direct shear test results under controlled suction for Madrid grey clay: shear strength versus suction for different values of the normal stress (modified after Escario and Saez (1986)).

Gan (1986) and Gan et al. (1988) performed multistage direct shear tests on saturated and unsaturated specimens of a compacted glacial till for suction range of (i.e. 0-500kPa). The experimental results for this large suction range showed a significant non-linearity (curved failure envelope) for the shear stress versus matric suction relationship (Figure 2.11). Several researchers' studies since then supported the nonlinear shear strength behavior of unsaturated soils (Toll, 1990; Vanapalli et al. 1996).

2.5.3 Prediction of shear strength of unsaturated soils using the *SWCC* and saturated shear strength parameters

The amount of water and the wetted contact area within the different pores of an unsaturated soil at a particular value of suction has a profound influence on the shear strength. In other words, shear strength of unsaturated soils can be related to the amount of water occupied within the pore space indirectly deriving this information from the *SWCC* (Vanapalli, 1994).

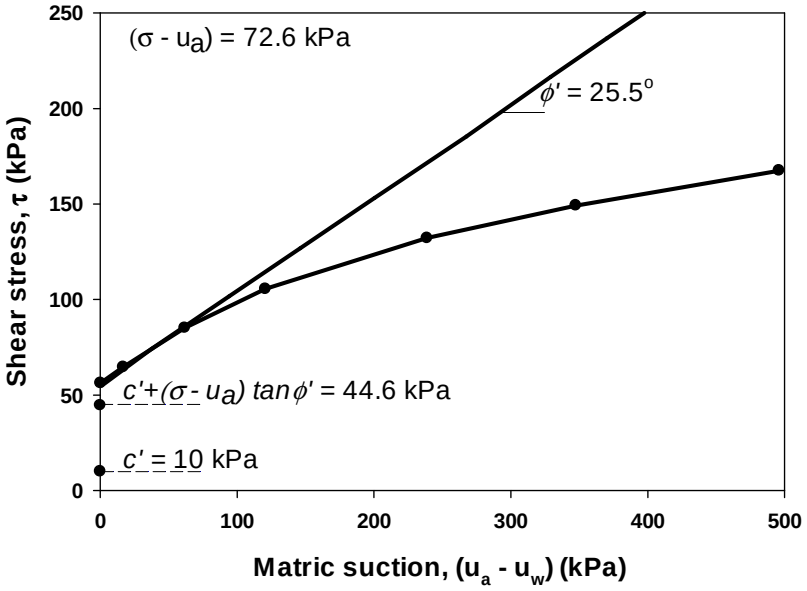

Figure 2.11 : Suction envelope and variation of ϕ^b with suction for glacial till soil sample (Fredlund et al., 1987).

Vanapalli et al. (1996) proposed two different approaches to predict the variation of shear strength with respect to matric suction using saturated shear strength parameters and the *SWCC*. The first proposed approach is given as follows:

$$\tau_{unsat} = c' + (\sigma_n - u_a)\tan\phi' + (u_a - u_w)\Theta^{\kappa}\tan\phi \qquad \textbf{(2.12)}$$

where Θ = the normalized water content which is a dimensionless parameter representing the amount of water in the soil to visualize the area of water which is in contact with the soil particles, κ = a fitting parameter which is a function of plasticity index of the studied soil to obtain a better agreement between predicted and measured shear strength data.

The normalized water content, Θ also equals to the degree of saturation, S. Thus, (2.12) can be rewritten by replacing Θ by S as (2.13). The fitting parameter, κ required can be obtained from relationship between the fitting parameter, κ and the plasticity index, I_p was presented by Vanapalli and Fredlund (2000) in Figure (2.12).

$$\tau_{unsat} = \left[c' + (\sigma_n - u_a)\tan\phi'\right] + \left[(u_a - u_w)S^{\kappa}\tan\phi'\right] \qquad \textbf{(2.13)}$$

The first part of the equation is the saturated shear strength when the pore-air pressure, u_a, is equal to the pore-water pressure, u_w. The second part of the equation is the shear strength contribution due to suction that can be derived from the *SWCC* using an appropriate value of κ.

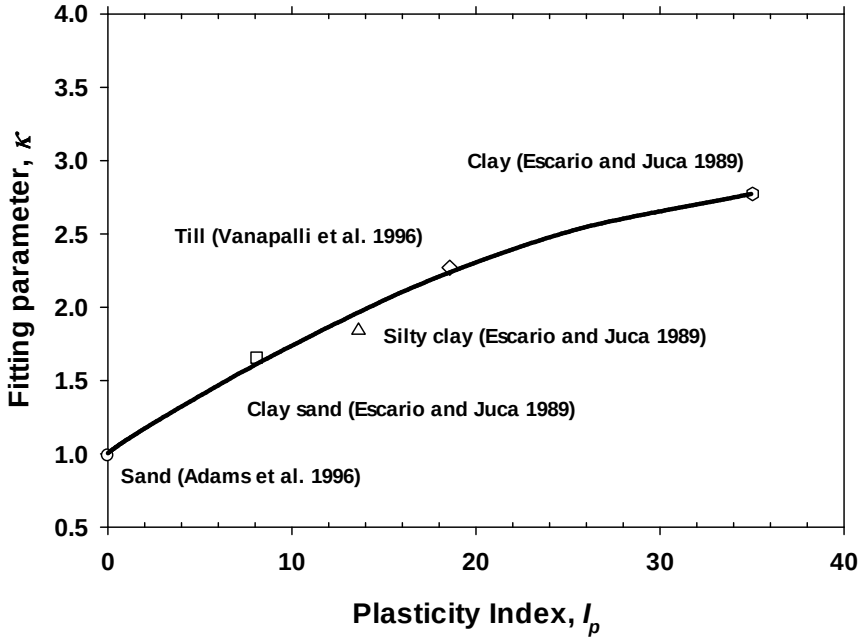

Figure 2.12 : The relationship between the fitting parameter, κ, and the plasticity index, I_p

The shear strength contribution due to suction in terms of normalized water content is mathematically expressed by Vanapalli et al. (1996) as:

$$\tau_{unsat} = (u_a - u_w)\Theta^{\kappa}\tan\phi' \qquad \textbf{(2.14)}$$

Differentiating (2.14) with respect to matric suction, $(u_a - u_w)$ gives the incremental shear strength contribution, $d\tau_{unsat}$ due to matric suction. This explains the nonlinear variation of shear strength with respect to matric suction (i.e. $tan\ \phi^b$) related to the rate of change of Θ.

$$\tan\phi^b = \frac{d\tau_{unsat}}{d(u_a - u_w)} = \frac{d((u_a - u_w)\Theta^\kappa \tan\phi')}{d(u_a - u_w)}$$

$$= d\left(u_a - u_w\right)\left[\left(\Theta^\kappa\right)(\tan\phi')\right] + (u_a - u_w)\left[d\left(\Theta^\kappa\right)(\tan\phi')\right] \quad \textbf{(2.15)}$$

$$= \left[\left(\Theta^\kappa\right) + (u_a - u_w)\frac{d\left(\Theta^\kappa\right)}{d\left(u_a - u_w\right)}\right](\tan\phi')$$

The derivation (2.15) supports the use of *SWCC* as a tool to develop a shear strength function of unsaturated soils (Vanapalli et al., 1996).

In the second proposed method, residual volumetric water content or residual degree of saturation is used as tool for predicting the matric suction contribution towards the shear strength (Vanapalli et al., 1996). The proposed equation (2.16) is given below:

$$\tau_{unsat} = \left[c' + (\sigma_n - u_a)\tan\phi'\right] + \left[(u_a - u_w)\left(\frac{(\theta - \theta_r)}{(\theta_s - \theta_r)}\tan\phi'\right)\right] \quad \textbf{(2.16)}$$

where, θ = volumetric water content at any suction, θ_s = volumetric water content at saturation, θ_r = residual volumetric water content. The volumetric water content values can be determined from the *SWCC*.

Figure 2.13 shows the relationship between the measured *SWCC* and shear strength of unsaturated soils. In the boundary effect zone, up to the *AEV* of the soil, the soil is essentially saturated and an increase in shear strength is similar to that of a saturated soil. In other words, the shear strength contribution due to suction, $\phi^b = \phi'$.

Beyond the *AEV*, as the soil begins to desaturate (i.e. transition zone), the effective area of contact between the water phase and the soil particles begins to decrease as air displaces the water within the soil pores. Consequently, further increase in matric suction is not as effective in producing an increase in the shearing resistance and hence ϕ^b contribution will be less than ϕ'.

Beyond the residual suction, the relationship between shear strength and suction is not well defined. The shear strength may increase, decrease, or remain the same depending on the soil type.

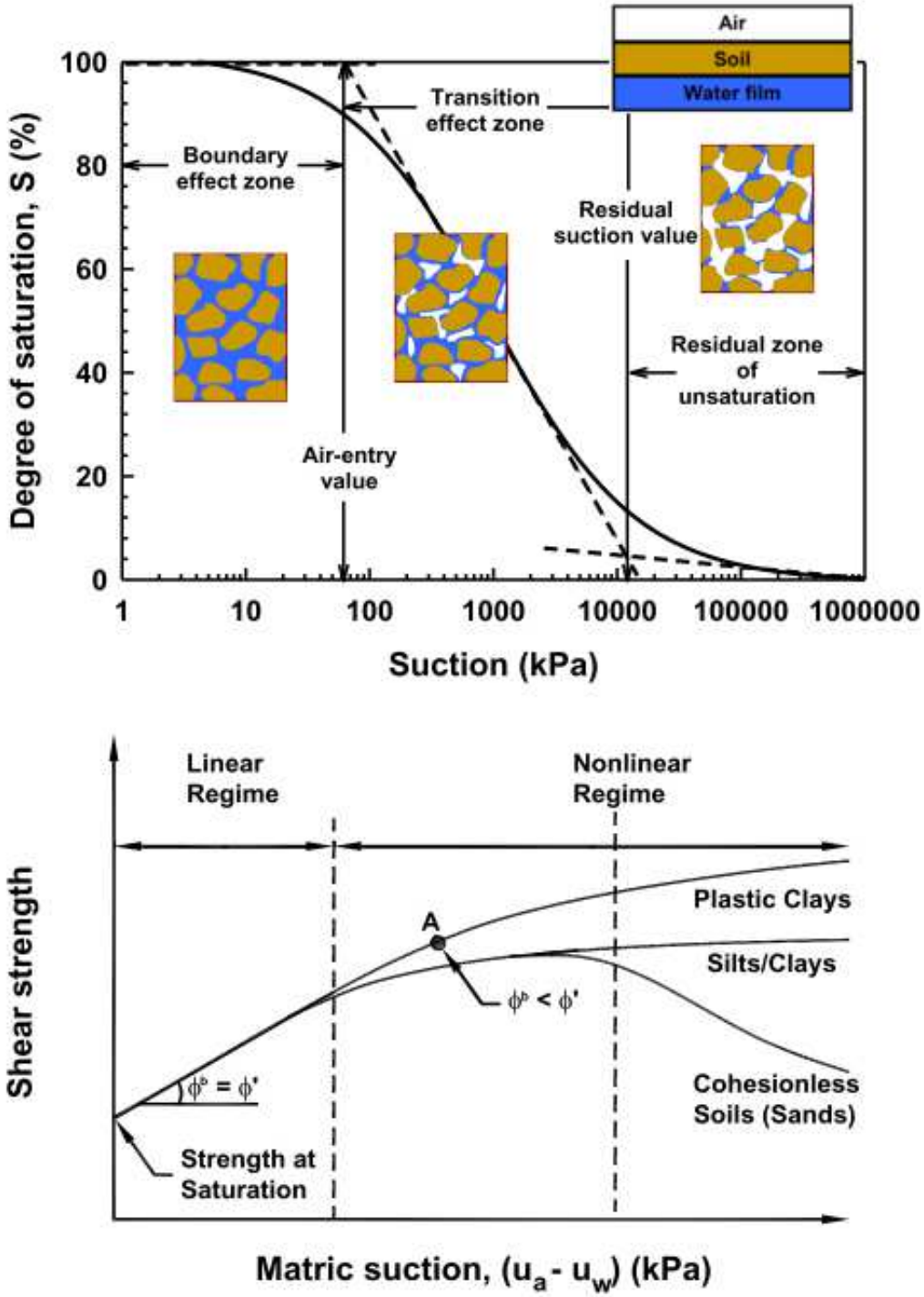

Figure 2.13 : The relationship between the *SWCC* and shear strength of unsaturated soils (Vanapalli, 2009).

2.5.4 Undrained shear strength of unsaturated soils

For saturated condition during undrained loading the deviator stress at failure, $(\sigma_1 - \sigma_3)$ remains constant regardless of the applied confining pressure. The undrained shear strength, c_u, for the soil remains constant at various confining pressures. As a

result, the unconfined compressive strength, q_u, is calculated as twice the undrained shear strength, c_u, for the saturated soil, regardless of the magnitude of the confining pressure (Figure 2.14a).

$$c_u = \frac{q_u}{2} \qquad \textbf{(2.17)}$$

However for an unsaturated soil, as the confining pressure increases, the undrained shear strength for the unsaturated soil also increases (Fig. 2.14b). Therefore, unconfined compression test results can be used for an unsaturated soil only when the total confining pressure, σ_3 is equal to zero (Fig. 2.14b). In that case, unconfined compressive strength, q_u can be approximated to the undrained shear strength; c_u (2.17). In other words, the compressive strength value may not be satisfactory in approximating the undrained shear strength, c_u, at a confining pressure greater than zero**.** (Fredlund and Rahardjo, 1993).

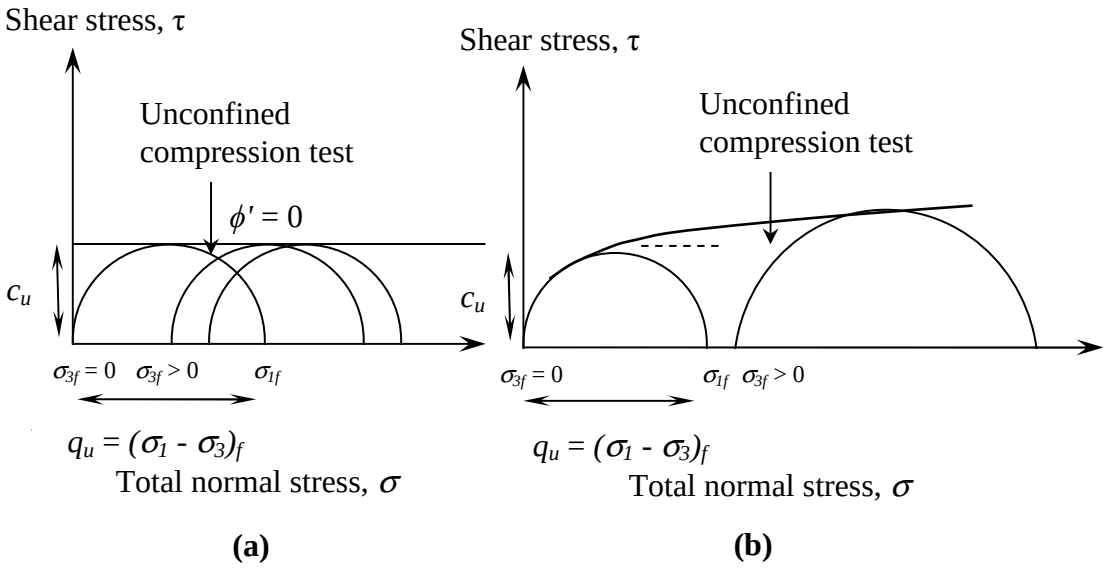

Figure 2.14 : (a) Relationship between τ and σ for a saturated soil (with negative pore-water pressures); (b) relationship between τ and σ for an unsaturated soil.

2.5.5 Prediction of unconfined shear strength of unsaturated soils using *SWCC* and saturated shear strength parameters

Oh and Vanapalli (2009) presented a model to predict the variation of shear strength of the unsaturated fine grained soils in (2.18) with respect to suction after analyzing six sets of unconfined compressive test results for various unsaturated fine grained

soils available in the literature. The model uses the unconfined compression strength test results for saturated condition and the *SWCC* along with two fitting parameters.

$$c_{u(unsat)} = c_{u(sat)}\left[1+\frac{(u_a-u_w)}{(P_a/101.3)}\left(S^{\nu}\right)/\mu\right] \qquad \textbf{(2.18)}$$

where: $c_{u(sat)}$, $c_{u(unsat)}$ =shear strength under saturated unsaturated conditions respectively, P_a = atmospheric pressure (i.e. 101.3 kPa) and υ, μ = the fitting parameters to obtain a better agreement between measured and predicted results. P_a / 101.3 = the normalization term which was used for maintaining consistency with respect to dimensions and units on both sides of the equation.

The fitting parameter, μ was found to be constant value of 9 for soils with I_p values in the range of 8% and 15.5%. The value of μ however increases linearly on semi-logarithmic scale with increasing I_p value following the given relationship in (2.19) and in Figure 2.15.

$$\begin{aligned} \mu &= 9 && \text{for } 8.0 \le I_p(\%) \le 15.5 \\ \mu &= 2.1088e^{0.0903(I_p)} && \text{for } 15.5 \le I_p(\%) \le 60.0 \end{aligned} \qquad \textbf{(2.19)}$$

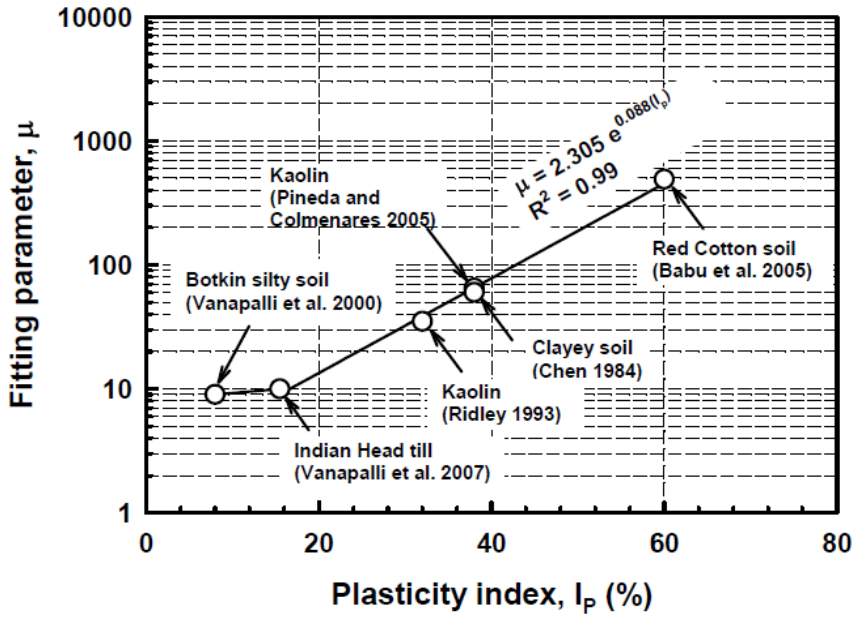

Figure 2.15 : Relationship between plasticity index, I_p and the fitting parameter, μ (Oh and Vanapalli, 2009).

2.6 Summary

Significant advances were made during the last 50 years towards better understanding the engineering behavior of unsaturated soils. These studies have contributed to develop theoretical frameworks, experimental methods and constitutive models including the numerical techniques. This chapter provides litreature review to introduce key unsaturated soil mechanics concepts and relevant background that is necessary for the proposed research. The effective stress concept, the role and meaning of suction for unsaturated soils and *SWCC* are also defined.

The focus of the research presented in this thesis is directed towards proposing tools for interpreting and estimating bearing capacity of single pile foundations. The carrying capacity of single piles in unsaturated soils is signficantly influened by the shear strength behavior. Due to this reason, literature review focus has been directed towards providing more background on shear strength of unsaturated soils both under drained and undrained loading conditions. The presented shear strength theoretical background information has been used for developing the semi-empirical modified α, β and λ methods for estimating the shaft bearing capacity of a single pile in unsaturated soil conditions. These details are summarized in Chapter 3.

3. THEORY

3.1 Introduction

Design procedures for many soil structures in conventional geotechnical engineering practice are based on theoretical methods (i.e; slope stability analysis and design of retaining walls). Acceptable theoretical methods for use in practice for the design of pile foundations however are still not available to date (Douglas, 1989; Jardine et al., 2005; Lehane et. al, 2012). Several practicing engineers believe that the load versus displacement behavior and the ultimate bearing capacity of pile can be determined with certainity only by performing in-situ load tests (Clausen, 2001). Terzaghi and Peck (1967) also stated that the "theoretical refinements in dealing with pile problems are completely out of place and can be safely ignored". Such a statement by these eminent geotechnical engineers clearly demonstrates the gaps in the measurements and the theoretical predictions of pile behavior.

Poulos (1989) in his Rankine address summarized the case study published by Douglas (1989) in the Fifth Australia–New Zealand conference on Geomechanics to highlight the differences in field studies results and computed theoretical and modeling results of several investigators. This study was an open competition of investigation inviting geotechnical engineers to predict the load-displacement behavior of two instrumented precast piles; one driven 25m depth into a clay layer underlain by very dense sand, and another pile that driven to a depth of 30.5m of dense sand layer.

Figure 3.1 summarizes the comparisons between the predicted and the actual load-displacement behavior of the longer pile which is driven to a depth of 30.5m. The results of the competition show significant differences between the estimated and measured load versus displacement behavior of a pile of many of these investigators. This study clearly highlights the limitations in the estimation of the pile performance based on theoretical studies by geotechnical engineers.

Design codes of many countries encourage testing about 1 in 10 piles on construction sites because of the limitations in the reliable estimation of pile performance from empirical, theoretical and computer modelling studies. However, in-situ pile testing in many cases is not possible due to high costs or practical limitations of the site for conducting the pile load tests. The practical and economical limitations encourage researchers proposing empirical, analytical or numerical techniques for reliable prediction of the load versus displacement behavior of piles (Lehane et al., 2012).

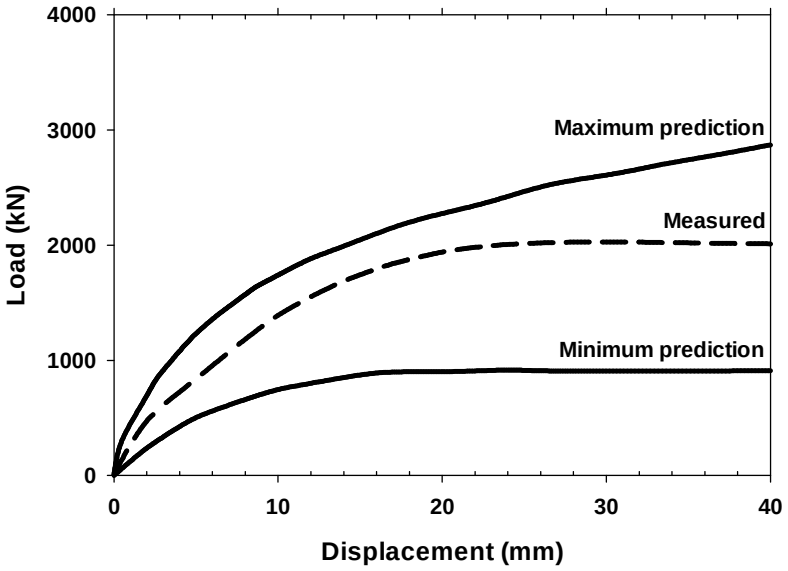

Figure 3.1 : Predicted and measured load-settlement behavior (Modified after Douglas, 1989).

The load versus displacement behavior of piles in clayey soils was studied by several investigators during the last 50 years (Tomlinson, 1957; Chandler, 1968; Vijayvergiya and Focht, 1972; Burland, 1973; Meyerhof, 1976; Kraft et al., 1981; Dennis and Olson, 1983a; Semple and Rigden, 1984; Randolph and Murphy, 1985; Azzouz, 1986; Mochtar and Edil, 1988; Sladen, 1991; Mirza, 1995; Kolk and Velde, 1996; Chow, 1996; Jardine and Chow, 1996; Mirza, 1997; Jardine et al., 2005; Gavin et al., 2010; Doherty and Gavin, 2011a; Doherty and Gavin, 2011b; Lehane et al., 2012).

Many studies were also undertaken to better understand the performance of piles in sandy soils (Robinsky and Morrison, 1964; Dennis and Olson, 1983b; Briaud and Tucker, 1989; Toolan et al., 1990; Kraft, 1991; Lehane et al., 1993; Randolph et al., 1994; Jardine and Chow, 1996; Chow et al., 1998; Lehane et al., 2004; Lehane et al.,

2005; Coop et al., 2005; Igoe, 2011). One of the key objectives of all these studies was to propose theoretical, empirical or computer-modeling procedures for estimating the ultimate load capacity of pile or the load versus settlement behavior using the in-situ pile load tests data.

In-situ tests such as standard penetration tests and cone penetration tests are commonly used for proposing indirect relationships for estimating or calculating the carrying capacity of piles in soils. These tests are typically perfomed during the dry season because of their relative ease in comparison to other seasons. The soil is typically in a state of unsaturated condition during the dry season. However, the interpretation of the test results is based on conventional soil mechanics principles assuming the soil is saturated. In other words, the influence of capillary stresses on the load versus displacement behavior of pile foundations is ignored for soils that are in a state of unsaturated condition. As discussed in the earlier chapters, the key objective of the present thesis is to propose simple procedures for engineering practice applications for reliable interpretation of the load carrying capacity of single piles considering the influence of capillary stresses (i.e. matric suction).

This chapter provides a theoretical background of conventional procedures used for estimation of the load carrying capacity of single piles in saturated soils. These procedures are modified such that they can be used taking account of the contribution of matric suction for interpreting model pile tests performed in a laboratory environment. Focus of the studies presented in the thesis is directed only to understand the shaft resistance of the single piles in both coarse and fine-grained soils.

3.2 Pile Foundations

Pile foundations are preferred in compresible soils with relatively low bearing capacity that are also susceptible to settlement problems. These foundations typically provide better solutions in comparsion to shallow foundations. Piles are also preferred as foundations for problematic soils such as expansive and collapsible soils (Prakash and Sharma, 1990). They are also commonly used as foundations where stability problems due to erosion or liquefaction potential are likely.

In many scenarios, pile foundations can carry the superstructure loads safely as an end bearing and/or friction piles. The ultimate bearing capacity of a single pile is derived from the combined contribution of the pile shaft skin friction, Q_f and the end bearing resistance, Q_p.

Several semi-empirical methods were proposed in the literature to estimate the shaft load carrying capacity of single piles. These methods are derived based on the results of a large number of field pile load tests performed in different soils. The most commonly used semi-empirical methods in geotechnical engineering practice are the α method which is based on the total stress approach, Skempton (1959), the β method extending the effective stress approach, Burland (1973) and the λ method, Vijayvergiya and Focht (1972).

3.2.1 Piles in clay

For saturated cohesive soils, the short-term bearing capacity of piles is critical because the strength of clay typically increases with respect to time due to consolidation or strength regain of disturbed soils. The most popular approach used in practice for short-term bearing capacity evaluation (i.e. to estimate the shaft capacity) for piles in saturated clays is the α method extending the total stress approach (i.e. $\phi = 0$ concept). The key parameter used in the estimation of the shaft resistance of piles is the average undrained shear strength (c_u). The other parameters that influence the short-term bearing capacity in clays are the undrained shear strength ratio (c_u / σ'_v), stress history (i.e. *OCR* effect), strain softening effect related to pile length, (L) and pile slenderness (L / D ratio).

Some recent studies question the validity of using the total stress approach in engineering practice. The need for using a transitional approach from total stress to effective stress approach is encouraged for reliable estimation of the ultimate bearing capacity of piles in clays (Mochtar and Edil, 1988).

3.2.2 Piles in sand

The effective stress approach known as the β method is commonly used for cohesionless soils to calculate the unit shaft friction mobilized at failure conditions. The mobilized shaft friction on the pile is dependent on the relative density of sand and stress level (Robinsky and Morrison, 1964; Meyerhof, 1959). The shaft

resistance of piles placed in sand can be better interpreted knowing the local shear stress along the pile shaft (Jardine et al., 2005).

Instrumented pile tests (i.e. model and in-situ tests) have been used to measure radial effective stress changes and the local shear stress developed along the pile shaft. The radial effective stress at failure, σ'_{rf}, and the interface friction angle, δ_f controls the unit shaft resistance following the Mohr-Coulomb failure criterion (Jardine et al., 2005).

3.2.3 Model pile load tests

The in-situ pile load tests provide reliable information with respect to the load versus displacement behavior. However, the high costs associated with conducting full-scale pile tests taking account of the variability of the field conditions make them impractical for conventional research studies (Al-Mhaidib, 2001). Due to this reason, model pile tests are conducted under controlled conditions in the laboratory to evaluate the effects of different parameters such as the soil type, loading history, pile material properties, shear strength and state of stress.

Table 3.1 summarizes the model pile and the test tank dimensions used to understand the load-transfer mechanism and the various parameters influencing the behavior of piles. One of the major problems associated with the pile model studies is related to the boundary and scale effects since the lateral boundaries of the testing tank can affect the stress and displacement behavior in the tested soil. Studies by several investigators have shown that the boundary effects influence will be negligible if the soil tank has a diameter of about 15 times the pile diameter in which the test is conducted (Vesic, 1977; Robinsky and Morrison, 1964; Cooke and Price, 1973; Randolph and Wroth, 1978). However, more recently, Mayoral et al. (2005) reported that the test tank-to-pile diameter ratio of 10 corresponds to an optimal testing tank size that minimizes the effect of the boundaries due to the lateral forces measured on the pile.

Table 3.1 : Dimension characteristics of model pile tests.

Reference	Test tank diameter (mm)	Model pile diameter (mm)	L/D	Test tank to pile diameter ratio
*Vesic (1963,1964)	2540	50.8 – 171.5	6-20	15-50
*Tan & Hanna (1974), Hanna & Tan (1973)	610 x 610	15.7-38	47-113	16-39
*Das et al. (1977)	457 x 610	25.4	12	23
*Chaudhuri & Symons (1983)	1100	25.4 -50	26-52	22-43
*Kerisel (1964)	6400	40-320	22-175	20-160
Robinsky & Morrison (1964)	501 x 711	20.5-37.5	25-13.5	24-13
Shin et al. (1993)	457 x 457	25.4	10-15	18
Al-Mhaidib (2001)	450	30		15
Mayoral et al. (2005)	510	51	5	10
Nanda & Patra (2011)	750	32	10-30	23.5

* adapted from Kraft et al. (1991)

3.2.4 Piles in unsaturated soils

The load bearing capacity of piles measured from in-situ load tests has been found to be typically higher in comparison to estimated values from analytical or empirical methods conventionally used in engineering practice. (Poulos, 1989; Douglas, 1989; Jardine et al., 2005). Such results can be due to the underestimation of the contribution from the shaft resistance along the length of the pile (Poulos, 1989). This behavior in part can be attributed to neglecting the contribution of matric suction and its influence on the soil-structure interface properites on load carrying capacity of piles.

The in-situ and model pile tests suggest that several parameters such as the soil compressibility, the development of initial skin friction, the loading history, the shear strength and the pile material properties influence the load carrying capacity and deformation behavior of a single pile (Law, 1982). However, there are limited studies reported in the literature that consider the influence of matric suction on the load carrying capacity of both shallow and deep foundations (Oloo et al., 1997; Douthitt et al., 1998; Georgiadis et al., 2002; Costa et al., 2003; Georgiadis et al., 2003;

Mohamed and Vanapalli, 2006; Vanapalli et al., 2007; Hamid and Miller, 2009; Hossain and Yin, 2010; Gurpersaud et al., 2013).

In the present study, modifications to the conventional α, β and λ methods are proposed to estimate the shaft bearing capacity of single piles taking account of the influence of matric suction. The modified α, β and λ methods are similar to the conventional techniques used in the design of piles in geotechnical engineering practice. There is a smooth transition between the modified and conventional methods and the proposed modified equations when the matric suction value is set to zero.

3.3 Bearing Capacity of Friction Piles: Basic Mechanisms

The load carrying capacity of a pile arises from the contribution of end and shaft resistance, irrespective of whether the pile is end bearing or friction pile (Fig. 3.1a). The shaft resistance contribution arises along the entire length of the pile-soil interface. The load transfer mechanism between the pile material and the surrounding soil has a significant influence on the ultimate carrying capacity of pile load (Vesic, 1973) (Fig.3.1b).

The shaft resistance or the skin friction is not necessarily equal to the shear strength of the soil. This can be attributed in part to the variation in the physical characteristics of the soil that arise during pile installation. In other words, the stress changes that occur in the soil during the pile installation influence the shear strength behavior of the soil (Randolph, 1985). From soil-structure interaction, the skin friction that is mobilized between the soil and the pile length can considered to be a function of the adhesion and angle of friction between pile and soil. Extending this reasoning, the shaft resistance has been suggested to have a functional relationship (3.1) as given below:

$$f_s = f\left(\sigma_v', \phi', c_u\right) \qquad \textbf{(3.1)}$$

This form of equation explains the fact that the shaft resistance can be analysed either in terms of total stresses or in terms of effective stresses considering the undrained and drained loading conditions, respectively. In total stress analysis since the drainage is not allowed, it is assumed that only the undrained shear strength is

developed along the pile shaft for fine-grained soils. On the otherhand for the effective stress analysis, the effective stresses gain significant importance since the cohesion component of shear strength is close to or equal to zero due to the remolding and softening effects along the pile shaft.

The local shear stresses at failure acting on the pile shaft, τ_f, follow the simple Coulomb failure criterion for coarse-grained soils:

$$\tau_f = \sigma'_{hf} \tan \delta_f \qquad \textbf{(3.2)}$$

where: σ'_{hf} = the horizontal (lateral, radial) effective stress acting on the shaft at failure and δ_f = the interface angle of friction. The shaft capacity can be estimated by integrating local shear stress over the external pile area. Jardine (2005) showed that in clays; as well as sands, the local shear failure is also governed by the Mohr-Coulomb effective stress interface friction law as given in (3.2).

Thus, pile-soil interface strength of the frictional capacity of a pile is primarily a function of the effective lateral pressure between the pile wall and the surrounding soil. These pressures are affected by the vertical and lateral effective stresses in the soil prior to installation and by the pile installation and loading stages. The secondary factors influencing the capacity of the pile include the soil composition, roughness of the pile and rate of loading (Bea, 1975).

Model tests have shown that the load-transfer behavior at the pile shaft takes place in a shearing zone of a thin interface zone (Fig. 3.3) which is surrounded by a soil mass that remains largely undeformed with minimum deformations and limits the shear-induced volume changes in the interface zone (Lehane and White, 2005). Change in lateral stress on the pile shaft arise from changes in volume of the shear zone and will increase with increasing level of confinement provided by the surrounding soil (Fig. 3.4).

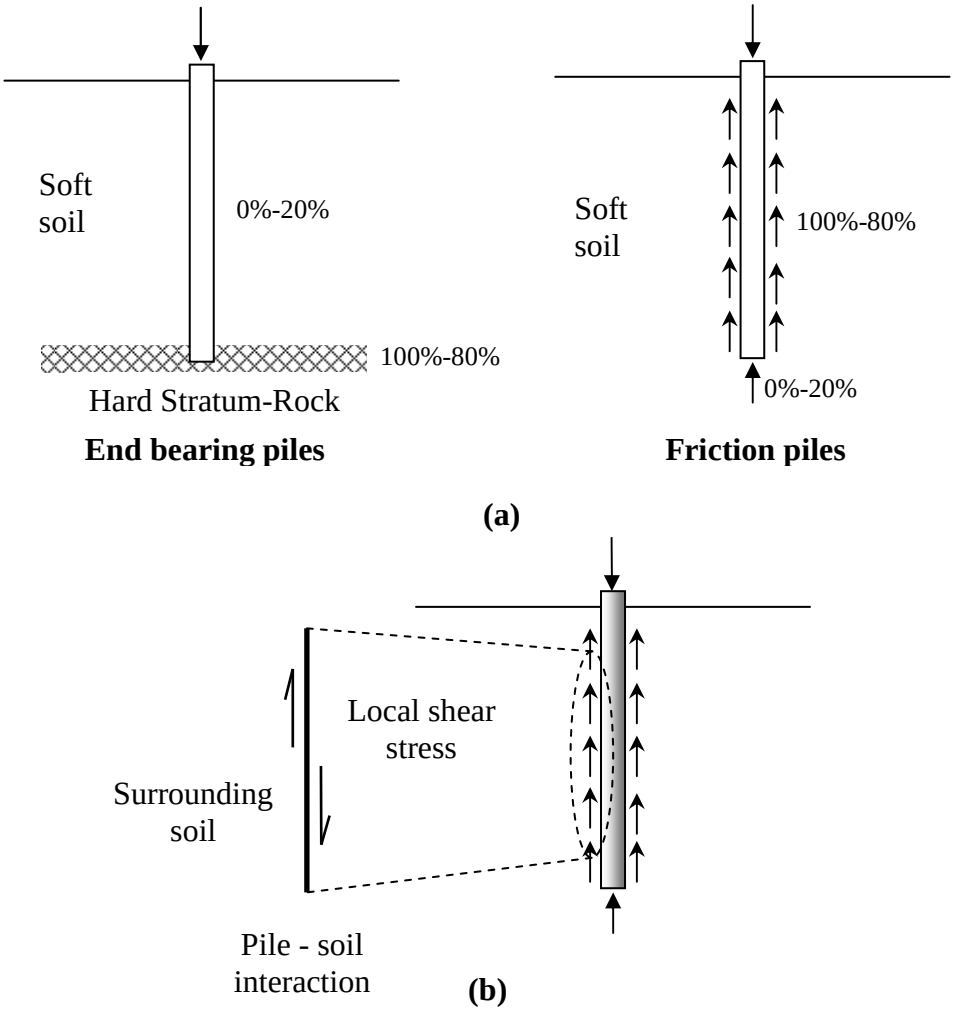

Figure 3.2 : (a) End bearing and friction piles, **(b)** Local shear stress mechanism at the soil-pile interface (modified after Vesic, 1973).

For slip to occur, a radial displacement, Δt, must develop in the thin interface shear zone in similar in magnitude to the average peak-to-trough centre-line roughness of the pile surface. This is approximately around 0.02mm for lightly rusted steel piles. This displacement induces a reactive change in the surrounding soil mass causing a radial effective stress change, $\Delta\sigma'_r$, which is inversely proportional to the radius. For piles with diameters greater than 1m the radial effective stress change, $\Delta\sigma'_r$, may contribute to the bearing capacity with less than 5%. However, it is important for medium-scale piles and can significantly dominate the behavior of small model piles (Jardine et al., 2005).

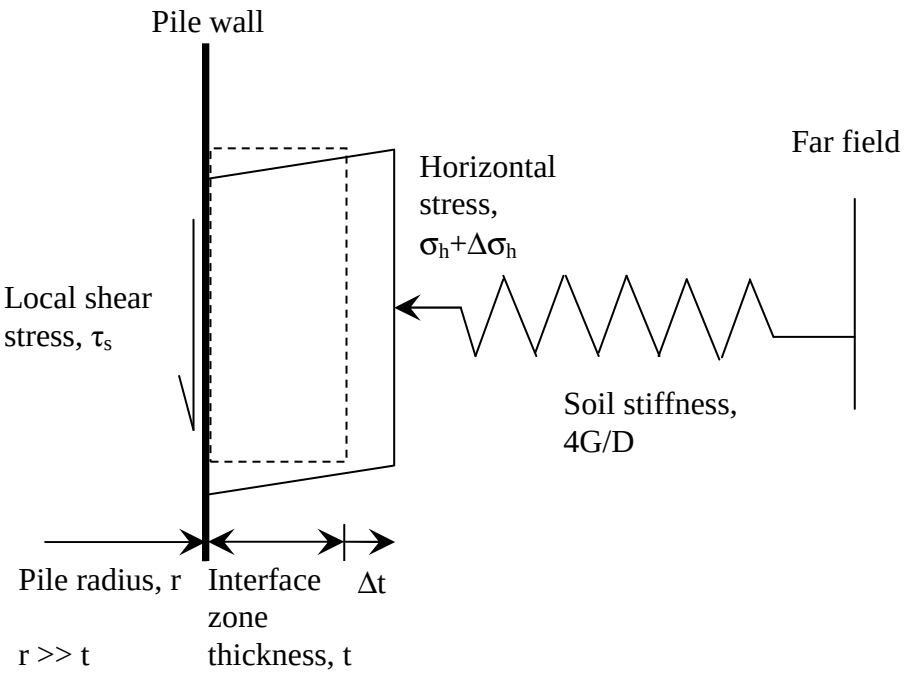

Figure 3.3 : Basic mechanism at the pile – soil interface under compression loading (modified after Lehane and White, 2005).

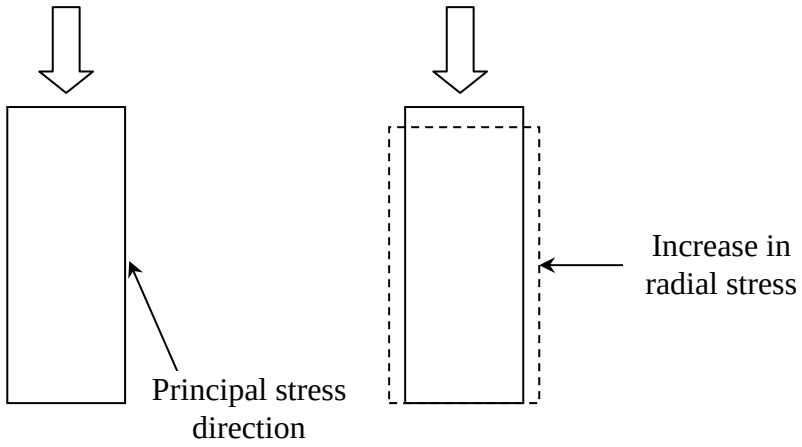

Figure 3.4 : Stresses and radial expansion during compression loading (modified after Jardine et al., 2005).

3.4 Empirical Methods for Predicting the Shaft Bearing Capacity of a Single Pile: Saturated Condition

The conventional α, β and λ methods can be summarized in dimensionless form (3.3a-c) (Randolph, 1985). This form explains the importance of understanding the influence of the parameters α, β and λ carefully such that they can be used with a greater degree of confidence in practice for estimating the load carrying capacity of single piles.

$$\alpha = \frac{\tau_s}{c_u} \tag{3.3a}$$

$$\beta = \frac{\tau_s}{\sigma'_v} \tag{3.3b}$$

$$\lambda = \frac{\tau_s}{\sigma'_v + 2c_u} \tag{3.3c}$$

3.4.1 Shaft friction in terms of effective stresses-β Method

Chandler (1968) suggested that the lateral effective stresses in the ground control the magnitude of pile shaft friction when rates of loading are slow enough to ensure drained conditions in the clay along the pile shaft. When the pile is subjected to axial loading, a relatively narrow clay zone deforms due to the simple shear around the pile shaft (Chandler, 1968; Cooke and Price, 1973; Burland, 1973). When the rate of loading is slow, drained conditions are going to be dominant along the pile shaft. The following simple relationship (3.4) can be used estimate the drained strength of the clay around the pile shaft:

$$\tau = c' + \sigma'_h \tan\phi' \tag{3.4}$$

where, τ_f = drained strength on the failure plane at failure, σ_h' = horizontal effective stress, δ = interface friction angle, c' = effective cohesion.

The expression given below for estimating the ultimate friction resistance per unit area, f_s:

$$f_s = c' + K_o \sigma'_v \tan\phi' \tag{3.5}$$

where K_o and σ'_v corresponds to the the mean values along the pile shaft.

The validity of the given equation was verified from pile test results performed in London Clay by several researchers (Skempton, 1959; Derrington, 1961; Frishmann and Flemming, 1962; Whitaker and Cooke, 1966; Burland et al., 1966).

However, it was observed that this method gives an overestimated shaft friction results for bored piles in London clay. The effect of softening due to remoulding and change in effective stress parameters were studied afterwards and it was concluded that the cohesion term is reduced to zero while effective internal friction angle ϕ' is not affected remarkably. Thus, (3.5) takes the following form (3.6) for shaft friction in normally consolidated clays:

$$f_s = K_o \sigma_v' \tan\phi' \qquad \textbf{(3.6)}$$

In 1973, Burland presented an approach for calculating the shaft resistance of piles in clay extending the simple effective stress principle based on the following assumptions:

(i) Excess pore pressures are considered to be completely dissipated before loading.

(ii) Drained conditions are available during loading due to the thin layer of disturbed zone,

(iii) Effective cohesion is negligible due to the remolding effect during pile installation regardless of the pile type.

In the light of the above discussion, shaft friction along a pile, f_s at any point including the soil-structure interface angle, δ is given by (3.7):

$$f_s = K_o \sigma_v' \tan\delta' \qquad \textbf{(3.7)}$$

The given equation can be expressed in nondimensional form using an empirical factor, β proposed by Burland (1973) as follows in (3.8):

$$\beta = \frac{f_s}{\sigma_v'} = K_o \tan\delta' \qquad \textbf{(3.8)}$$

where β = Bjerrum-Burland coefficient, it can be clearly seen that β is a function of earth pressure coefficient K_o and effective angle of friction between the soil and the pile shaft, δ.

Burland (1973) had extended the given relationship for estimating the local peak shaft friction as given in (3.9). This approach assumes a linear relationship between the shaft resistance at static failure and the initial effective overburden pressure, $\sigma_v^{'}$.

$$Q_f = f_s \times A_s = \sum_{i=1}^{i=n} K_i(\sigma_v') \tan\delta'(\pi dL) \qquad \textbf{(3.9)}$$

where $\beta = K_o \tan\delta$

$$f_s = \beta\sigma_z^{'}$$

$$Q_f = f_s \times A_s = \sum_{i=1}^{i=n} \beta(\sigma_v')(\pi dL) \qquad \textbf{(3.10a)}$$

Assuming a linearly increase in stress distribution along the pile shaft, the average vertical stress along the pile is $\sigma_z{'} = \frac{\gamma' L}{2}$, in which γ' is the effective unit weight of the soil. Therefore, (3.10a) can be rewritten in the following form as given in (3.10b):

$$Q_f = \sum_{i=1}^{i=n} \left(\beta \sigma_z^{'}\right)(\pi\, d\, L) = \sum_{i=1}^{i=n} \beta \left(\frac{\gamma' L}{2}\right)(\pi\, d\, L) \qquad \textbf{(3.10b)}$$

The shaft resistance is approximately proportional to depth if β is assumed to be constant value (Fig.3.5a). The pile test results compiled by Burland (1973) based on a wide variety of clays shows a remarkably small scatter (Fig.3.5a) giving a mean value of 0.3 for the β parameter for normally consolidated clays.

Murphy (1985) and later Burland (1993) also considered the stress history of clays and interpreted the relationship between β and undrained shear strength ratio, $c_u / \sigma_v^{'}$. It has been shown that β value increases with an increase in the $c_u / \sigma_v^{'}$ (Figure 3.5b). In other words, β value is lower for lightly consolidated or normally consolidated clays than the values for over consolidated clays. Burland (1973) and Meyerhof (1976) suggested the correlation as: $\beta = (1 - \sin\phi')\tan\phi'(OCR)^{0.5}$ in order to include the effect of overconsolidation ratio into the calculations.

For sands, β values were estimated according to suggestions made by McClelland (1974), Meyerhof (1976), and API (1984) using the internal friction angle of sand, ϕ', and the soil/steel friction angle, δ. For driven piles in sand McClelland (1974) suggested β values of 0.15 to 0.35 for compression and 0.10 to 0.24 for tension shaft

resistance of driven piles in sand. Meyerhof (1976) proposed β values of 0.44 to 1.20 for soils with a friction angle, ϕ' in the range of 28^o to 37^o. API (1984) recommended the correlation of $\beta = 0.7 \tan(\phi' - 5^o)$. Briaud and Tucker (1997) estimated β values from the relative embedment of the pile and the frictional resistance of the soil/pile interface and the type of pile installation. For bored piles in sand Meyerhof (1976) proposed β values of 0.1 to 0.35 for soils with a friction angle ϕ' in the range of 33^o to 37^o.

The shaft friction depends on the compressibility of the soil, the original horizontal stress in the ground and on pile type and shape. However, the changes in lateral earth pressure coefficient, K_i and in the interface characteristics, $\tan\delta$ along the pile shaft are generally not known after the pile installation. The appropriate β values therefore can be determined by back-calculations from pile load test results if effective stress conditions along the soil/pile interface are known.

3.4.2 Total stress analysis- α Method

Effective stress approach can be used for all soil types (i.e. for sands and clays), whereas the total stress approach is used for piles in saturated clays considering the critical short-term design parameters (i.e. $\phi = 0$ concept). Total stress approach is an empirical method based on simple in-situ and laboratory tests with correlations. The adhesion that arises between the pile and soil, c_a plays a prominent role in the calculation of the shaft resistance of piles in clays carried out in terms of total stresses. Several national foundation design codes and other studies suggest estimating c_a reducing the undrained cohesion c_u by a coefficient that is equal to α. The α coefficient represents a fraction of c_u mobilized by the pile-soil adhesion mechanism. The coefficient, α that is named as the adhesion factor is conventionally considered to be an empirical parameter.

Sladen (1991) however has shown that the adhesion factor, α has a theoretical basis to explain the stress transfer mechanism of load transfer in saturated clays along the soil and pile interface. It is suggested that both the effective and the total stresses at the pile soil interface is influenced by the same factors.

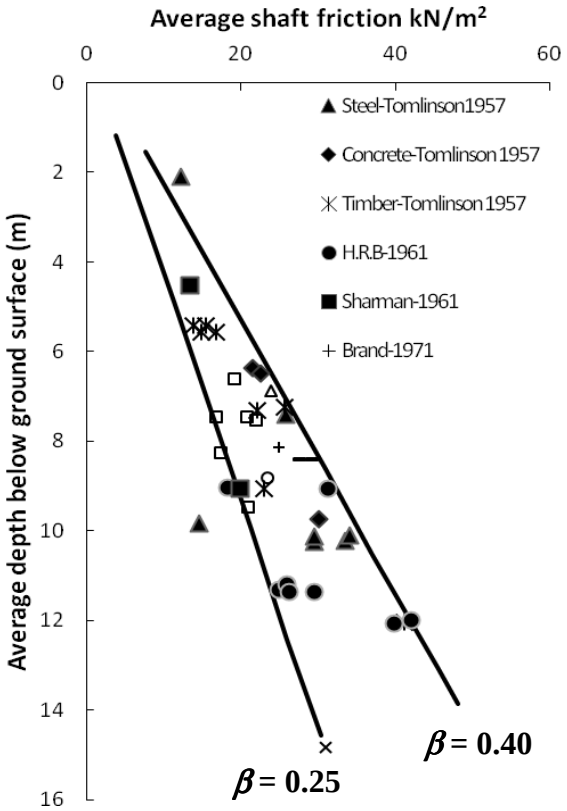

(a)

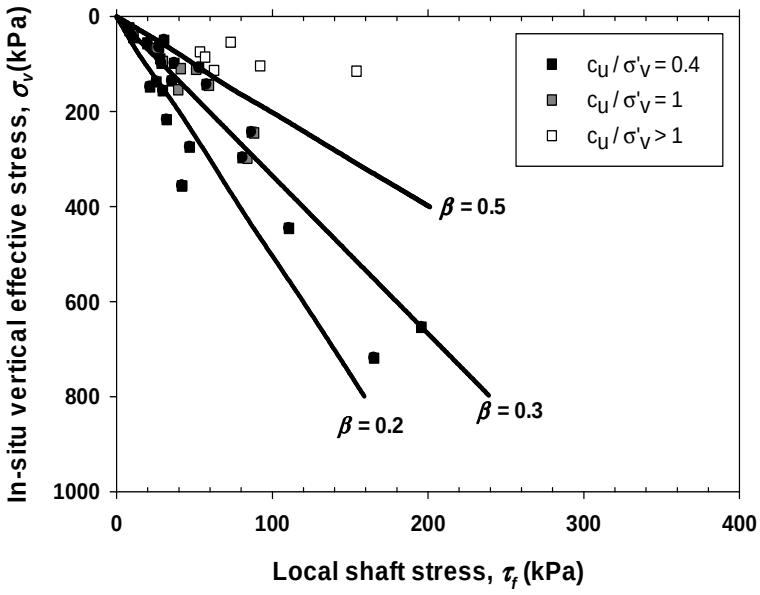

(b)

Figure 3.5 : (a) Relationship between average shaft friction and average depth for driven piles placed in clay (modified after Burland, 1973) **(b)** Variation in β parameter for different undrained shear strength ratios (modified after Doherty and Gavin, 2011).

The mobilized interface strength (i.e. the total stress) can be explained using the undrained shear strength as a tool because the horizontal effective stress at the interface can be related to undrained shear strength (Sladen, 1991). The shaft bearing capacity of piles in clay can be estimated in terms of total stresses using the simple correlation shown in (3.11).

$$f_s = c_a$$

$$c_a = \alpha c_u \qquad \textbf{(3.11)}$$

$$Q_f = f_s \times A_s = \sum_{i=1}^{i=n} \alpha c_u \pi dL$$

where c_a = the average adhesion between the clay and the pile shaft, A_s = the area of the pile shaft in the clay, α = adhesion factor, c_u = undrained shear strength, d = pile diameter, L = pile length. The adhesion, c_a is related to the average undisturbed shear strength of clay, c_u within the depth of penetration of the pile in clay.

The above relation states that the shaft resistance is directly proportional to the undrained shear strength for assessing the short term carrying capacity but is not equal to it mainly because of the effects of disturbance during installation.

Since the early studies by Tomlinson (1957), Skempton (1959), Semple and Ridgen (1984) and Fleming et al. (1985), it became apparent that the backcalculated values of α from load tests reduce with increasing shear strength, c_u which was also understood to depend on the sample quality and the test method.

The evaluation of α was also carried out using series of equations and by design charts as a function of undrained shear strength, c_u by Kerisel (1965), Tomlinson (1957), Woodward and Boitano (1961), Peck (1958), Dennis and Olson (1983), API (1974), Sowers and Sowers (1979) and McCarthy (1977) in Figure 3.6. All the studies show that the adhesion parameter α, decreases with increasing soil undrained shear strength from close to unity to about 0.3 for undrained shear strength higher than 150 kPa.

In order to simulate the complete stress history of a soil element adjacent to a pile, including the over consolidation and pile installation, the adhesion factor is defined as a function of vertical effective stress and undrained shear strength known as the

undrained shear strength ratio, (c_u/σ'_v). The theoretical derivation of the adhesion factor shows that α is the function of over consolidation ratio *(OCR)*, vertical effective stress (σ'_v), lateral earth pressure coefficient at rest (K_o), swelling (C_s) and compression (C_c) indices, installation factor *(k)* and the interface friction angle (δ) (Sladen, 1991). All these parameters may be related to each other by means of the undrained shear strength ratio (c_u/σ'_v).

Several investigators; Semple and Rigden (1984), Randolph and Murphy (1985), API (1987) and Sladen (1991) over the years proposed formulations to define the adhesion factor, α as a function of undrained strength ratio, (c_u / σ'_v) given in Figure 3.7 and in Table 3.2.

3.4.3 λ method

A method that is referred to as the λ method for calculating the shaft capacity of piles driven into clay has been suggested by Vijayvergiya and Focht (1972) using the *API* database. The conventional λ method combines the total (i.e. undrained) and effective (i.e. drained) stress approaches. This method draws together existing total and effective stress approaches for calculating pile capacity, in a manner, which reduces the sensitivity of the calculation to the measured shear strength of the soil, Vijayvergiya and Focht (1977) using the total and effective stress analysis. The total shaft capacity is calculated using the equation (3.12).

$$f_{s(avg)} = \lambda(\sigma'_{v(avg)} + 2c_u) \qquad \textbf{(3.12)}$$

where $\sigma'_{v(avg)}$ = the mean effective stress along the pile shaft, c_u = undrained shear strength along the pile length, λ = frictional capacity coefficient which is a function of entire embedded depth of pile.

Table 3.2 : Shaft resistance determination from laboratory strength data (modified after Poulos, 1989).

Soil type	Relation	Remarks	Reference
Clay	$f_s = \alpha c_u$	α = 0.45 (London clay)	Skempton (1959)
		$\alpha = 1.0$ ($c_u \leq 25$kPa) $\alpha = 0.5$ ($c_u \leq 70$kPa)	API (1984)
		$\alpha = 1.0$ ($c_u \leq 35$kPa) $\alpha = 0.5$ ($c_u \leq 80$kPa)	Semple & Rigden (1984)
		$\alpha = \left(\frac{c_u}{\sigma'_v}\right)^{0.5}\left(\frac{c_u}{\sigma'_v}\right)^{-0.5}$ for $\left(\frac{c_u}{\sigma'_v}\right) \leq 1$ $\alpha = \left(\frac{c_u}{\sigma'_v}\right)^{0.5}\left(\frac{c_u}{\sigma'_v}\right)^{-0.25}$ for $\left(\frac{c_u}{\sigma'_v}\right) \geq 1$	Fleming et al. (1985)
		$\alpha = 0.5\left(\frac{c_u}{\sigma'_v}\right)^{-0.5}$ for $\left(\frac{c_u}{\sigma'_v}\right) \leq 1$ $\alpha = 0.5\left(\frac{c_u}{\sigma'_v}\right)^{-0.25}$ for $\left(\frac{c_u}{\sigma'_v}\right) > 1$	Randolph & Murphy (1985)
		$\alpha = 0.5\left(\frac{c_u}{\sigma'_v}\right)^{-0.45}$	Sladen (1991)
		$\alpha = 0.5\psi^{-0.5}$ if $\psi \leq 1$ $\alpha = 0.5\psi^{-0.25}$ if $\psi > 1$ where $\psi = c_u/\sigma'_v$ and σ'_v = vertical effective stress	API (2000)

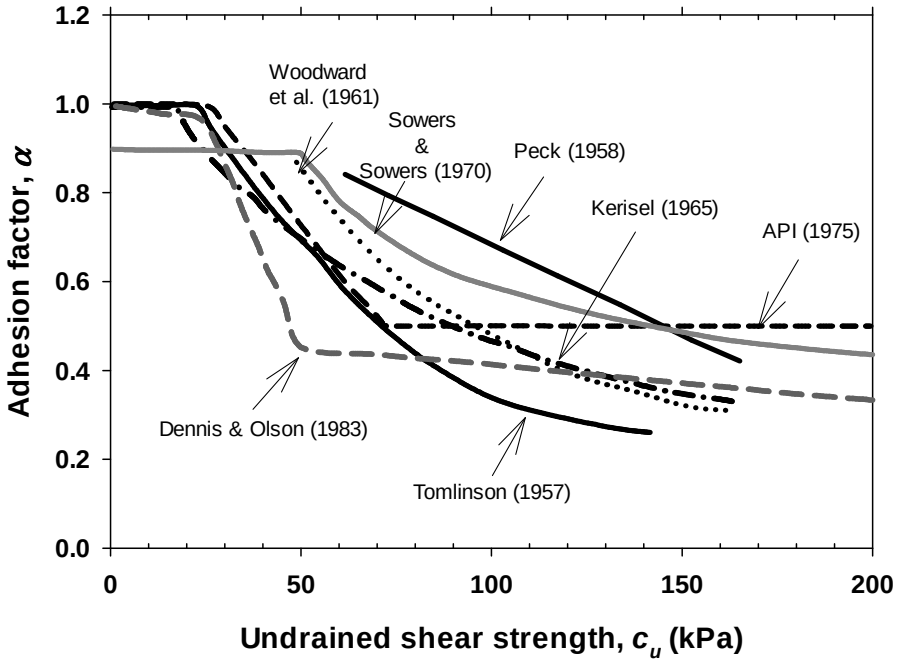

Figure 3.6 : Trends for the adhesion factor recommended by various authors (modified after Sladen, 1992).

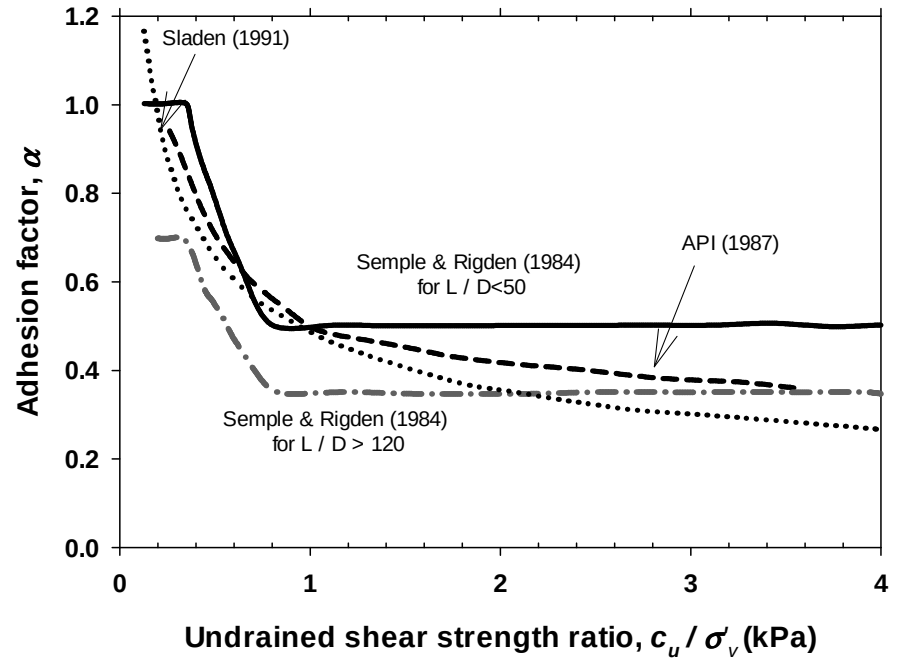

Figure 3.7 : Variation of α with undrained shear strength ratio (Dohert and Gavin, 2011).

The λ value varies from 0.12 to 0.5 for pile penetration of 0 to 70 m for the 42 piles load test data gathered and presented by Vijayvergiya and Focht (1972). The λ value is a function of pile length which can be determined from Figure 3.8 for estimating the load capacity of piles in-situ. The research data analysed Vijayvergiya and Focht

(1972) is revisited and plotted differently as a relationship between the λ and the ratio of pile diameter, d to pile penetration depth, L (Figure 3.9). A best-fit linear curve is plotted through the data which exhibits some scatter.

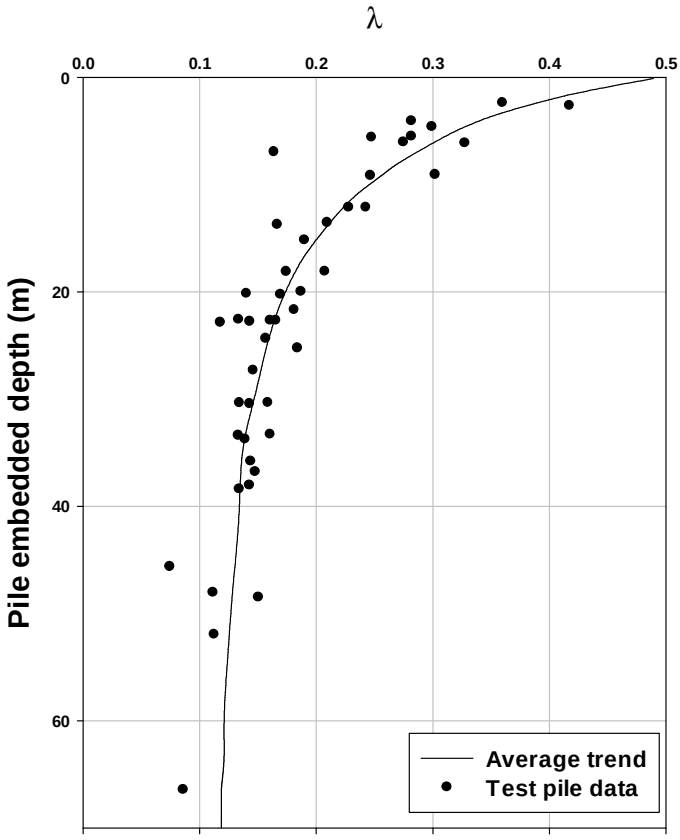

Figure 3.8 : Frictional capacity coefficient, λ vs. pile penetration, L (modified after Vijayvergiya and Focht, 1972).

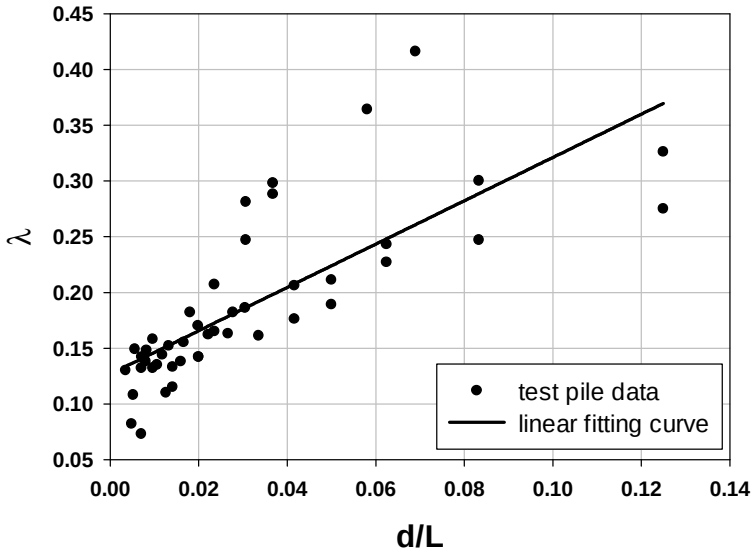

Figure 3.9 : Relationship between the variation of λ coefficient and the ratio betwee pile diameter, d to pile penetration, L (data from Vijayvergiya and Focht, 1972).

3.5 Extending the Unsaturated Shear Strength Equation for Predicting the Shaft Bearing Capacity of Single Pile in Unsaturated Soils

3.5.1 Modified β method-effective stress analysis

In the case of unsaturated conditions, a general expression for estimating the shaft resistance of piles in unsaturated sands $Q_{f(us)}$ with the contribution of matric suction can be expressed as shown in (3.13):

$$Q_{f(us)} = Q_f + Q_{(u_a - u_w)} \tag{3.13}$$

The contribution of ultimate shaft resistance due to matric suction $Q_{(ua\text{-}uw)}$ can be determined by extending the equation for predicting shear strength of unsaturated soils in (3.14) proposed by Vanapalli et al. (1996) and Fredlund et al. (1996) using the *SWCC* and the effective shear strength parameters.

$$\tau = \left[c' + (\sigma_n - u_a)\tan\phi'\right] + \left[(u_a - u_w)(S)^{\kappa}(\tan\phi')\right] \tag{3.14}$$

where, c' = effective cohesion, ϕ' = angle of internal friction , κ = fitting parameter used for obtaining a best-fit between the measured and predicted values, and S = degree of saturation.

The second part of (3.14) constitutes the shear strength contribution due to matric suction as:

$$\tau_{us} = \left[(u_a - u_w)(S)^{\kappa}(\tan\phi')\right] \tag{3.15}$$

Extending the same philosophy, the contribution of ultimate shaft resistance due to matric suction, $Q_{(ua\text{-}uw)}$ along the pile and soil interface can be estimated since the shaft resistance is explained by the shear strength theory (Hamid and Miller, 2009). The shaft capacity then will be equal to τ_{us} times the surface area of the pile, A_s.

$$Q_{(u_a - u_w)} = \tau_{us} \times A_s \tag{3.16}$$

Thus, a general expression for estimating shaft resistance of piles for unsaturated conditions can be obtained by substituting (3.15) and (3.16) in (3.13) as given below:

$$Q_{f_{us}} = Q_f + Q_{(u_a - u_w)} = \beta\left(\frac{\gamma L}{2}\right)(\pi\, d\, L) + \left[(u_a - u_w)(S)^{\kappa}(\tan\delta')\right]\pi dL \tag{3.17}$$

In the above equation, the fitting parameter κ is provided from the relationships studied by Vanapalli and Fredlund (2000). Furthermore, in order to determine the shaft resistance of a single pile by using (3.17), matric suction, $(u_a - u_w)$, along the pile shaft or the average matric suction value, $(u_a - u_w)_{avg}$ and the corresponding degree of saturation, S must be known.

3.5.2 Modified α method-total stress analysis

Vanapalli et al. (2007), presented a technique for determination of undrained shear strength for unsaturated soils as the summation of two components as undrained shear strength for fully saturated condition and the shear strength contribution due to matric suction (3.18).

$$c_{u(unsat)} = c_{u(sat)} + (u_a - u_w)\tan\phi^b \qquad \textbf{(3.18)}$$

where, ϕ^b = the angle of internal friction with respect to matric suction.

Oh et al. (2009) proposed a model to estimate the undrained shear strength under unsaturated condition based on the unconfined compression test results for saturated condition and the *SWCC* along with two fitting parameters as given in (3.19).

$$c_{u(unsat)} = c_{u(sat)}\left[1+\frac{(u_a-u_w)}{(P_a/101.3)}\left(S^{\upsilon}\right)/\mu\right] \qquad \textbf{(3.19)}$$

where $c_{u(sat)}$, $c_{u(unsat)}$ = shear strength under saturated and unsaturated conditions respectively, υ, μ = fitting parameters which are the function of plasticity index, I_p. The term $(P_a/101.3)$ is used to maintain consistency with respect to the dimensions and units on both sides of the equation.

Thus, a general expression (3.20) for estimating shaft resistance of piles for unsaturated conditions for total stress analysis can be obtained by substituting (3.19) in (3.11) as given below:

$$Q_{f(us)} = \alpha c_{u(sat)}\left[1+\frac{(u_a-u_w)}{(P_a/101.3)}S^{\upsilon}/\mu\right]\pi dL \qquad \textbf{(3.20)}$$

3.5.3 Modified λ method

The conventional λ method modified to propose (3.21) including the influence of matric suction in the estimation of shaft resistance of piles in unsaturated soil condition by substituting (3.19) in (3.12) as given below:

$$Q_{f(us)} = \lambda\left[\sigma'_v + 2c_{u(sat)}\left(1+\frac{(u_a-u_w)}{(P_a/100)}S^{\upsilon}/\mu\right)\right]\pi dL \qquad \textbf{(3.21)}$$

where σ'_v = the mean effective stress for entire embedded length and λ = the coefficient which depends on entire embedded depth of the pile.

The form of this equation will be same as the conventional λ method once the matric suction, $(u_a - u_w)$ component is set to zero.(3.21) can also be used to predict the variation of total shaft resistance of pile, $Q_{f(us)}$ with respect to matric suction. The required information using this equation are the undrained shear strength under saturated condition, $c_{u(sat)}$ and the *SWCC.*

3.6 Summary

Several semi-empirical methods were proposed in the literature to estimate the shaft load carrying capacity of single piles. The most commonly used semi-empirical methods in geotechnical engineering practice extending the mechanics of saturated soils are the α Skempton (1959), the β, Burland (1973) and Meyerhof (1976) and the λ, Vijayvergiya and Focht (1972) methods. These methods were derived based on the results of a large number of field pile load tests performed in different soils.

However, the predicted load bearing capacities by using the developed analytical/semi-empirical methods show differences from the bearing capacities measured by the in-situ load tests which is mainly due to the underestimation of the shaft resistance. This is because the in-situ pile load test results are commonly interpreted without taking account of the influence of matric suction although the pile load tests are commonly performed on the soils that are in a state of unsaturated condition during the dry season.

In the present study, the modification to these methods are proposed to estimate the variation of ultimate shaft capacity of single piles with respect to matric suction using the *SWCC* and the conventional shear strength parameters. There is a smooth

transition between the modified and conventional α, β and λ methods once the matric suction is set to zero. The main objective of the proposed modified methods is to implement the unsaturated soil mechanics into conventional geotechnical practice by introducing simple and reliable techniques.

4. ESTIMATION OF THE SHAFT BEARING CAPACITY OF MODEL TEST PILES IN NON-PLASTIC UNSATURATED SOILS

4.1 Introduction

This chapter provides details of a technique to estimate the contribution of matric suction towards the shaft bearing capacity of single piles in compacted unsaturated coarse-grained soils. This technique is proposed using the results of test program performed on a series of model test piles in two different sands. The key objectives of the study summarized in this chapter include:

- To assess the carrying capacity of single piles under tension and compression loading conditions.
- To evaluate the relationship between the *SWCC* and the shaft bearing capacity of a single pile.
- To develop a simple technique to estimate the the shaft bearing capacity of a single pile by using the *SWCC* and the saturated shear strength parameters.

Some experiments presented in this chapter on model pile testing were originally intitated under the supervision of Prof. Eigenbrod and Prof. Vanapalli at Lakehead University. This research was continued and supervised by Prof. Vanapalli, after Prof. Eigenbrod passed away. Further investigations were undertaken at the University of Ottawa and supplemented in the present study to interpret and estimate the shaft resistance of test (model) piles in two different sands under saturated and unsaturated conditions under the supervison of Prof. Vanapalli. In addition to model pile load tests, other tests that include CPT and determination of the shear strength behavior of the soil and the soil/steel interfaces were performed along with the measurement of total stresses, pore water pressures, and matric suction.

The test results show that the shaft resistance of piles increases both in compression and tension due to the contribution of matric suction. The conventional β method originally proposed by Burland (1973) is modified to include the contribution of

matric suction and used for interpretation of bearing capacity of single piles tested in unsaturated soils.

4.2 Model Pile Testing Program: Equipment and Methodology

A specially designed test tank was used in the research program for vertical loading of the model pile in compacted coarse grained soil. Model pile load tests were performed for compression and tension loadings under saturated and unsaturated soil conditions. All the required data related to the soil properties, shear strength parameters, *SWCC* and suction measurements were also collected during the testing program for interpretation of the model pile test results using the modified β method.

4.2.1 Soil properties and equipment details

The test tank used for conducting the model pile tests has the dimensions of 2200 mm in width, 4400 mm in length and 2500 mm in height. This was divided into two smaller units as A and B by a timber lagging at the centre of the tank length. The soil sample was placed in tank A. Tank B was initially left empty and is used to add and remove water for saturation and desaturation process of the compacted soil in tank A. The capillary stresses of the compacted soil in tank A can be controlled by changing the height of the water in tank B (Figures 4.1 and 4.2).

Soil # 1 is well graded silty sand and Soil #2 is poorly graded commercially available washed concrete sand. The soil was placed in the test tank A in layers of 150 mm thickness and compacted with a vibratory plate compactor. The compaction process was consistent for all the layers in the test box and an average dry density of 104% and 100% of the optimum was achieved respectively for silty sand and clean sand. The density of the compacted soils was checked during placement using a nuclear densometer and sand cone. The compaction curves for both soils (Soil #1 and Soil # 2) are shown in Figure 4.3. Table 4.1 summarizes the properties of the soils used in the test program.

Table 4.1 : Properties of the tested soils.

Property	Soil #1	Soil #2
Sand (%)	58	100
Silt (%)	42	-
Clay (%)	-	-
Soil friction angle, ϕ'(°)	40	40
Effective cohesion, c'(°)	0	0
Soil-steel interface friction (δ')	36/28	24/22
Optimum water content, w_{opt} (%)	12.50	12.20
Maximum dry unit weight, $\gamma_{dry\text{-}max}$, (kN/m^3)	18.70	18.95
Total unit weight γ_{total}, (kN/m^3)	21.00	19.70
Saturated unit weight, γ_{sat} (kN/m^3)	22.00	21.50
Placed water content, w (%)	8.50	6.50
Placed dry unit weight, γ(kN/m^3)	19.40	18.90
Degree of compaction, (%)	104	100

4.2.2 Instrumentation

The applied force and the displacement on the model pile were recorded during the test through a data acquisition system *(DAS)*. Tensiometers, pressure cells and a vibrating wire piezometer were used to collect data during testing. Commercially available jet fill-type tensiometers were installed at three levels in the soil at 300 mm, 600 mm and 1200 mm below the ground surface (Figure 4.1) to quickly and reliably measure the matric suction in the range of 0 to 90 kPa. Total pressure cells were installed at four different elevations along the tank wall**.** A vibrating wire piezometer was placed in the tested soil with the tip located at 1067 mm below the ground surface to measure pore water pressures in the soil during the fluctuations of water levels.

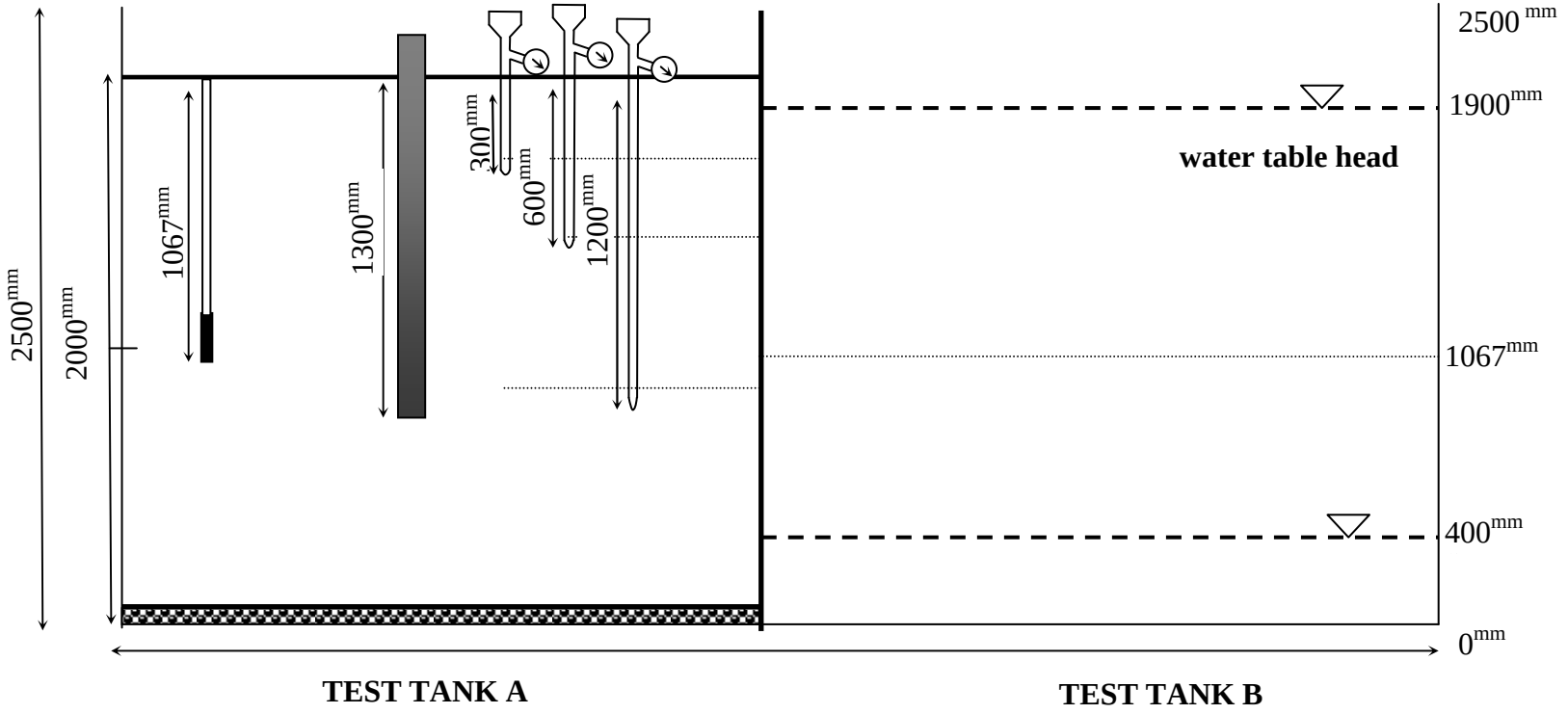

Figure 4.1 : Schematic cross section view of the geotechnical test tank.

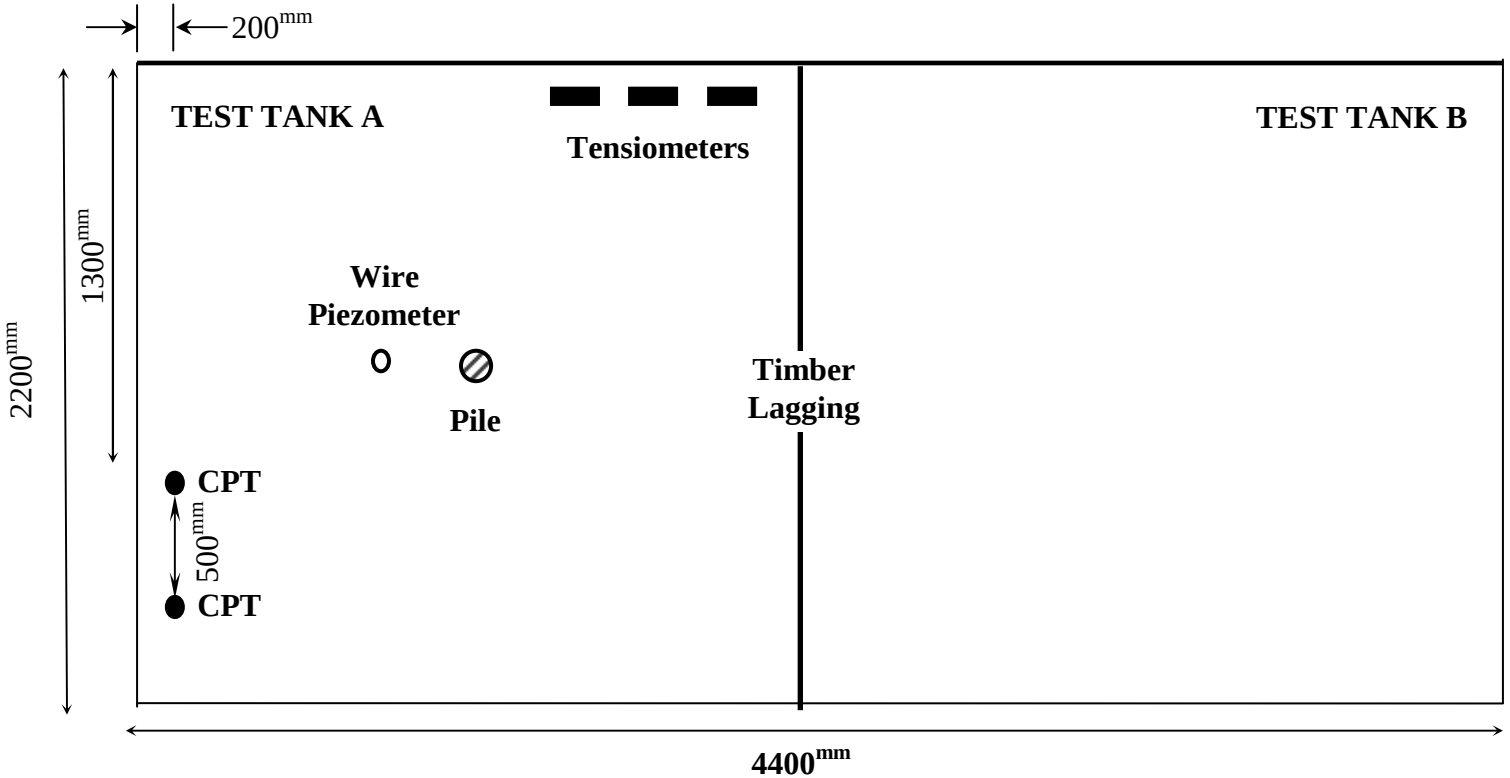

Figure 4.2 : Schematic plan view of the geotechnical test tank.

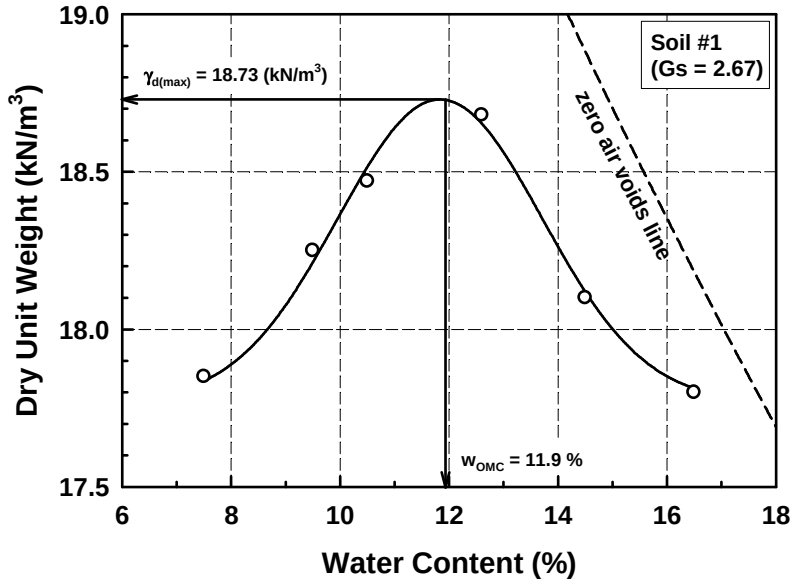

(a)

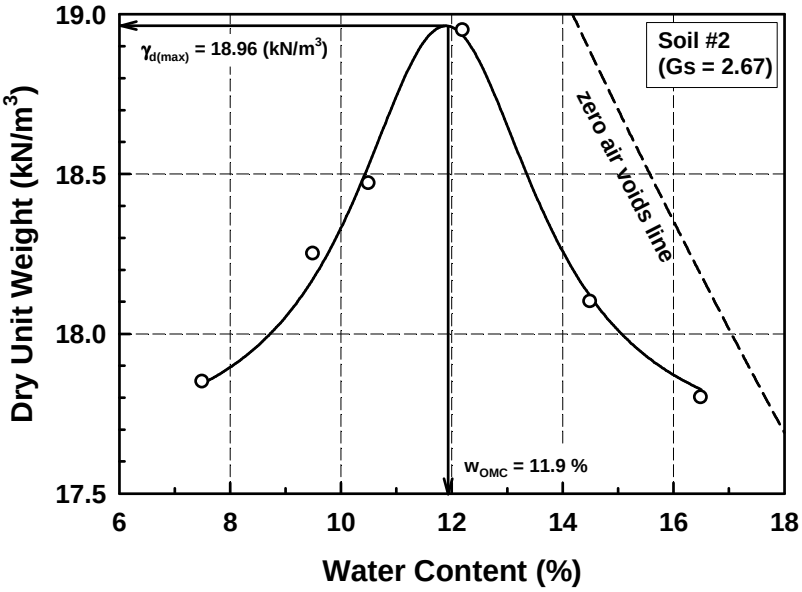

(b)

Figure 4.3 : Compaction curves for (a) Soil #1 and for (b) Soil #2.

4.2.3 Pile properties and installation

Blank stainless steel and coated mild steel open end pipe piles of 65 mm outer diameters were jacked to an embedment depth of 1300 mm from the ground surface (Figure 4.1). The piles were not instrumented. In the following section, only the results from the stainless steel pile will be presented as the mild steel pile experienced corrosion along the shaft in spite of the protective coating, which resulted in an uncontrollable change of interface characteristics.

A load frame with 10 ton capacity was used for pile installation and testing. Figure 4.4 shows the test setup for the loading of the piles in compression and tension, respectively. The penetration resistances measured at maximum depth of 1350 mm during the installation of the blank stainless steel pile in Soil # 1 and Soil # 2 was 13 kN and 21 kN, respectively (Figure 4.5a-4.5b).

The plug formation during the pile installation was recorded in both soils. In both soils plug length was less than 400 mm which has developed after approximately 400 mm of pile penetration. They remained constant until 800 mm of penetration in Soil # 1 which is silty sand in nature and until 900 mm in Soil # 2 which is clean sand. At these points the plugs moved again, gaining approximately 20 mm in length but remained constant during continued penetration up to the final pile depth of 1350 mm (Figure 4.6a-4.6b).

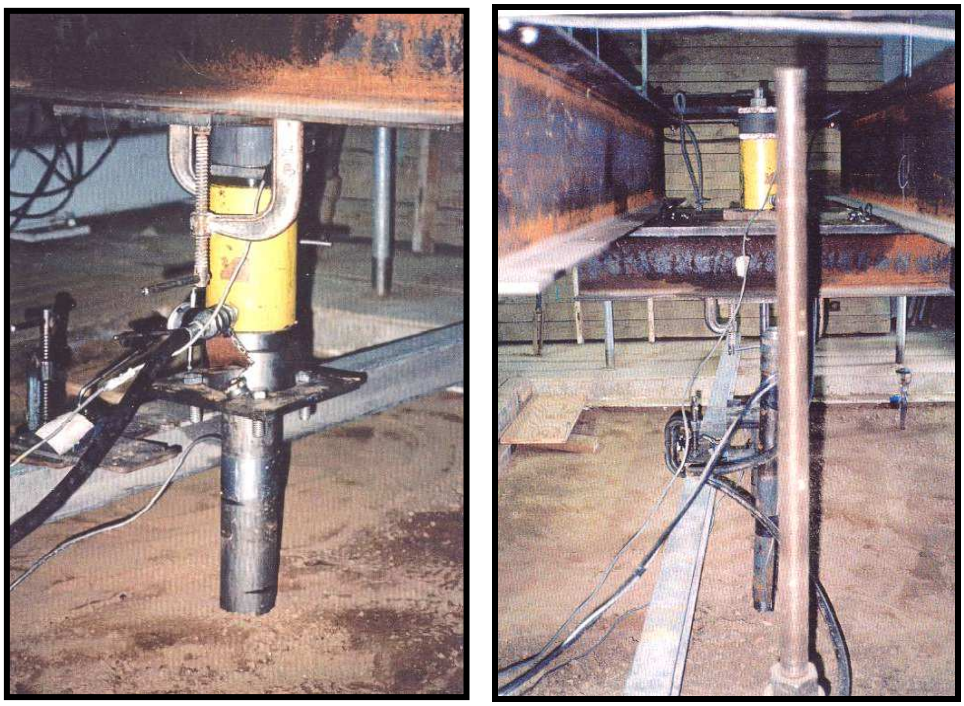

Figure 4.4 : Test setup of model pile loading of pile in compression and pile in tension.

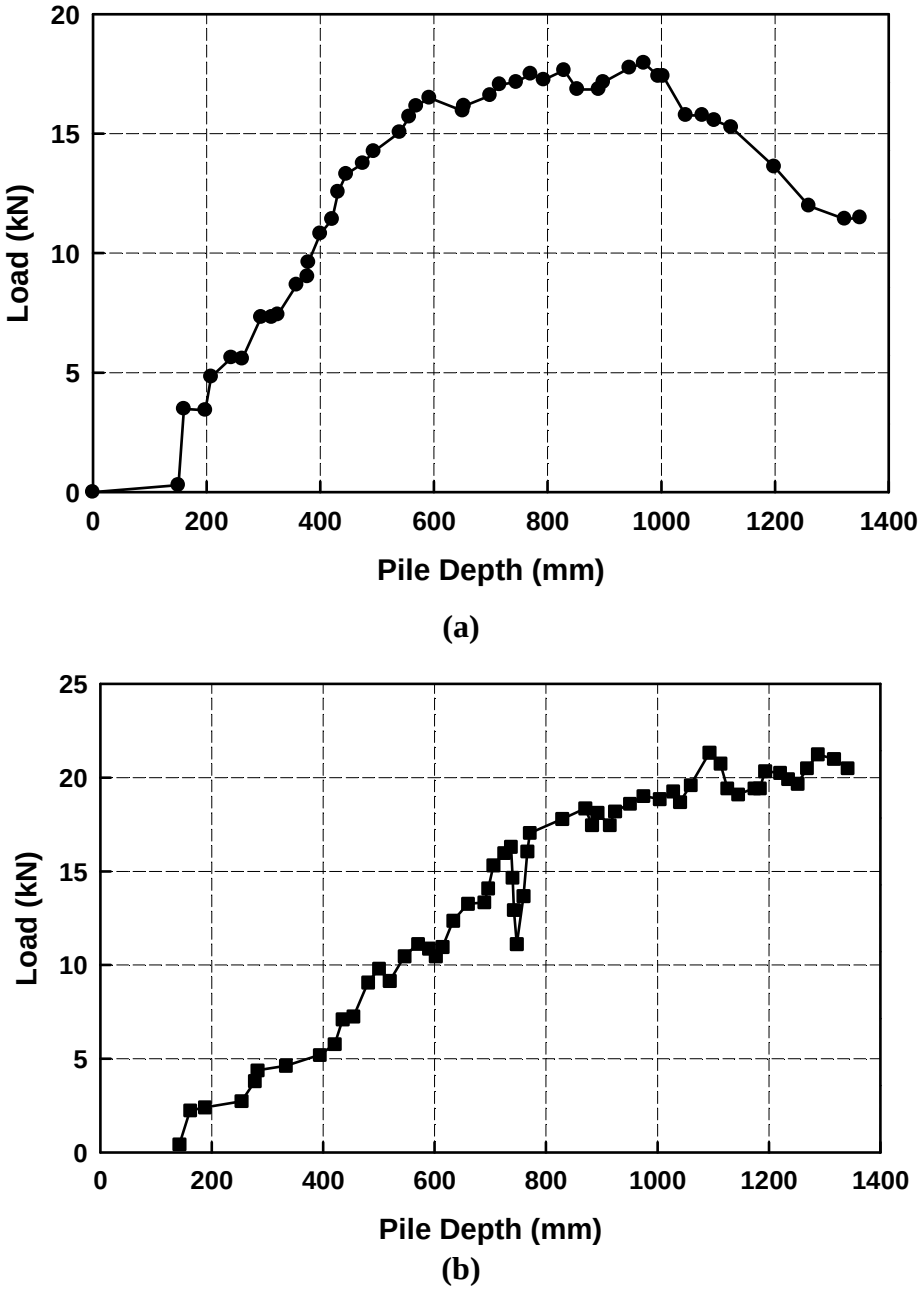

Figure 4.5 : Penetration resistance during installation of stainless steel pipe pile (a) in Soil # 1 and in (b) Soil #2.

After the pile was installed at the desired depth, the soil inside the pile was removed with a hand auger and a void was created below the toe of the pile by augering to a depth of approximately 200 mm below the pile toe. Much care was taken to expand the void laterally beyond the pile shaft dimensions. The loosened soil was removed with a vacuum hose inserted into the hollow pile. The void below the pile was visually inspected with a flashlight for proper soil removal. The intent of the void below the pile toe was to eliminate the toe resistance during compressive loading, thus permitting direct measurement of shaft resistance in compression and in tension.

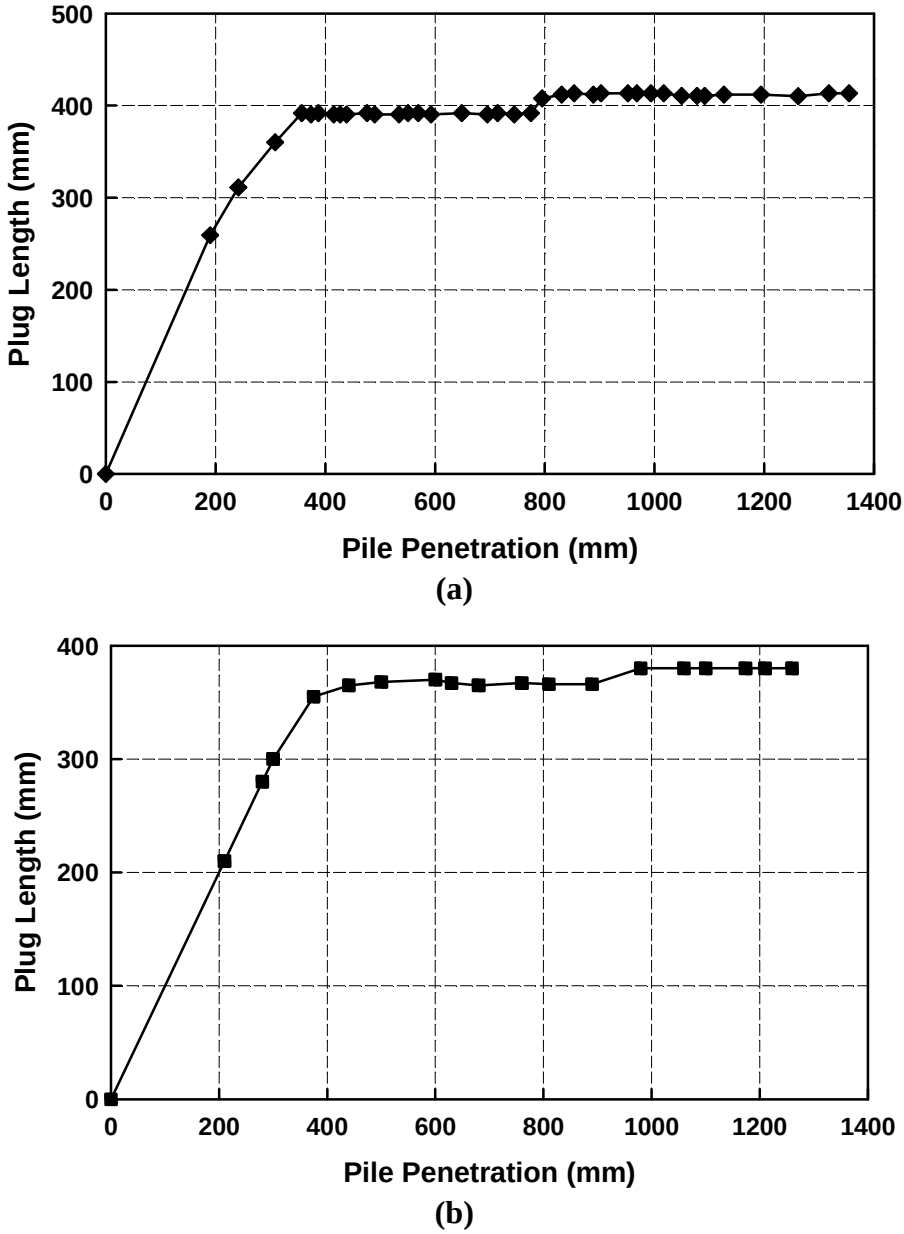

Figure 4.6 : Plug length vs. pile penetration during installation of stainless steel pipe pile in (a) Soil #1 and in (b) Soil #2.

4.2.4 Saturation and desaturation process

The compacted sand in the test box was saturated by adding water in test tank B and increasing the water level up to the ground surface. Subsequently the water level was lowered in the test tank B by pumping.

4.2.5 Testing program and pile testing procedure: methodology

A series of model pile tests were performed in two different compacted sands for both saturated and unsaturated conditions under identical conditions. Four different sets of test were conducted and the results were presented for Soil #1 as follows: Test

No.1: Unsaturated condition, Test No. 2: Saturated condition, Test No. 3: Unsaturated condition which was performed after one week. Finally Test No. 4 was performed with the new pile installation in unsaturated soil condition.

Three key tests were conducted on Soil #2. Test No. 1: Unsaturated condition, Test No. 2: Unsaturated condition, the pile was tested again after a period of 4 days. Finally the soil was saturated and Test No. 3 was performed under saturated condition. A total of seven pile tests with several cycles of compression and tension were performed during this study. The pile was repeatedly tested, alternating between tension and compression which resulted in continuously decreasing shaft capacities.

The piles were tested in axial compression and tension by loading in increments of approximately 20 N up to the point at which no further load increment could be sustained (Figure 4.7). Each load increment was held until the rate of movements decreased to zero. After reaching the maximum sustainable load, which was defined as failure load, the piles were unloaded in two steps back to zero. After a pause of at least four hours the next load test was carried out. Usually a testing set was started with a compression test, followed by a tension test. Maximum loads were reached in Soil # 1 after 1 to 2 mm movement and in Soil # 2 after 3 to 4 mm. In Soil # 1 the shaft resistances in compression were generally larger than in tension, whereas in Soil # 2 the opposite was the case.

Immediately after the compacted soil was placed in the test tank and during the pile testing, the coefficient of lateral earth pressure, K_o values were measured in the test tank by using the total pressure cells installed at four different elevations along the tank wall. The measured horizontal stresses increased almost linearly with depth resulting in earth pressure coefficients of approximately 0.7 for both soils in terms of total stresses. No total stress changes were recorded during testing by the load cells that were installed in the walls of the test tank.

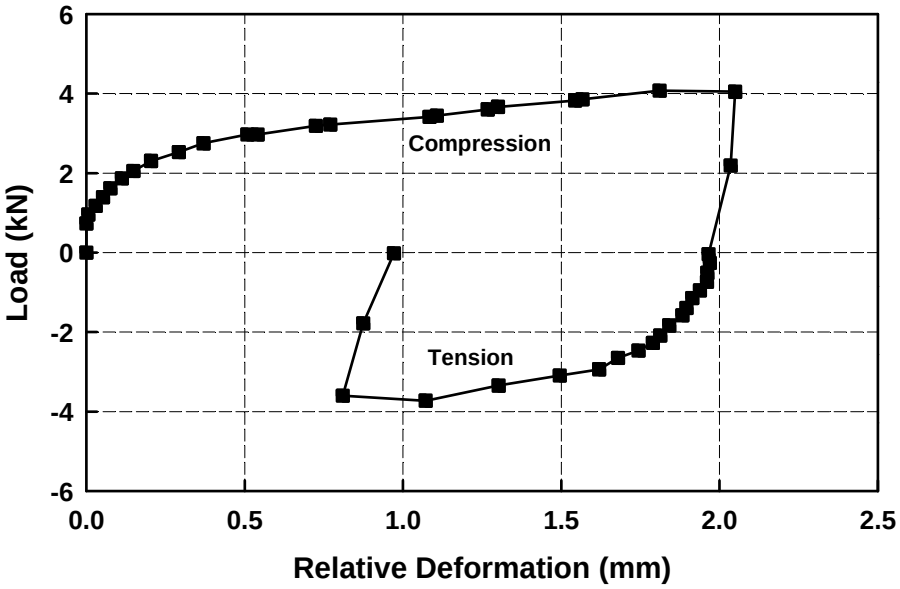

Figure 4.7 : Typical load deformation curve for pile in compression and tension for Soil#1 (Test Series 1 , 2nd cycle).

4.3 Experimental Results

4.3.1 Laboratory pile load test results

For each test, the maximum initial loads and the maximum loads that were experienced after the last load application are shown for compression and tension. The results of the pile tests that were accompanied by tensiometer readings are summarized for Soil #1 and Soil #2 in Figure 4.8 and in Figure 4.12.

For both soils, the test results show that the shaft capacities in tension and compression decreased during the repeated loading. In each case, it was apparent that the cavity below the pile toe had collapsed after the water table had been raised to the soil surface. This was confirmed from the observations of soil movement into the hollow pile shaft which contributed to the development of some end bearing. In addition, the soil portions adjacent to the lower pile shaft had loosened up, resulting in a decrease of the shaft capacity. In both cases, the shaft capacities in tension and in compression decreased during repeated loading, similar to observations reported previously, for example by Poulos (1989).

4.3.1.1 Silty sand-Soil No.1

Tests were carried out by varying (raising/lowering) water levels representing the saturated and unsaturated conditions. Four different tests were conducted for Soil #1

as follows: Test 1: unsaturated, Test 2: saturated, Test 3: unsaturated again and tested after one week, and finally Test 4: the new pile installation.

Referring to Figure 4.8, the pile shaft bearing capacities obtained in Test No. 2 are considerably lower than the results obtained in Test No. 1 after the soil was saturated by raising the water table level to the ground surface. Such a behavior was anticipated on the basis of the associated decrease in effective stress. Subsequently, the water table was lowered again. Surprisingly, the pile tests which were carried out one week after the water table lowered and was near the base of the pit (Test No. 3), resulted in capacities that were only slightly higher than those observed during saturated condition in compression and even lower in tension.

After the water table had been raised to the soil surface it was apparent that the cavity below the pile toe had collapsed and that soil had moved several centimetres into the hollow pile shaft. It can be visualized that due to this process some end bearing had developed and that the soil portions adjacent to the lower pile shaft had loosened up, resulting in a decrease of the shaft capacity. This may explain the low shaft capacities measured in Test No.3 after raising and lowering of the water table. For this reason, the pile results of Test No. 2 and Test No. 3 are considered not fully comparable to Test No. 1. Hence, the pile was removed and subsequently reinstalled about 0.6 m away from the original location. The subsequent load tests (Test No. 4) after the new pile installation, showed slightly higher capacities than Test No. 1, reflecting the slightly densified conditions due to the effective stress changes experienced during the preceding water table fluctuations.

After completion of the testing program in Soil # 1, sand was removed from the tank with the pile in place and samples were taken from the sand along the pile shaft. Thin-sections from these samples identified a concentration of fine particles within a zone of 1 to 2 mm adjacent to the pile surface, as well as orientation of elongated particles parallel to the pile shaft. This indicates that the soil conditions had changed along the pile shaft as a consequence of installing and testing of the pile. Such a behavior will influence the friction angle of the soil-steel interface required for the determination of the β parameter. More discussions on the β parameter will follow later in the chapter.

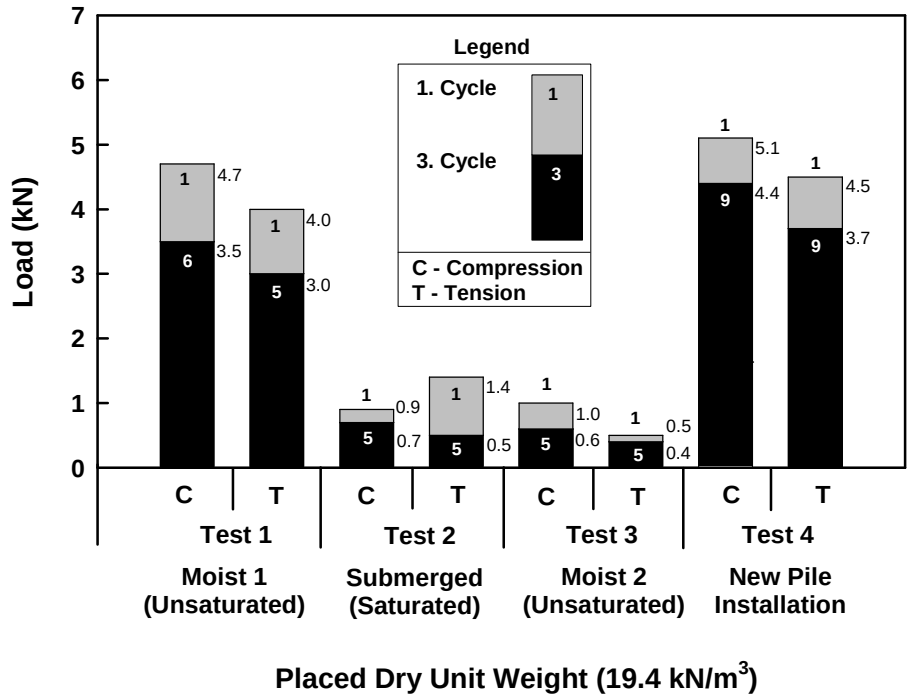

Figure 4.8 : Summary of pile test schedule and results for Soil #1.

Figure 4.9 and Figure 4.10 show the matric suction and pore water pressure changes (expressed in terms of piezometric head above piezometer tip) with time within the soil observed during raising and lowering the water table in tank B. The matric suction values measured in Soil # 1 immediately after placement in the test tank were 14 kPa, 15 kPa and 14.5 kPa at depths of 300 mm, 600 mm and 1200 mm, respectively given in Figure 4.9 indicating an approximately uniform suction profile along the pile shaft. After completing Test No.1 in unsaturated condition, water table was raised to the ground surface by adding water in tank B to saturate the compacted soil sample in tank A and subsequently lowered by pumping.

A time delay of 14 hours occurred between the free water table in pit B and the equalized pore-water pressure in the soil. The delay between free water table and response of the tensiometers (Figure 4.9) was shorter than that for the piezometer readings (Figure 4.10). The time span between the point when a stable free water surface was established and the point at which stable capillary stresses or matric suction values were achieved was approximately 12 hours. At fully saturated condition, the matric suction values from the three respective tensiometers were in the range of 0.9 to 1.5 kPa.

4.3.1.2 Clean concrete sand-Soil No. 2

Three key tests were conducted using Soil #2. Test No. 1 was conducted under unsaturated condition. After a period of 4 days the pile was tested again under unsaturated condition (Test No. 2), and finally the soil was saturated and tested (Test No. 3).

In Soil # 2, the pile was repeatedly tested, alternating between tension and compression. Changing the direction of loading resulted in continuously decreasing shaft capacities from 2.2 kN after the first load application to 1.7 kN after the sixth load application in compression and, respectively, from 3.1 kN to 1.9 kN in tension for Test No. 1 (Figure 4.11). After a period of 4 days waiting, the pile was retested (Test No. 2). The shaft capacities of the pile in compression and in tension had decreased further to 1.5 kN and 1.6 kN in compression and tension respectively at the end of the first cycle load application.

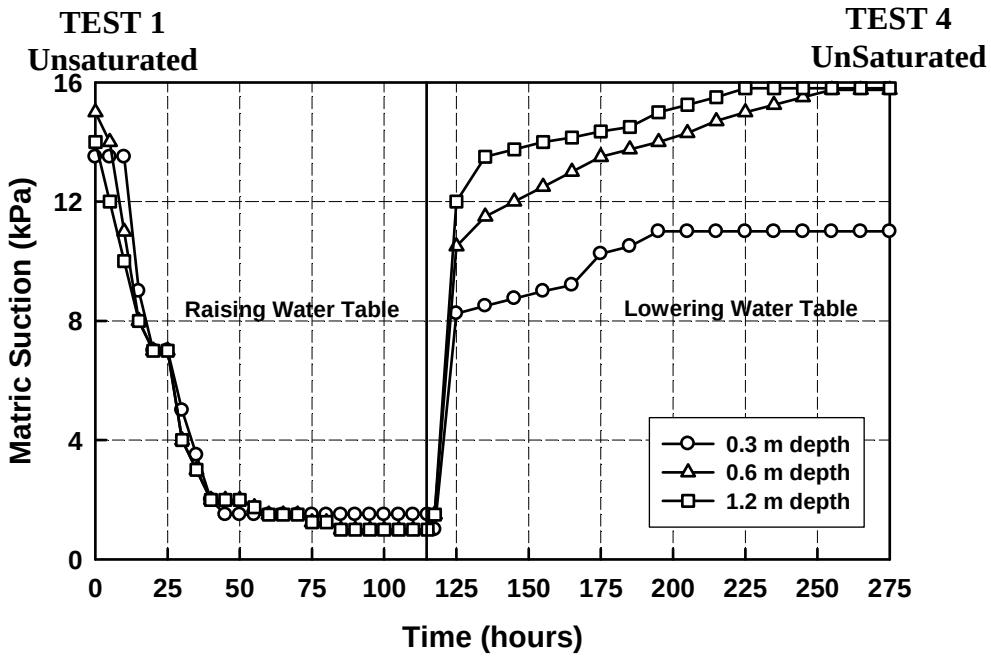

Figure 4.9 : Changes in capillary stresses (matric suction) during raising and lowering the water table (Soil #1).

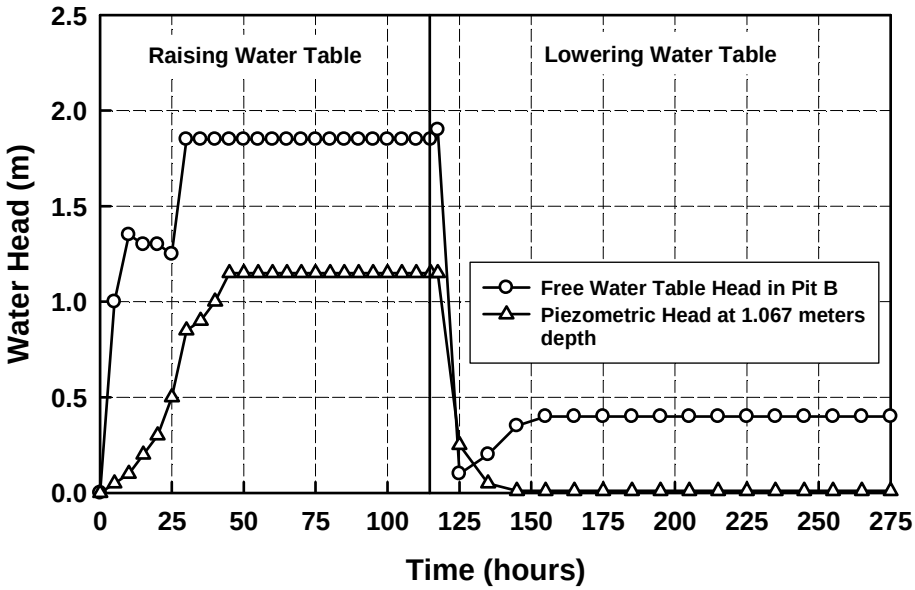

Figure 4.10 : Pore water pressures measured with piezometer at 1.067 m below ground surface during raising and lowering of the free water table in pit B (Soil #1).

The matric suction values measured in Soil # 2 immediately after placement of the soil sample in the test tank was 10 kPa, 11.5 kPa and 18 kPa at 300 mm, 600 mm and 1200 mm, respectively (Figure 4.12). Lowest value of matric suction value was measured near the surface and the highest at the larger depth. Two days before performing the Test No. 2 water was added to the soil surface using a garden-sprinkler resulting in decrease in matric suction values at all three tensiometer levels. The largest decrease was observed near the surface, changing from 10 kPa to 3 kPa almost immediately. The smallest change occurred at the lowest tensiometers with 6 hours delay from 18 kPa to 16.2 kPa (Figure 4.12). The tensiometer readings increased again when the application of water to the soil surface was stopped. The matric suction values before, during and after water application to the soil surface of Soil # 2 are plotted against depth in Figure 4.13.

Finally, the soil was saturated and the pile was tested again, applying three load cycles. However, for Soil # 2 in saturated soil condition, only the tensile capacities were recorded due to the same reasoning in Soil #1 that the cavity below the pile toe had collapsed when the water table was raised.

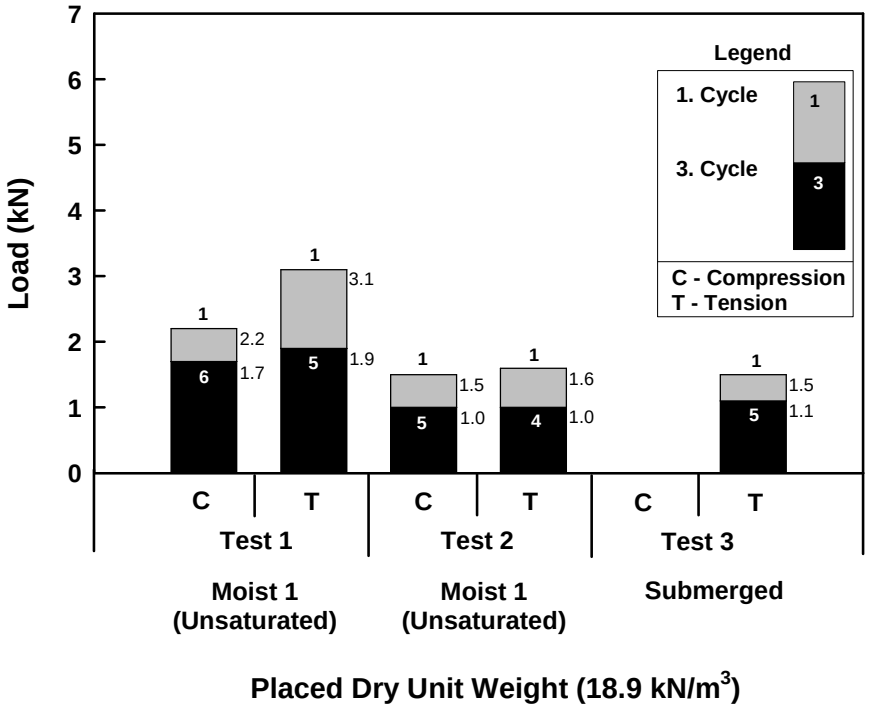

Figure 4.11 : Summary of pile test schedule and results for Soil #2.

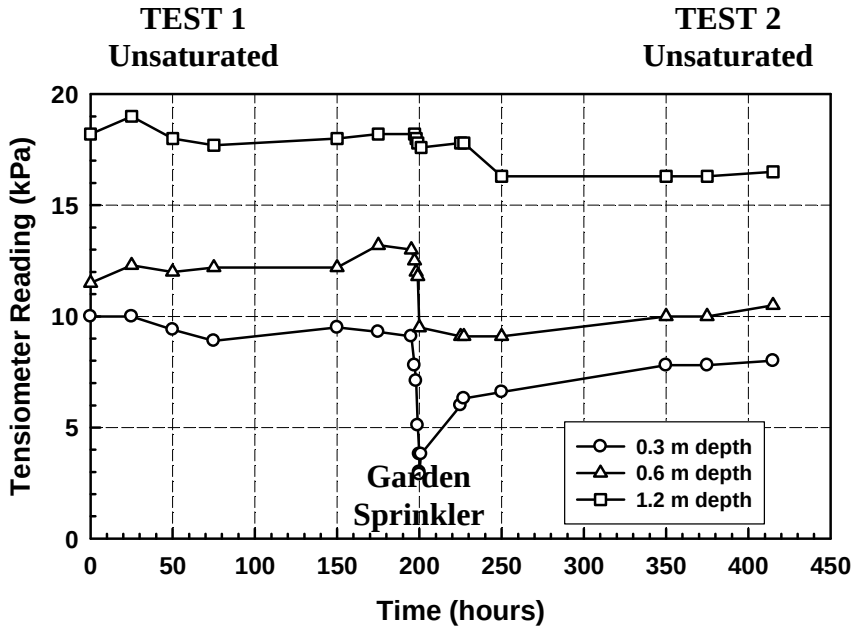

Figure 4.12 : Variation of tensiometer readings in Soil # 2 with time prior to and after water sprinkling.

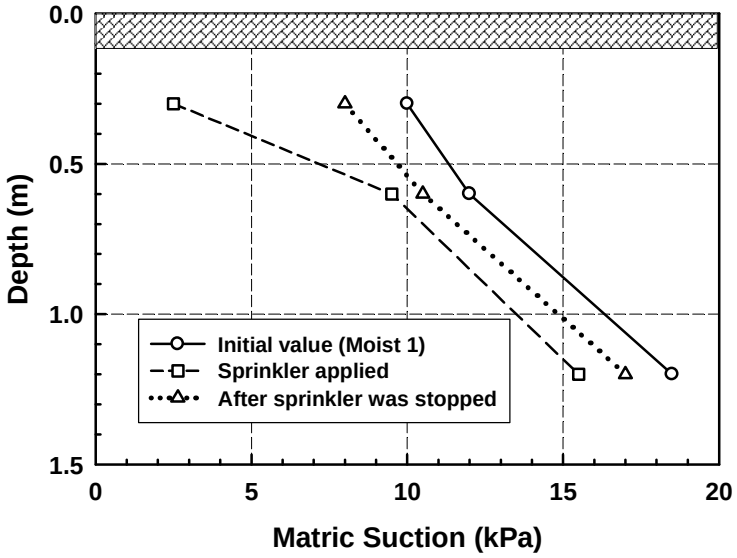

Figure 4.13 : Profile of matric suction before, during and after sprinkler application in Soil # 2.

4.3.2 Cyclic direct shear test results

The shear strength along the soil-steel interface was determined by performing cyclic direct shear tests at constant normal load *(CNL).* The shear strength along the soil-steel interface was measured by placing the upper half of the shear box (height of 25 mm) on a plane steel plate, filling it with soil and compact it before shearing at a specified load along the steel surface. Cyclic direct shear tests were carried out to simulate the load reversals applied during pile load testing. Both soils experienced contractive behaviour during cyclic shearing, which became more pronounced at higher stress levels (Figure 4.14 and Figure 4.15). Particularly for Soil # 1 the shearing resistances were consistently lower during load reversals. Similar observations had been reported from *CNL* direct shear tests along sand-steel interfaces by Hanke (2001) and Lehane and Jardine (1994).

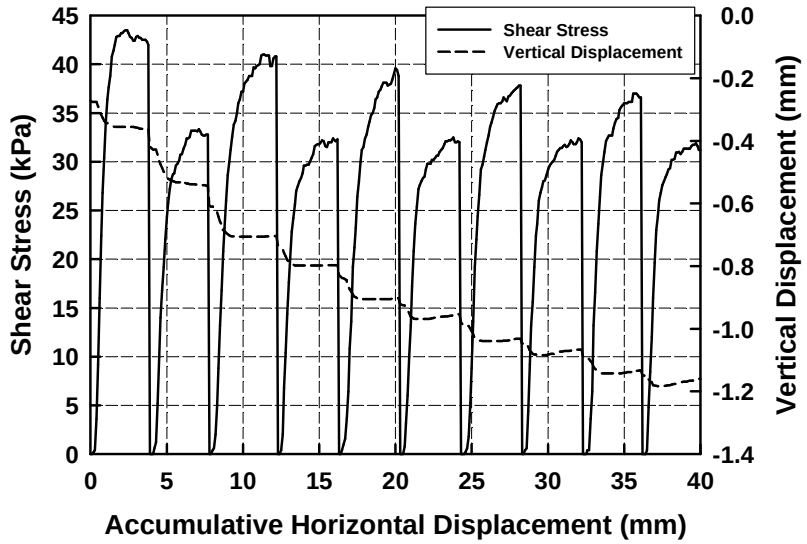

Figure 4.14 : Results from cyclic shearing test, along interface of steel and Soil #1 at normal stress of 60 kPa.

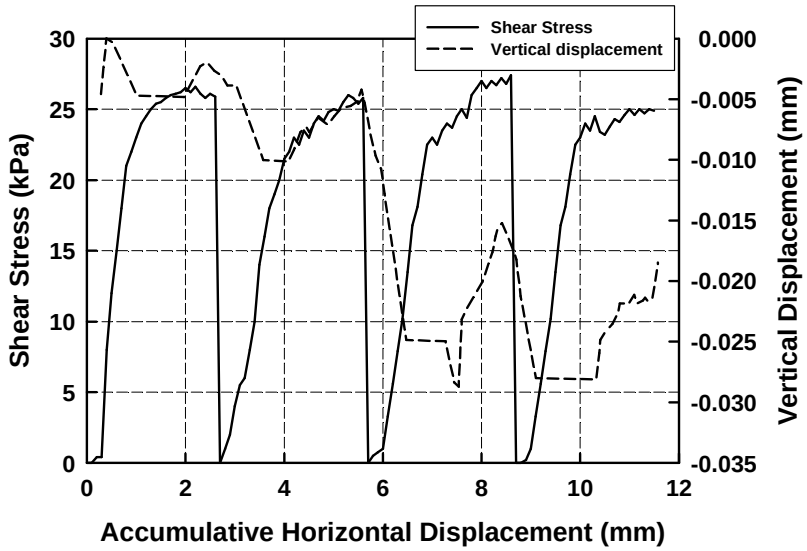

Figure 4.15 : Results from cyclic shearing test along interface of steel and Soil #2 at normal stress of 60 kPa.

The direct shear test results of the interface of steel and Soils # 1 and # 2 are summarized in Figure 4.16 and 4.17, respectively. The friction angles, ϕ' and δ' determined for both soils and for the respective soil-steel interfaces, are summarized in Table 4.1.

4.3.3 Determination of the SWCCs

The *SWCC* (drying curve) was plotted as a relationship between the degree of saturation, *S* and matric suction, $(u_a - u_w)$, by using three different methods.

(i) *SWCCs* were measured using pressure plate apparatus.

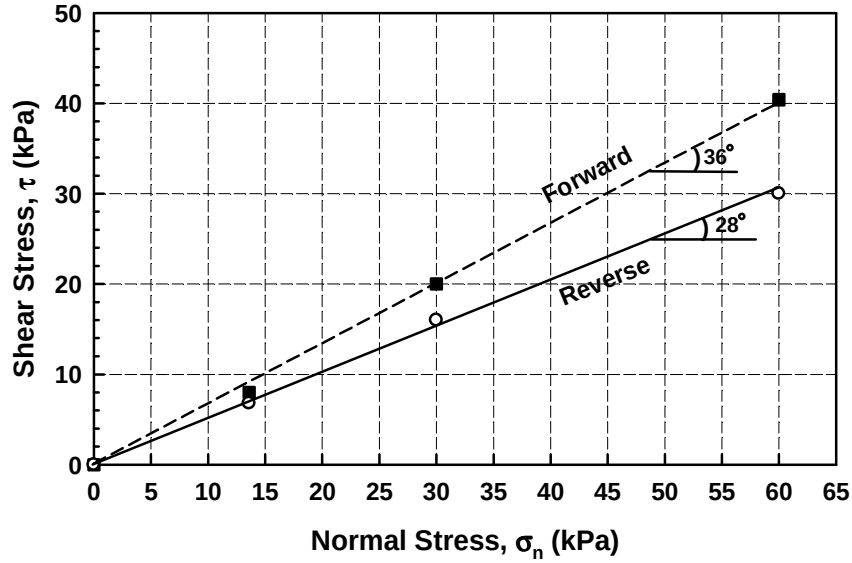

Figure 4.16 : Shear strength along soil/ steel interface (Soil #1).

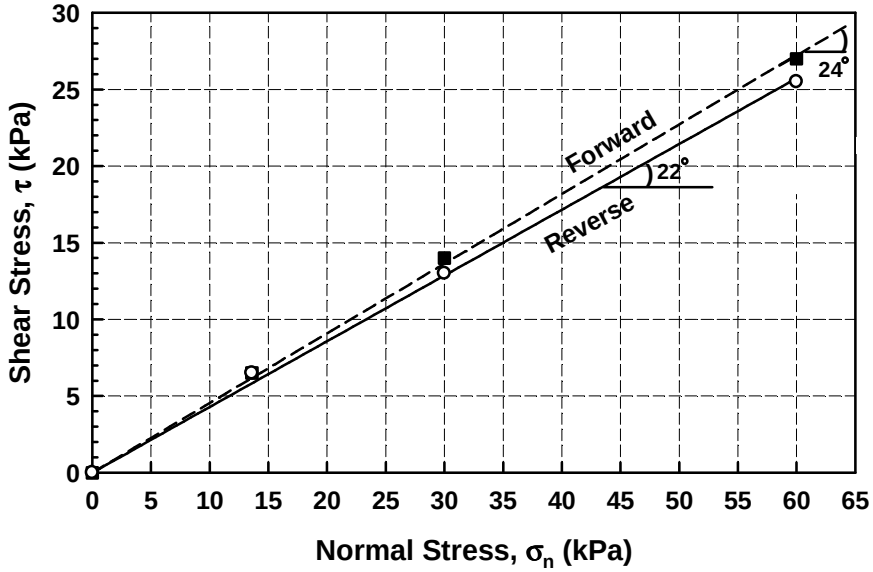

Figure 4.17 : Shear strength along soil/ steel interface (Soil #2).

(ii) The measured *SWCC* results were also compared and supported with the estimated values obtained by using computer software; SoilVision 2000 which uses the grain size analysis data and the volume-mass properties (Fredlund et al. 2002).

(iii) One-point prediction technique proposed by Vanapalli and Catana (2005) was used to obtain *SWCC*. There are several models based on the fitting curve equations by using one or more fitting parameters for the determination of *SWCC*. The one point measurement technique builds up a relation between the easily obtained soil properties and fitting parameters of widely used equations and models proposed by Brutsaert (1966), van Genuchten (1980) and Fredlund and Xing (1994) but only

needs one experimental data point of matric suction. The results will be given within test results section. There is a good comparison between the *SWCCs* obtained using all three different methods (Figure 4.18 and Figure 4.19).

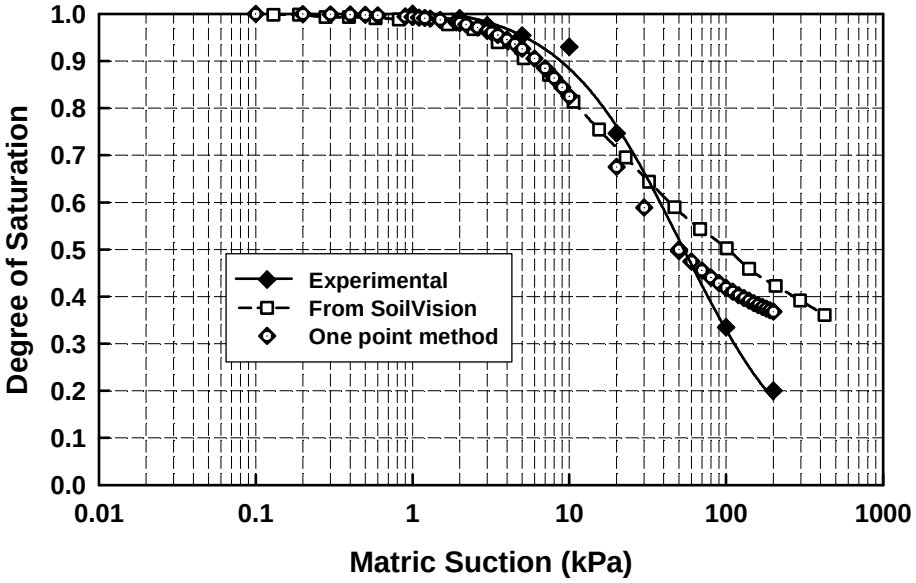

Figure 4.18 : Measured and predicted soil-water characteristic curve for Soil # 1.

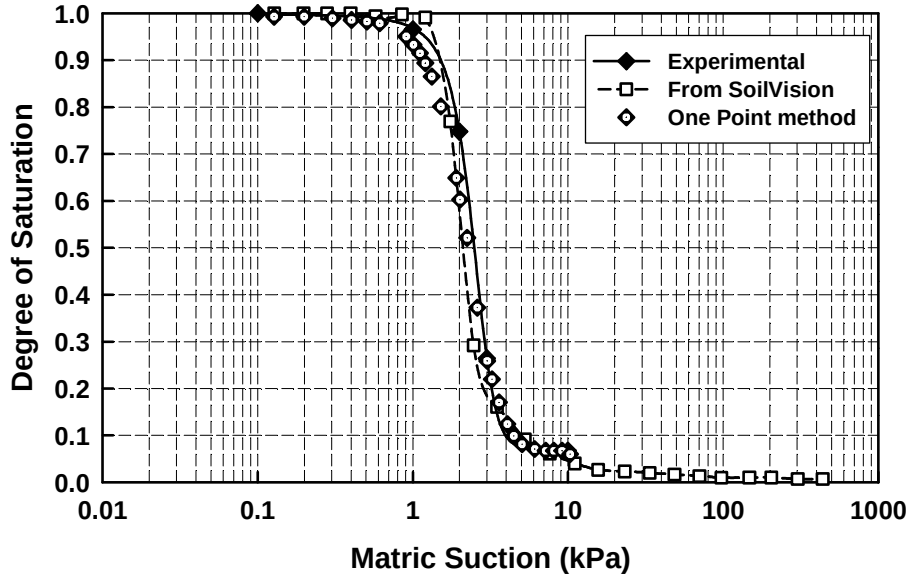

Figure 4.19 : Measured and predicted soil-water characteristic curve for Soil # 2.

4.4 Estimating the Shaft Resistance by the Proposed Modified β-Method

The shaft bearing capacities of the tested piles in unsaturated soils were calculated using the modified β method (4.1) which has been derived in detail in the preceeding chapter.

$$Q_{f_{us}} = Q_f + Q_{(u_a - u_w)} = \beta\left(\frac{\gamma L}{2}\right)(\pi\, d\, L) + \left[(u_a - u_w)(S)^{\kappa}(\tan\delta')\right]\pi dL \quad \textbf{(4.1)}$$

where: β = Bjerrum-Burland coefficient, γ = unit weight of the soil, L = embedded length of the pile, effective cohesion, S = degree of saturation, δ = interface friction angle, κ = fitting parameter used for obtaining a best-fit between the measured and predicted values.

The predicted and measured results are summarized in Table 4.2 through Table 4.5 for Soil #1 and Soil #2 respectively for comparisons. The contribution of matric suction to the total shaft resistance was evaluated for both soils using β values of 0.24, 0.35 and 0.60 in tension and compression. The chosen range is widely used in the conventional analyses. Thus, it also appeared appropriate to obtain β values directly from back-calculations of the pile test results and the vertical effective stress conditions along the soil/pile interface. The back calculated values can be compared with the values obtained from the analytical method using the relationship given in (4.2) and with the values suggested in literature.

$$\beta = K_o \tan\delta' \quad \textbf{(4.2)}$$

where K_o = lateral earth pressure coefficient at rest. It is observed that the choice of β affects the contribution of matric suction to the shaft resistance.

In the present study, matric suction values and their variations were measured by the tensiometer readings located at three different depths in the soil bed of the test tank. However, the water contents at these locations were not measured directly. The *SWCC* data were used as a tool to obtain the corresponding degree of saturation, *S* values at these depths by back calculation which is separately summarized in Table 4.3 and Table 4.5.

Soil #1 –Silty Sand

Table 4.2 : Contribution of matric suction to the total shaft resistance given with measured and computed results for Soil #1.

Test No.	$Q_{f(predicted)}$ (kN)						$Q_{f(meas.)}$ (kN)
	β = 0.35		β = 0.24		β = 0.60		-
	$Q_{(\mathbf{u_a - u_w})}$	$Q_{f(us)}$	$Q_{(\mathbf{u_a - u_w})}$	$Q_{f(us)}$	$Q_{(\mathbf{u_a - u_w})}$	$Q_{f(us)}$	$Q_{f(sat,\ unsat)}$
Test 1-UNSAT	1.84	3.11	1.82	2.70	1.82	4.00	4.7
Test 2-SAT	0.0	0.74	0.0	0.51	0.0	1.26	0.9
Test 4-UNSAT	1.82	3.09	1.82	2.70	1.82	4.00	5.1

Table 4.3 : Measured matric suctions and estimated normalized water contents at various depths for Soil # 1.

Test No.	Depth (m)	Matric Suction $(u_a - u_w)$, *kPa*	Degree of Saturation (S, *%)*
Test 1	0.00 – 0.45	13.5	0.780
	0.45 - 0.90	15.0	0.765
	0.90 – 1.30	14.0	0.775
Test 2	0.00 – 0.45	1.5	0.985
	0.45 - 0.90	1.0	0.990
	0.90 – 1.30	0.9	0.990
Test 4	0.00 – 0.45	11.0	0.810
	0.45 - 0.90	16.0	0.755
	0.90 – 1.30	16.0	0.755

Soil #2 –Clean Sand

Table 4.4 : Contribution of matric suction to the total shaft resistance given with measured and computed results for Soil #2.

Test No.	$Q_{f(predicted)}$ (kN)						$Q_{f(meas).}$ (kN)
	for $\beta = 0.35$		for $\beta = 0.24$		for $\beta = 0.60$		
	$Q_{(\mathbf{u_a - u_w})}$	$Q_{f(us)}$	$Q_{(\mathbf{u_a - u_w})}$	$Q_{f(us)}$	$Q_{(\mathbf{u_a - u_w})}$	$Q_{f(us)}$	$Q_{f(sat, unsat)}$
Test 1-UNSAT	0.057	1.25	0.06	0.88	0.06	1.25	2.2
Test 2-UNSAT	0.056	1.25	0.056	0.87	0.056	2.10	1.5
Test 3-SAT	0.00	0.71	0.00	0.48	0.00	1.21	N/A

Table 4.5 : Measured matric suctions and estimated normalized water contents at various depths for Soil # 2.

Test No.	Depth (m)	Matric Suction $(u_a - u_w)$, *kPa*	Degree of Saturation, (S)
Test 1	0.90 – 1.30	10.0	0.050
	0.45 – 0.90	12.0	0.048
	0.00 – 0.45	18.0	0.025
Test 2	0.90 – 1.30	8.0	0.060
	0.45 – 0.90	10.0	0.050
	0.00 – 0.45	16.5	0.030
Test 3 (Saturated)	0.00 - 0.45 0.45 - 0.90 0.90 - 1.30	N/A	N/A

The estimated shaft bearing capacity values using the proposed modified β method given in (4.1) versus the measured shaft capacities are plotted in Figure 4.20. Two key observations can be made from the summarized results as the contribution of matric suction to the total shaft resistance, and the difference between the measured and predicted total shaft bearing capacities.

The contribution due to matric suction to the total shaft resistance was found to be 45%-50% of the total shaft capacity in the Soil #1 which was silty in nature. For Soil #1 the contribution of matric suction to the shaft resistance is approximately 50% of the measured total shaft resistance for the unsaturated cases. However, contribution of matric suction to the total shaft resistance was almost negligible in Soil # 2 which was clean concrete sand. For Soil #2, the matric suction contribution towards shaft resistance is quite low for unsaturated conditions.

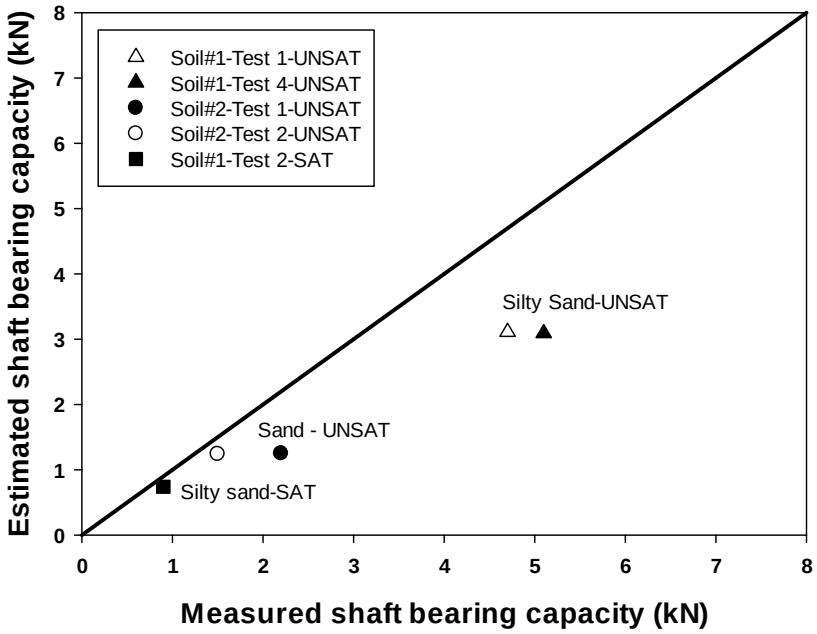

Figure 4.20 : Estimated values versus measured shaft bearing capacity for model single pile tested under saturated and unsaturated conditions for $\beta = 0.35$.

As discussed earlier this can be attributed to the rapid reduction in degree of saturation even with small increases in matric suction values (Figure 4.19). Similar rapid decreases in shear strength values were reported when degree of saturation decreased with small increases in matric suction (Vanapalli et al., 1996). This behavior can be attributed to the soil approaching residual stage of desaturation. In the residual stage of desaturation, the shear strength generally decreases, especially for sands and silts (Vanapalli et al., 1996; Vanapalli et al., 1998). The water content or degree of saturation in the residual stage is typically low for sands and silts and may not transmit suction effectively to the soil particle or aggregate contact points.

Since the matric suction contribution is the same for the possible estimated shaft bearing capacities, it can be concluded that the difference between the measured and estimated shaft bearing capacities can be attributed to the β values which are

dependent on the stress condition of the soil. For this reason, β values were back calculated to understand the influence of unsaturated soil conditions dependent on the stress condition of the soil.

4.5 Discussion: Back Calculated β-values

The difference between the estimated shaft bearing capacities obtained by using the proposed equation (4.1) and the measured shaft bearing capacity values can be due to the selected β parameter. The β value is a function of in-situ stress conditions, frictional resistance and mode of pile installation. Although the coefficient of lateral earth pressure, K_o values were measured in the test tank by using the total pressure cells installed along the tank wall, this does not fully define the lateral stress changes in the shearing zone of thin interface between the pile wall and the surrounding soil.

Thus, the β values were back calculated from the measured shaft capacities in compression and tension (i) for fully saturated condition (4.3); (ii) for unsaturated condition considering the contribution of matric suction (4.4) and (iii) for unsaturated condition without considering the contribution of matric suction (4.5) using the following equations, respectively.

Equation (4.3) is used to back calculate the β values from the model pile load tests performed under the fully saturated soil conditions based on the conventional β method. The modified β method (4.1) is used to obtain the given equation in (4.4) to back calculate the β values from the tests performed under unsaturated soil conditions considering the matric suction contribution. However, in conventional engineering practice the matric suction contribution is not included in the calculations and the conventional approaches are followed although the soil is in an unsaturated condition. Thus, (4.5) is used to demonstrate this situation and the β values are back-calculated by ignoring the contribution of matric suction.

The back calculated values by using the (4.3), (4.4) and (4.5) are summarized in Table 4.6 and in Table 4.7 using first cycle loads for Soil # 1 and Soil # 2. The back calculated β values using (4.3) to (4.5) - varying from 0.24 to 1.41, which are in close agreement with values reported in the literature but show considerable scatter. However, this scatter in β values considerably decreases, if contribution of matric suction is taken into account by using (4.4).

For Soil # 1 the β values that were back calculated for unsaturated soil conditions without considering soil suction were greater than 1.0, whereas the β values including soil suction ranged between 0.6 and 0.9. Thus, β values calculated with considering the influence of matric suction are between 36% and 45% lower than the situation when it is ignored. As it is unlikely that the angle of friction valid along the soil pile interface is different for saturated and unsaturated conditions, it can be concluded that the normal stress acting against the pile shaft is less in unsaturated soils than in saturated soils. This assessment agrees with the notion that soils when unsaturated will experience contraction as a result of the capillary tension between the soil particles.

The equations for back calculation of β parameter are given as follows:

$$\beta = \frac{Q_f}{\left(\frac{\gamma' L}{2}\right)(\pi d L)} \quad \textbf{(4.3)}$$

$$\beta = \frac{Q_{f(us)} - Q_{(u_a - u_w)}}{\left(\frac{\gamma L}{2}\right)(\pi d L)} \quad \textbf{(4.4)}$$

$$\beta = \frac{Q_{f(us)}}{\left(\frac{\gamma L}{2}\right)(\pi d L)} \quad \textbf{(4.5)}$$

The β values that were back calculated for saturated conditions were much lower in both soils than for the unsaturated soils, reflecting the effect of looser soil conditions near the pile shaft after the soil had sloughed into the cavity below the pile tip after being saturated. Under saturated conditions the back calculated β values were much lower, ranging between 0.24 and 0.43 but this time representing a loose soil condition.

For Soil #2, β values, calculated with and without soil suction, are similar. This result can be attributed to very little contribution of matric suction towards shaft resistance. Because of zero fine content in Soil # 2, water cannot be retained and hence the behaviour of Soil # 2 is similar to dry sand or saturated sand, in spite of the unsaturated conditions.

The back calculated β values shows that as the matric suction increases the β values tend to increase also. In other words the saturation degree and the β values are inversely proportional.

Table 4.6 : The β values back calculated from measured shaft capacities for Soil # 1.

Test No.	$Q_{f(meas.)}$	$Q_{f(meas.)}$	Back calculated β values					
	kN	kN	(4.3)		(4.4)		(4.5)	
	C*	T^{ξ}	C	T	C	T	C	T
Test 1 (UNSAT)	4.7	4.0	-	-	0.80	0.60	1.30	1.10
Test 4 (UNSAT)	5.1	4.5	-	-	0.90	0.74	1.41	1.24
Test 2 (SAT)	0.9	1.4	0.43	0.24	-	-	-	-

* Compression, ξ Tension

Table 4.7 : The β values back calculated from measured shaft capacities for Soil # 2.

Test No.	$Q_{f(meas.)}$	$Q_{f(meas.)}$	Back calculated β values					
	kN	kN	(4.3)		(4.4)		(4.5)	
	C*	T^{ξ}	C	T	C	T	C	T
Test 1 (UNSAT)	2.2	3.1	-	-	0.64	0.88	0.66	0.90
Test 4 (UNSAT)	1.5	1.6	-	-	0.43	0.45	0.44	0.47
Test 2 (SAT)	-	1.5	N/A	0.54	-	-	-	-

4.6 Summary

The objective of this study is to determine the contribution of matric suction towards the total shaft resistance of piles and propose a technique to estimate the shaft resistance in unsaturated soil conditions.

The shaft capacities of steel pipe piles which had been jacked hydraulically into two sands tested under saturated and unsaturated conditions were evaluated in terms of the matric suction that was measured in the unsaturated soils.

The contribution of matric suction was found out to be between 45%-50% of the total shaft capacity of the test piles for silty sand but almost negligible for clean sands. Thus, it can be concluded that in unsaturated soils, with the exception of clean sands and granular soils, the contribution of matric suction to the total shaft capacity of piles cannot be neglected. In addition, a simple technique was proposed to estimate the shaft resistance in unsaturated soil conditions using the *SWCC* and the conventional shear strength parameters.

In Soil # 2, which is clean sand with zero fine content, the back calculated β values were approximately the same with and without consideration of soil suction. Because of the low fine content, the effect of soil suction is almost negligible on the β values and thus on the normal stress against the pile shaft.

The results of this study are promising to predict the contribution of matric suction towards shaft resistance using well established β-method for sandy soils in the literature. However, more pile load tests need to be performed and evaluated for a better understanding of the contribution of matric suction towards the shaft capacity of piles in different types of sandy soils.

5. EQUIPMENT AND ACCESSORIES DETAILS USED FOR DETERMINING THE SHAFT BEARING CAPACITY OF MODEL PILES IN FINE GRAINED SOILS

5.1 Introduction

This chapter presents details of the equipment that were used to determine shaft bearing capacity of model piles under axial loading in statically compacted fine-grained soils. Model piles were loaded in a specially designed test tank under both saturated and unsaturated conditions. The key objective of the testing program was to determine the contribution of the matric suction towards the shaft bearing capacity of the model piles under axial loading.

In addition to the model pile tests, the *SWCC* of the compacted fine-grained soils were determined using the soil pressure-plate apparatus. The matric suction of the compacted soil specimens were determined using the modified null pressure plate apparatus. The variation of matric suction in the compacted soil specimen with respect to depth in the test tank were measured using the Tensiometers. Theoretical background and working principles associated with the key equipment and the other accessories used in the research study are also presented in this chapter. Detailed experimental procedures with respect to model pile testing are however summarized in the next chapter.

5.2 Model Pile Testing Set-up

The shaft capacity of model piles were to be placed and axially loaded in compacted fine grained soil in a specially designed test tank to determine shaft bearing capacity under both saturated and unsaturated conditions. The tank used in the study is a cylindrical high strength plastic container with the dimensions of 300 mm both in diameter and height with a wall thickness of 12.7 mm. Three clamps were wrapped around the high strength plastic container to eliminate the possible strain effects on

the container during compaction of the sample and while loading the model pile. Three holes were placed in the tank wall depth at equal distances to introduce Tensiometers into the compacted soil for determining the matric suction. This tank was originally designed by Vanapalli et al. (2007) for determining the bearing capacity of surface model footings of fine-grained compacted soils (Figure 5.1).

The soil will be placed in the plastic mould and statically compacted using a specially designed compactor. The compactor consists of two concentric circular plates (300 mm in diameter × 9.85 mm in thickness and 160 mm in diameter × 9.85 mm in thickness) placed on each other with a solid cylindrical bar (50 mm in diameter × 230 mm in height) fastened on top of the 160 mm diameter plate. The smaller metal circular plate was fastened on larger aluminium circular plate to prevent possible bending while compacting the soil in the mould. Four holes drilled through the larger circular plate allow drainage. The proving ring will be used to measure the applied compaction stress to the soil in the test tank (Figure 5.2).

Solid stainless steel model piles with diameters of 10, 15, 20, 30 and 45 mm referred to as D10, D15, D20, D30, D45 with total length of 450 mm were used in the present study. A cylindrical hole was created to a depth of 220 mm in the compacted soil using thin wall tubes to reduce the disturbance and the generation of excessive stresses adjacent to soil during the pile installation. The thin wall tube diameters were slightly less than the model piles to develop a good contact between the pile and the soil along the shaft length. After the hole drilling was completed, model pile will be jacked down to an embedment depth of 200 mm. A void of 20 mm in length was intentionally left below the pile toe. This void facilitates in the measurement of shaft resistance over a length of 20 mm without any contribution from the end bearing resistance.

The conventional triaxial testing equipment (ELE Int. Ltd- *TRI-FLEX 2*) is used as the loading frame for compacting the soil in the test tank. The same equipment also is used for loading of model piles. The load and displacement were measured by a load cell and a Linearly Variable Displacement Transducer *(LVDT)*. A Data Acquisition System *(DAS)* was used to collect the data. The model pile test set-up used for the test program is shown in Figure 5.3.

Figure 5.1 : Testing tank and compactor details
(photo adapted from Vanapalli et al., 2007).

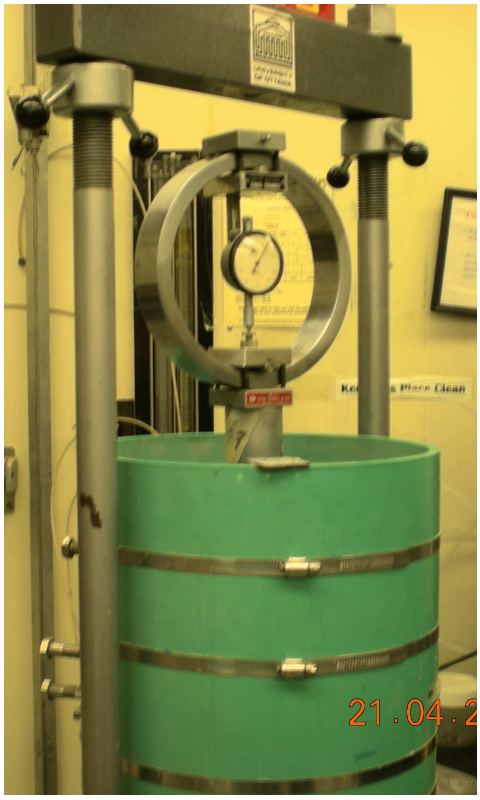

Figure 5.2 : Test tank assembly and the loading frame with the proving ring.

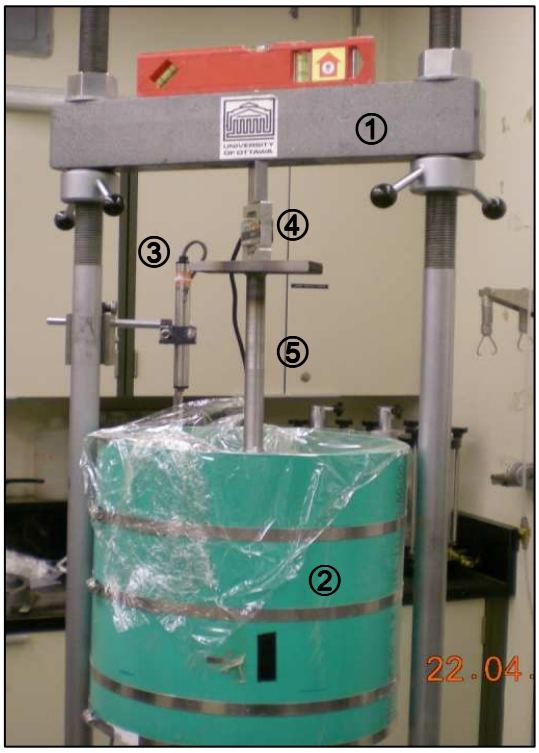

Figure 5.3 : Test setup for model pile loading in fine-grained soil. (① Adjustable height loading frame ② Test tank ③ LVDT ④ Load cell ⑤ Model pile).

5.3 Compaction Equipment

The compaction characteristics of the tested soil were determined by statically compacting it in standard consolidation rings. The soil samples used in the study were prepared at different initial water contents. The soil was compacted in one layer into the brass compaction equipment shown in Figure 5.4.

The compaction equipment consists of a brass mold (two semi-cylinders attached) with 120 mm in height and 52 mm in inner diameter and a compactor ram with a tapered teflon base to reduce friction. The Teflon base also formed a tight seal with the mold to prevent the soil particles from jamming the ram. A 25 mm circular piece of porous plastic was inserted into the Teflon base leading to an air vent to eliminate the possibility of vacuum developing inside the mold during compaction. The vent would allow any trapped air to escape out of the mold (Figure 5.4). More details of this equipment are available in Catana (2005).

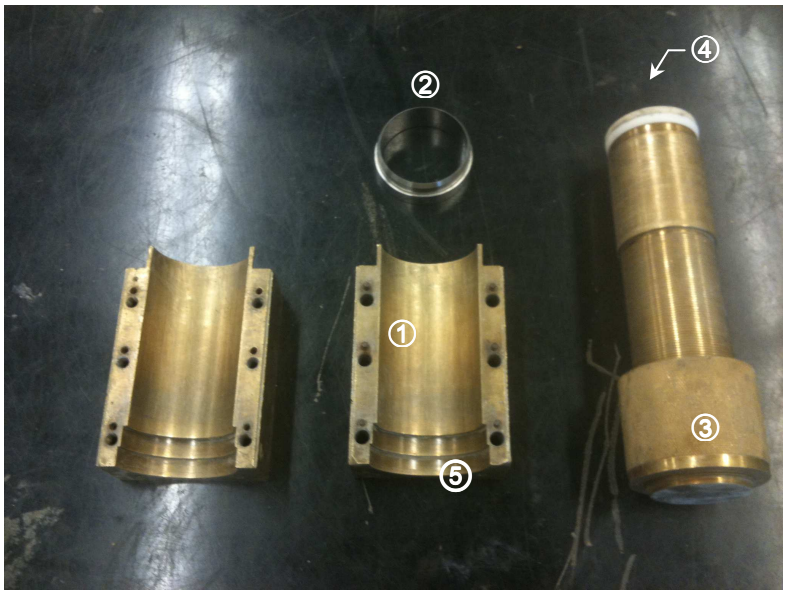

Figure 5.4 : Specimen compactor mold and ram: ① brass mold separated into two halves, ② specimen ring, ③ ram, ④ tapered Teflon base, ⑤ grooves to hold the specimen ring.

5.4 Soil Suction Measurement Techniques

Soil suction measurement techniques are summarized in Figure 5.5 based on the working suction range and suction (i.e. matric or total) measured. In the present research, Tensiometers and axis-translation were used for direct measurement of the negative pore water pressure (matric suction). Both the Tensiometers and the axis translation technique rely on the use of high-air entry (here after referred to as *HAE*) materials made of ceramic to measure matric suction.

5.4.1 Properties of High-Air-Entry *(HAE)* materials

HAE ceramic materials consists of relatively uniform microscopic pores. Once these pores are filled with water and the ceramic material is saturated, a contractile skin or a membrane is formed due to the influence of surface tension. This membrane separates the air and water phases and offers resistance to the flow of air but allows free passage of water through the pores as long as the *HAE* ceramic pores are saturated (Figure 5.6). The maximum pressure that can be resisted by the surface tension offering resistance for air to pass through the saturated pores is referred to as the air-entry value; $(u_a - u_w)_b$, of the material. The air-entry value of ceramic is inversely proportional to the pore size and can be estimated using the principle of capillary forces equation (5.1) below.

$$\left(u_a - u_w\right)_b = \frac{2T_s}{r} \qquad \textbf{(5.1)}$$

where T_s = the surface tension at the air-water interface, r = the radius of the pore size of the *HAE* material or the ceramic.

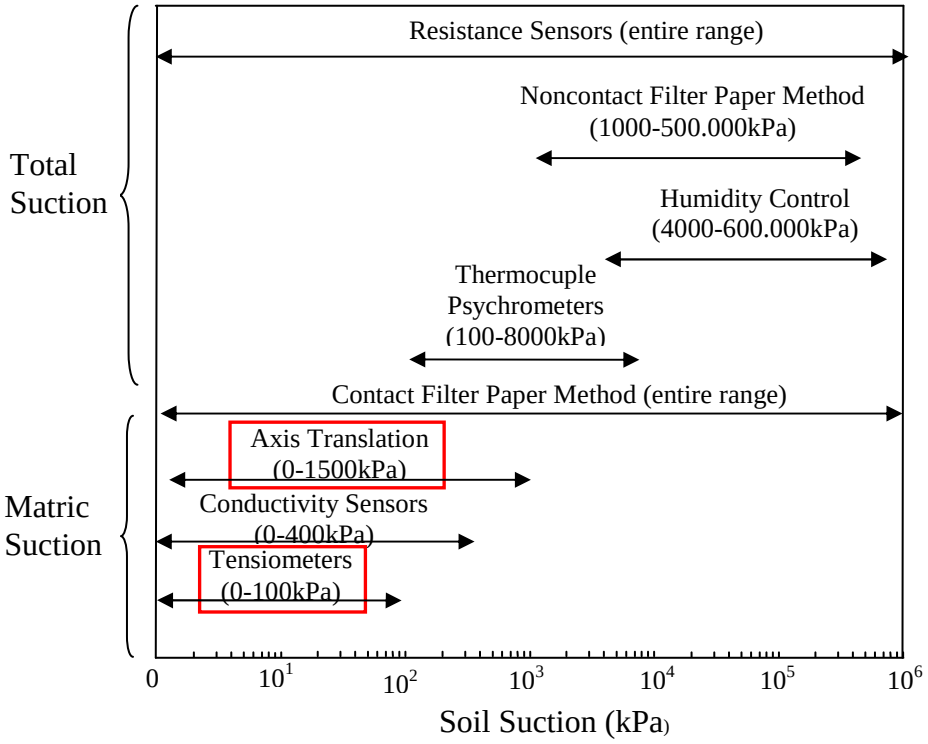

Figure 5.5 : Different suction measurement techniques (adopted from Lu and Likos, 2004).

The maximum matric suction that can be applied for testing unsaturated soils extending axis translation technique is the air-entry value of the ceramic. Free air starts passing through the pores of the *HAE* material when this specific value is exceeded. More details about the axis translation technique are available in a later section.

The *SWCC* (i.e. drying path) for a typical soil and idealized *SWCC* for a *HAE* material are shown to highlight the differences in the pore structure of the two different materials (Figure 5.7). The water drainage through the soil pores shows a smooth transition with increasing suction due to the non-homogeneous pore-size distribution. However, there is sudden transition in the *HAE* material beyond the air-entry value due to uniform pore-size distribution.

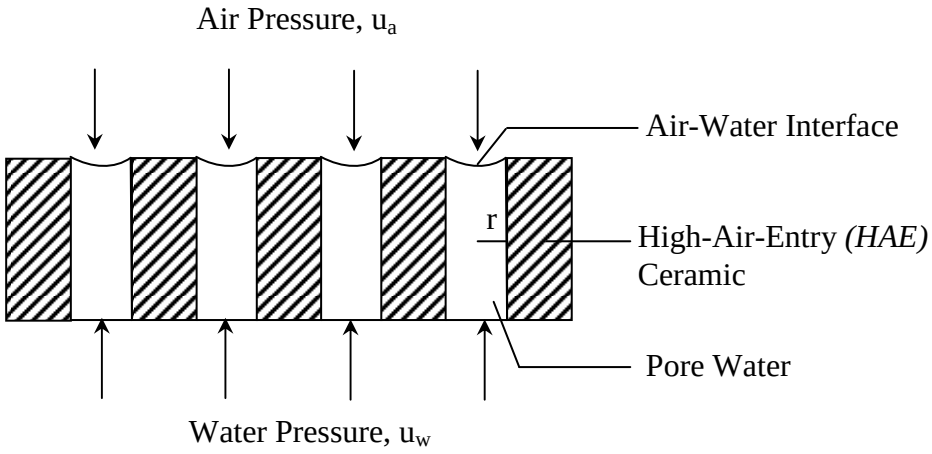

Figure 5.6 : Schematic representation of an High-Air-Entry *(HAE)* ceramic disc (Lu and Likos, 2004).

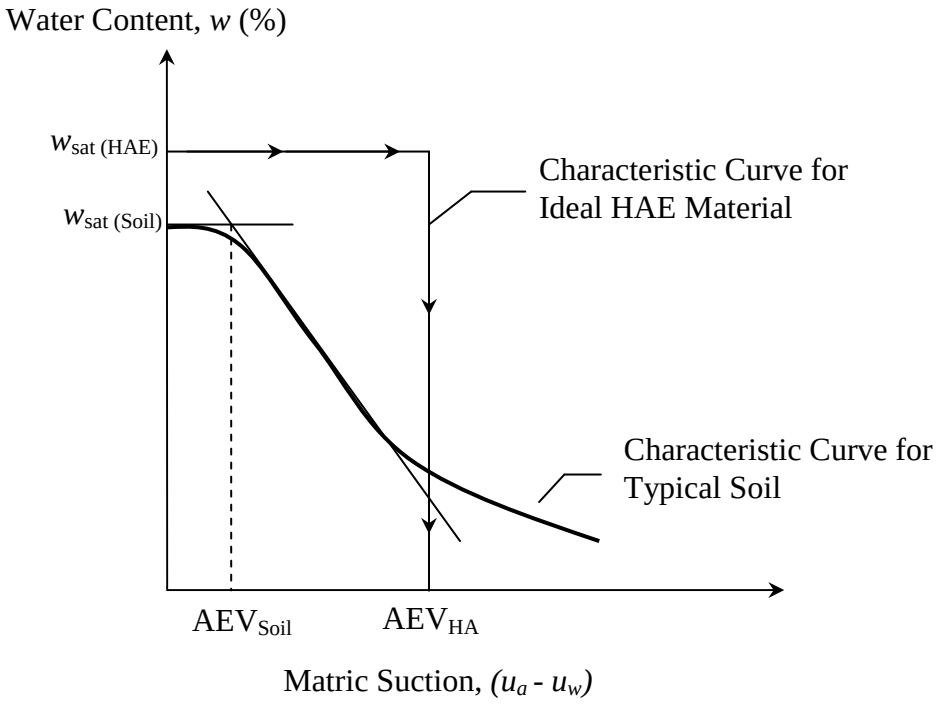

Figure 5.7 : Comparison of characteristic curves of a typical soil and HAE material (Lu and Likos, 2004).

5.4.2 Tensiometers

From a theoretical stanpoint of view, conventional Tensiometers are capable for measuring matric suction values of 100 kPa in soil samples without cavitation problems. However, several studies report problems associated with cavitation when suction of values of 80 kPa are measured (Vanapalli et al., 2003; Stannard, 1990; Vanapalli and Oh, 2011). Cavitation problems are enhanced due to the influence of impurities, dissolved gasses and air bubbles generated within the system.

Tensiometers consist of three main parts as: i) the sensing probe unit with a HAE ceramic tip, ii) water-filled body tube unit, and iii) measuring unit connected to the tube (i.e. pressure gauge) (Figure 5.8). A good contact is required between the saturated sensor tip and the soil in order to reliably measure matric suction. The negative pore water pressure in the soil results in flow of water from the Tensiometer to the soil through the saturated ceramic sensor tip. The water in the measurement system is in tension and is measured as the matric suction of the soil once the system reaches equilibrium condition (i.e. no flow of water occurs in or out of the Tensiometer at equilibrium conditions).

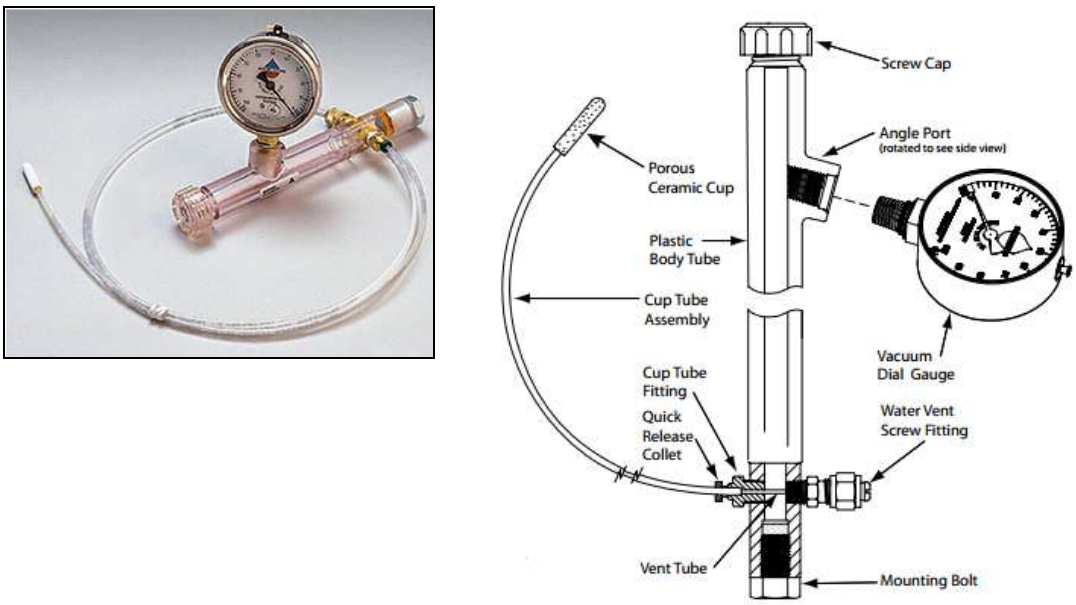

Figure 5.8 : A schematic diagram of laboratory tensiometer (Soilmoisture Equipment Corp., 2009).

5.4.3 Axis translation technique (ATT)

Hilf (1956) suggested axis translation technique for testing unsaturated soils with matric suction values greater than 101. 3 kPa (i.e. pore-water pressure lower than -101.3 kPa) without cavitation problems. This is achieved by elevating the atmospheric air pressure ($u_a = 0$) and negative water pressure ($u_w < 0$) to a condition of positive air pressure ($u_a > 0$) and pore-water pressure (to $u_w = 0$ or higher)) in a controlled environment (i.e. typically a chamber) for performing tests with unsaturated soil specimens (Figure 5.9).

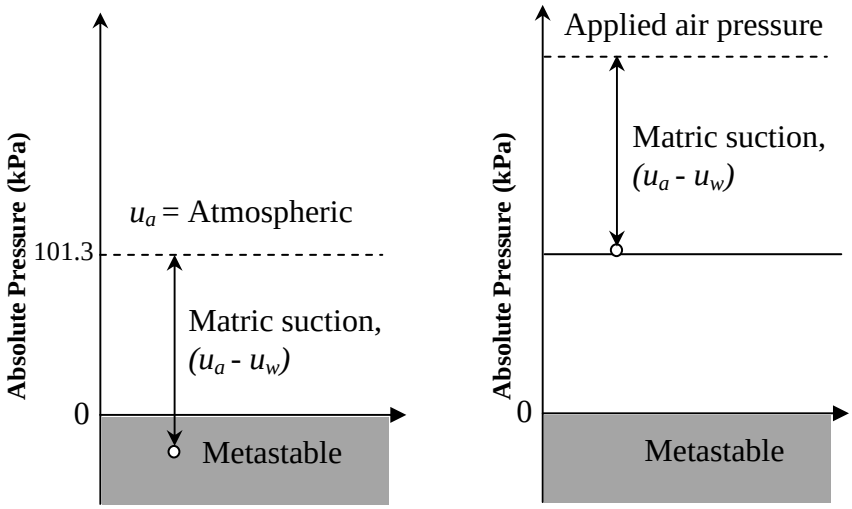

Figure 5.9 : Meaning of axis translation technique (Lu and Likos, 2004).

5.4.3.1 Modified null type pressure plate apparatus

The modified null pressure plate apparatus is used for the measurement of matric suction in statically compacted specimens (i.e. in the range of 20 – 500 kPa) applying the axis translation technique (Power and Vanapalli, 2011) (Figure 5.10). The apparatus consists of two main parts: i) Suction measurement unit, and ii) Flushing unit. The suction measurement unit has a pressure chamber which consists of brass cylinder and a brass cap through which the air pressure can be applied, an acrylic base with inlet and outlet tubes attached at the bottom connecting the pressure chamber to the flushing system, and a *HAE* ceramic disc (Figure 5.10a). The acrylic base has a special housing for placing a specimen ring of 20 mm in height and 50 mm in diameter (Figure 5.10b). The *HAE* disc with an air-entry value of 500 kPa is embedded inside this acrylic base maintaining a good contact with the test specimen. The *HAE* disc in the modified null pressure apparatus was saturated before performing matric suction measurements.

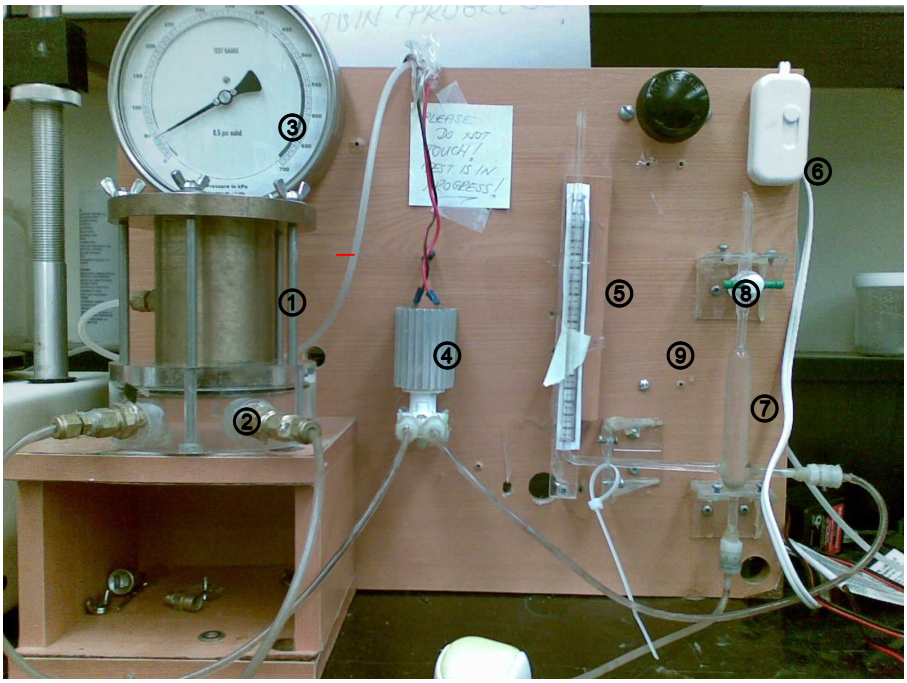

(a)

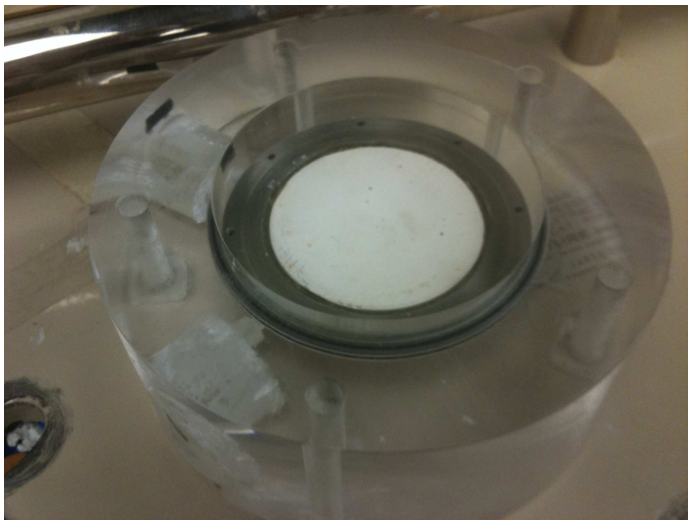

(b)

Figure 5.10 : (a) Modified null pressure plate apparatus for measurement of suction using the axis translation technique (①brass chamber, ② acrylic base,③pressure gauge, ④ peristaltic pump, ⑤ glass tube, ⑥ dimmer switch, ⑦air trap, ⑧stop-cock, ⑨reference marking), (b) acrylic base with *HAE*.

The initial, intermediate and equilibrium stages for measuring the matric suction of an unsaturated soil specimen are shown in Figure 5.11 (Power and Vanapalli, 2011). The initial position of the water level has to be marked on the glass tube as a reference level (i.e. approximately the mid-height of the specimen in the ring) before placing the specimen in the apparatus.

When an unsaturated soil specimen is placed on the saturated *HAE* disk, the water in the glass–tube tends to go into tension and level of water in the glass tube starts decreasing as water is imbibed into the specimen (Figure 5.11a).

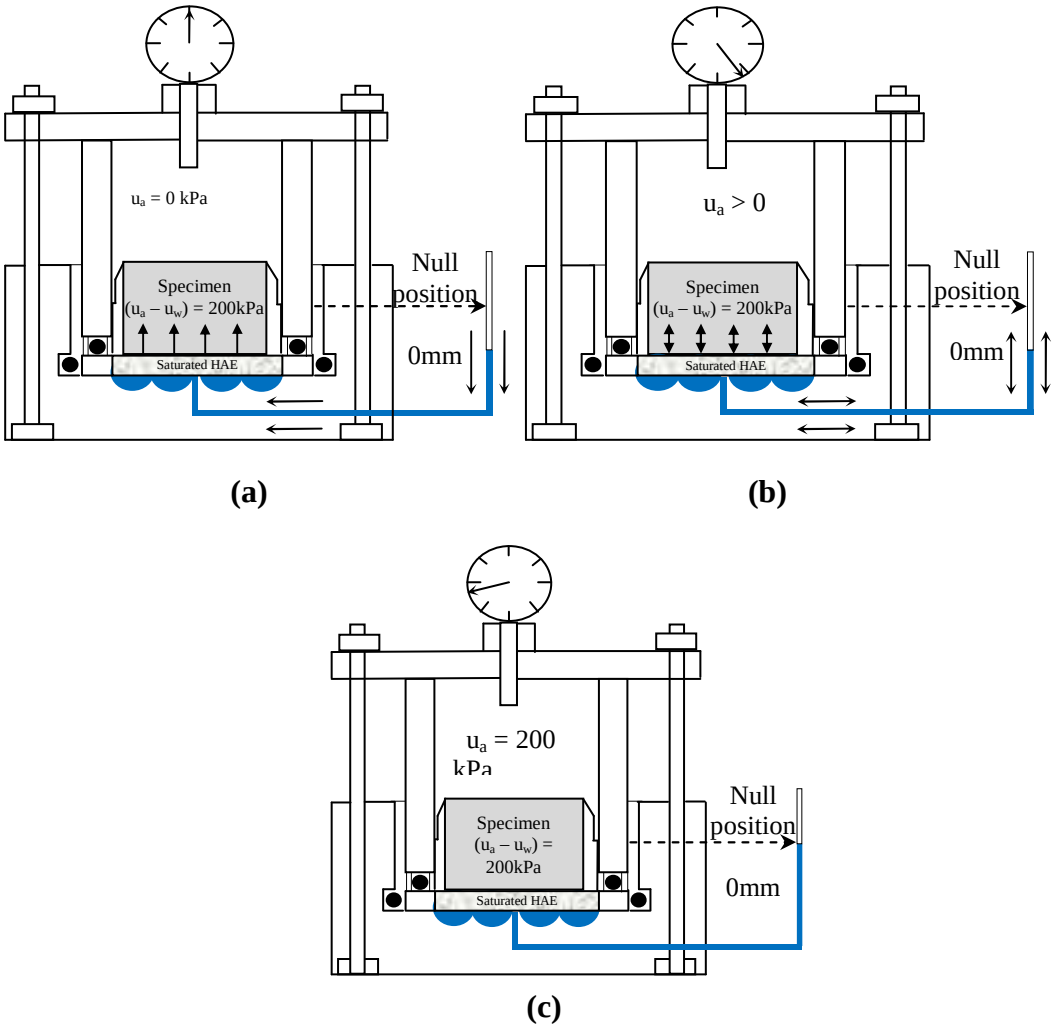

Figure 5.11 : Key stages followed during measuring matric suction with the modified null pressure plate apparatus: (a) İnitial condition (u_a = 0kPa), (b) Intermediate stage, (c) Final stage (u_a = matric suction value of the specimen). (modified after Power and Vanapalli, 2011).

The tendency of the water to go into tension should not be allowed by increasing air pressure (i.e. u_a > 0 kPa) in the chamber to bring the level of water back to its original position (Figure 5.11b). Eventually, an equilibrium condition will be attained (i.e. attains a “null” condition). At this stage water in the specimen will not further go into tension. The applied air pressure in the chamber to achieve “null” condition is the matric suction value as water pressure is equal to zero (i.e. numerically the negative pore-water pressure with respect to atmospheric pressure) (Figure 5.11c).

Air can get dissolved within the system and flows through the *HAE* disc and gets collected at the bottom of the disc when the axis translation test is performed for relatively longer period of times. The flushing unit of the modified null pressure plate apparatus is used for removing the accumulated air bubbles beneath the *HAE* disc to prevent erroneous measurements. The inlet and outlet tubes circulate water underneath the *HAE* disc with the help of peristaltic pump. The air-trap with stopcock allows to remove the accumulated air from the system to the atmosphere. The spiral grooves located within the acrylic base below the *HAE* ceramic disc provides a path to circulate water and helps to remove the accumulated air bubbles (Figure 5.12). The acrylic base is advantageous in comparison to metallic base as it facilitates seeing any air bubbles formed during testing with the naked eye.

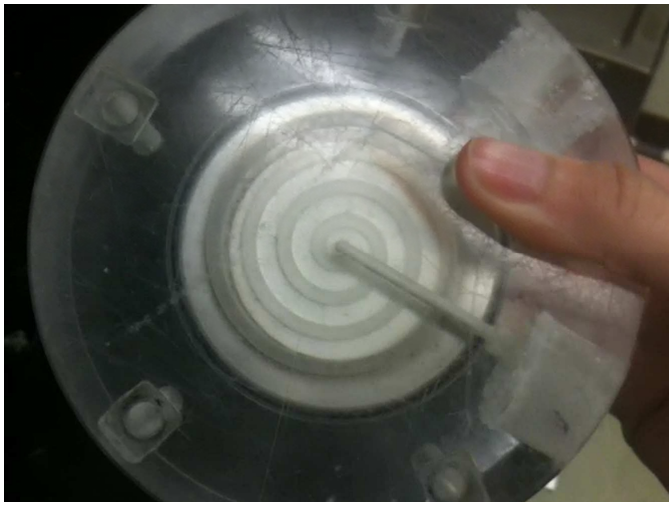

Figure 5.12 : Bottom view of the acrylic base with spiral grooves and the *HEA* ceramic disc.

5.4.4 Pressure plate apparatus for measuring *SWCC*

The *SWCC* are conventionally measured by using pressure plate apparatus for coarse and fine-grained soils (ASTM D 2325). Soil Moisture Equipment Corporation 1600 Model 5Bar Ceramic Plate Extractor was used in the present study. The equipment consists of a steel pressure chamber, measurement unit and a *HAE* porous ceramic disc. The working principle is the same as the modified null pressure plate apparatus. The suction application range is limited to the air-entry value of the ceramic plate which is 500 kPa. Figure (5.13a-b) shows a schematic drawing and a picture of a pressure plate apparatus.

The pressure plate apparatus consists of a ceramic plate covered on one side by thin Neoprene diaphragm sealed to the edges of the plate. An internal screen between the plate and the diaphragm provides a passage for the flow of water. The water reservoir is vented to the atmosphere through an outflow tube located on top of the plate, thus allowing the air pressure in the vessel and the water pressure in the reservoir to be separated across the air-water interfaces bridging the saturated pores of the *HAE* material (Figure 5.13a). An outlet stem running through the plate connects this passage to an outflow tube fitting, which connects to the atmosphere outside the extractor (Soilmoisture Equipment Corp., 2008).

The saturated soil specimens prepared in metal rings are placed on top of the previously saturated ceramic disc. Air pressure in the vessel is then increased to a desired level while pore water is allowed to drain from the specimens. As soon as air pressure inside the chamber is raised above atmospheric pressure, the higher pressure inside the chamber forces excess water through the microscopic pores in the ceramic plate and out through the outflow stem (Soil Moisture Equipment Corporation 1600 Model 5Bar Ceramic Plate Extractor Manual).

The outflow tube is connected to a burette with a piece of small diameter tubing and the outflow of water is monitored with this burette until it ceases. The burette reading will not measurably change for many hours or days once equilibrium condition is attained. At this point of time, it can be assumed that the specimen has reached equilibrium condition. The equilibrium period depends on the applied suction and the saturated coefficient of permeability of the soil specimen. The test is continued by increasing the pressure to determine the new equilibrium water content. Typically, six to eight pressures are applied with successive increments to be plotted as a relationship between the water content and the soil suction; this relationship is referred to as the soil-water characteristic curve (*SWCC*). The water content of the specimen at different equilibrium condition is determined from mass-volume relationships using back calculations after determining the water content of the specimen tested at the highest (and the last test) by oven drying. This equipment facilitates placing several specimens on the ceramic disk at the same time to simultaneously measure the soil-water characteristic curves.

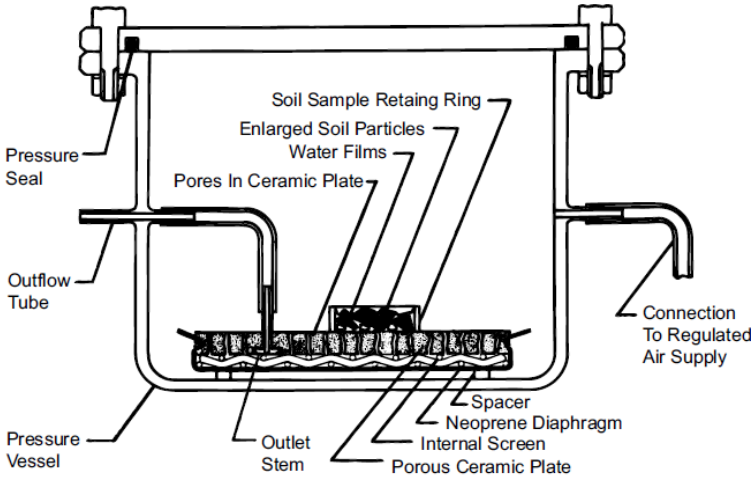

(a)

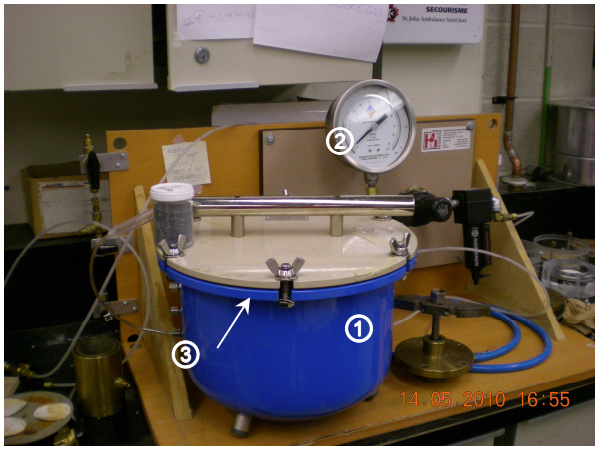

(b)

Figure 5.13 : (a) Schematic cross section of pressure plate axis translation apparatus (Soil Moisture Equipment Corp, 2008) and (b) photograph of pressure plate apparatus set up (University of Ottawa Geotechnical Lab.) ① Pressure vessel, ② Pressure gauge, ③ Outflow tube.

6. LABORATORY PROGRAM AND METHODOLOGY FOR TESTING MODEL PILES IN FINE-GRAINED SOILS

6.1 Introduction

This chapter provides the details of the laboratoy program and the methodology for testing model piles in fine-grained compacted soils. The proposed laboratory testing program to determine the influence of matric suction on the shaft bearing capacity of a single model pile is conducted in three stages. The first stage (i.e. Experimental Program-I) includes the soil sample preparation, determination of the soil properties and the compaction characteristics. In the second stage (i.e. Experimental Program-II), the matric suction values of the compacted soil specimens were measured using both the axis-translation technique and Tensiometers. In addition, the *SWCC* of compacted soil specimens were measured using the pressure plate apparatus. In the third stage (i.e. Experimental Program-III), the model pile load tests were carried out. The third stage also involves details related to the shear strength tests: direct shear (i.e. interface tests) and unconfined compression tests on statically compacted specimens to determine the shear strength behavior of pile-soil interaction.

6.2 Experimental Testing Program

The key objective of the test program was to determine the influence of matric suction on the ultimate shaft capacity of model piles placed in unsaturated fine grained soils. To achieve this objective, several series of model pile load tests were performed in both saturated and unsaturated compacted fine-grained soils under drained and undrained loading conditions. Table 6.1 summarizes the model pile load tests performed for different initial compaction water contenst, pile diameters, and drainage conditions. In total thirty model pile load tests were conducted.

Table 6.1 : Experimental Test Program.

Drainage Condition	Model Pile Diameters (mm)	INDIAN HEAD TILL						LOAM SOIL	
		w = % 13.2 (dry of optimum)		w = % 16.2 (dry of optimum)		w = % 18.8 (optimum)		w = % 13 (dry of optimum)	
		Saturated	As Compacted	Saturated	As Compacted	Saturated	As Compacted	Saturated	As Compacted
UNDRAINED (1.14mm/min)	10	✓	✓						
	15		✓						
	20	✓	✓		✓		✓	✗	✓
	30	✓	✓		✓		✓	✗	✓
	45	✓	✓		✓		✓		
DRAINED (0.012mm/min)	10								
	15		✓					✗	✓
	20	✓	✓		✓✓		✓	✗	✓
	30	✓	✓						
	45	✓	✓						

6.3 Determination of Properties of the Soils (Experimental Program-I)

Two different soils were studied in the research program. The first soil used in the study was Indian Head till from Saskatchewan, Canada. The second soil was Loam which is a low plasticity fine-grained soil obtained from Ottawa region, Ontario, Canada. In this first stage of the experimental testing program, the soil properties and compaction characteristics of both the tested soils were determined.

6.3.1 Soil suitability

The Indian Head till and Loam soil samples were chosen for this particular research study because of the reasonable equilibration times required for saturation/desaturation processes. Indian Head till soil is sandy clay and requires 5-7 days for reaching equilibrium conditions with respect to different matric suction values used in the present study. Loam soil is a low plasticity silty clay that requires about 2-3 days to reach equilibrium conditions.

The desaturation stages (capillary zone, transition zone, residual zone) for the *SWCCs* for both the soils, Indian Head till and Loam soil fall in the range of 0 – 500 kPa. The *SWCCs* for this range can be measured using the pressure plate apparatus. The matric suction values of the individually compacted soil specimens with different initial water contents were measured using the modified null pressure plate apparatus.

Both the Indian Head till and Loam soil are low plasticity fine grained soils that show engineering behavior characteristics in between the sandy and clayey type of soils. The shear strength behavior of both the soils have a significant influence due to the contribution of matric suction. Hence, it is also expected that there would be significant influence of matric suction on the ultimate shaft capacity of model piles for both these soils.

The unconfined compression test results for the Indian Head till and Loam soil compacted with different initial water contents are required for interepreting the model pile load test results. The compacted soil specimens can be prepared and tested relatively easily for determining the unconfined strength and *SWCC* for both the soils. Also, soil specimens have to be collected from the bearing capacity test

tank for conducting unconfined compression tests both under saturated and unsaturated conditions for intepretation of the test results. This is possible with both these soils.

6.3.2 Soil sample preparation

The soil collected from the field was first air-dried for several days and then subjected to gentle pulverization using a grinding machine. The grinding process lasted for two hours for preparing one bucket of soil that meets the standards for testing. The pulverized soil was then passed through a sieve with opening size of 2 mm (i.e. #10 sieve). The prepared soil for the entire testing program was put in a drum and rolled and stored (Figure 6.1). The soil required for testing was collected from the drum and oven dried for 24 hours. The oven dry soil was brought to the room temperature and pre-determined quantity of distilled water was added to achieve the required initial water content conditions for testing. The calculated amount of distilled water was sprayed on the dry soil sample using a spray bottle. The spraying was done in several layers on the soil and mixed with a spatula. The mixing was done carefully to achieve a homogenous soil-water mixture. The occluded soil particles formed, if any, during the soil mixing were removed.

Figure 6.1 : Rolling the sample in a barrel to obtain a uniform soil for use in the entire testing.

The prepared soil samples were put in tightly covered double plastic bags and stored in a humidity controlled box (moist room) for 3 days for curing. This procedure resulted in a uniform soil-water mixture with little or no soil-water clods for both dry and optimum water contents. After the standard 3 day curing period was completed, small samples were taken from each single plastic bag in order to check the water contents. Three different samples were taken from different locations of the bag. The water contents of the mixtures in all bags were approximately the same (i.e. ± 0.5 %). The small differences in water content may be attributed to evaporation losses or humidity changes during the mixing of soil and water.

6.3.3 Static compaction test

The compaction curves for both soils were obtained by statically compacting specimens at different water contents with a compaction stress of 350 kPa in a brass compaction equipment. The equipment details along with the compacted soil specimen are shown in Figure 6.2. The specimens were compacted in one layer into the specimen ring and the excessive part was trimmed by using a wire saw. The compaction effort was applied manually and controlled by a calibrated proving ring. The compaction curves for Indian Head till and Loam soil are shown in Figure 6.3 and Figure 6.4, respectively.

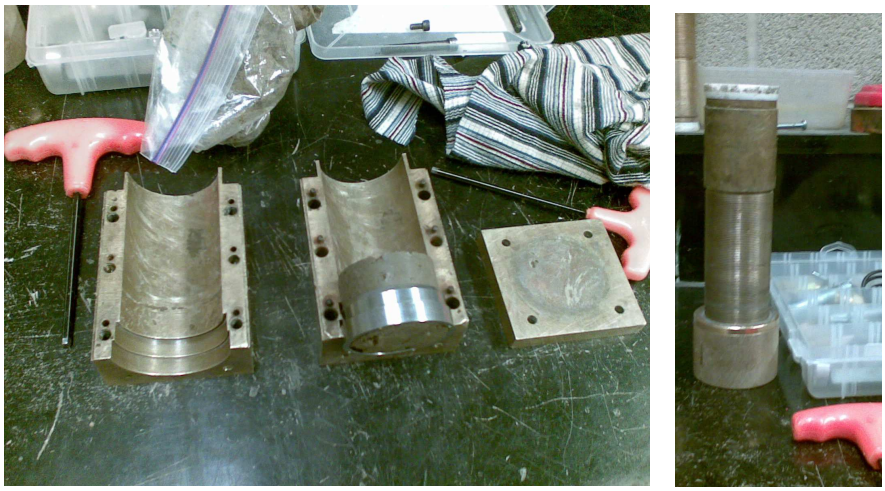

Figure 6.2 : Brass compaction mold and ram used for static compaction.

Three different water contents with values of 13% (dry of optimum), 15.5% (dry of optimum) and 18% (close of optimum) were chosen from the compaction curve for Indian Head till for testing. A water content value of 13% was chosen for Loam soil for this particular research study. The water contents chosen cover a wide range of

matric suction values. The matric suction measurements for different corresponding water contents of the compacted soil specimens was determined using the modified null pressure plate extending the axis translation technique. The details of the tests related to matric suction measurements are provided in later sections.

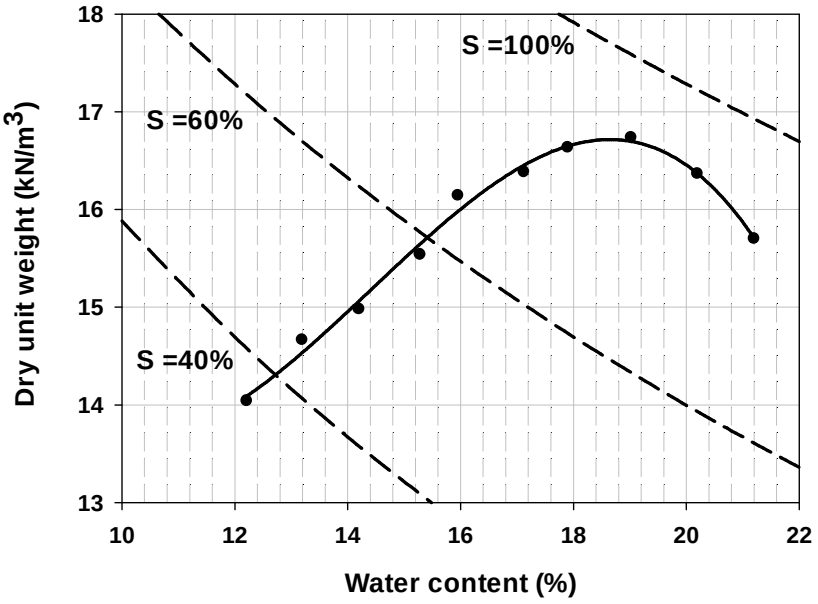

Figure 6.3 : Compaction curve for Indian Head till.

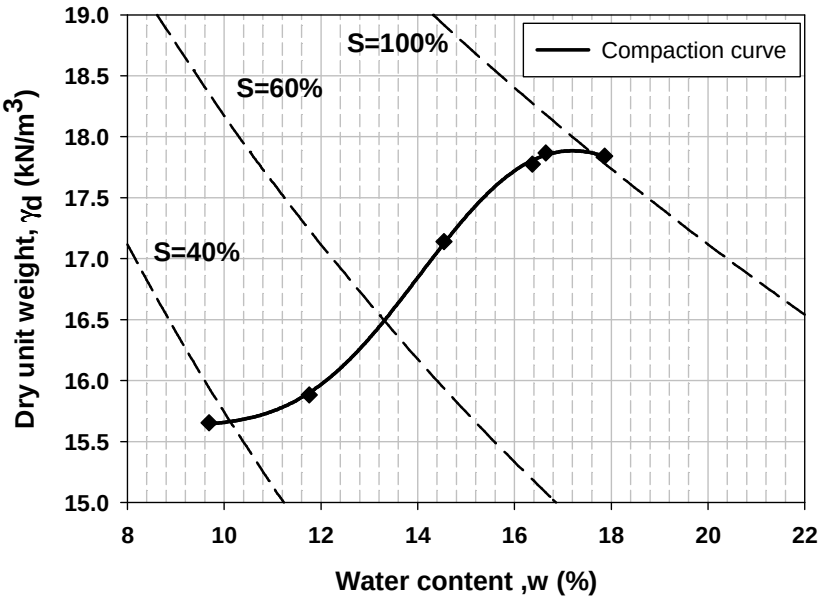

Figure 6.4 : Compaction curve for Loam soil.

6.3.4 Sieve analysis and Atterberg limit tests

The soil index properties, grain size distribution data and compaction results are summarized in Table 6.2.

Table 6.2 : Basic soil properties of the studied soils.

	Indian Head till	Loam soil
Soil Properties	Value	Value
Optimum water content, w_{opt} (%)	18.6	17.4
Maximum dry unit weight, γ_{dmax} (kN/m^3)	16.7	17.9
Saturated unit weight, γ_{sat} (kN/m^3)	20.0	21.0
Sand *(%)*	28	15
Silt *(%)*	42	75
Clay *(%)*	30	10
Liquid limit, *LL* (%)	32.5	25
Plastic limit, *PL* (%)	17	18.5
Plasticity index, I_p (%)	15.5	6.5
USCS	CL	CL-ML

6.4 Suction Measurements (Experimental Program-II)

6.4.1 Matric suction measurements using axis translation technique

Matric suction measurements were carried out on the statically compacted specimens prepared for the compaction curves (see 6.3.4) using modified null pressure appratus extending axis translation technique. Three Indian Head till soil specimens compacted at the water contents of 13% (dry of optimum), 15.5% (dry of optimum) and 18% (close of optimum) and one Loam soil specimen compacted at the water content of 13% were used. In addition, matric suction values of the specimens collected from the test tank after pile load tests were also measured. The specimens used for measuring matric suction were collected into metal rings of 50 mm in diameter and 20 mm in height using thin walled tubes attached to the rings.

The high air-entry (i.e. *HAE*) disc in the modified null pressure apparatus was saturated overnight by adding distilled water on top of the disc. The next day, low air pressures (i.e. less than 10 kPa) were applied to in the null apparatus further accelerate the saturation process. The stop-cock at the end of the air-trap was left open such that the air in the system can freely escape through it. The initial, intermediate and equilibrium stages were followed during the measurement of the matric suction of an unsaturated soil specimen with the modified null pressure plate apparatus as detailed in section 5.4.3.1. The measured matric suctions are summarized in Table 6.3 for the representative soil specimens that were used in the experiments.

Table 6.3 : The matric suction values measured by the axis translation technique.

Soil Type	$w_{initial}$	$(u_a - u_w)$	γ	γ_{dry}	e	S
	(%)	kPa	kN/m^3	kN/m^3	-	%
IHT	13.0	205	16.0	14.3	0.85	45
IHT	15.5	110	18.6	16.2	0.64	65
IHT	18.0	55	19.2	16.4	0.61	76
LS	13.0	80-90	18.0	16.0	0.6	55-58

6.4.2 Matric suction measurements using tensiometers : calibration and installation

The accuracy of matric suction measurements using the conventional Tensiometers are dependent on the degree of saturation of the sensor tip. Due to this reason, prior to testing, the sensor tips of the conventional Tensiometers were fully saturated (Figure 6.5). The ceramic probe acts as a hydraulic connection between the soil pore water and the water filled body tube and should be fully saturated before measuring the suction values.

The ceramic sensor tip was immersed in de-aired distilled water for several hours to fill the pores with water. Tensiometer system (i.e. plastic body tube) was filled with de-aired water and temporary vacuum was applied to remove air bubbles from the system. The sensor tip must be periodically resaturated through the service port if measurements over prolonged testing periods are required. The accumulated air in the nylon tube and in the plastic body tube must be removed. This precautionary measure assures the system to be sensitive to changes in soil suction values and provide reliable and reproducible measured suction values.

In addition, a good contact is required between the sensor tip and the soil in order to maintain a saturated link between the pore water and the measurement system. A thin wall tube with 6 mm diameter was used to create a hole in the soil for placing the sensor tip. The value on the guage measured after acheving equilibrium conditons is the soil suction (see Figure 6.5).

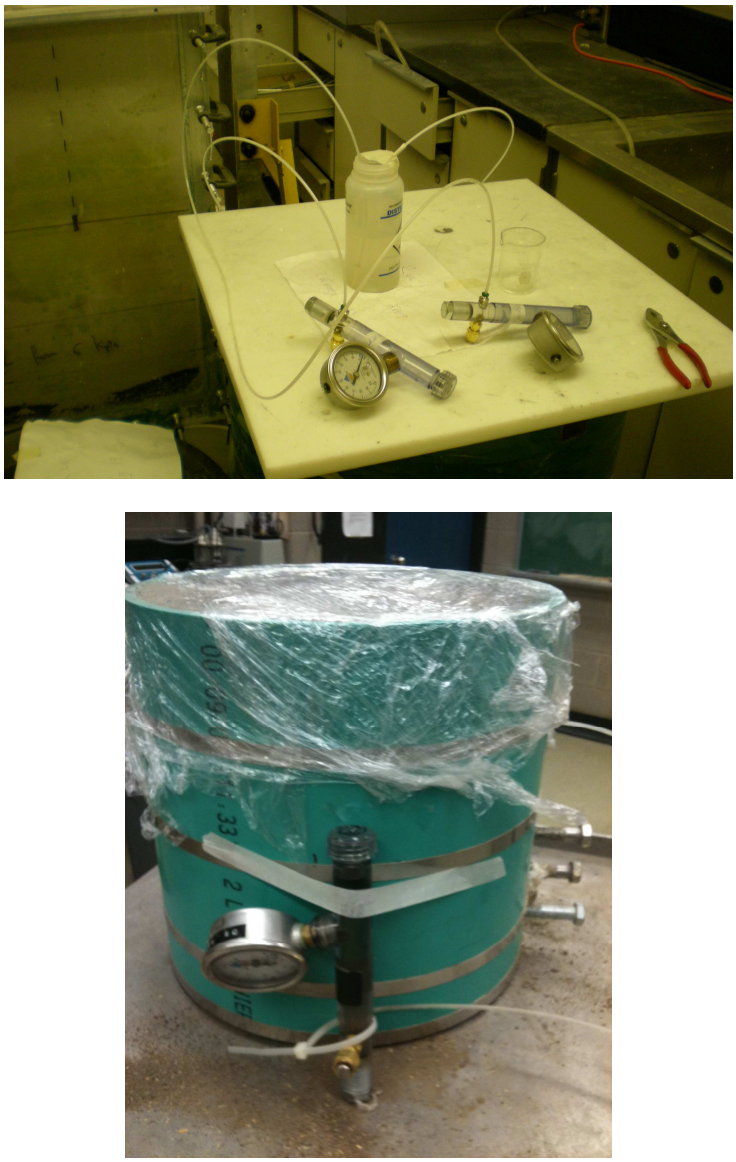

Figure 6.5 : Tensiometer saturating and its installation for measuring soil suction.

6.4.3 Testing procedure for developing the SWCC*s* using the pressure plate apparatus

The *SWCC* for drying path was established using the pressure plate apparatus for the specimens prepared by following the procedures detailed in section 5.4.4. Three Indian Head till specimens with initial water contents of 13%, 15.5% and 18% were prepared and two Loam soil specimens with the same initial water content of 13% were prepared. The soil specimen diameter was 50 mm and 20 mm height. The mass of the specimen ring (i.e. M_{ring}) and initial total mass of prepared specimens (i.e. $M_{ring} + M_{soil}$) were measured.

After saturating the ceramic plate, the soil specimens prepared in the rings were placed on the ceramic of the pressure plate apparatus for saturating them. The top and bottom of the specimens were covered with a filter paper in order to avoid loss of soil particles during saturation. A porous metal was placed on top of the specimens to prevent the possible swelling during the saturation process. The specimens were left submerged into the water with application of air pressure. Trial measurements showed that a time period of 5 days was required for saturating the specimen by reaching the target saturated water content determined by using the volume-mass relationships. The total mass of each individual samples were measured and recorded $(M_{ring} + M_{sat\text{-}soil})$. The specimen volume-mass properties were determined after saturation.

The saturated soil specimens were placed back into the chamber (Figure 6.6) to start the desaturation process for measuring the *SWCC* by applying a known value of air pressure. After reaching equilibrium condition under the applied air pressure (i.e. with respect to matric suction), the specimens were taken out and mass of specimen holder and specimen $(M_{ring} + M_{soil})$ were determined using a sensitive laboratory scale.

Figure 6.6 : Specimens placed into the pressure plate apparatus for SWCC measurements.

The water content/degree of saturation of the specimen at different equilibrium condition is determined from mass-volume relationships from back calculations after determining the water content of the specimen tested at the highest matric suction

(i.e. last test) by oven drying. Air-pressure values of 10, 20, 50, 100, 150, 200, 250, 300, and 400 kPa were respectively applied with successive increments in the present study for establishing the *SWCC*. A time period of 2 days was required for achieving equilibrium conditions under each applied value of suction.

6.5 Testing Procedures for Model Pile Load Tests (Experimental Program-III)

As summarized in Table 6.1, Experimental Program-III involves the model pile load tests, interface tests (i.e. direct shear) and unconfined compression tests performed on statically compacted specimens. Model piles were tested under saturated and as compacted condition under drained and undrained loading conditions.

The soil sample in the test tank was compacted statically in five layers with a compaction energy 350 kPa using loading rate of approximately 5 mm/min with a specially designed compactor. The static compaction energy was controlled by a calibrated loading ring. After completion of compaction of each layer, the soil surface was scarified in order to maintain continuity between the successive layers of the compacted soil.

The flow chart shown in Figure 6.7 summarizes model pile load testing program.

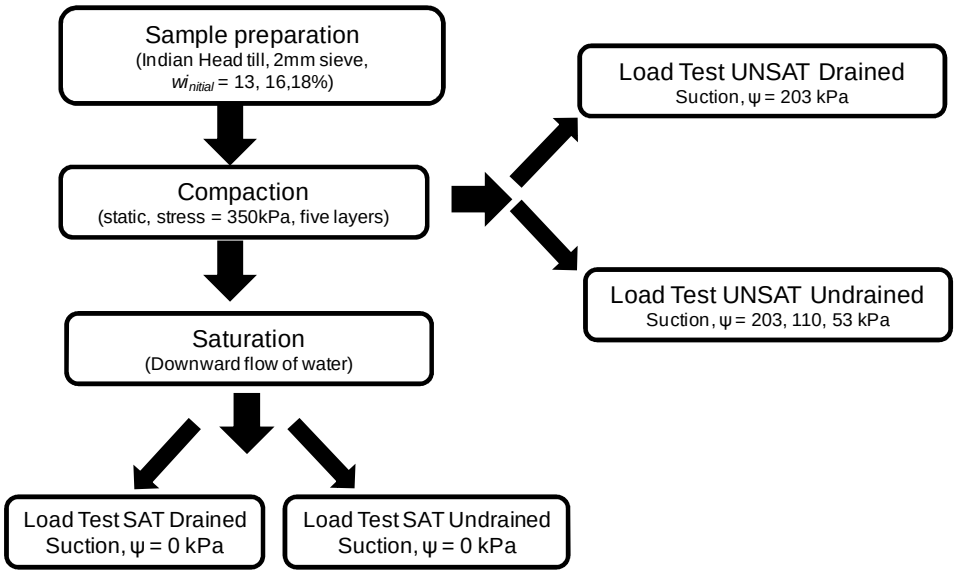

Figure 6.7 : Flow chart for testing program using Indian Head till.

6.5.1 Model pile load tests in compacted soil with uniform suction profile

After statically compacting the soil in the bearing capacity tank, thin wall tube was pushed down to a depth 220 mm to create a hole for pile installation without

overstressing the soil that will surrounding the model pile. Penetration of the tube and model piles was conducted by operating a loading machine at a rate of approximately 5.0 mm/min.

After the thin wall tube reached to a depth of 220 mm down in the compacted soil, it was removed with the soil by operating the loading machine in the opposite direction (Figure 6.8). The outer diameter of the tube is slightly less than the model pile diameter. This procedure was followed to ensure a good contact between the soil and the surface of model pile shaft for determining the total shaft resistance. One of the important precautions is to assure perfect alignment of the model pile with the created hole.

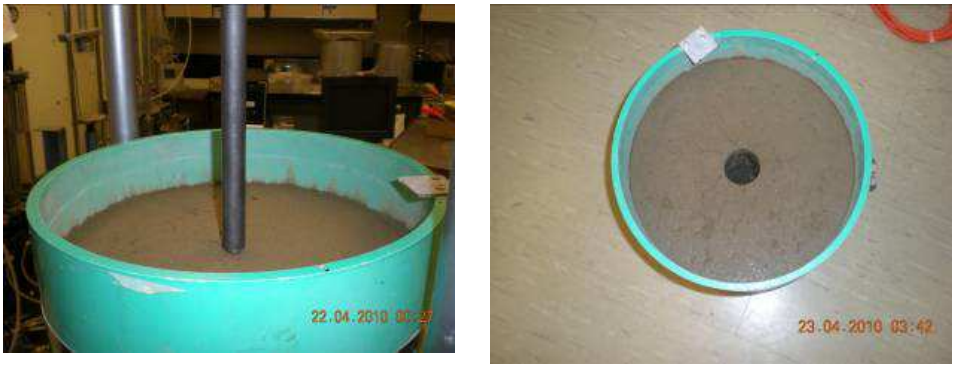

Figure 6.8 : A hole created in the compacted soil using thin-wall steel tube for installing the model pile.

6.5.2 Model pile load tests under saturated condition (SAT)

The compacted soil in the tank was saturated by gradually allowing downward flow of water from top of the soil through the compactor which had apertures. During the saturation process, the compactor plate was placed on top of the compacted soil sample and fixed to the loading frame to avoid possible volume change due to swelling, if any. A piezometer attached to the side of the tank was used to check saturation of the compacted soils. The saturation of the compacted soils was assumed to have been achieved when the level of water in the piezometer reached the same water level within the test tank (Figure 6.9). Matric suction was also directly measured with a Tensiometer that was placed in the compacted soil to check the degree of saturation. The Tensiometer reading of $(u_a - u_w)$ = 0 kPa provided another indication that the compacted soil is saturated. In addition to these checks, small chunks of soil specimens were collected from the tank for water content measurements after determining the ultimate shaft capacity of the model pile. The

average water content from these tests was determined and the corresponding degree of saturation was calculated from mass-volume relationships.

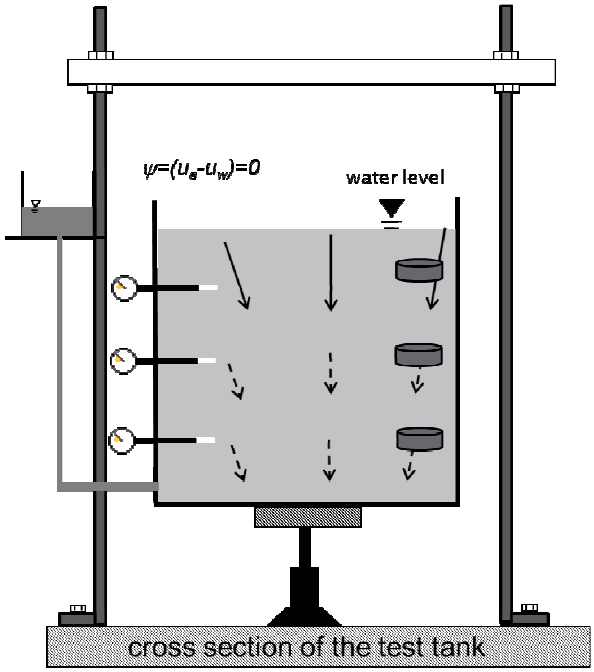

Figure 6.9 : Schematic representation of the bearing capacity tank saturation.

The model pile was jacked down to a depth of 200 mm in the drilled hole, leaving a void of 20 mm in length below the pile toe. In other words, the void facilitates in the measurement of shaft resistance over a length of 20 mm during model pile loading without any contribution from the end bearing resistance (Figure 6.10). The same procedure as in the installation of the casing is followed while installing the model pile.

The drained and undrained tests differ from each other in terms of loading rate. Previous studies on Indian Head till compacted samples show that drained conditions can be achieved in soil specimens when they are loaded at a strain rate of 0.0102 mm/min to 0.0132 mm/min (Gan et al., 1988; Vanapalli et al., 1996). In the present study, a strain rate of 0.0120 mm/min was chosen for loading the model pile to achieve drained loading conditions. A relatively fast loading rate of 1.14 mm/min was used to simulate undrained loading conditions.

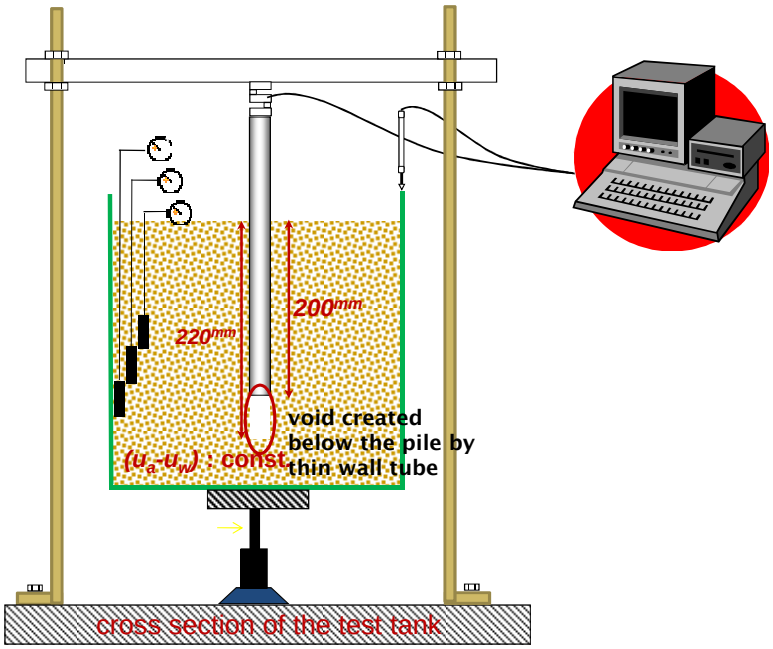

Figure 6.10 : Schematic of the model pile test set-up.

6.6 Determination of the Shear Strength Parameters of the Studied Soils

Pile shaft resistance developed along the pile-soil interface is controlled by the shear strength parameters of the soil. The local shaft failure is governed by the Coulomb effective stress interface friction law for drained loading conditions. However, the failure characteristics are dependent on the undrained shear strength, c_u, of soil for undrained loading condition. The shear strength parameters determined from these tests were used to interpret the pile load test results using the proposed modified α, β, and λ methods.

6.6.1 Single stage direct shear tests: interface tests

The direct shear box interface tests were conducted on Indian Head till and Loam soil specimens prepared at 13%, 15.5%, 18% and 13% of initial water contents respectively for both saturated and unsaturated (i.e. as compacted condition) conditions. The interface strength parameters (i.e. c_a and δ) were used to estimate the ultimate shaft resistance of tested model piles for drained loading conditions using the modified proposed β method.

The direct shear box dimensions were 60 mm x 60 mm. The interface plate with same dimensions was prepared using the same material and roughness characteristics as the model pile to simulate the actual loading conditions. Interface plate was placed

into the lower part of the shear box. The top and lower parts of the direct shear box were fastened each other and the prepared soil sample was compacted in one layer using 350 kPa of stress level into the upper box. Porous plate and loading cap were placed afterwards. Tests were conducted applying three normal stress values of 200 kPa, 350 kPa and 450 kPa.

For conducting direct shear tests, the soil specimens were first saturated for a period of 24 hours and then consolidated for another 24 hours under the applied normal stress. The vertical movements of the specimen during the consolidation stage were monitored until no further settlements were observed. The specimen was sheared at a rate of 0.012mm/min after it was consolidated. The photograph given below in Figure 6.11 shows the contact surfaces after the test was completed.

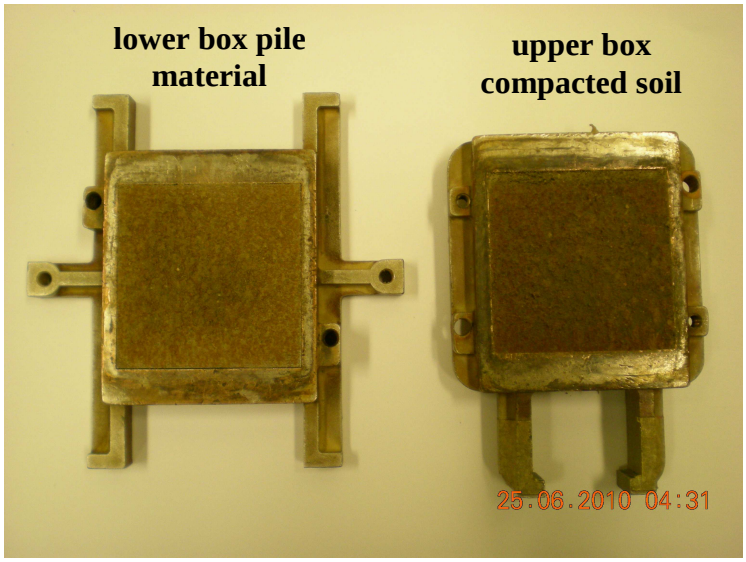

Figure 6.11 : Interface Direct shear box test (after the test).

6.6.2 Testing procedure for unconfined compression tests

The undrained strength of the soil specimens were determined from unconfined compression tests. The undrained shear strength values determined were used to estimate the ultimate shaft resistance of tested model piles for undrained loading conditions using the modified α and λ methods. The unconfined compression tests were conducted on both saturated and unsaturated (i.e. as compacted condition) soil specimens.

6.6.2.1 Saturated tests

Soil specimens of 50 mm in diameter and 100 mm in length were extracted from at least two different locations of the test tank immediately after completing the model pile load tests using the thin wall sampling tubes (50mm in diameter and 120 mm in length) (Figure 6.12a). The specimens were collected approximately at a distance of 4*d* or greater (*d* = diameter of the model pile) from the tested pile outside the displacement envelope to ensure that the stresses associated with pile loading on the collected soil specimens were negligible (Robinsky and Morrison, 1964; Vesic, 1977). The tubes were pushed down into the soil slowly and the specimen was extracted from the sampling tube with care to minimize the disturbance. (Figure (6.12b)).

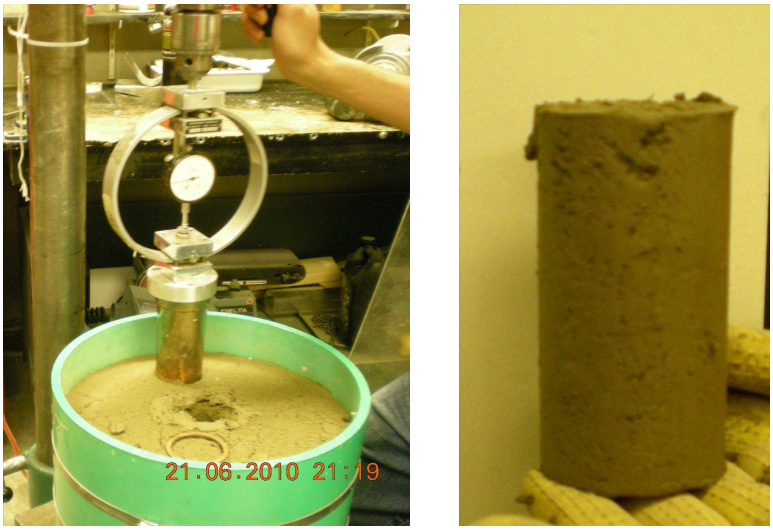

(a) **(b)**

Figure 6.12 : (a) Soil specimen extraction technique from the bearing capacity test tank (b) Specimen extracted from the test tank for conducting unconfined compression test (saturated sample).

6.6.2.2 Unsaturated tests (as compacted condition)

Information of unconfined compression test results is necessary for interpreting the model pile tests that were conducted in the compacted soil. The soil specimens required for conducting these tests were prepared at the same water content and compaction stress. In addition, soil specimens were also extracted from the bearing capacity tank for conducting unconfined compression tests after completing the model pile load tests. The unconfined compressive strength was determined from soil

specimens by loading them at a rate of 1.14 mm/min. The same rate of strain was also used for conducting the model pile load tests under undrained loading condition.

6.7 Summary

A comprehensive experimental program was undertaken to study the influence of matric suction on the shaft bearing capacity of model single pile placed in two different fine-grained compacted soils (i.e. Indian Head till and Loam soil). Model pile diameters of 10 mm, 15 mm, 20 mm, 30 mm and 45 mm were used in the study. In addition to model pile tests; several other tests that include the matric suction measurements, *SWCC* determination and strength measurements were also conducted. These tests are necessary for the interpretation of the model pile load test results using the modified α, β, and λ methods. The results of the testing program undertaken are reported and analysed in the next chapter.

7. PRESENTATION AND INTERPRETATION OF MODEL PILE LOAD TEST RESULTS IN COMPACTED FINE-GRAINED SOILS

7.1 Introduction

The proposed test program summarized in Table 6.1 were performed following the procedures described in Chapter 6. The results of model pile tests, matric suction and shear strength measurements are presented and interpreted in this chapter. The difficulties associated with performing some of these tests are also detailed.

Model pile load tests were conducted on two different soils : i) Indian Head till, ii) Loam soil prepared at different initial compaction water contents.

The tests on Indian Head till soil sample compacted at an initial water content of $w_{initial}$ = 13% (i.e. dry of optimum condition) and for saturated condition. The soil compacted at two other different initial water contents, one with an $w_{initial}$ =16% (i.e. also representing dry of optimum condition) and another wih an $w_{initial}$ = 18% (i.e. close to optimum) were also tested As compacted condition tests (hereafter referred to as ASCOMP) provide uniform matric suction profile throughout the bearing capacity tank in which the model piles were tested.

The tests on Loam soil were performed for as compacted condition on samples prepared at an initial water content of $w_{initial}$ = 13% (i.e. dry of optimum).

7.2 Suction Measurements and SWCC*s*

The *SWCCs* were established using pressure plate apparatus following the procedures detailed in Chapter 6 (see section 6.4.3) on specimens that were compacted in metal rings with a compaction stress of 350 kPa. The static compaction stress used for preparing soil sample in the bearing capacity tank for testing the model piles and the specimens for measuring the *SWCC*s was the same. In other words, identical conditions were maintained for reliable interpretation of the

test results. The *SWCCs* for Indian Head till and Loam soil are given in Figure 7.1 and Figure 7.2, respectively.

The measured *SWCCs* of the Indian Head till compacted at different initial water contents are different from each other due to the effect of soil structure. The soil compacted at an initial water content of 13% (i.e. dry of optimum condition) exhibits flocculated structure (i.e. more open pores) and desaturates at a relatively faster rate in comparison to the same soil compacted at higher initial water contents of 16% and 18%. The soil compacted at 16% is less flocculated and the soil compacted at 18% exhibits close to dispersed structure. The soil compacted with a higher water content offers more resistance to desaturation due to influence of soil structure. The *SWCC* results in the present study are consistent with the results of Vanapalli et al. (1999).

7.3 Model Pile Load Tests

Model pile load tests were performed as displacement controlled tests. Previous studies on Indian Head till compacted samples show that drained conditions can be achieved in soil specimens when they are loaded at a strain rate of 0.0102 mm/min to 0.0132 mm/min (Gan et al., 1988; Vanapalli et al., 1996). In the present study, a strain rate of 0.0120 mm/min was chosen for loading the model pile to achieve drained loading conditions. A relatively fast loading rate of 1.14 mm/min was used to simulate undrained loading conditions. In this section, model pile load test results performed under both drained and undrained loading conditions.

7.3.1 Procedure to estimate and control the matric suction

The soil was compacted in the test tank following the procedures detailed in Chapter 6 to achieve uniform water content and matric suction profile. Thin walled sampling tubes (20 mm of inner diameter, 100 mm of length and 0.02 mm of wall thickness) and stainless steel metal rings (20 mm of height and 50 mm of diameter) were used to collect samples from different depths of the test tank for water content, *(w)*, degree of saturation, *(S)*, void ratio, *(e)* and matric suction measurements after the pile laod test was completed. Model pile test results load versus displacement (p-δ) plots are presented with the corresponding water content and matric suction profile.

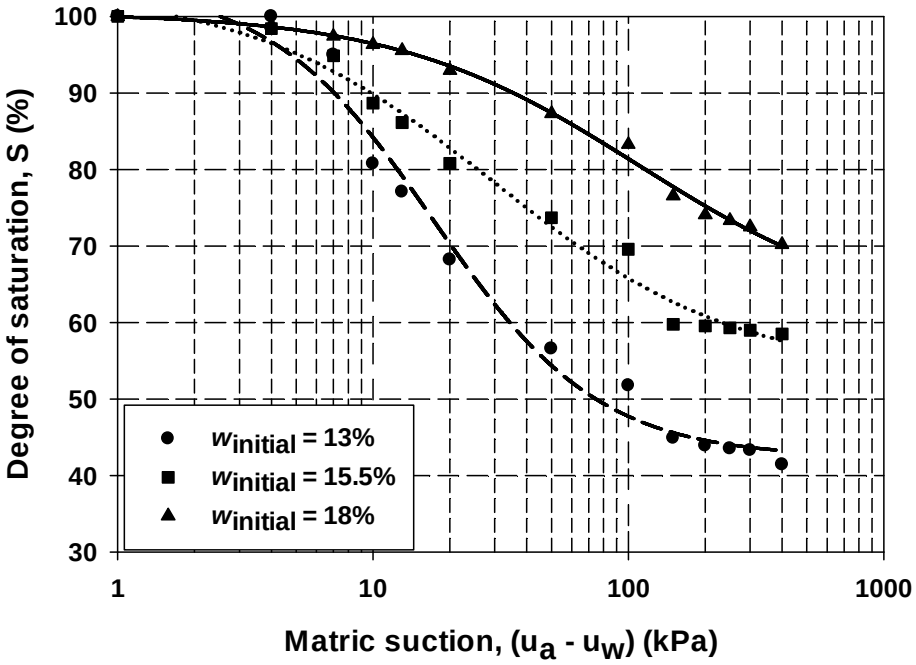

Figure 7.1 : *SWCCs* for Indian Head Till specimens prepared at different inital water contents.

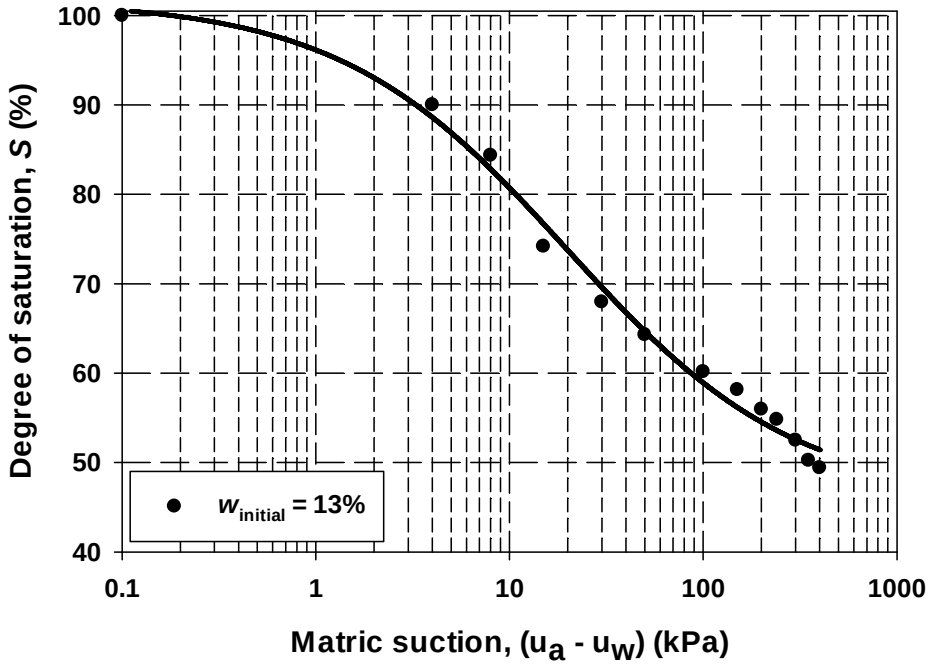

Figure 7.2 : *SWCC* for Loam soil specimen prepared at an inital water content of 13%.

7.3.2 Model pile failure criteria

In engineering practice, it is typically assumed that the ultimate total load bearing capacity of a single pile is reached at vertical displacement of 10% of the pile diameter (Potts and Zdravkovic, 2001). However, the ultimate shaft resistance for the model piles mobilized at smaller displacements which is less than 1%~2% of the pile diameter. This displacement is assumed to be the failure criteria in the present study to define the ultimate shaft bearing capacity for model pile load tests.

7.4 Model Pile Load Test Results: Indian Head till (Test Series No. 1)

In Test Series No.1, model piles were tested placed in Indian Head till soil sample at different compaction water contents ($w_{initial}$ = 13%, 15.5%, 18%). Each individual test is named refering to the Soil Type - Test Condition - Initial compaction water content - loading condition (i.e. IHT.ASCOMPAC.13.UD).

7.4.1 Test results of IHT.ASCOMPAC.13 : (matric suction = 205 kPa)

The variation of water content with respect to depth conducted for model pile results conducted on soil samples (i.e. as compacted condition) compacted at an initial water content of 13% are summarized in this section. This water content corresponds dry of optimum condition (i.e. -5% of OMC) having an average matric suction value of 205 kPa. The dry of optimum conditions were chosen for this first test series since it is relatively easier to achieve uniform conditions throughout the specimen and also relatively quicker to saturate the sample in tank due to the flocculated soil structure.

Water content values obtained along the compacted soil profile are summarized in Table 7.1. The matric suction distribution diagram obtained from the *SWCC* using the measured water content data is presented in Figure 7.3. Two additional soil specimens were also collected at depths of 50 mm and 100 mm from the surface for matric suction measurement using the axis translation technique (Table 7.2).

Table 7.1 : Water content values with depth.

Depth (mm)	0	20	75	150	200	300
w (%)	12.5	13.1	13.3	13.0	12.8	13.0

The matric suction values measured by axis translation technique on the soil samples collected from the test tank were also shown in Figure 7.3. The results are summarized in Table 7.2.

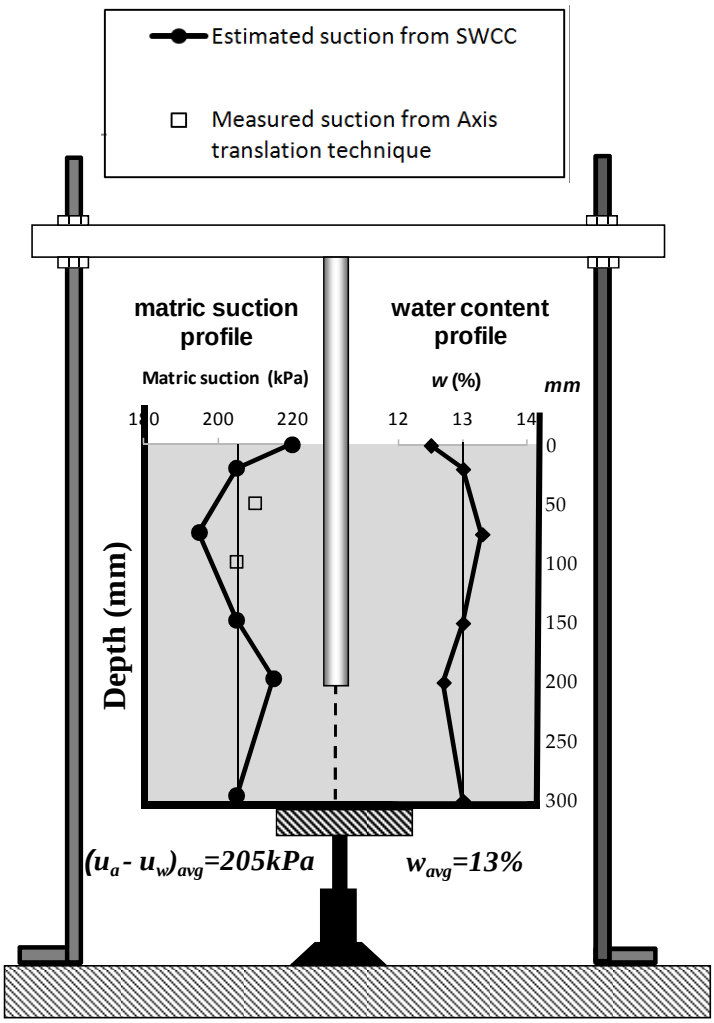

Figure 7.3 : A schematic illustration of the matric suction and water content profile for IHT.ASCOMPAC.13.

The water content values summarized in Table 7.1 shows that the water content was uniform throughout the depth. To avoid air-drying during testing, wet paper towels were placed on the surface of the compacted soil and the surface of the test tank was covered with a plastic wrap to minimize the evaporation losses. All the tests were conducted in humidity controlled laboratory environment.

Table 7.2 : Soil properties for the compacted saturated soil in the test tank for IHT.ASCOMPAC.13.

Depth	Sample type	$(u_a - u_w)$	γ_n	γ_{dry}	e	w	S
mm		kPa	kN/m^3	kN/m^3	-	%	%
50	Ring	215	19.14	14.5	0.87	12.7	0.43
100	Ring	205	18.90	14.5	0.87	12.8	0.45

7.4.1.1 Test results of IHT.ASCOMPAC.13.UD

IHT.ASCOMPAC.13.UD tests were performed using piles of different diameters; namely, 10 mm, 15 mm, 20 mm, 30 mm and 45 mm and are referred as D10-D15-D20-D30-D45 model piles. The p-δ behavior of different pile diameters are summarized in Figure 7.4. From the p-δ behavior for the tested piles, it can be seen that the shaft capacity is fully mobilized of between 0.2 mm to 0.5 mm of vertical displacement which corresponds to 1-2% of the pile diameter defined with the failure criteria. Reasonably well defined peak value can be observed for D10-D15 and D20 piles however this behavior is not observed for piles D30 and D45.

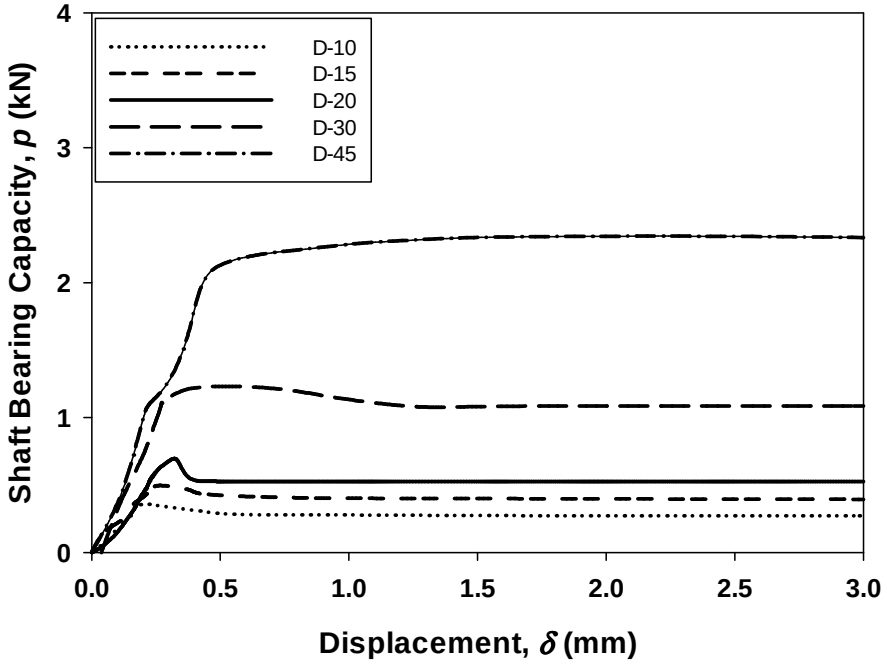

Figure 7.4 : p-δ behavior of IHT.ASCOMPAC.13.UD for piles D10-D15-D20-D30-D45.

7.4.1.2 Test results of IHT.ASCOMPAC.13.D

IHT.ASCOMPAC.D refer to the the model pile tests performed on as compacted Indian Head till and tested under drained loading condition. Tests were performed for piles D20, D30 and D45. The test results are summarized in Figure 7.5. The p-δ behavior of piles D20 and D30 shows a peak value as expected around 0.2 to 0.3 mm of vertical displacement. The trends of the p-δ behavior are consistent with the expected trends. These results indirectly suggest a good contact between the pile material and the surrounding soil.

The load-displacement behavior of model pile-D45 however shows no significant peak value but reaches a constant value of ultimate shaft capacity at a displacement value of 1.2 mm. This value is higher than the expected failure displacement value which may be associated with loss of contact between the pile and soil and also due to some degree of disturbance during installation.

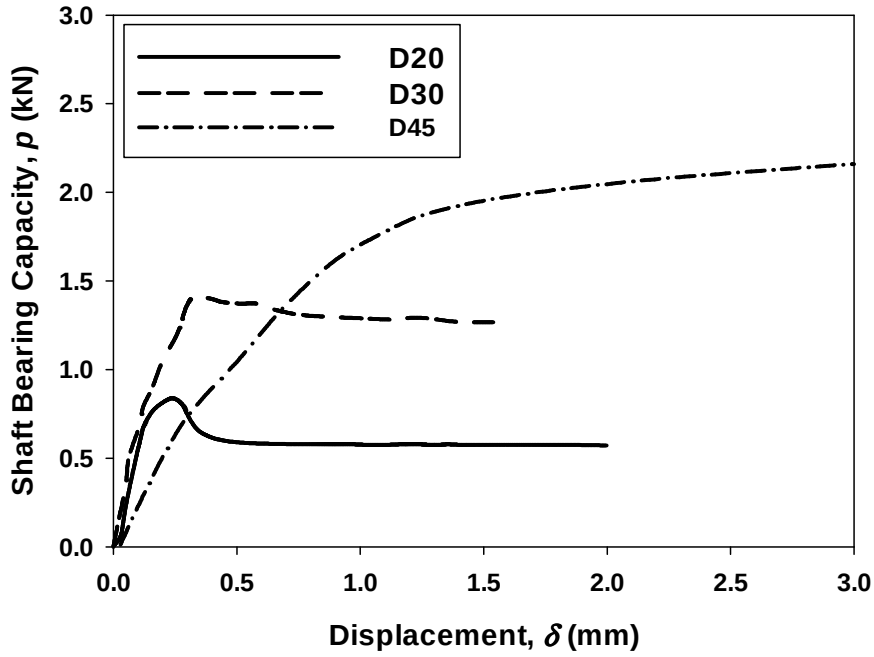

Figure 7.5 : p-δ behavior of IHT.ASCOMPAC.13.D test for Pile-D20-D30-D45.

7.4.2 Test results of IHT.SAT.13

The second set of tests were performed with the compacted soil under saturated condition with an initial compaction water content of 13%. The saturation process was performed following the procedures detailed in Chapter 6 (see 6.5.2). The compacted soil in the test tank was saturated using a downwards flow of water

simulating natural flow behavior in field conditions (i.e. infiltration and flooding). Saturation of the compacted soil in the tank was confirmed using three different methods; which included Tensiometer measurements, piezometer reading observations, and from volume-mass relationships.

Prior to starting the tests, three Tensiometers were placed in the compacted soil of the bearing capacity tank at depths of 50, 100 and 150 mm from the surface. All the Tensiometer recorded zero matric suction confirming the saturated conditions of the compacted soil. In addition, the water level in the piezometer connected to the base of the plastic tank was the same as the water level in the test tank assuring saturated condition of the compacted soil. Water content values were measured collecting samples from various depths after the model pile tests were conducted. The samples were collected in the region where the soil was not disturbed due to the loading of the model pile. The average water content was determined as 31% which corresponds to the degree of saturation of 96% or higher from the volume-mass relationships (Table 7.3). All the three techniques provide evidence that the soil sample compacted in the bearing capacity tank was saturated. Figure 7.6 shows a schematic illustration of the model pile load test under saturated condition. The following table summarizes the data obtained from saturation checks.

Table 7.3 : Soil properties for the compacted saturated soil in the test tank for IHT.SAT.13.

Depth	Sample Type	$(u_a - u_w)$*	γ_n	γ_{dry}	e	w	S
mm	-	kPa	kN/m^3	kN/m^3	-	(%)	(%)
0	Tube+M.Can	0	19.14	14.5	0.87	32	100
50	Tube	0	18.90	14.5	0.87	31	96
150	Tube	0	19.00	14.5	0.87	31	96
250	M. Can	-	-	-	-	30	-

*Measured by using the conventional tensiometers.

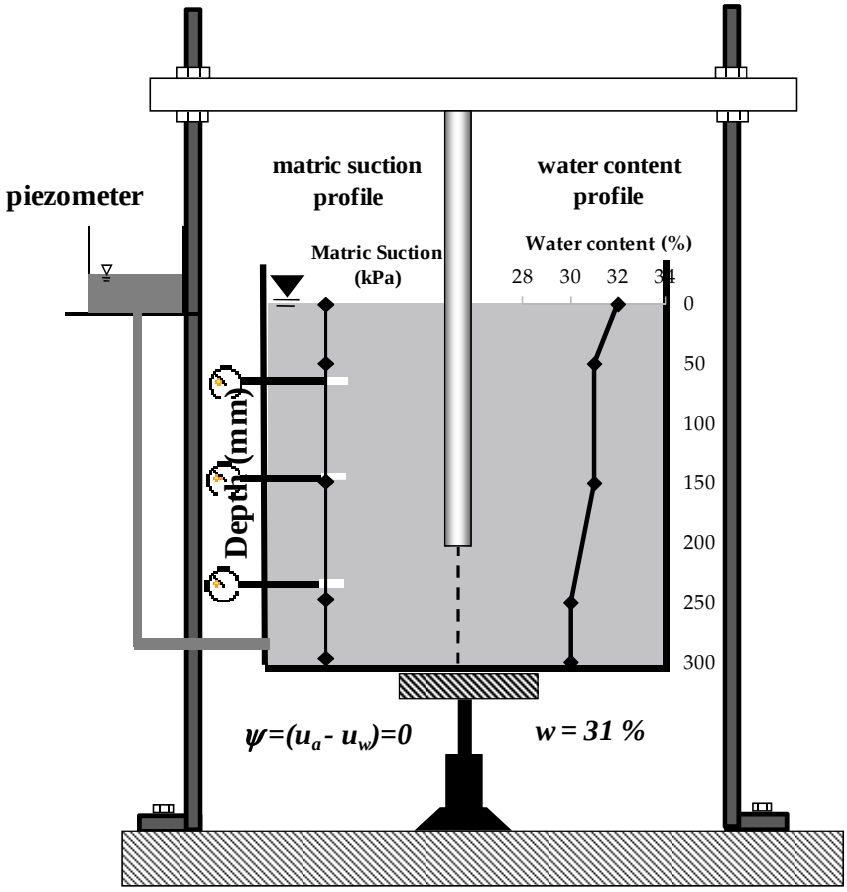

Figure 7.6 : A schematic illustrating the saturation process and saturation control for IHT.SAT.13.

7.4.2.1 Test results of IHT.SAT.13.UD

Model pile test results IHT.SAT.13.UD (i.e. Indian Head till saturated soil sample for undrained loading condition) are summarized in Figure 7.7. The ultimate shaft bearing capacity was observed at 0.02 mm of vertical displacement which is less than 1%~2% of the pile diameter as stated in the failure criteria for D20 and D30 piles. The load test results for pile D20 and D30 show that once the ultimate shaft resistance is reached, the load-displacement curves are parallel to each other with further displacement. This behavior is observed in saturated soil samples and soil samples tested with lower matric suction values. The load tests on pile D45 are not reported as the compacted soil sample was highly disturbed during the placement of the model pile.

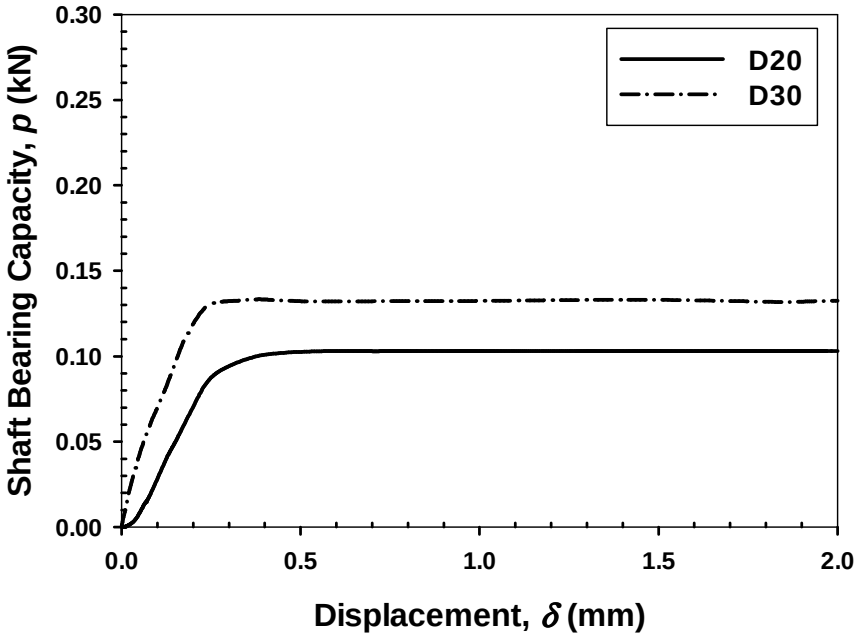

Figure 7.7 : p-δ behavior of IHT.SAT.13.UD for Pile D20 and D30.

7.4.2.2 Test results of IHT.SAT.13.D

IHT.SAT.13.D tests were performed on pile D20 and D30 (Figure 7.8). Pile-D45 was not conducted due to some disturbance. Model pile tests were started with the smallest diameter of the pile. After the test was completed, the next higher size model pile was placed in the same hole and then loaded; however sufficient time was allowed for regaining the strength (i.e. overnight). For saturated condition tests, special care was taken to reduce the possible disturbance both during the pile installation and removal. In spite of the all the precautions, some is expected. Due to this reason, disturbance effect was considered in the analysis and interpretation of the obtained results.

Since the drained loading tests are slow tests (i.e. loading rate 0.012 mm/min), total vertical displacement of 3 mm takes 5-6 hours. During this period, the soil sample should be assured to saturated conditons. In other words, evaporation losses should be controlled during the long periods of testing from the surface of the test tank. This was acheived by covering the surface with plastic sheets.

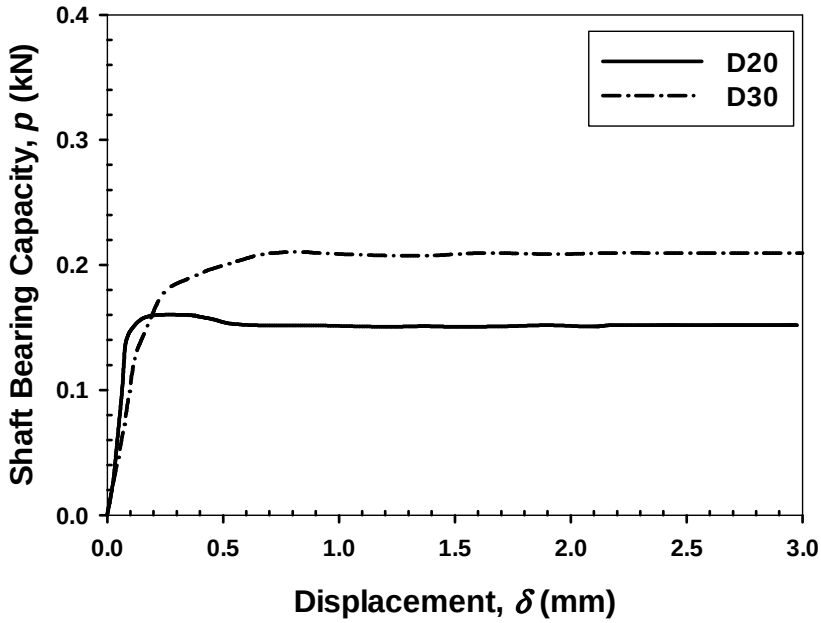

Figure 7.8 : p-δ behavior of IHT.SAT.13.D for Pile D20 and D30.

7.4.3 Test results of IHT.ASCOMPAC.15.5 : (matric suction=110 kPa)

The next set of tests were performed on soil sample compacted an initial water content of 15.5% (-3% of OMC) with an average matric suction value of 110 kPa. The measured water content values along the compacted soil profile are summarized in Table 7.4. The water content profile and the associated matric suction distribution diagram obtained from the *SWCC* is illustrated in Figure 7.9.

The distribution diagram for water content show small fluctuations with depth around the average value of 15.5%. These variations are within the acceptable limits of ± 2%. All the precautions discussed in the preceding sections were also taken during testing to reduce air-drying on the surface of the compacted soil.

Table 7.4 : Water content values with depth.

Depth (mm)	0	50	50	100	100	150	200	250	300
w (%)	16.0	16.0	15.3	15.4	15.0	15.2	15.2	15.2	15.2

Matric suction values of the soil speciemens collected from depths of 100 mm and 150 mm were measured using axis translation technique. These results are summarized in Table 7.5.

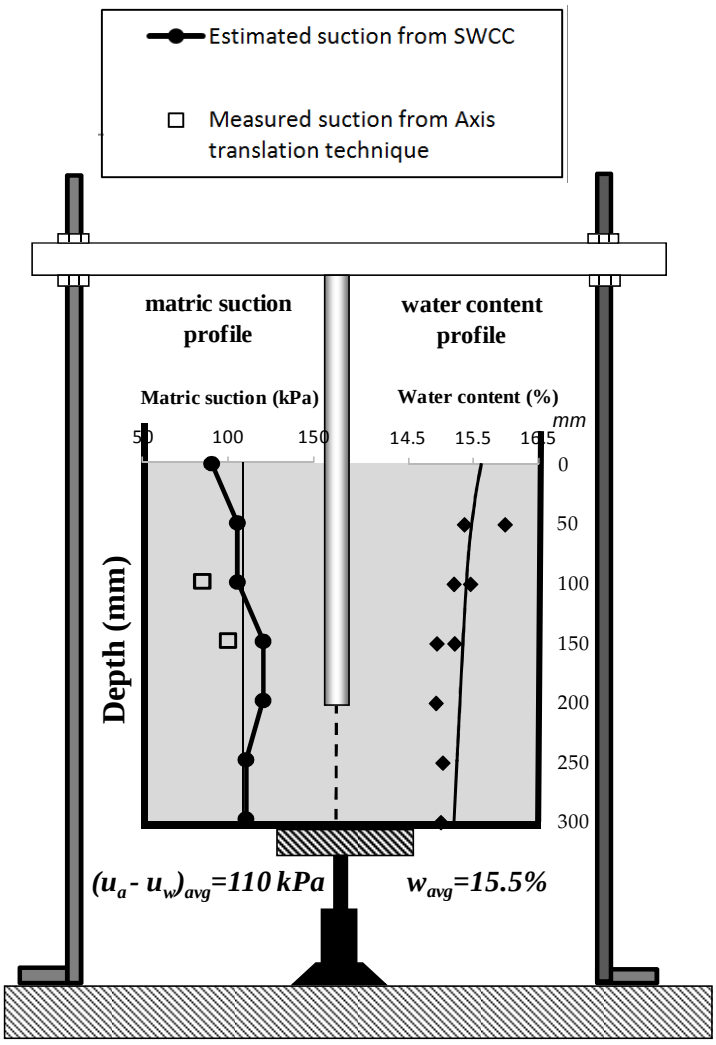

Figure 7.9 : A schematic illustrating for the controlled uniform matric suction and water content profile for IHT.ASCOMPAC.15.5.

Table 7.5 : Soil properties for the compacted saturated soil in the test tank IHT.ASCOMPAC.15.5.

Depth	Sample Type	$(u_a - u_w)$	γ_n	γ_{dry}	e	w	S
mm		kPa	kN/m^3	kN/m^3	-	%	%
100	Ring	85	18.3	15.50	0.65	15.6	65
150	Tube+Ring	105	18.6	16.20	0.65	15.3	63

7.4.3.1 Test results of IHT.ASCOMPAC.15.5.UD

The model pile test results performed for the as compacted soil condition prepared at an initial water content of 15.5% (-3% of OMC) under undrained loading condition are given in Figure 7.10.

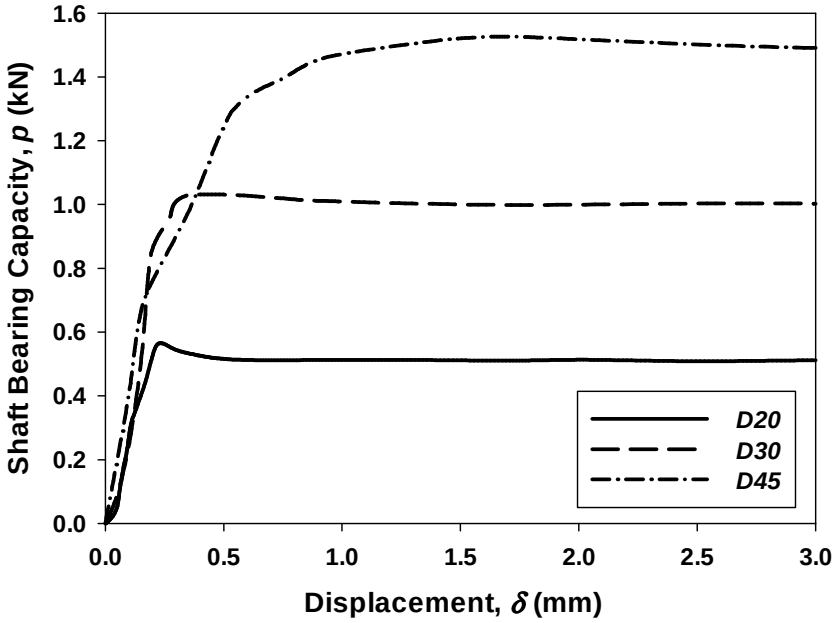

Figure 7.10 : *p*-δ behavior of IHT.ASCOMPAC.15.5.UD for Pile D20-D30-D45.

7.4.3.2 Test results of IHT.ASCOMPAC.15.5.D

The model pile test results performed for the as compacted soil condition prepared at an initial water content of 15.5% under drained loading condition are given in Figure 7.11.

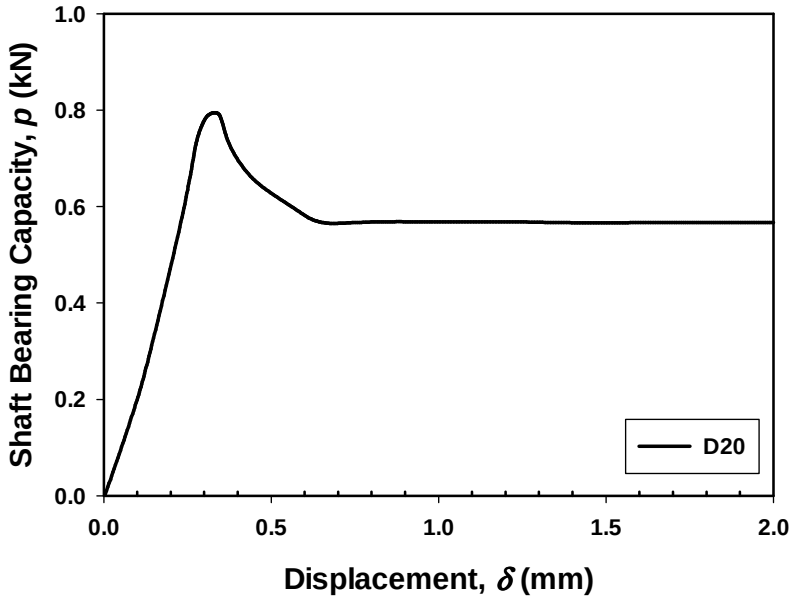

Figure 7.11 : *p*-δ behavior of ASCOMPAC.15.5.D for Pile D20.

7.4.4 Test results of IHT.UNSAT.15.5.D : (average matric suction = 60 kPa)

In this series of model pile load test, the soil was compacted in the test tank at an initial water content of 15.5% (-3 % of OMC) and a downward flow of water was applied through the drainage holes of the compaction plate for a period of three days following the test procedures described in the earlier chapter. The intial matric suction of the compacted specimen will reduce due to the water infiltration. In other words, the matric suction profile will vary with respect to the depth. The objective of this particular series of tests is to understand the influence of varying matric suction on the carrying capacity of the model pile. In addition, using the test results, a technique has been developed to intepret the model test results based on the average matric suction value. Such a technique is useful for interpreting the field test results as such scenarios are common.

After the model pile test was completed, soil samples were collected for determination of water content and matric suction measurements at depths of 0 mm, 50 mm, 100 mm, 150 mm and 200 mm from the surface of the compacted soil along the pile shaft. Four of the specimens were used to measure matric suction using the axis translation technique. The results are summarized in Table 7.6 and Table 7.7. Figure 7.12 summarizes the results.

Table 7.6 : Water content check after the test.

Depth (mm)	0	50	100	150	200
w (%)	23.0	20.5	18	17.0	15.8

Table 7.7 : Soil properties for the compacted unsaturated soil in the test tank.

Depth	Sample type	$(u_a - u_w)$	γ_n	γ_{dry}	E	w	S
mm	-	kPa	kN/m^3	kN/m^3	-	%	%
0	Can	0	-	-	-	24	-
50	Tube+Ring	20	19.3	16.9	0.58	20.5	86
100	Ring	35	20.0	16.7	0.59	18	76
150	Ring	50	19.2	16.9	0.61	17	72
200	Tube+Ring	100	18.6	16.2	0.65	15.6	66

The measured matric suction values using axis translation technique for the corresponding degrees of saturation were plotted on the measured *SWCC* (Figure 7.13). The measured p-δ behavior for drained loading condition is shown in Figure 7.14.

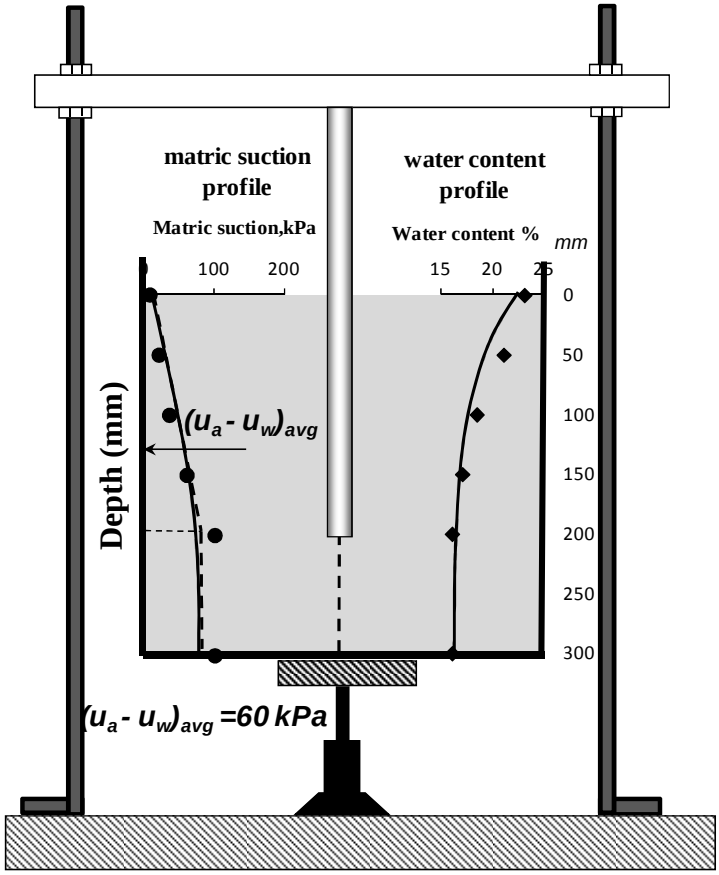

Figure 7.12 : A schematic illustrating the varying matric suction and water content profile for IHT.UNSAT.15.5.

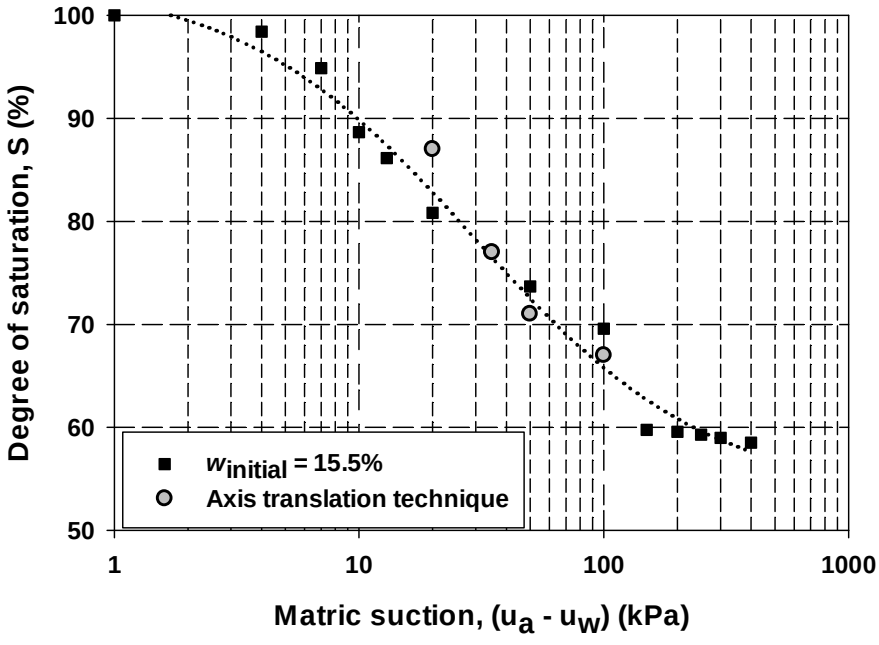

Figure 7.13 : *SWCC* for Indian Head till with compaction water content for IHT.UNSAT.15.5.

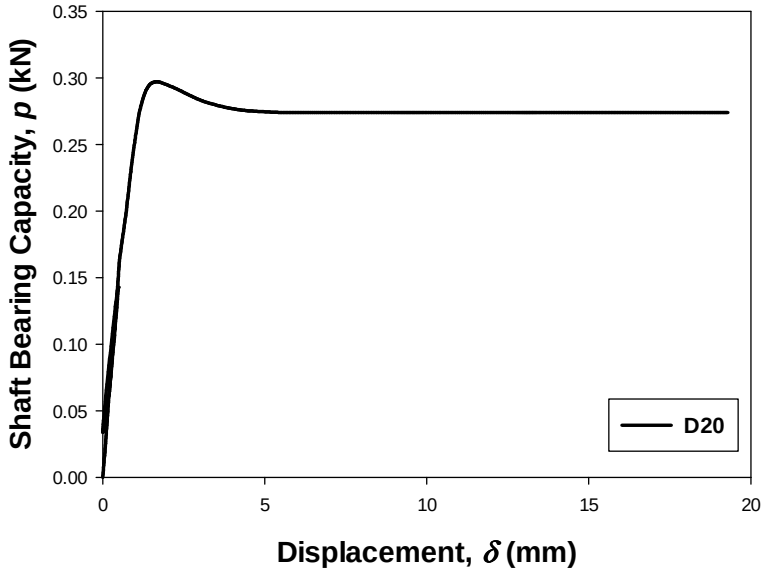

Figure 7.14 : p-δ behavior of IHT.UNSAT.15.5.D for pile D20.

7.4.4.1 Procedure for calculating the average matric suction value

In this test series (i.e. IHT.UNSAT.15.5.D), average matric suction is determined which corresponds to the centroid of the suction distribution diagram from surface to the pile embedment depth of 200 mm.

Vanapalli and Mohamed (2007) and Oh et al. (2009) have suggested a procedure for the determination of average matric suction value for shallow foundations (i.e. footing) within the stress bulb region. The stress bulb depth typically extends from the base of the foundation to a depth of 1.5 to 2.0 times the width of the foundation (i.e. d = 1.5B to 2B). The average matric suction value has been defined as the matric suction value at the centroid of the matric suction distribution diagram assuming a hydrostatic distribution profile.

The diagram in Figure 7.15 shows the technique used for estimating the average matric suction value based on the measured matric suction distribution diagram by Oh and Vanapalli (2011). The measured non-linear matric suction profile was simplified as two straight lines.

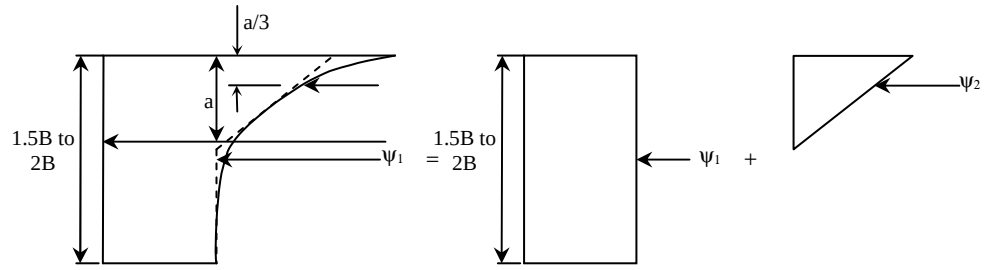

Figure 7.15 : Estimation of average matric suction value based on matric suction distribution diagram (Oh and Vanapalli, 2011).

In a similar manner, for the model pile test series, the average matric suction value, $(u_a - u_w)_{avg} = \psi_{avg}$ was estimated simplifying the actual matric suction distribution diagram (Fig. 7.12) as two straight lines (Figure 7.16). The matric suction distribution diagram along the pile shaft (i.e. 200 mm = pile embedment length) was considered for the calculation of average matric suction. The matric suction value, $\psi_{avg\,(1)}$, corresponding the centroid of the triangular diagram was equal to 60 kPa.

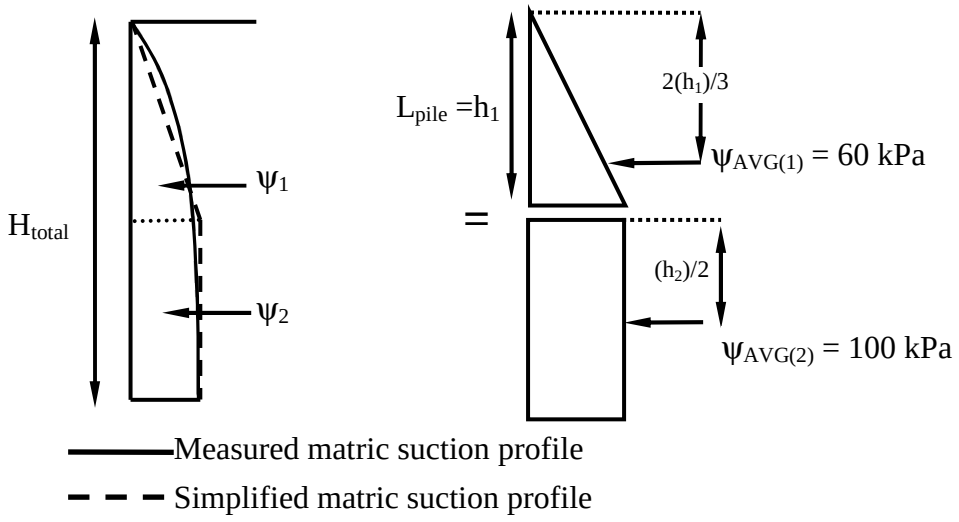

Figure 7.16 : Estimation of average matric suction value based on matric suction distribution diagram in the varying suction profile pile test series.

7.4.5 Test results of IHT.ASCOMPAC.18 : (matric suction=55 kPa)

IHT.ASCOMPAC.18 tests were performed for close to optimum condition with an initial water content value of 18 % (- 0.6% of OMC). The matric suction of the soil sample compacted at this water is equal to 55 kPa. The measured water content values along the compacted soil profile are summarized in Table 7.8. The water content profile and the associated matric suction distribution diagram obtained from

the *SWCC* is illustrated in Figure 7.17. The data of unit weight, degree of saturation and water contents directly collected from the test tank are summarized in Table 7.9.

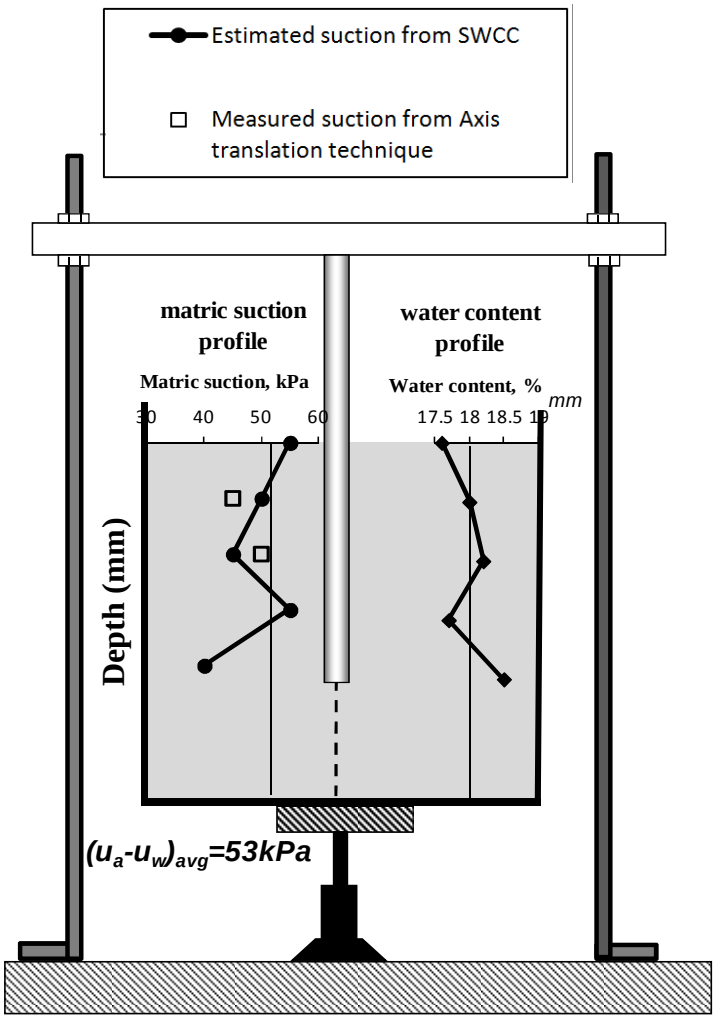

Figure 7.17 : A schematic illustrating for the controlled uniform matric suction and water content profile for IHT.ASCOMPAC.18.

Table 7.8 : Water content check.

Depth (mm)	0	50	100	150	200
w (%)	17.5	18.0	18.2	17.7	18.5

Table 7.9 : Soil properties for the compacted unsaturated soil in the test tank.

Depth	Sample Type	$(u_a - u_w)$	γ_n	γ_{dry}	*e*	*w*	*S*
mm		kPa	kN/m^3	kN/m^3	-	%	%
100	Ring	45	19.0	1.73	0.59	18.2	85
150	Ring	55	18.7	1.70	0.63	17.7	82
200	Tube	-	19.0	1.70	0.58	18.5	80
200	Can	-	-	-	-	18.5	-

7.4.5.1 Test results of IHT.ASCOMPAC.18.UD

Figure 7.18 summarizes the model pile test results performed on Indian Head till compacted soil condition at an initial water content of 18% under undrained loading condition**.** The p-δ behavior of pile D45 shows a lower value of ultimate shaft capacity than the expected value. Such a behavior can be associated with improper installation and/or disturbance during installation. The measured and expected p-δ curves for D45 pile is given in Figure 7.18.

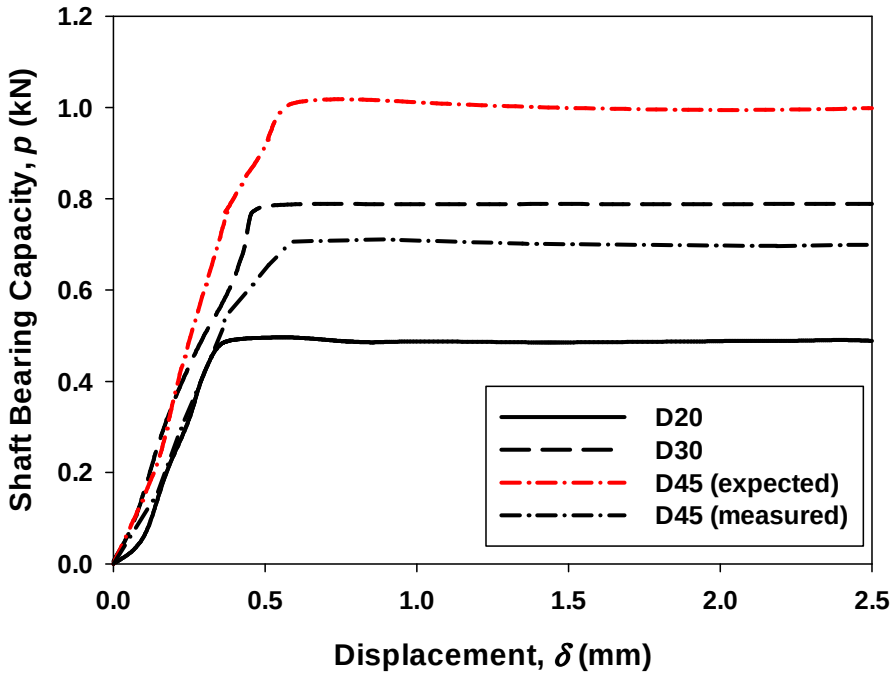

Figure 7.18 : p-δ behavior of IHT.ASCOMPAC.18.UD for Pile D20-D30-D45.

7.4.5.2 Test results of IHT.ASCOMPAC.18.D

The model pile test results performed for the as compacted soil condition prepared at an initial water content of 18 % under drained loading condition are given in Figure 7.19.

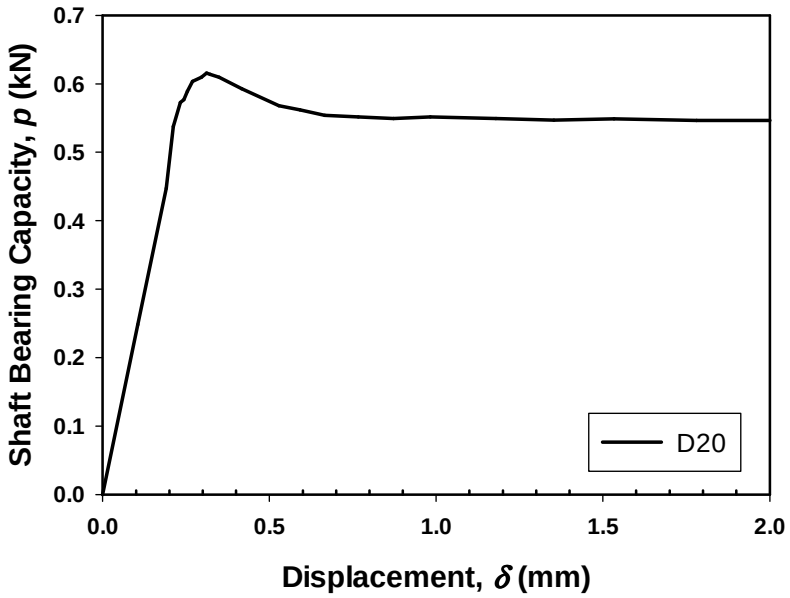

Figure 7.19 : p-δ behavior of IHT.ASCOMPAC.18.D for Pile D20.

7.5 Model Pile Load Test Results: Low Plastic Loam Soil (Test Series No.2)

An attempt is made to estimate the shaft bearing capacity of a single pile placed in unsaturated Loam soil with a low plasticity (I_p = 6.5%) in this section. The measured matric suction values are reported in Table 7.10 and shown in Figure 7.20 on the compaction curve.

Table 7.10 : Matric suction values measured by using the axis translation technique.

Sample Type	$(u_a - u_w)$	γ_n	γ_{dry}	e	w	S
	kPa	kN/m^3	kN/m^3	-	%	%
Ring	115	18.0	16.0	0.60	13.6	60-56
Ring	107	18.0	16.0	0.60	13.2	58-55
Ring	80	18.0	16.0	0.60	13.4	59-57
Ring	50	18.8	16.5	0.60	14.7	65-66

The measured matric suction values using the axis translation technique are presented in Table 7.10 and the corresponding degree of saturation fell on the measured *SWCC* using the pressure plate for the studied Loam soil as shown in Figure 7.21.

It was decided to work with an initial compaction water content value of 13% which is the dry of optimum condition (i.e. w_{opt} = 17.4%) where the degree of saturation varies between 50%-60% and which corresponds to a relatively higher matric suction value and falls within the range of 80-100 kPa.

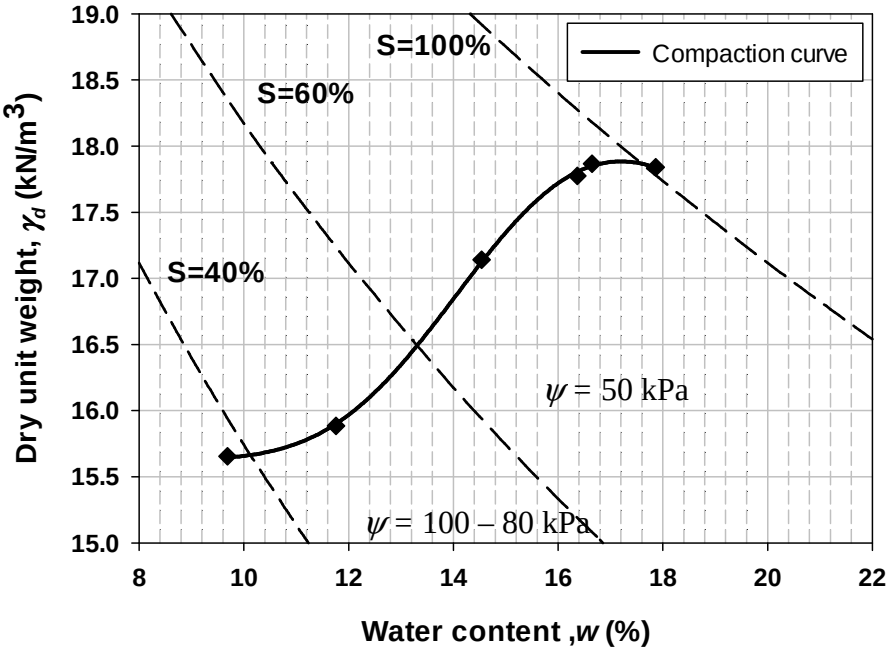

Figure 7.20 : Matric suction values measured for the as-compacted condition.

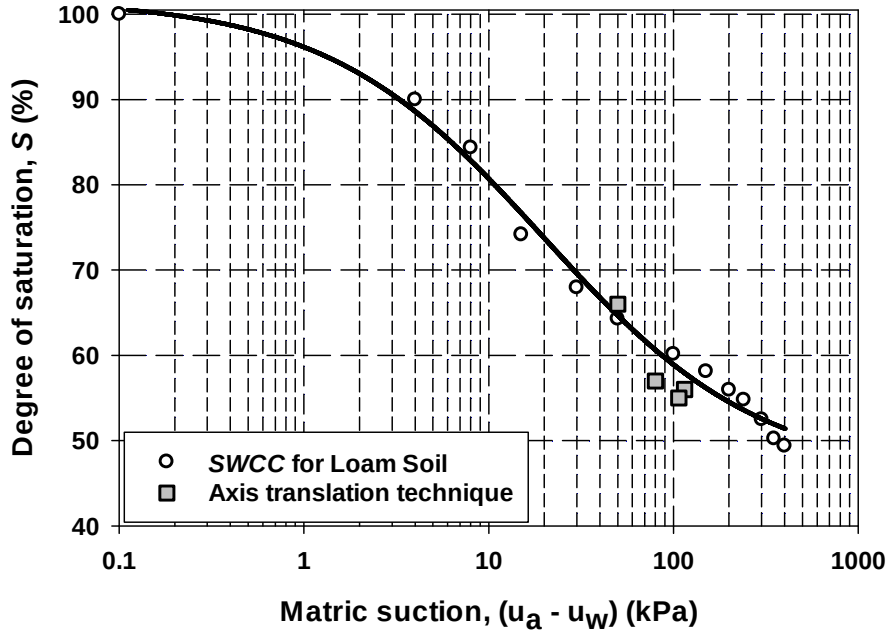

Figure 7.21 : SWCC for Loam Soil and axis translation technique measurement results.

7.5.1 Test results of LS.ASCOMPAC.13 : (matric suction = 85 kPa)

The first experimental measurements were performed on unsaturated soil sample prepared at an initial water content of 13% which corresponds to a suction value of 80-90 kPa. The pile loading were performed both under drained and undrained loading rates for as compacted soil condition on Pile-D20 and D30. The suction control before and after the tests were done by water content check and also by axis

translation technique measurements performed on the soil samples collected from the test tank after completion of the loading tests. Water content profile for the compacted soil and the associated matric suction distribution diagram is illustrated in Figure 7.22 and in Table 7.11. The estimate matric suction profile was obtained based on the measured water contents using the *SWCC*. The model pile test results performed for the as compacted soil condition prepared at an initial water content of 13% under undrained and drained loading conditions are shown in Figure 7.23 and Figure 7.24 respectively.

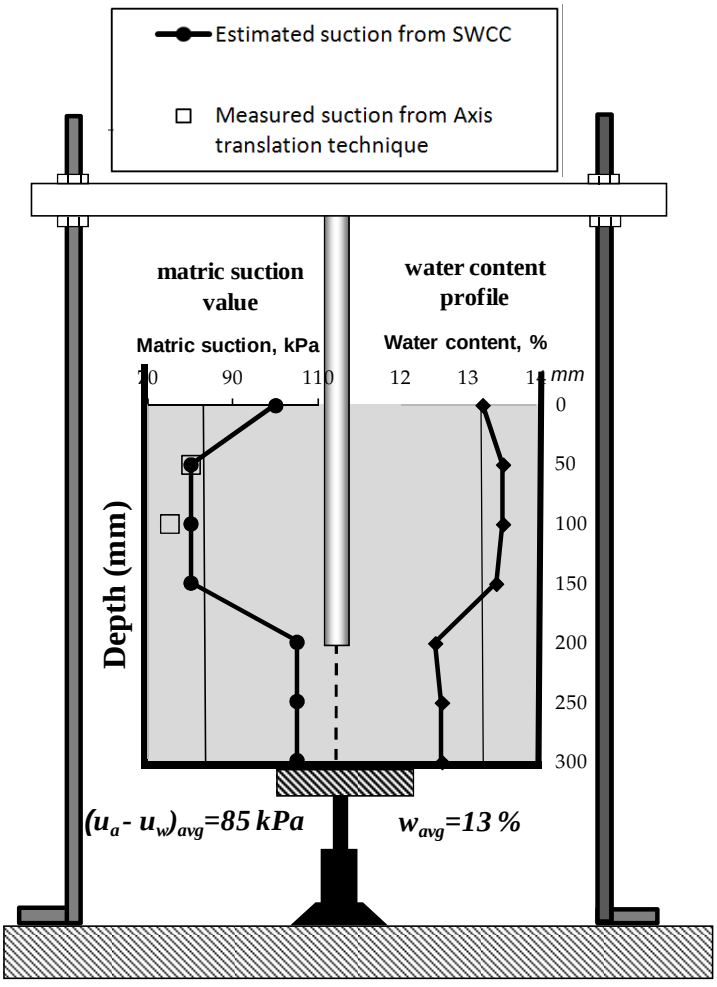

Figure 7.22 : A schematic illustrating for the controlled uniform matric suction and water content profile for LS.ASCOMPAC.13.

Table 7.11 : Water content check.

Depth (mm)	0	50	100	150	200	250	300
w (%)	13.2	13.5	13.5	13.4	12.6	12.6	12.6

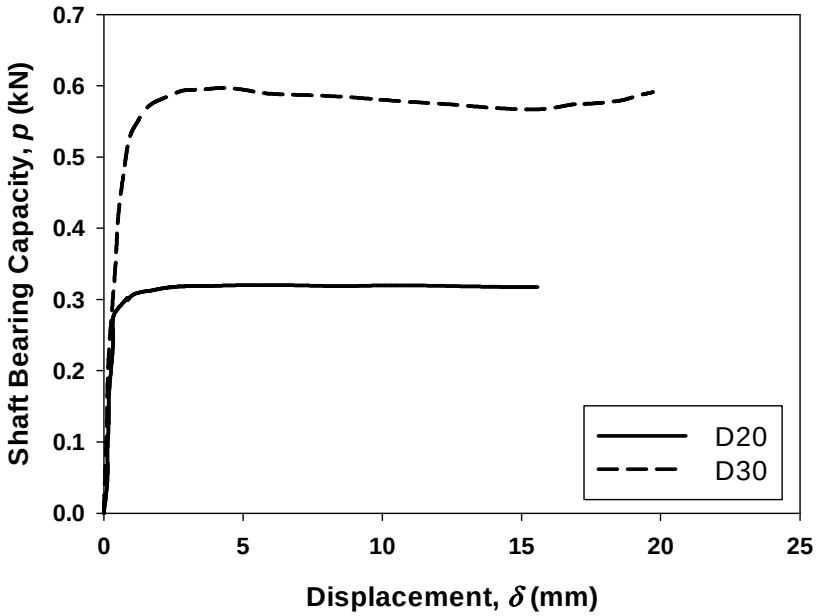

Figure 7.23 : Shaft bearing capacity versus displacement curves for LS.ASCOMPAC.13.UD.

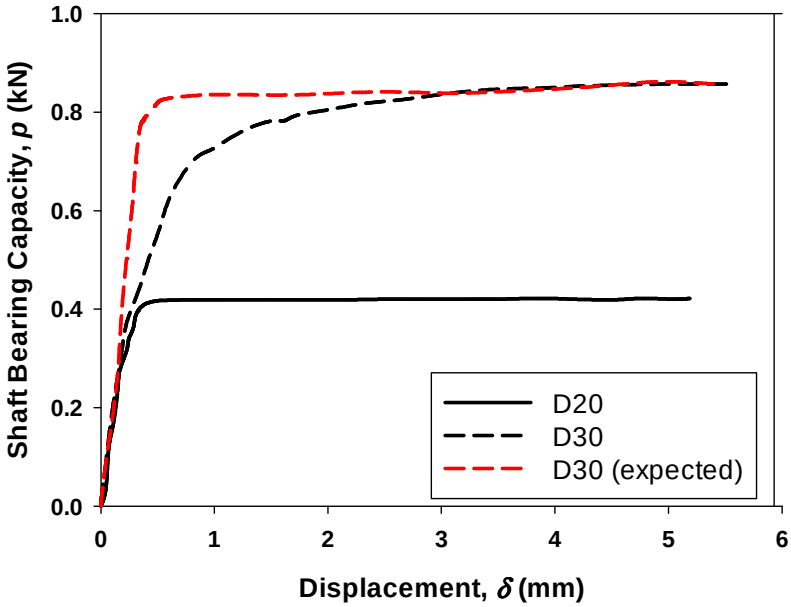

Figure 7.24 : Shaft bearing capacity versus displacement curves for LS.ASCOMPAC.13.D.

7.6 Shear Strength Measurements: Interface Direct Shear Tests

Single stage interface direct shear tests were performed on Indian Head till and Loam soils to measure the interface friction angle, δ and adhesion, c'_a between the soil and the pile material. The specimens were loaded with applied normal stress values of 200-350 and 450 kPa and sheared at a constant rate of 0.0120 mm/min. The shearing rate used for model pile loading was the same as the rate used for shearing for

interface direct shear testing. The shear stress versus the normal stress relationships and the shear strength parameters for the saturated and as compacted conditions for both Indian Head till and Loam soil are summarized in the following sections.

7.6.1 Test results of interface direct shear for Indian Head till

The interface direct shear test results for saturated and as compacted condition and the interface shear strength parameters for Indian Head till are given in Table 7.12 and in Figure7.25 and Figure 7.26.

Table 7.12 : Shear strength parameters obtained from the interface direct shear test results for saturated (SAT) and as compacted (ASCOMPAC) condition.

Test Series	SAT		ASCOMPAC	
$w_{initial}$ (%)	c'_a (kPa)	δ'(°)	c'_a (kPa)	δ'(°)
13	20.0	23	50	25
15.5	15.0	23	22	23
18	12.0	23	19	23

7.6.2 Test results of interface direct shear tests for Loam soil

The interface direct shear test results for saturated and as compacted condition and the interface shear strength parameters for Loam soil are given in Table 7.13 and in Figure 7.27.

Table 7.13 : Interface direct shear test results for saturated (SAT) and as compacted (ASCOMPAC) condition for Loam soil.

Test Series	SAT		ASCOMPAC	
$w_{initial}$ (%)	c'_a (kPa)	δ(°)	c'_a (kPa)	δ(°)
13	7	25	26	25

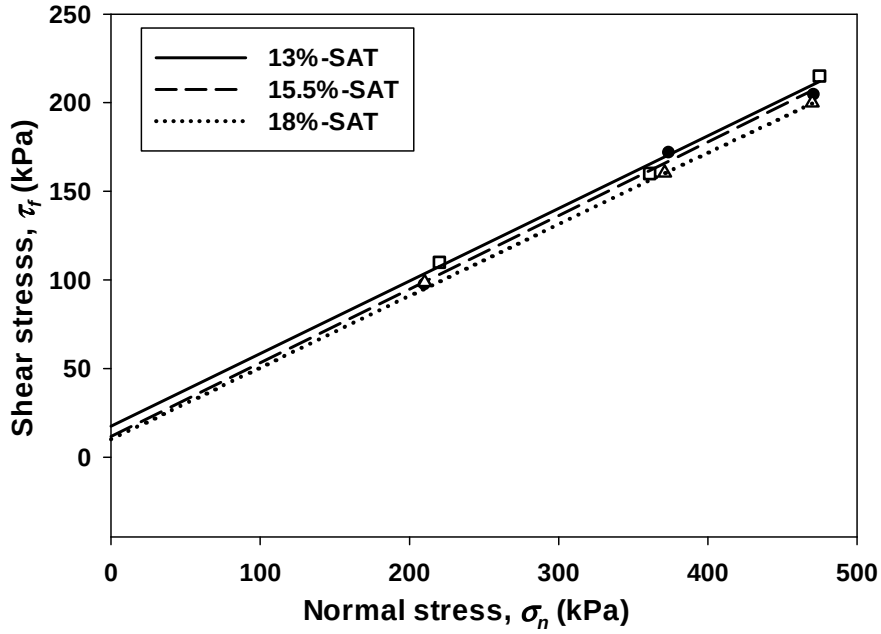

Figure 7.25 : Saturated interface shear strength results for Indian Head till.

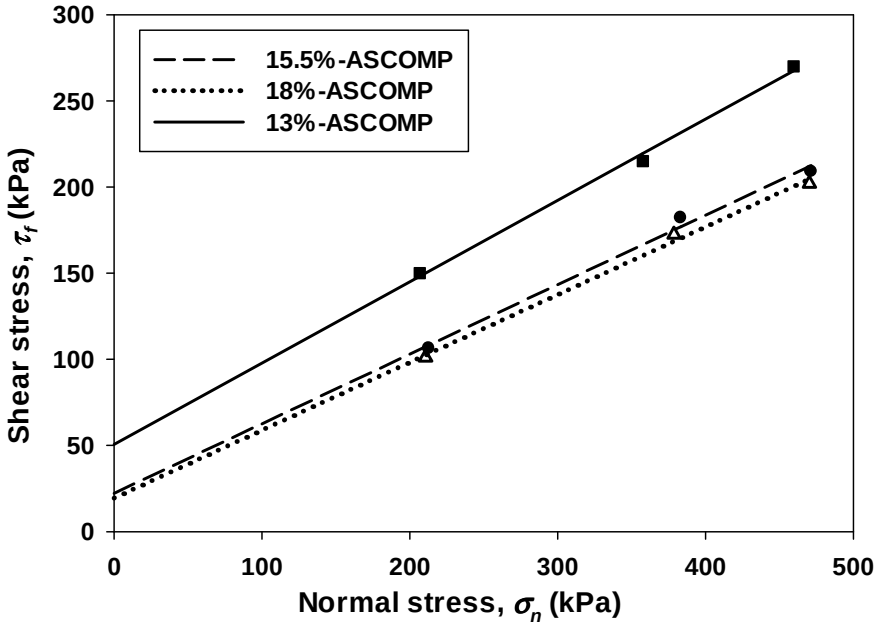

Figure 7.26 : As compacted interface shear strength results for Indian Head till.

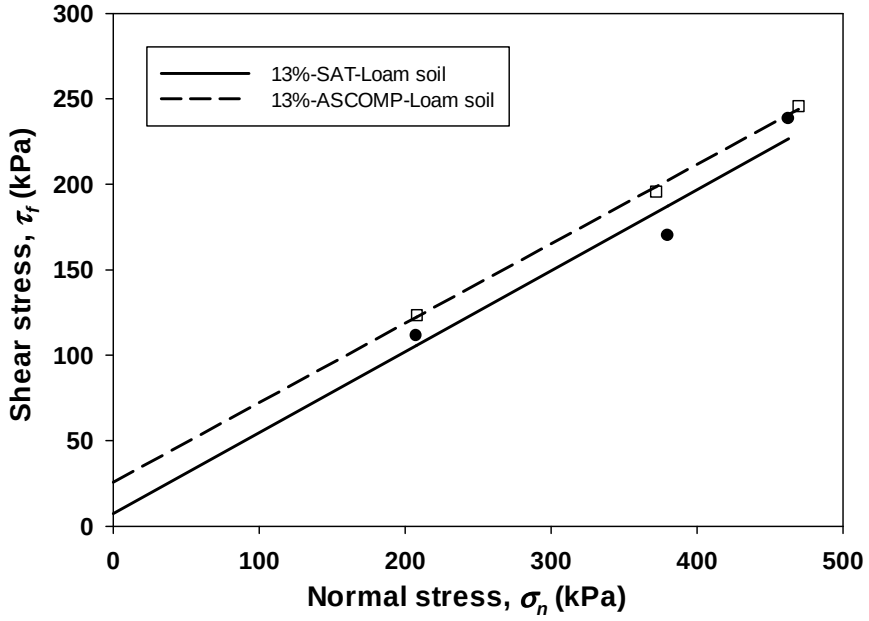

Figure 7.27 : As compacted and saturated interface shear strength results for Loam soil.

7.7 Shear Strength Measurements : Unconfined Compression Tests

The unconfined compression tests were perfromed on samples that were obtained in two different ways for saturated and as compacted testing conditions:

i. Thin wall tubes were penetrated into the test tank with saturated compacted soil to extract samples from them.

ii. For ASCOMPAC condition tests, samples were prepared by compacting in the compaction mold separately to avoid the possible external factors affecting the results. This methodology was decided since the extraction process (i.e. force to push sample out from the tube) of the collected samples from the thin-wall tubes causes decrease in the volume due to the high friction between the soil sample and the thin-wall tube leading to an increase in the unconfined compressive strength. This phenomenon was not observed for the SAT sample due to the low friction between the soil sample and the thin-wall tube leading to a negligible volume change during the extraction process.

7.7.1 Test results of unconfined compression test for IHT and LS

The unconfined compression test results are shown in the following figure for Indian Head till and Loam soil samples (Figure 7.28, Figure 7.29 and Table 7.14, Table 7.15).

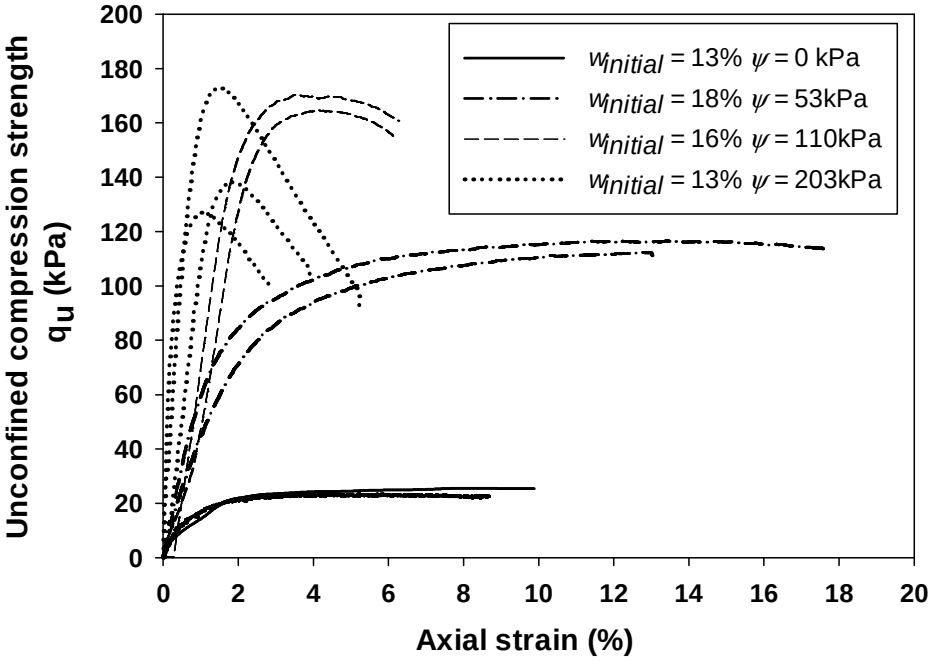

Figure 7.28 : Unconfined compression test results for Indian Head till sample.

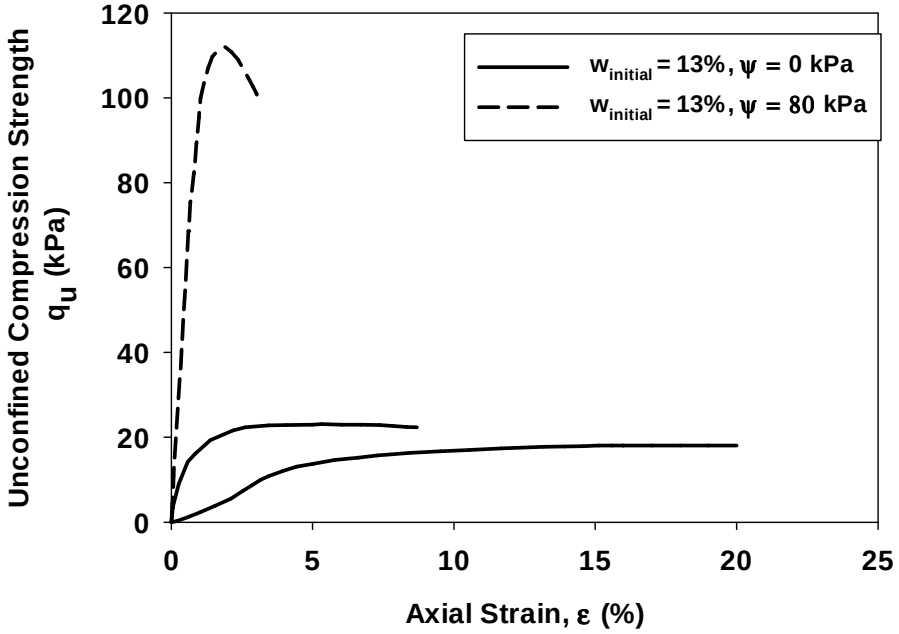

Figure 7.29 : Unconfined compression test results for Loam Soil sample.

The results show that the undrained shear strength of specimens compacted at dry of optimum condition is higher than those compacted at optimum condition. This is due to higher matric suction in the specimens. However, for the specimens compacted at two different dry of optimum conditions (i.e. 13% and 15.5%) show that the one with higher initial water content and lower matric suction shows slightly higher undrained strength when compared to the sample prepared at a lower water content. Post-peak softening behavior is more pronounced for specimens with higher matric suction.

Table 7.14 : Unconfined compression test results for Indian Head till sample.

w	$(u_a - u_w)$	q_u	c_u
%	kPa	kPa	kPa
13SAT1-UU	0	23	11.5
13SAT2-UU	0	22	11.0
Avg(13SAT-UU)	0	23	11.5
13ASCOMPAC1-UU	205	125	62.5
13ASCOMPAC2-UU	205	140	68.0
13ASCOMPAC3-UU	205	178	89.0
Avg(13ASCOMP-UU)	205	150	75.0
16 ASCOMPAC1-UU	110	170	85.0
16ASCOMPAC2-UU	110	163	81.5
Avg(16ASCOMPAC-UU)	110	166.5	83.0
18 ASCOMPAC1-UU	55	118	59.0
18ASCOMPAC2-UU	55	112	56.0
Avg(18ASCOMPAC-UU)	55	115	58.0

Table 7.15 : Unconfined compression test results for Loam Soil sample.

w	$(u_a - u_w)$	q_u	c_u
(%)	kPa	kPa	kPa
13SAT1-UU	0	22	11
13SAT2-UU	0	18	9
Avg(13SAT-UU)	0	20	10
13 ASCOMPAC1-UU	80	110	55
Avg(13ASCOMPAC-UU)	80	166.5	55.0

7.8 Interpretation of Test Results

The model pile load test results are interpreted in this section using three different approaches considering the drained and undrained loading conditions as; i) Modified α method following the total stress approach (TSA), ii) Modified β method following the effective stress approach (ESA), and iii) Combining total stress and the effective stress approaches in the modified λ-method. Comparisons are provided between the measured and estimated ultimate shaft capacities (hereafter referred to as USC) for each methods.

7.8.1 Estimation of USC by the modified α method - (TSA)

The model pile tests conducted under undrained loading condition were interpreted using the modified α method (7.1) (see section 3.5.2).

$$Q_{f(us)} = \alpha c_{u(sat)} \left[1 + \frac{(u_a - u_w)}{(P_a / 101.3)} S^{\upsilon} / \mu \right] \pi dL \qquad \textbf{(7.1)}$$

where, $Q_{f(us)}$ = ultimate shaft bearing capacity of a pile for unsaturated condition, α = adhesion factor, $c_{u(sat)}$ = undrained shear strength under saturated and unsaturated conditions, respectively, P_a = atmospheric pressure (i.e. 101.3 kPa), $(u_a - u_w) = \psi$ =matric suction, S = degree of saturation and ν, μ = fitting parameters.

The fitting parameters, ν and μ were determined based on the I_p values of the studied two soils (i.e. IHT and LS). For Indian Head till soil sample (i.e. I_p =15.5) ν = 2 and μ =9 (see section 2.5.5 and Figure 2.16). This is further discussed for Loam soil in the following sections.

The undrained strength of the soil specimens were determined from unconfined compression tests. The measured undrained shear strength values, c_u were used for the estimation of ultimate shaft bearing capacities. The estimated undrained shear strength values using the (3.19) in section 3.5.1 are given for comparison purposes. The adhesion factors (i.e. $\alpha_{cal} = \alpha_{sat/unsat}$) were also back calculated from the model pile test results and presented along with the analysis results.

The analysis results of the model pile tests performed for Indian Head till with the initial water contents of 13% -15.5% and 18% under undrained loading condition are summarized through Table 7.16 to Table 7.19. The comparison between the measured and those estimated shaft bearing capacities using the modified α method are provided in Figure 7.30.

7.8.1.1 IHT.ASCOMPAC.13.UD : (matric suction=205 kPa)

Table 7.16 : Measured and estimated *USC* values using the modified α method for IHT.ASCOMP.13.UD.

D	$w_{initial}$	$(u_a - u_w)$	Meas. c_u	Est. c_u	$\alpha_{sat/unsat}$	Est. $Q_{f(us)}$	Meas. $Q_{f(us)}$	α_{cal}
mm	(%)	kPa	kPa	kPa	-	kN	kN	-
10						0.37	0.35	0.78
15						0.55	0.50	0.74
20	13	205	68	64	0.90/0.75	0.73	0.68	0.80
30						1.10	1.25	0.89
45						1.64	2.30	1.20

7.8.1.2 IHT.SAT.13.UD : (matric suction=0 kPa)

Table 7.17 : Measured and estimated *USC* values using the modified α method for IHT.SAT.13.UD.

D	$w_{initial}$	$(u_a - u_w)$	Meas. c_u	α_{sat}	Est. $Q_{f(us)}$	Meas. $Q_{f(us)}$	α_{cal}
(mm)	(%)	kPa	kPa	-	kN	kN	-
20	13	0	11.5	0.90	0.13	0.10	0.70
30					0.19	0.14	0.64

The measured *USC* from model pile tested on compacted saturated soil is lower than the estimated *USC*. This result is attributed to the problems encountered during the drilling and jacking procedures which caused softening and soil disturbance. It was challenging to conduct the model pile tests in saturated condition in the present research program without disturbance. A low value of *USC* (i.e. 0.10 kN) and associated low α value (i.e. 0.70) may be attributed to the disturbance of the soil sapme. The expected *USC* for saturated condition is 0.13 kN for the measured $c_{u(sat)}$ of 11.5 kPa. The back calculated α value for *USC* of 0.13 kN is 0.9 which is consistent with the results published in the literature.

7.8.1.3 IHT.ASCOMPAC.15.5.UD: (matric suction=110 kPa)

Table 7.18 : Measured and estimated *USC* using the modified α method IHT.ASCOMPAC.15.5.UD.

D	$w_{initial}$	$(u_a - u_w)$	Meas. c_u	Est. c_u	$\alpha_{sat/unsat}$	Est. $Q_{f(us)}$	Meas. $Q_{f(us)}$	α_{cal}
mm	%	kPa	kPa	kPa	-	kN	kN	-
20						0.74	0.55	0.55
30	15.5	110	83	65	0.90/0.67	1.11	1.00	0.67
45						1.66	1.50	0.66

7.8.1.4 Analysis results for IHT.ASCOMPAC.18.UD: (matric suction=55 kPa)

Table 7.19 : Measured and estimated *USC* using the Modified α method for IHT.ASCOMPAC.18.UD.

D	$w_{initial}$	$(u_a - u_w)$	Meas. c_u	Est. c_u	$\alpha_{sat/unsat}$	Est. $Q_{f(us)}$	Meas. $Q_{f(us)}$	α_{cal}
mm	%	kPa	kPa	kPa	-	kN	kN	-
20						0.64	0.50	0.67
30	18	55	58	52	0.90/0.82	0.95	0.77	0.70
45						1.44	0.70*	0.61

*disturbance/improper installation

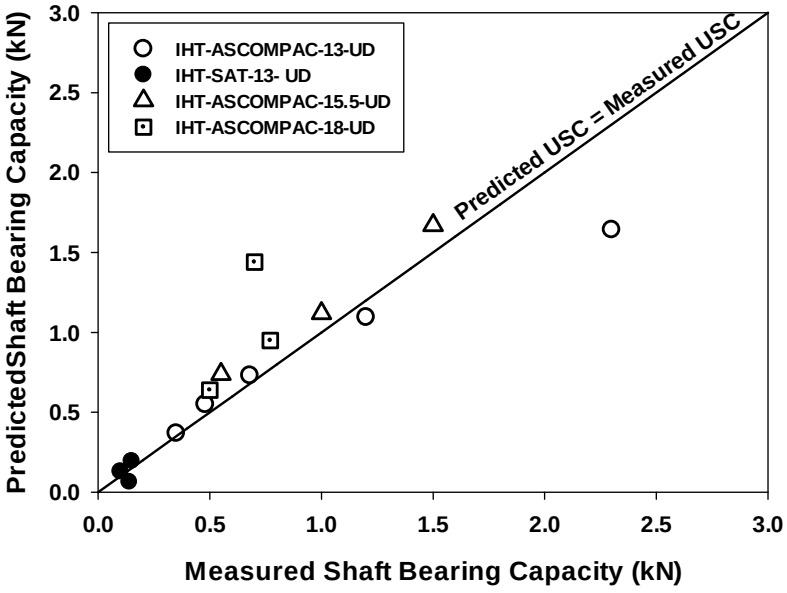

Figure 7.30 : Comparison between the measured and the predicted *USC*s using the Modified α method for Indian Head till soil sample.

7.8.1.5 LS.ASCOMPAC.13.UD: (matric suction=80-90 kPa)

As discussed earlier, the proposed method uses the undrained shear strength derived from unconfined compression test results for saturated condition and the *SWCC* along with the two fitting parameters, ν and μ. The fitting parameter, ν =2 can be used for fine grained soils for the I_p values in the range of 8% to 15.5%; however, I_p value of the tested loam is 6.5%. Therefore, the analyses were carried out for both ν =1 and 2 with different μ values following the work of Oh (2012). Table 7.20 and Figure 7.31 provide the comparison between the measured and those estimated shaft bearing capacities using the modified α method.

Table 7.20 : Measured and estimated *USC* using the modified α method for LS.ASCOMPAC.13.UD.

D	$w_{initial}$	$(u_a - u_w)$	Meas. $c_{u(sat)}$/ $c_{u(unsat)}$	Est. $Q_{f(us)}$				Meas. $Q_{f(us)}$
mm	%	kPa	kPa	kN				kN
				μ=5	μ=6	μ=7	μ=8	
20	13	80	10/60	0.61	0.53	0.45	0.42	0.32
30				0.92	0.79	0.68	0.63	0.60

The best results were obtained for the fitting parameters of (ν =2, μ =7-8). The results estimated by using the fitting parameter ν =1 did not provided good results.

7.8.2 Estimation of USC by the modified β method (effective stress approach)

The modified β method is proposed for the interpretation and prediction of the shaft bearing capacity of a single pile placed both in saturated and unsaturated fine and coarse grained soils for drained loading conditions. The proposed technique was developed by extending the concept for predicting the shear strength of unsaturated soils and the conventional β method used for estimating the shaft capacity of piles in sandy type of coarse grained soils.

The general expression proposed for estimating the ultimate shaft capacity of piles in unsaturated soils, $Q_{f(us)}$ is given as in (7.2). The derivation of this equation is detailed in Chapter 3 (see section 3.5.1).

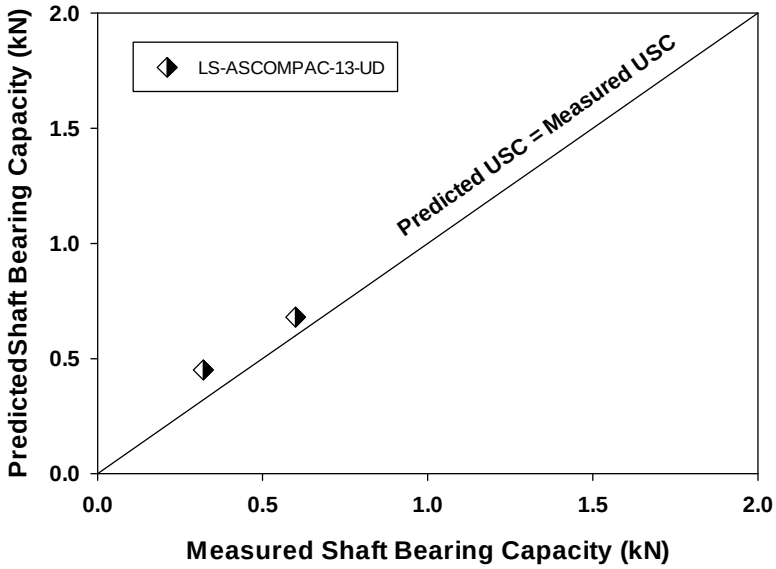

Figure 7.31 : Comparison between the measured and the predicted *USC*s using the Modified α method for Loam Soil.

$$\begin{aligned} Q_{f(us)} &= Q_{f(sat)} + Q_{f(u_a - u_w)} \\ &= \left[\beta \sigma_v' + \left\{ (u_a - u_w)(S^{\kappa})(\tan \delta') \right\} \right] \pi d\, L \end{aligned} \qquad \textbf{(7.2)}$$

Equation (7.2) shows that there is a smooth transition between the ultimate shaft capacity of a single pile from an unsaturated to saturated condition. This relationship will be the same as conventional β method when matric suction is equal to zero (i.e. saturated condition).

However, the contribution of cohesion component associated with the adhesion, c_a' under drained loading condition may not be negligible for evaluating the pile capacity of fine-grained soils for the β method. In other words, there will be some contribution of adhesion, c_a' towards the ultimate shaft capacity which will be mobilized with time after the installation of the pile. Therefore, the ultimate shaft capacity of piles in unsaturated fine-grained soils under drained loading conditions can be estimated as given in (7.3). The shaft capacity of the model pile is estimated using (7.3).

$$Q_{f(us)} = \left[c_a' + \beta(\sigma_z') + (u_a - u_w)(S^{\kappa})(\tan \delta') \right] \pi d\, L \qquad \textbf{(7.3)}$$

where, c_a' = adhesion component of cohesion for saturated condition, δ'= effective angle of interface along the soil/pile.

The analysis results of the model pile tests performed in Indian Head till with the initial water contents of 13 %, 15.5% and 18% under drained loading condition are

summarized through Table 7.21 to Table 7.25 and in Figure 7.32. The analysis results of the model pile tests performed in Loam soil with the initial water content of 13 % is summarized in Table 7.26 and in Figure 7.33.

7.8.2.1 IHT.SAT.13.D: (matric suction=0 kPa)

Table 7.21 : Measured and estimated *USC* using the Modified β method for IHT.SAT.13.D.

D	$w_{initial}$	$(u_a - u_w)$	β	δ	c_a'	Est. $Q_{f(us)}$	Meas. $Q_{f(us)}$
mm	%	kPa	-	°	kPa	kN	kN
20	13	0	0.5	23	20	0.26	0.16
30						0.39	0.22

7.8.2.2 IHT.ASCOMPAC.13.D: (matric suction = 205 kPa)

Table 7.22 : Measured and estimated *USC* values using the modified β method for IHT.ASCOMPAC.13.D.

D	$w_{initial}$	$(u_a - u_w)$	β	δ	c_a'	Est. $Q_{f(us)}$	Meas. $Q_{f(us)}$
mm	%	kPa	-	°	kPa	kN	kN
20	13	205	0.5			0.50	0.82
30	13	205	0.5	23	20	0.73	1.40
45	13	205	0.5			1.10	2.00

7.8.2.3 IHT.ASCOMPAC.15.5.D: (matric suction =110 kPa)

Table 7.23 : Measured and estimated *USC* values using the modified β method for IHT.ASCOMPAC.15.5.D.

D	$w_{initial}$	$(u_a - u_w)$	β	δ	c_a'	Est. $Q_{f(us)}$	Meas. $Q_{f(us)}$
mm	%	kPa	-	°	kPa	kN	kN
20	15.5	110	0.5	23	15	0.45	0.80

7.8.2.4 IHT.UNSAT.15.5.D: (avg. matric suction = 60 kPa)

Table 7.24 : Measured and estimated *USC* values using the modified β method for IHT.UNSAT.15.5.D -varying suction profile.

D	$w_{initial}$	$(u_a - u_w)$	β	δ	c_a'	Est. $Q_{f(us)}$	Meas. $Q_{f(us)}$
mm	%	kPa	-	°	kPa	kN	kN
20	15.5	60	0.5	23	15	0.33	0.29

7.8.2.5 IHT.ASCOMPAC.18: (matric suction = 55 kPa)

Table 7.25 : Measured and estimated *USC* values using the modified β method for IHT.UNSAT.18.D.

D	$w_{initial}$	$(u_a - u_w)$	β	δ	c_a'	Est. $Q_{f(us)}$	Meas. $Q_{f(us)}$
mm	%	kPa	-	°	kPa	kN	kN
20	18	55	0.5	23	12	0.40	0.62

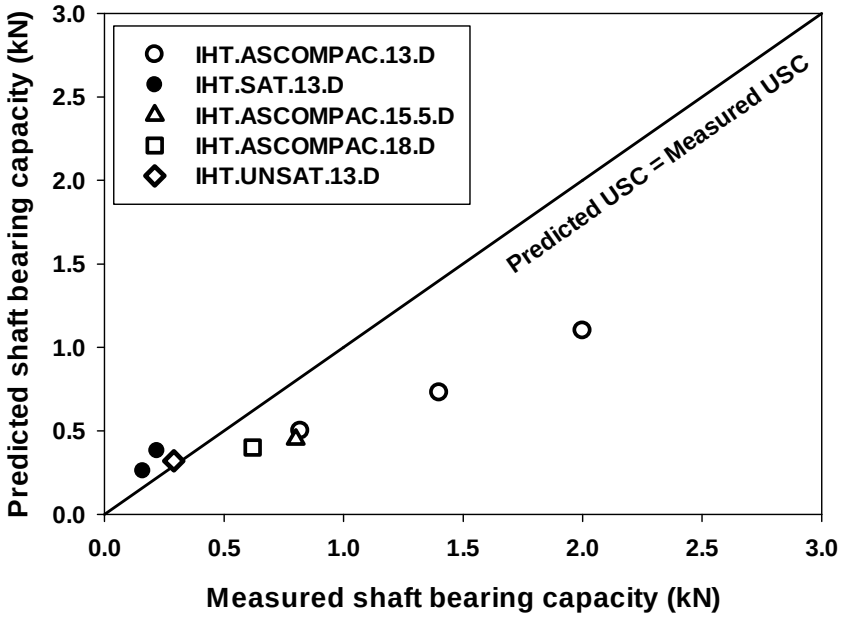

Figure 7.32 : Comparison between the measured and the predicted *USC*s using the modified β method for Indian Head till.

7.8.2.6 LS.ASCOMPAC.13 : (matric suction = 80-90 kPa)

Table 7.26 : Measured and estimated *USC* values using the modified β method for LS.ASCOMP.13.D.

D	$w_{initial}$	$(u_a - u_w)$	β	δ	c_a'	Est. $Q_{f(us)}$	Meas. $Q_{f(us)}$
mm	%	kPa	-	°	kPa	kN	kN
20	13	90	0.3	26	7	0.30	0.40
30						0.45	0.80

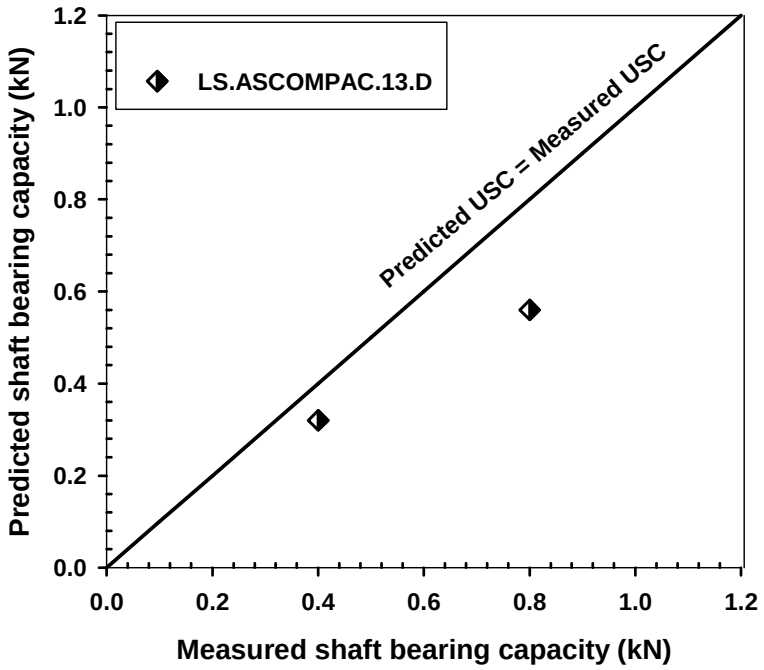

Figure 7.33 : Comparison between the measured and the predicted *USC*s using the modified β method for Loam Soil.

7.8.3 Estimation of USC by the modified λ method

The λ method was modified to propose (7.4) to include the influence of matric suction effect in the estimation of shaft resistance of piles in unsaturated soils.

$$Q_{f(us)} = \lambda\left[\sigma'_{v(avg)} + 2c_{u(sat)}\left(1 + \frac{(u_a - u_w)}{(P_a / 101.3)} S^{\upsilon} / \mu\right)\right]\pi dL \qquad \textbf{(7.4)}$$

The form of this equation will be same as the conventional λ method once the matric suction, $(u_a - u_w)$ component is set to zero. The required information using this equation are the undrained shear strength under saturated condition, $c_{u(sat)}$ and the *SWCC*.

The λ value is a function of pile length which can be determined from Figure 7.34 for estimating the load capacity of piles in-situ. The data of Vijayvergiya and Focht (1972) is revisited and plotted differently as a relationship between the λ and the ratio of pile diameter, d to pile penetration depth, L in Figure 7.35. A best-fit linear curve is plotted through the data which exhibits some scatter. This relationship is useful for interpreting the model pile results compared to the relationship shown Figure 7.34. The λ values for interpreting the model pile test results is determined

based on the *d/L* ratio as shown in Figure 7.35. The shaft capacity of the model pile is estimated using (7.4).

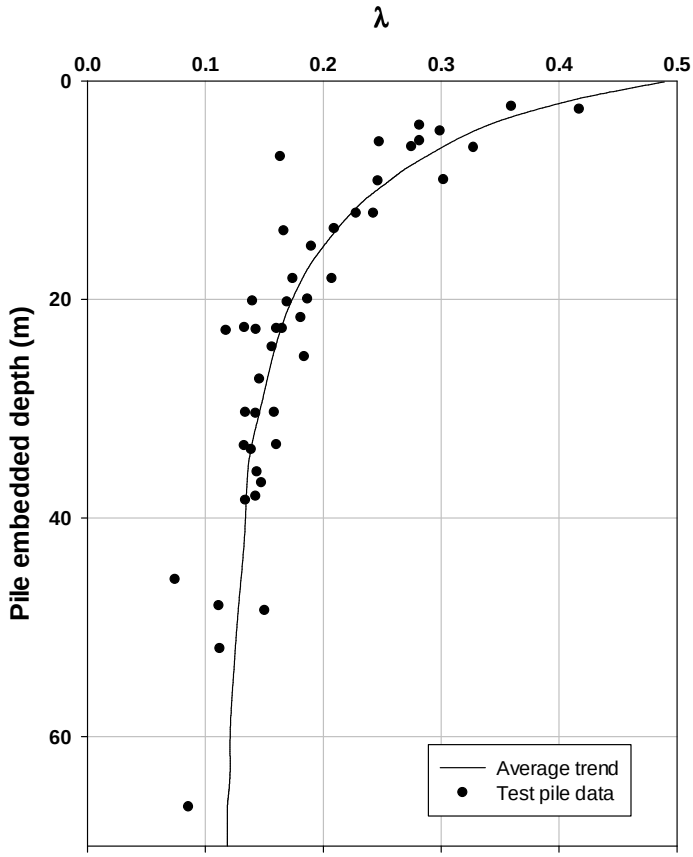

Figure 7.34 : Frictional capacity coefficient, λ vs. pile penetration (modified after Vijayvergiya and Focht, 1972).

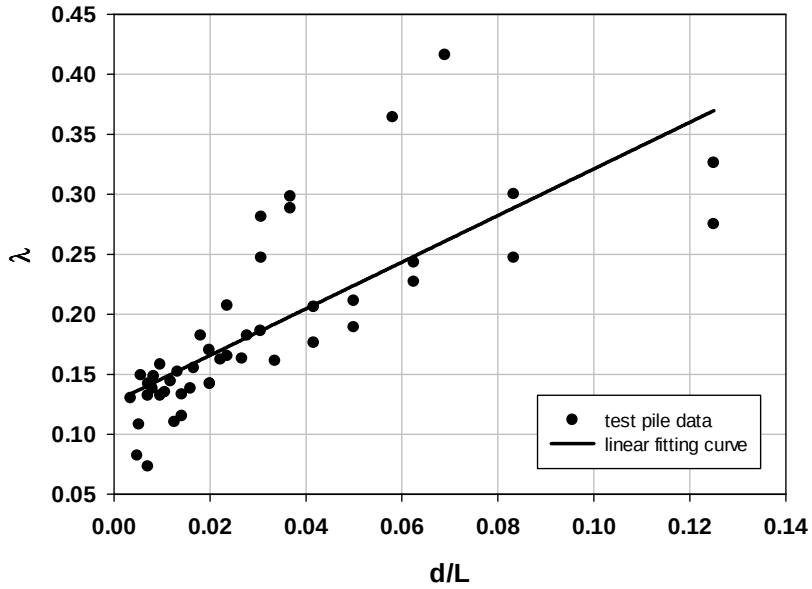

Figure 7.35 : Relationship between the variation of λ coefficient and the ratio between pile diameter, *d* to pile penetration, *L* using the data from Vijayvergiya and Focht (1972).

The analysis results of the model pile tests performed in Indian Head till with the initial water contents of 13 % -15.5% and 18% under undrained loading condition are summarized through Table 7.27 to Table 7.30 and in Figure 7.36. The analysis results of the model pile tests performed in Loam soil with the initial water content of 13 % is summarized in Table 7.31 and in Figure 7.37.

7.8.3.1 IHT.ASCOMPAC.13.UD : (matric suction=205kPa)

Table 7.27 : Measured and estimated *USC* values using the modified λ method for IHT.ASCOMP.13.UD.

D	$w_{initial}$	$(u_a - u_w)$	Meas. c_u	Est. c_u	d/L	λ	Est. $Q_{f(us)}$	Meas. $Q_{f(us)}$
mm	(%)	kPa	kPa	kPa	-	-	kN	kN
10					0.050	0.23	0.19	0.35
15					0.075	0.27	0.33	0.50
20	13	205	68	64	0.100	0.32	0.53	0.68
30					0.150	0.40	0.99	1.20
45					0.225	0.40	1.48	2.30

7.8.3.2 IHT.SAT.13.UD : (matric suction=0kPa)

Table 7.28 : Measured and estimated *USC* values using the modified λ method for IHT.SAT.13.UD.

D	$w_{initial}$	$(u_a - u_w)$	Meas. c_u	d/L	λ	Est. $Q_{f(us)}$	Meas. $Q_{f(us)}$
(mm)	(%)	kPa	kPa	-	-	kN	kN
20	13	0	11.5	0.10	0.32	0.09	0.10
30				0.15	0.40	0.19	0.14

7.8.3.3 IHT.ASCOMPAC.15.5.UD: (matric suction=110kPa)

Table 7.29 : Measured and estimated *USC* using the modified λ method for IHT.ASCOMP.15.5.UD.

D	$w_{initial}$	$(u_a - u_w)$	Meas. c_u	Est. c_u	d/L	λ	Est. $Q_{f(us)}$	Meas. $Q_{f(us)}$
mm	%	kPa	kPa	kPa	-	-	kN	kN
20					0.100	0.32	0.53	0.55
30	15.5	110	83	65	0.150	0.40	1.00	1.00
45					0.225	0.40	1.50	1.50

7.8.3.4 IHT.ASCOMPAC.18.UD: (Suction=55 kPa)

Table 7.30 : Measured and estimated *USC* using the Modified λ method for IHT.ASCOMP.18.UD.

D	$w_{initial}$	$(u_a - u_w)$	Meas. c_u	Est. c_u	d/L	λ	Est. $Q_{f(us)}$	Meas. $Q_{f(us)}$
mm	%	kPa	kPa	kPa	-	-	kN	kN
20					0.100	0.32	0.46	0.50
30	18	55	58	52	0.150	0.40	0.86	0.77
45					0.225	0.40	1.30	0.70*

*disturbance/improper installation

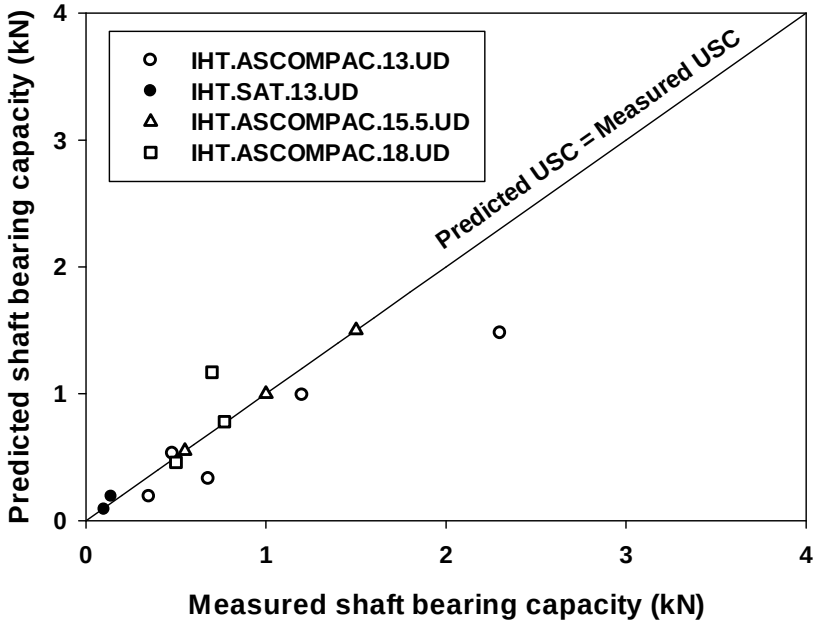

Figure 7.36 : Comparison between the measured and the predicted *USC*s using the modified λ method for Indian Head till.

7.8.3.5 LS.ASCOMPAC.13.UD: (matric suction=80-90 kPa)

The fitting parameters were chosen as $\nu = 2$, $\mu = 7$ for Loam soil with the plasticity value equal to $I_p = 6.5\%$. (Table 7.31 and Figure 7.37).

Table 7.31 : Measured and estimated *USC* using the modified λ method for LS.ASCOMP.13.UD.

D	$w_{initial}$	$(u_a - u_w)$	Meas. $c_{u(sat)}$/ $c_{u(unsat)}$	Est. c_u	d/L	λ	Est. $Q_{f(us)}$	Meas. $Q_{f(us)}$
mm	%	kPa	kPa	kPa	-	-	kN	kN
20	13	90	10/60	40	0.100	0.32	0.27	0.32
30					0.150	0.40	0.51	0.60

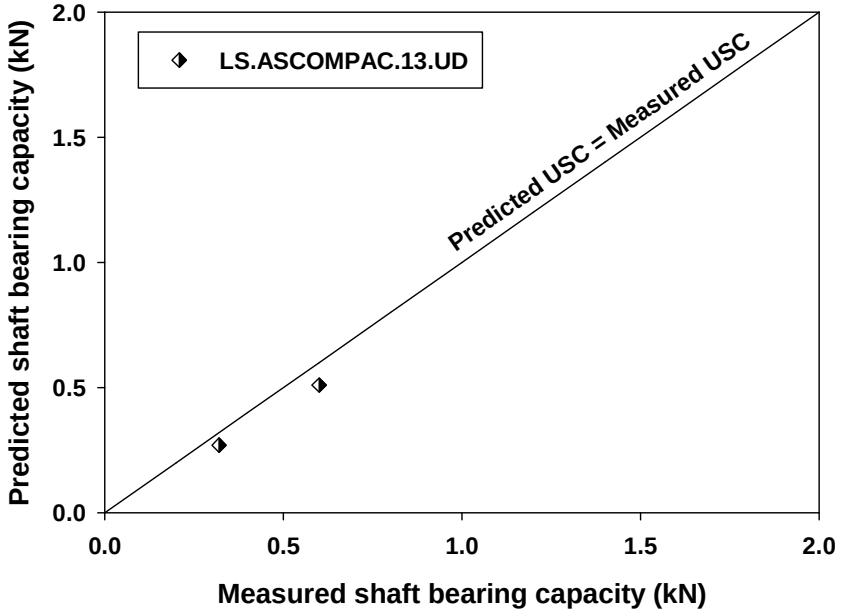

Figure 7.37 : Comparison between the measured and the predicted *USC*s using the modified λ method for Loam soil.

7.9 Summary

In this chapter, the results of the model pile load tests performed under saturated and unsaturated conditions on two different compacted fine grained soils (i.e. Indian Head till and Loam soil) were presented and analysed to study the influence of matric suction on the shaft bearing capacity. The ultimate shaft bearing capacites of model piles with different diameters (10 mm, 15 mm, 20 mm, 30 mm and 45 mm)

were determined from the measured p-δ curves following the assigned failure criteria. The difficulties associated with performing some of these tests are detailed.

The presented model pile load test results were then interpreted by using the modified α, β, and λ methods considering the effect of matric suction. Other test results including the matric suction measurements, *SWCC* determination and strength measurements were also reported and used as a tool for interpretation and prediction of shaft capacities under unsaturated condition.

The experimental shaft bearing capacity of a single pile under unsaturated condition was found to be approximately 5 to 6 times higher than the shaft bearing capacity of the same soil under fully saturated conditions. The results of this experimental program suggest that the conventional procedures for the estimation of pile shaft capacity of a single pile used in engineering practice are conservative when they are applied for unsaturated soil conditions.

8. MODELLING THE LOAD VERSUS DISPLACEMENT BEHAVIORS OF A SINGLE PILE IN UNSATURATED FINE GRAINED SOILS

8.1 Introduction

The load-displacement (i.e. p-δ) behavior of pile foundations can be determined from in situ load tests. However, in many cases it is not possible due to high costs or practical limitations of the site for conducting the pile load tests. The practical and economical limitations have encouraged researchers to propose empirical, analytical or numerical techniques for reliable and quick prediction of the p-δ behavior of piles. However, these conventional interpretation procedures/techniques are based on the mechanics of saturated soils.

Experimental results of model pile load tests conducted on unsaturated coarse and fine-grained soils in a laboratory environment and described in earlier chapters showed that the load-displacement behavior is significantly influenced by matric suction. The matric suction contribution due to shaft resistance of a single pile was determined to be between 40-50% for silts and silty sand type of soils and is around 30-120% for tills. In previous chapters conventional α, β and λ methods were modified to estimate and interpret the contribution of matric suction to the ultimate shaft bearing capacity. Numerical modeling studies in this direction also would be of value to understand the influence of matric suction on the ultimate shaft capacity of piles and to predict the p-δ behavior. Some studies in this direction were reported in the literature to understand the influence of suction on the performance of piles behavior (Georgiadis et al., 2003; Muraleetharan et al., 2008; Muraleetharan and Ravichandran, 2009; Ravichandran, 2009; Krishnapillai and Ravichandran, 2011)

Georgiadis et al. (2003) proposed a constitutive model for unsaturated soils extending the critical state concepts and incorporated into the Imperial College Finite Element Program (here after referred as *ICFEP*). This model was used to estimate the p-δ behavior of a single pile under axial loading using the critical state model

parameters. The contribution of matric suction to the bearing capacity behavior of a full-scale single pile (i.e. 20 m in length and 1 m in diameter), placed in glacial till, was investigated considering the influence of capillary stresses above the ground water table. Different scenarios with varying groundwater table conditions have been assumed such that both the positive and negative pore water pressure influence the pile behavior. The conventional and unsaturated analyses have been performed assuming drained loading conditions using the *ICFEP*.

In this chapter, the single pile analyses undertaken by Georgiadis et al. (2003) were reanalyzed using a commercially available finite element analysis program *SIGMA/W* (Geostudio 2007) software which is a product of GEO-SLOPE (Krahn, 2007). These analyses were carried out using the elastic-perfectly plastic model extending the Mohr-Coulomb yield criterion. The conventional shear strength parameters (i.e. c' and ϕ'), the soil-water characteristic curve (*SWCC*), the elastic modulus for saturated (i.e. E_{sat}) and unsaturated conditions (i.e. E_{unsat}) are required for modelling the p-δ behavior of single pile behavior. The numerical technnique is based on the elastic-plastic Mohr-Coulomb model that is incorportated into the *SIGMA/W* as one of the failure criterion models. The *SIGMA/W* analyses performed were compared with the *ICFEP* analysis results of Georgiadis et al. (2003).

8.2 Background

8.2.1 Elastic-plastic constitutive model extending the Mohr-Coulomb theory

Elastic-plastic framework can be used as a tool to propose simple constitutive models to describe the general soil behavior. A yield function, a plastic potential function and hardening/softening rules are required to formulate an elasto-plastic material.

A yield function defines the starting point of plastic straining. This function seperates elastic behavior from the elasto-plastic behaviour. A yield function is a scalar function in the form of $F(\{\sigma\},\{k\}) = 0$ where $\{\sigma\}$ = stress components or stress invariants and $\{k\}$ = state parameters. On the other hand, a plastic potential function of the form $P(\{\sigma\},\{m\}) = 0$ determines the direction of the plastic straining where $\{m\}$ = vector of state parameters (Potts and Zdravkovic, 2001). In the axial loading condition, the plastic strains take place in the same direction as the applied stresses.

However, for multi-axial loading it is necessary to define the plastic strain under different stress states.

A hardening/softening rule is required as the material hardens or softens for modeling. The hardening/softening rules determines how the state parameters $\{k\}$ vary with plastic straining. If the material is perfectly plastic, no hardening or softening rules are required. However, for materials which harden and/or soften during plastic straining, rules are required to specify how the yield function changes.

Elastic-plastic framework together with the Mohr-Coulomb failure criterion can be used to propose simple constitutive model to describe the general soil behavior in terms of effective stresses. The plastic behavior is governed by the shear strength parameters (c' and ϕ') and dilatancy angle (ψ); however, the elastic behavior is dependent on the Young's modulus (E) and Poisson's ratio (μ).

There is no need for hardening/softening law if the Mohr-Coulomb model is assumed to be perfectly plastic. The state parameter $\{k\}=\{c',\phi'\}^T$ can be assumed to be constant, independent of plastic strain or plastic work. In spite of assuming the Mohr-Coulomb model to be perfectly plastic, the calculated plastic strains results in a dilatant plastic volumetric strain behavior which is dependent on the angle of dilatation, ψ. This is one of the main shortcomings of the model as it can contribute to unreasonable predictions for some boundary value problems (Potts and Zdravkovic, 1999).

8.2.2 Critical State Model (*CSM*) for saturated soils

Mohr-Coulomb failure envelope is not capable to model adequately many basic features of soil behaviour such as the dilatancy during yield. The constitutive critical state model presents a framework to define mechanical behavior of soils considering both the shear strength and the volume change characteristics. The original critical state framework for saturated soils used in the Cam clay model was later extended into the Modified Cam clay model (Georgiadis et al., 2003; Potts and Zdravkovic, 2001). These models define a unique failure surface in q-p'-v space and use the M, λ, κ, v and v_o as the basic model parameters to define critical state line (Figure 8.1) through the following relationships (8.1) and (8.2):

$$q = Mp' \quad \textbf{(8.1)}$$

$$v = v_o - \lambda \ln(p') \quad \textbf{(8.2)}$$

where, q = deviator stress, M = the slope of the critical state line projected into p'- q stress space, p'= effective mean stress, v = specific volume = (1+ e), v_o = the specific volume at critical state, λ = slope of the virgin compression line and slope of the critical state line projected into $ln\ p'$-v space and κ= slope of the swelling line.

The critical state parameters are also related to the conventional soil properties such as the angle of internal friction, ϕ' and the compression index, C_c .The slope of the critical state line in the q-p' plane, M can be obtained from a series of triaxial compression tests and can be related to the ϕ' using (8.3) as given below:

$$M = \frac{6\sin\phi'}{3-\sin\phi'} \quad \textbf{(8. 3)}$$

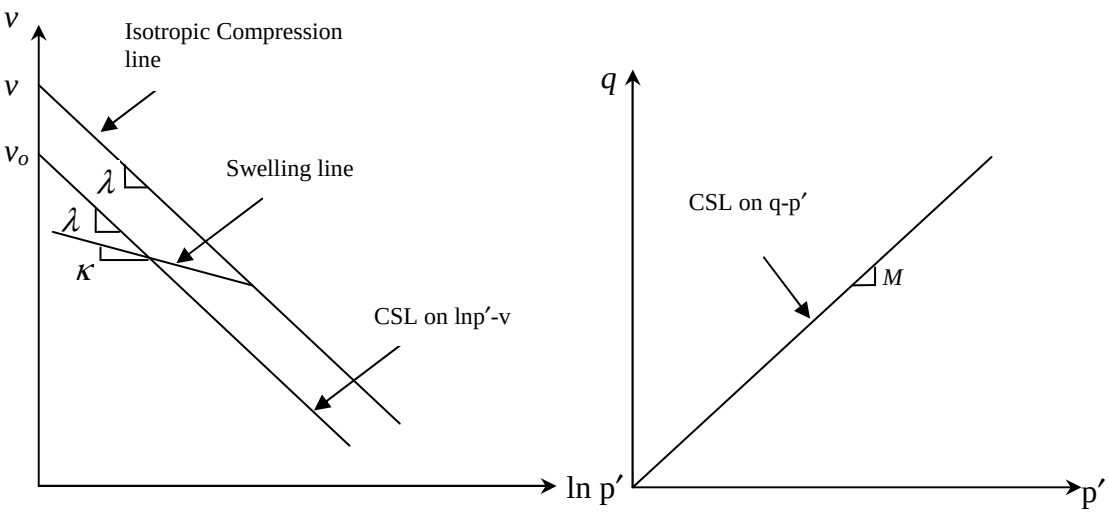

Figure 8.1 : Critical state model parameters.

8.2.3 Critical state model (*CSM*) extended for unsaturated soils

One of the first constitutive models to be developed for unsaturated soils was the Barcelona basic model (Alonso et al., 1987; Alonso et al., 1990). This model was based on the modified Cam clay model for fully saturated soils, and was extended for unsaturated soils through the introduction of the concept of the loading-collapse yield surface. Most constitutive models for unsaturated soils are extensions of critical state constitutive models originally proposed for saturated soils (Alonso et al., 1990;

Kohgo et al., 1993; Wheeler and Sivakumar, 1995; Bolzon et al., 1996). These constituve models consider the change in degree of saturation during the variation of volumetric deformation due to swelling-shrinkage or net normal stress.

Georgiadis et al. (2003) presented a constitutive model for unsaturated soils based on the loading-collapse yield surface concept by defining an additional equivalent suction space. The proposed constitutive model for unsaturated soils based on the loading-collapse yield surface concept by defining two yield surfaces. The equation for yield surface and associated plastic potential surface is extended to the equivalent suction space by introducing a suction term, $k\, s_{eq}$. This term represents the expansion of the yield surface into the tensile total stress (stress-suction space) region and defines the amount of increase in apparent cohesion. In Georgiadis et al. (2003) model, the cohesion increase parameter, k can either have a constant value leading to a linear increase of apparent cohesion with suction, or be set equal to the degree of saturation (S_r). The *SWCC* data is required when the parameter, k is assumed to be equal to S_r.

In order to model mechanical behavior of unsaturated soils, the critical state line equation and compression line equation are modified by including the above assumptions in (8.1) and (8.2) to obtain equation (8.4a), (8.4b) and (8.5) as given below.

$$q = M(p + k.s_{eq} + s_{air}) \quad \text{if } k = \text{constant} \qquad \textbf{(8.4a)}$$

$$q = M(p + S_r.s_{eq} + s_{air}) \quad \text{if} \quad k = S_r \qquad \textbf{(8.4b)}$$

$$v = v(s_{eq}) - \lambda(s_{eq}) \ln p_o \qquad \textbf{(8.5)}$$

where, $s_{eq} = s - s_{air}$, S_r = the degree of saturation, s_{eq} = the equivalent suction, s = soil suction value, s_{air} = air entry suction value.

8.3 Single Pile Analysis by Georgiadis et al. (2003)

Georgiadis et al. (2003) summarized two common scenarios of pore pressure distribution profiles which are illustrated in Figure 8.2; (a) Profile 1: Conventional analysis and (b) Profile 2: Unsaturated analysis. In conventional analysis, the influence of negative pore water pressure above the groundwater table (GWT) is ignored. The pore water pressure is considered to be equal to zero above the

saturated zone as it is a conservative assumption. For unsaturated analysis case, in general, three different negative pore-water pressures profiles are possible when the soil is in a state of unsaturated condition. These include: (i) excessive evaporation condition, (ii) hydrostatic condition, and (iii) flooding desiccated soil condition.

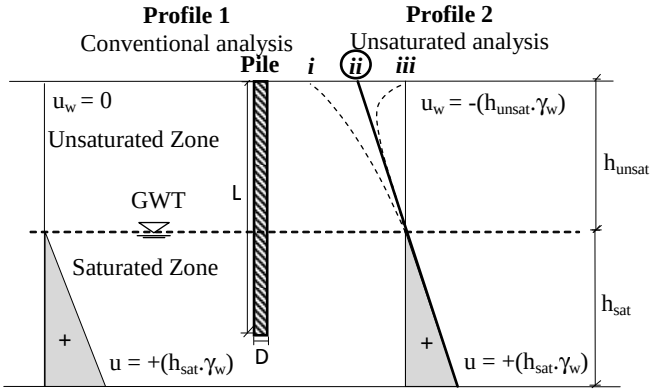

Figure 8.2 : The variation of pore-water pressure with respect to depth considering the initial ground water table level condition (modified after Georgiadis et al. 2003).

The proposed critical state model extended for unsaturated soils has been implemented into the *ICFEP* and used to investigate the influence of suction and the ground water fluctuations on the behavior of a single pile placed in a glacial till deposit. The single pile used in the study was 20 m in length and 1 m in diameter. The analyses were performed considering different ground water table levels from the ground surface (i.e. 0 m (saturated condition), 2 m, 6 m, 10 m, and 25 m) for both conventional (Profile 1) and unsaturated analysis (Profile 2-ii) for the hydrostatic pore-water pressure profile condition. The soil considered in the study Lower Cromer till (hereafter referred to as LC till), which was assumed to be isotropic and homogeneous. This soil can be categorized as sandy clay with low plasticity. All the analyses were performed assuming drained loading condition.

The cohesion increase parameter, *k* was chosen as a constant value of 0.8 due to the the low suction values associated with the pore-water pressure profile. Assuming the parameter *k* as constant value eliminates the need for using the *SWCC* (8.4a). An air-entry suction value, s_{air}, was assumed to be zero for the unsaturated analyses cases and the soil between the ground surface and the ground water table was considered to be unsaturated. In other words, the capillary saturated zone extending from the water table up to the air-entry head has been ignored.

In the numerical modeling analyses performed by Georgiadis et al. (2003), eight-noded axisymmetric isoparametric quadrilateral elements with reduced integration were used. The critical state model parameters, α and μ which control the shape of the defined yield surfaces were selected in a way that the model for saturated soil conditions is the same as modified Cam-clay model.

8.4 Estimation of *p*-δ Behavior of In-situ Single Pile in Unsaturated Glacial till Deposit Using Elastic-Plastic Mohr-Coulomb Model in SIGMA/W

The in-situ single pile behavior studied by Georgiadis et al. (2003) was reanalyzed using the commercially available finite element software, *SIGMA/W* (GeoStudio 2007) extending the elastic-plastic Mohr Coulomb model for unsaturated soils.

8.4.1 Definition of the analysis problem and soil properties

An independent finite element analyses (here after referred as *FEA*) were undertaken by using *SIGMA/W* to evaluate load carrying capacity of a single pile for different scenarios of positive and negative pore-water pressures as shown in Profile 1 and Profile 2: (ii) hydrostatic condition given in Figure 8.2. The unsaturated zone above the *GWT* level was defined by assigning the water table level at different depths from the ground surface as 0 m (saturated condition), 2 m, 6 m, 10 m, and 25 m. The soil profile at the site is assumed to be isotropic and homogeneous. The pile dimensions, groundwater table conditions, soil properties and the analysis steps for the problem defined in this paper were parallel to the example problem presented by Georgiadis et al. (2003). All the analyses were performed for drained loading conditions.

Due to the lack of *SWCC* information of LC till, the *SWCC* of Indian Head till (adopted from Vanapalli et al. (1996)) was used in the present study. The *LC* till and Indian Head till have similar grain size distribution, index properties and engineering properties. Therefore, it is reasonable to use the *SWCC* for Indian Head till in this study. For comparison purposes, the soil properties of Indian Head till are summarized along with the *LC* till in Table8.1. The *SWCC* of the Indian Head till used in the present study is summarized in Figure 8.3.

8.4.2 Shear strength of unsaturated soils

The shear strength behavior of unsaturated soils for Profile 2 shown in Figure 8.2 can be interpreted using the Fredlund et al. (1978) equation in terms of two stress state variables, net normal stress and matric suction (8.6):

$$\tau_{unsat} = c' + (\sigma_n - u_a)\tan\phi' + (u_a - u_w)\tan\phi^b \qquad \textbf{(8.6)}$$

where τ_{unsat} = shear strength of an unsaturated soil, c' = effective cohesion, $(\sigma_n - u_a)$ = net normal stress, ϕ' = effective internal friction angle, $(u_a - u_w)$ = matric suction and ϕ^b = angle of shearing resistance due to an increase in matric suction.

Table 8.1 : Soil properties used in the study.

Soil Properties	**Lower Cromer Till** Gens (1982), Maswoswe (1985), Bell (1991)	**Indian Head Till** Vanapalli (1994) & Vanapalli et al. (2007)
Effective cohesion, c'(kPa)	12	15
Effective friction angle, ϕ'(deg)	26	23
Specific gravity, G_s	2.70	2.73
Total unit weight, γ(kN/m^3)	17.0	19.2
Plasticity Index, I_p (%)	12	15.5
Sand (%)	38-64	28
Silt (%)	18-32	42
Clay (%)	17-30	30

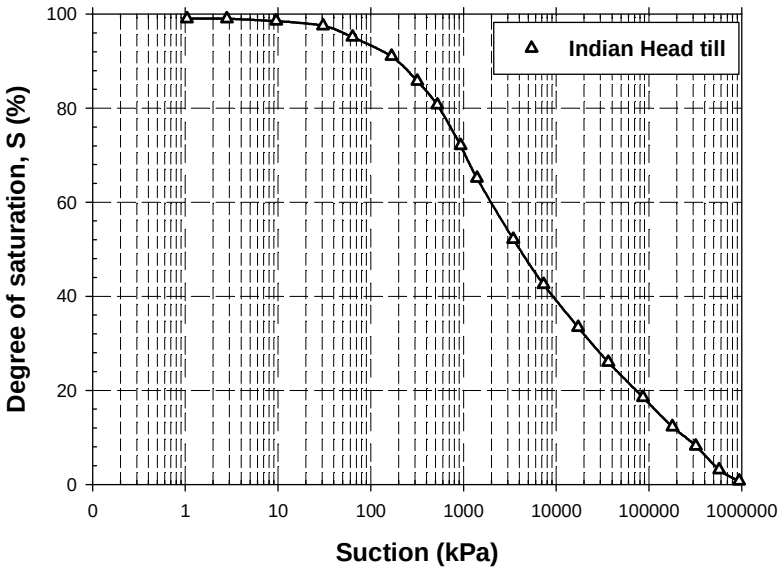

Figure 8.3 : Soil-water characteristic curve for Indian Head till.

Vanapalli et al. (1996) provided a semi-empirical equation (8.7) to predict the variation of shear strength of unsaturated soils using the conventional shear strength parameters (i.e. c' and ϕ') and the *SWCC*.

$$\tau_{unsat} = c' + (\sigma_n - u_a)\tan\phi' + (u_a - u_w)\left[\frac{(\theta - \theta_r)}{(\theta_s - \theta_r)}\tan\phi'\right] \quad \textbf{(8.7)}$$

where, θ = the volumetric water content at any suction, θ_s = the volumetric water content at saturation, θ_r = the residual volumetric water content. The various volumetric water content values can be determined from the *SWCC*.

The *SWCC* function can be defined in the *SIGMA/W* software in terms of volumetric water content *(θ)* versus suction *(u_a - u_w)* such that the contribution of suction towards total cohesion can be estimated. The user defined effective cohesion, c' for saturated condition along with the *SWCC* (θ *vs.* *(u_a - u_w)*) data is used to calculate the variation of total cohesion with respect to suction using the following relationship given in (8.8):

$$c = c' + (u_a - u_w)\left[\frac{(\theta - \theta_r)}{(\theta_s - \theta_r)}\tan\phi'\right] \quad \textbf{(8.8)}$$

Georgiadis et al. (2003), in their study reported the slope of the critical state line, *M* to be equal to 1.2. The internal friction angle ϕ' for LC till was derived from Eq. 8.3 for use in the Mohr-Coulomb model. The back calculated ϕ' value of 26º is also consistent with the reported values in the literature for LC till soil samples (Bell, 1991).

8.4.3 Definition of the pore water pressure profile

In *SIGMA/W*, the variation of pore water pressure with respect to depth can be simulated in two different ways: i) by defining an initial water table (h_{sat}) and a maximum negative pressure head (h_{max}) based on the assumption that it varies hydrostatically with distance above and below the initial ground water table level (Fig. 8.4), and ii) by defining a spatial function to simulate the pore water pressure change as excessive evaporation condition, hydrostatic condition or as flooding desiccated condition.

In the former case, if the defined maximum pressure head is lower than the thickness of the unsaturated soil layer (i.e. $h_{max} < h_{unsat}$) the negative pore water pressure is

constant up to the ground surface beyond once the maximum negative pressure head is reached. If maximum negative pressure head is greater than the height of unsaturated soil layer (i.e. $h_{max} > h_{unsat}$) then the negative pore-water pressure can be defined to be increasing hydrostatically up to ground surface (Fig. 8.4).

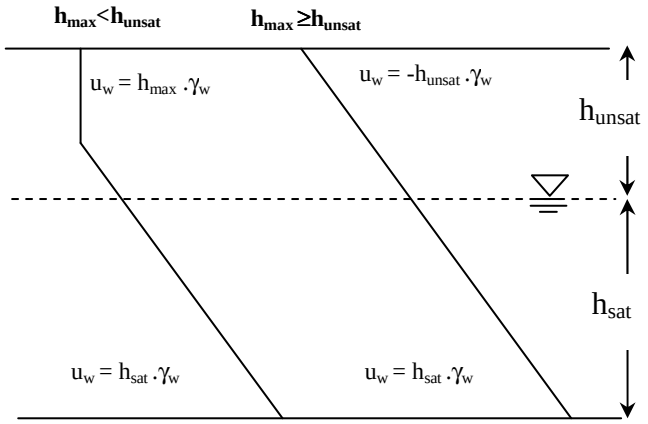

Figure 8.4 : Defining pore water pressure in SIGMA/W by assigning an initial water table (modified after Oh and Vanapalli, 2011).

8.4.4 Elastic modulus for unsaturated soil condition

Oh et al. (2009) proposed a semi-empirical model for predicting the variation of modulus of elasticity of unsaturated soils, E_{unsat} using the *SWCC* and the modulus of elasticity under saturated condition, E_{sat} (8.9). This relationship is used for the analysis to estimate the elastic modulus for the unsaturated soil zone above the *GWT*.

$$E_{unsat} = E_{sat}\left[1+\alpha\frac{(u_a-u_w)}{P_a/101.3}S^{\beta}\right] \qquad \textbf{(8.9)}$$

where E_{sat}, E_{unsat} = elastic modulus under saturated and unsaturated conditions, respectively, and α, β = fitting parameters. β = 2 for fine-grained soils regardless of I_p. Vanapalli and Oh (2010) have shown that the fitting parameter α can be defined by a relationship shown in (8.10). The relationship shows that the inverse of α nonlinearly increases with increasing, I_p.

$$(1/\alpha) = 0.5 + 0.063(I_p) + 0.036(I_p)^2 \qquad \textbf{(8.10)}$$

The fitting parameters values of α =1/10 and β = 2 suggested by Vanapalli and Oh (2011) for Indian Head till with I_p value of 15.5 were used in the present study.

In *SIGMA/W*, the elasticity modulus can be simulated in two different ways: i) by defining the variation of elastic modulus with depth, and ii) by defining an average value of elastic modulus for the entire soil profile. Both approaches were used in the present analyses obtaining close results.

i) The variation of the elastic modulus with respect to matric suction and the corresponding E_{unsat} values for the unsaturated zone (i.e. hydrostatic negative pore water pressure profile assumption) is calculated by (8.10) using the *SWCC* data *and* E_{sat} value. The obtained relationship is given in Figure (8.5). These values are defined as data point function in *SIGMA/W* to plot the variation of elastic modulus with depth considering different depths for *GWT* location (i.e. 0 m, 2 m, 6 m, 10 m and 25 m). The elastic modulus for the saturated zone below the GWT is assumed to be constant and equal to E_{sat}.

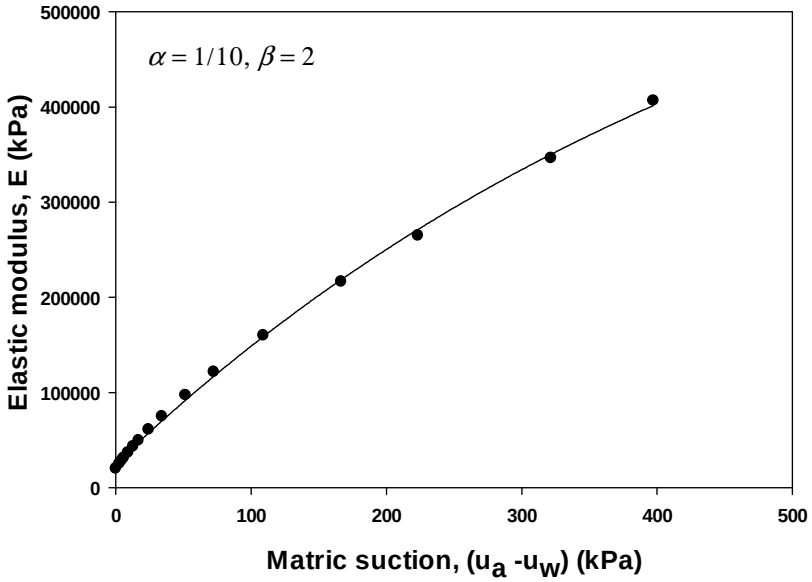

Figure 8.5 : Variation of the estimated elasticity modulus with respect to matric suction.

ii) An average value of elastic modulus as $E_{unsat(avg)}$ is defined for the given soil profile. This value of $E_{unsat(avg)}$ is determined by calculating the average of the data point function values obtained in (i). The calculated input $E_{unsat(avg)}$ for various depths are summarized in Table (8.2).

Table 8.2 : Elasticity modulus values used for calculations in unsaturated analysis.

GWT level (m)	$E_{sat/unsat(avg)}$ (kPa)
0	20000
2	21920
6	33196
10	57127
25	90815

8.4.5 Model parameters

The model parameters used for predicting the load versus displacement (i.e. p-δ) behavior using the elastic-plastic Mohr-Coulomb model are summarized in Table 8.3. Axisymmetric analysis was performed using quadrilateral elements with single nodes considering appropriate boundary conditions. Figure 8.6 summarizes the key details; however, it is not drawn to scale. The space coordinates extend to 50 m and 55 m in the x and y directions, respectively. The pile and soil material properties were defined separately. The pile itself is modeled as linear elastic material with a relatively high modulus of elasticity compared to the soil. The loading on the pile was applied by increments of vertical displacement to its top.

Table 8.3 : Model parameters used in SIGMA/W analysis.

Model Parameters	Soil	Pile
Model	Elastic Plastic	Linear Elastic
c'(kPa)	12	-
ϕ'(°)	26	-
E_{sat} (kPa)	20000	20×10^6
γ(kN/m^3)	17	24
K_o	1	-
μ	0.334	0.15
ψ(°)	0	-

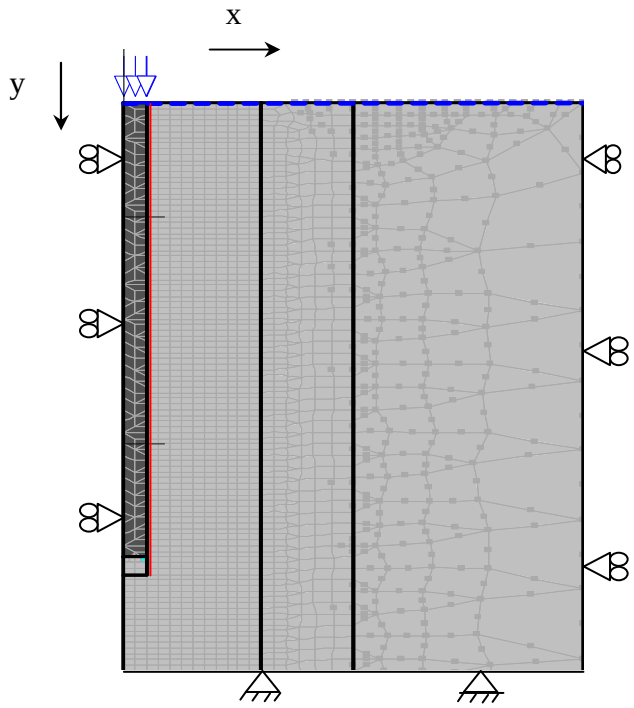

Figure 8.6 : Finite element modeling in SIGMA/W (not drawn to scale).

8.4.6 Finite element analysis results

The FEA results of the present study using the *SIGMA/W* are compared with the *ICFEP* results reported by Georgiadis (2003). In Figure 8.7, the load-displacement (i.e. $p–\delta$) behavior of the single pile for saturated soil condition is summarized. The $p–\delta$ behavior for the conventional analysis based on the pore pressure Profile 1 shown in Figure 8.8 through Figure 8.11. The $p–\delta$ curves show the analysis results assuming *GWT* at 2 m, 6 m, 10 m and 25 m depths from the ground surface. The unsaturated analysis results based on the hydrostatic pore water pressure assumption in Profile 2 is summarized in Figure 8.12 through Figure 8.15.

The contribution of matric suction to the load carrying capacity of pile for shallow *GWT* depth of 2 to 6 m in comparison to saturated soil conditions is not significant. This behavior can be observed from the conventional and the unsaturated analysis (Fig. 8.16a-b). However, bearing capacity of a single pile increases with an increase in the *GWT* depth from the ground surface. The increase in bearing capacity for unsaturated analyses is due to the contribution of suction to the shaft resistance. The analysis results also show that the end bearing capacity is not significantly influenced by the unsaturated zone for the fine-grained soil investigated in the present study.

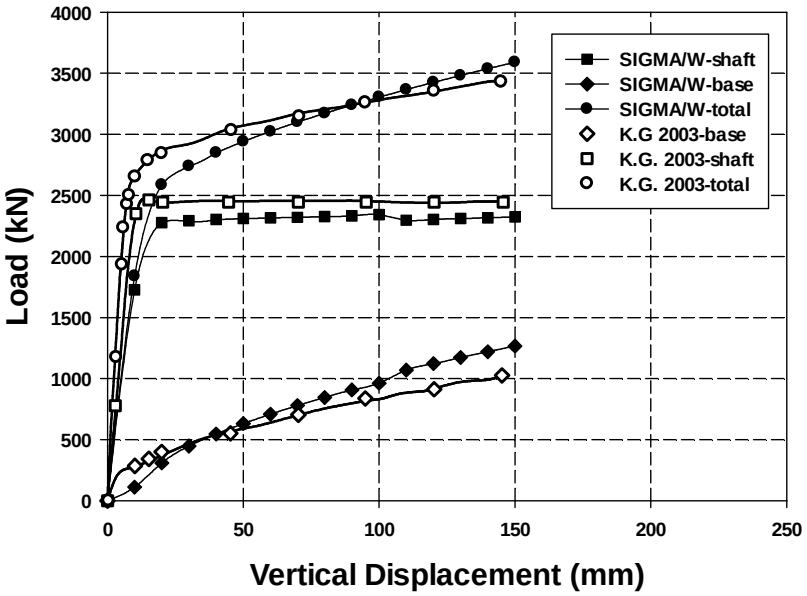

Figure 8.7 : Load-displacement curve for drained loading analyses for saturated soil condition when GWT = 0m.

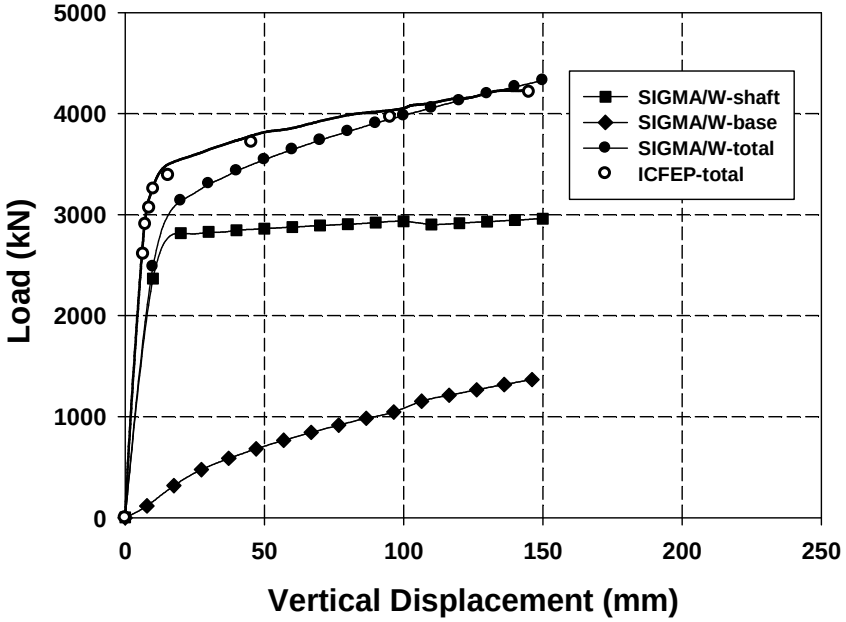

Figure 8.8 : Load-displacement curve results for conventional analyses when GWT = 2m.

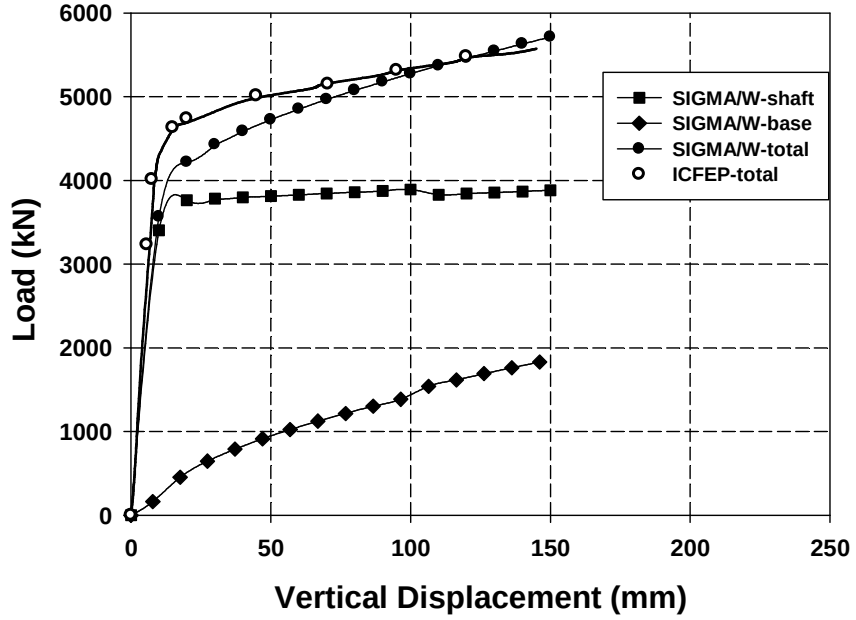

Figure 8.9 : Load-displacement curve results for conventional analyses when GWT = 6m.

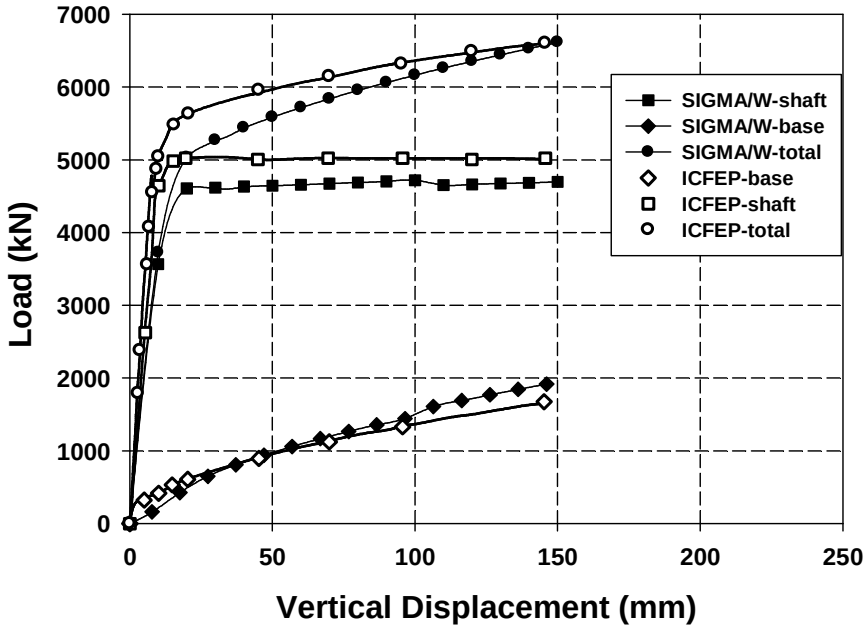

Figure 8.10 : Load-displacement curve results for conventional analyses when GWT = 10m.

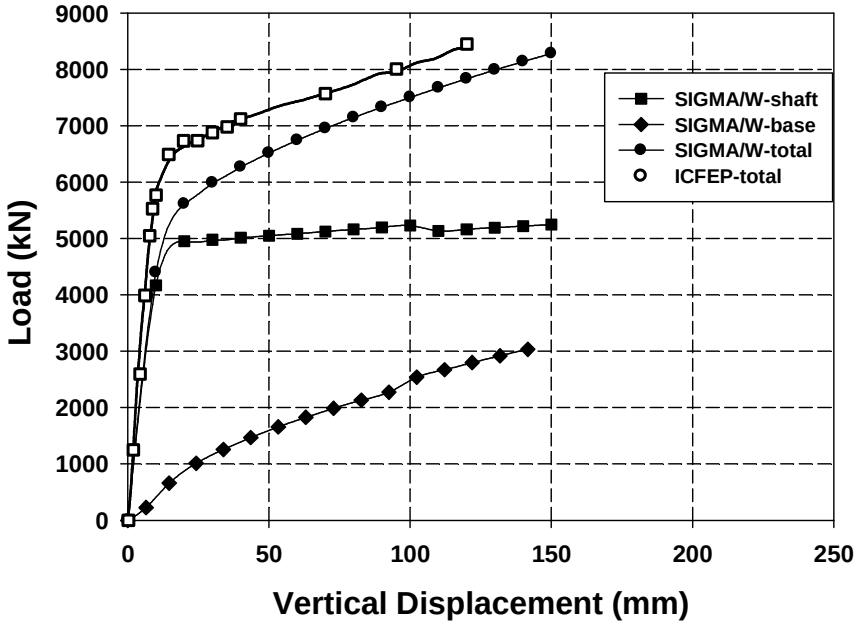

Figure 8.11 : Load-displacement curve results for conventional analyses when GWT = 25m.

The conventional analysis underestimates the load carrying capacity of the pile approximately by 2, 4, 12 and 45% compared to the unsaturated analysis for GWT located at 2 m, 6 m, 10 m and 25 m from the ground surface, respectively. As the GWT level changes over time and moves to a greater depth (i.e. dewatering or underdrainage) after pile installation, the pile load capacity increases. The pile load tests can result in higher bearing capacities when compared to the saturated condition. However, if GWT rises to the ground surface again then an overprediction of 293% would be observed for the two extreme conditions of GWT at 25 m depth and at natural ground surface (i.e. the fully saturated case).

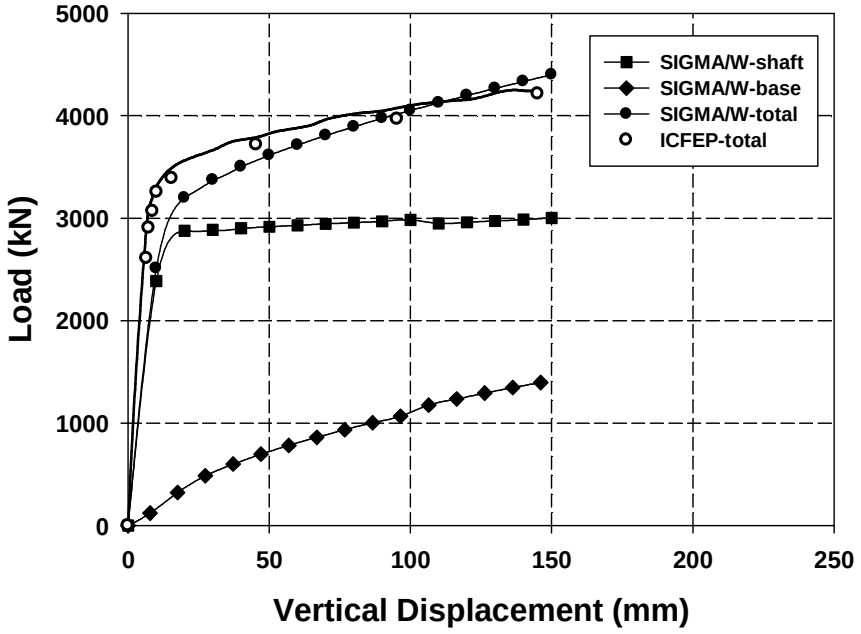

Figure 8.12 : Load-displacement curve results for unsaturated analyses when GWT = 2m.

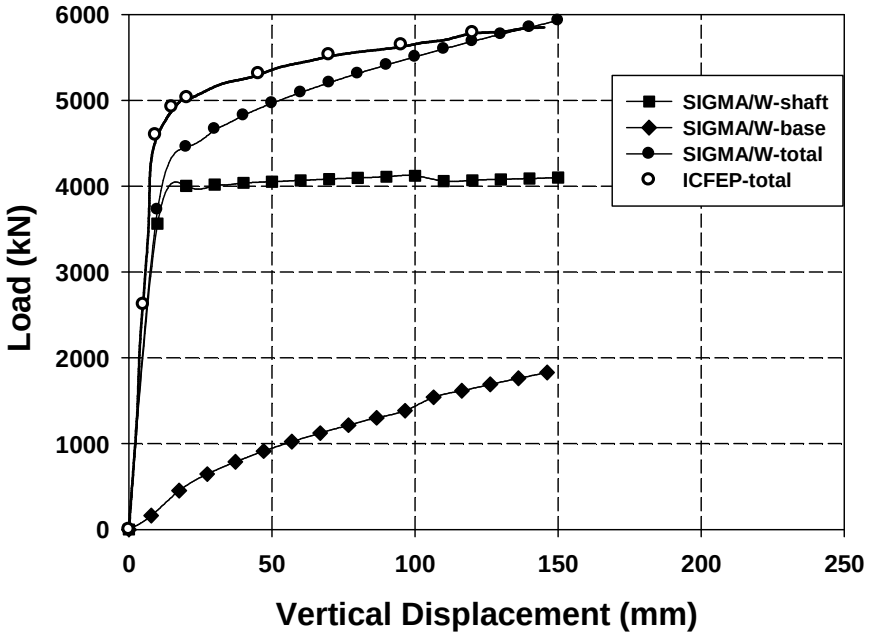

Figure 8.13 : Load-displacement curve results for unsaturated analyses when GWT = 6m.

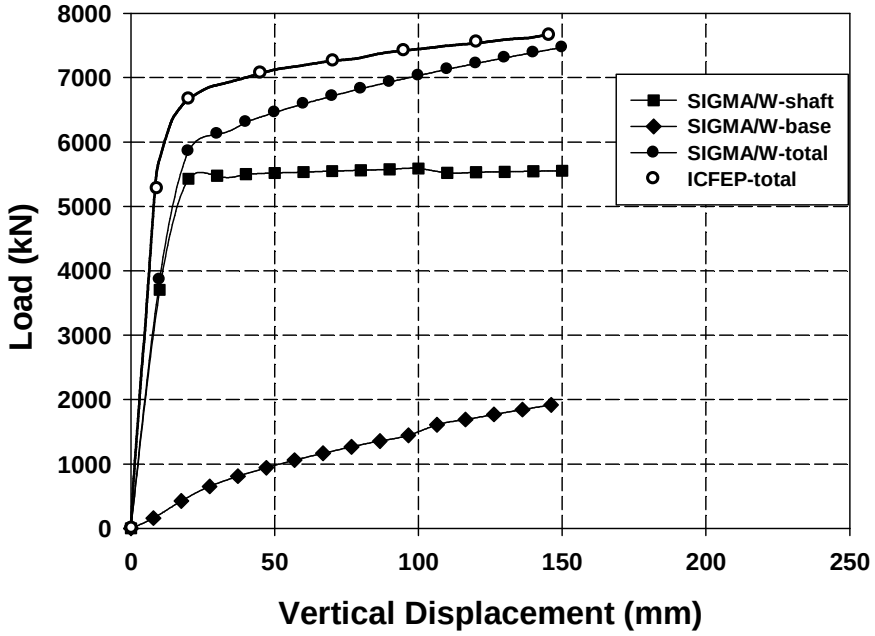

Figure 8.14 : Load-displacement curve results for unsaturated analyses when GWT = 10m.

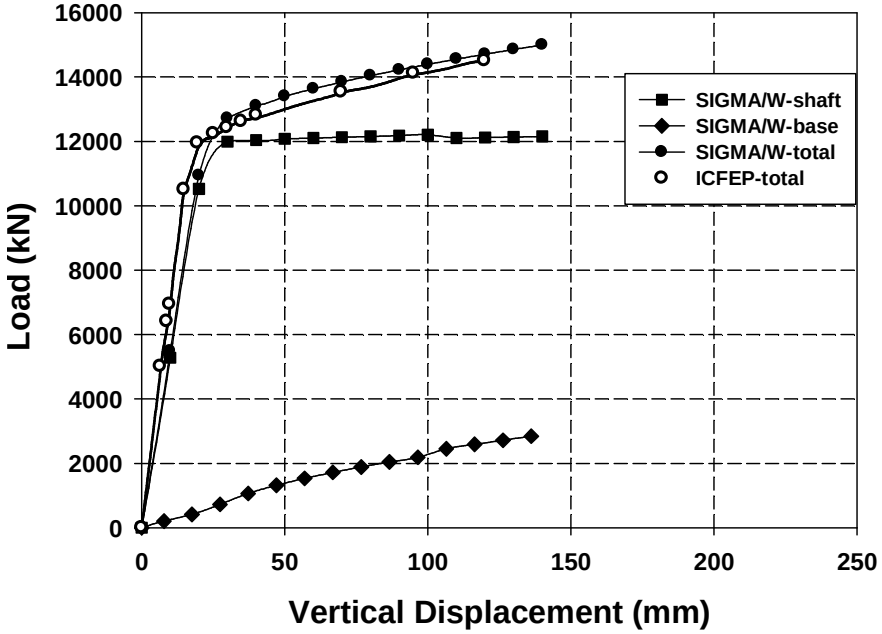

Figure 8.15 : Load-displacement curve results for unsaturated analyses when GWT = 25m.

There is a reasonably good agreement between the two models discussed in this study both for the conventional and the unsaturated analyses results. This agreement shows that the elastic-plastic Mohr-Coulomb model can be used in modeling the pile foundation behavior in unsaturated conditions considering the influence of suction. The proposed approach has the advantage of working with conventional shear strength parameters and the *SWCC* using commercial software.

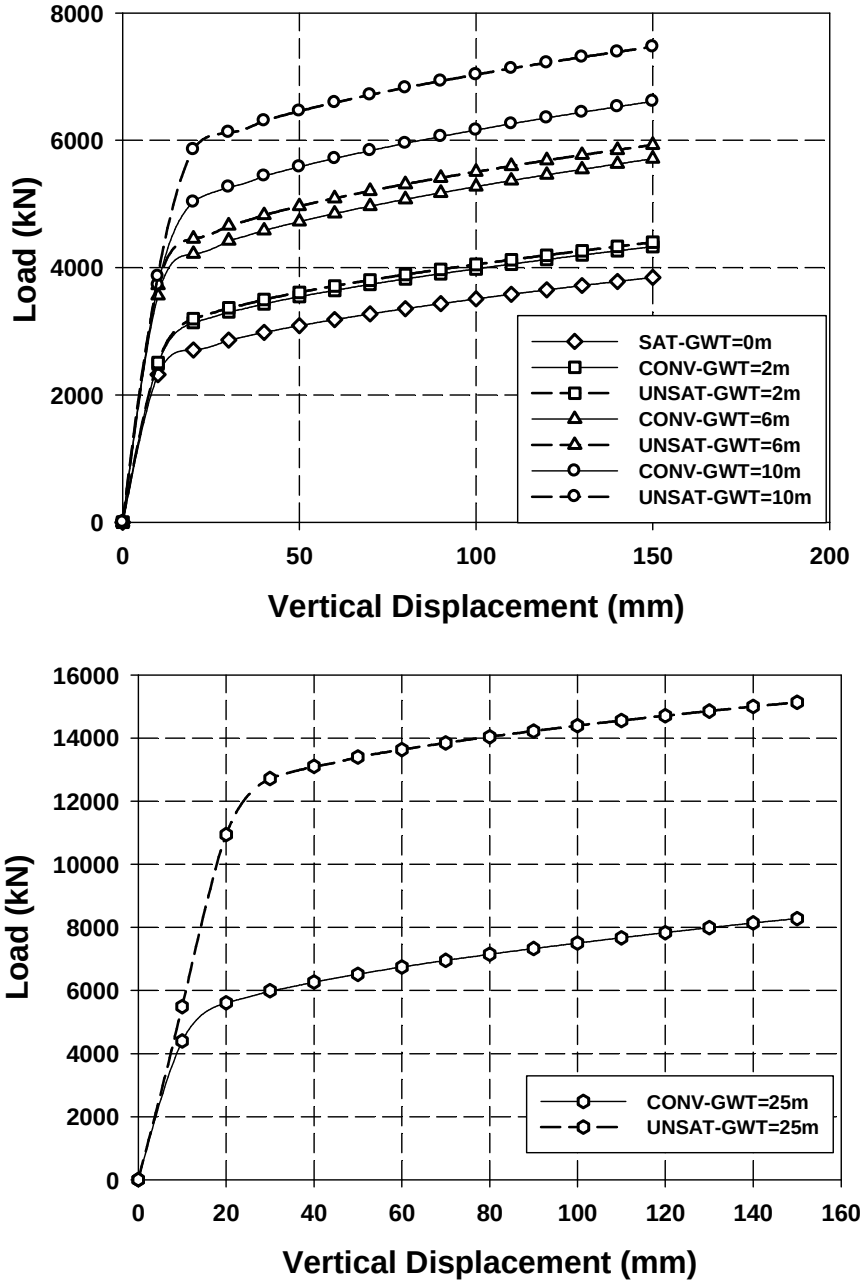

Figure 8.16 : Comparison of the load-displacement curve results for conventional and unsaturated analysis results for GWT = 0-2-6-10-25m.

8.4.7 Validation of the elastic-plastic model for unsaturated soils

Comparisons were provided between the load versus displacement (p-δ) behavior of a single pile placed in a glacial deposit under saturated and unsaturated soil conditions using two different numerical analysis techniques. The numerical technique proposed by Georgiadis et al. (2003) is a comprehensive constitutive model based on critical state soil mechanics concepts for unsaturated soils. The technique presented in this paper is based on an elastic-plastic Mohr-Coulomb model which uses the conventional shear strength parameters and the *SWCC* that can be

implemented with the commercial software program *(SIGMA/W)*. There is a reasonably good comparison between the simulated results using both these approaches.

Two key conclusions can be derived from the present study. Firstly, the conventional calculation methods for estimating the load-displacement (i.e. p-δ) behavior of pile foundations are conservative when they are extended for unsaturated fine-grained soils. Secondly, the elastic-plastic Mohr-Coulomb model supported by the commercial software (i.e. *SIGMA/W*) can be used as a tool to estimate the load-displacement (i.e. p-δ) behavior of pile foundations for both the saturated and unsaturated soil conditions.

8.5 Analytical Calculation of UBC for Conventional and Unsaturated Analysis Using the Modified β Method

The modified β Method (8.11) was used for calculating the ultimate shaft bearing capacity. More details of this method were discussed in Chapter 3 (see section 3.5.1).

$$\begin{aligned} Q_{f(us)} &= Q_{f(sat)} + Q_{f(u_a - u_w)} \\ &= \left[\beta \sigma'_z + (u_a - u_w)(S^{\kappa})(\tan \delta') \right] \pi d L \end{aligned} \qquad \textbf{(8.11)}$$

where, κ = fitting parameter used for shear strength, and S = degree of saturation, $(u_a - u_w)$ = matric suction, δ = internal friction angle between pile and soil, $\beta = K_o \tan \delta$, where $K_o = (1-\sin \delta)$ which is the average lateral earth coefficient at rest.

The effective adhesion between the pile and soil, c'_a was neglected on account of the local remoulding assumed to occur during pile installation (Potts and Martins 1982). The end bearing resistance of the pile is also calculated in the present study using the conventional formulation given in (8.12) and the matric suction effect was not taken into account.

$$Q_p = N_q \sigma'_v A_b \qquad \textbf{(8.12)}$$

where, Q_p = ultimate pile tip bearing capacity, N_q = bearing capacity factor which is the function of effective internal friction angle different, σ'_v= effective overburden pressure at the pile tip, A_b= area of the pile tip. A value of 8 is used for N_q for piles (Prakash and Sharma 1990).

The ultimate load bearing capacity values for conventional and unsaturated analysis calculated from the conventional and modified β method are respectively plotted on the same figures. The failure criteria (i.e. ultimate bearing capacity) is typically estimated to be reached at 10% of the pile diameter (ASTM D1143). The ultimate bearing capacity values corresponding to the 0.1 m of vertical displacement are calculated and shown on Figure (8.17).

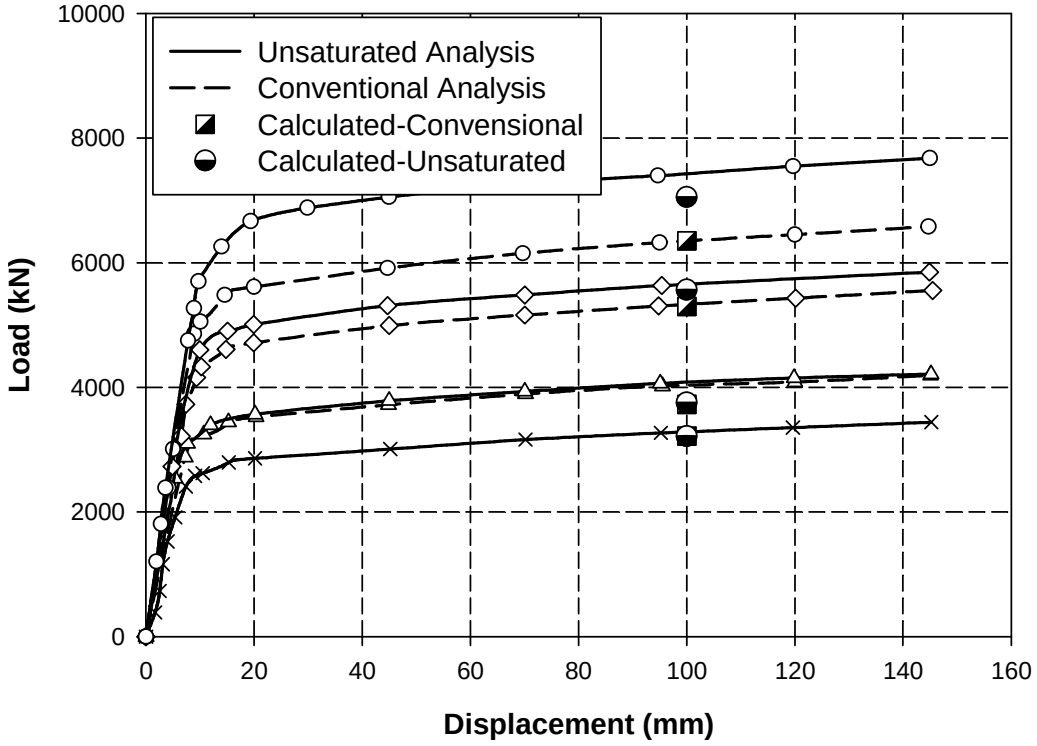

Figure 8.17 : Load-displacement curves and analytical calculation results using the modified β method for conventional and unsaturated analysis for GWT = 0-2-6-10.

The biggest difference for the calculated loads is observed for the unsaturated analysis when GWT = 25 m. The predicted results using the modified β method given in Figure 8.17 shows a good comparison with the numerical analyses results where the GWT is comparatively at shallow depths (i.e. 0 m to 10 m). However for the condition where GWT is located at 25 m depth, the modified β method underestimates the bearing capacity by 20%. This may be explained by the matric suction contribution due to end bearing since pile tip is also located within the unsaturated soil zone when GWT = 25 m which is ignored in the calculations (Figure 8.18).

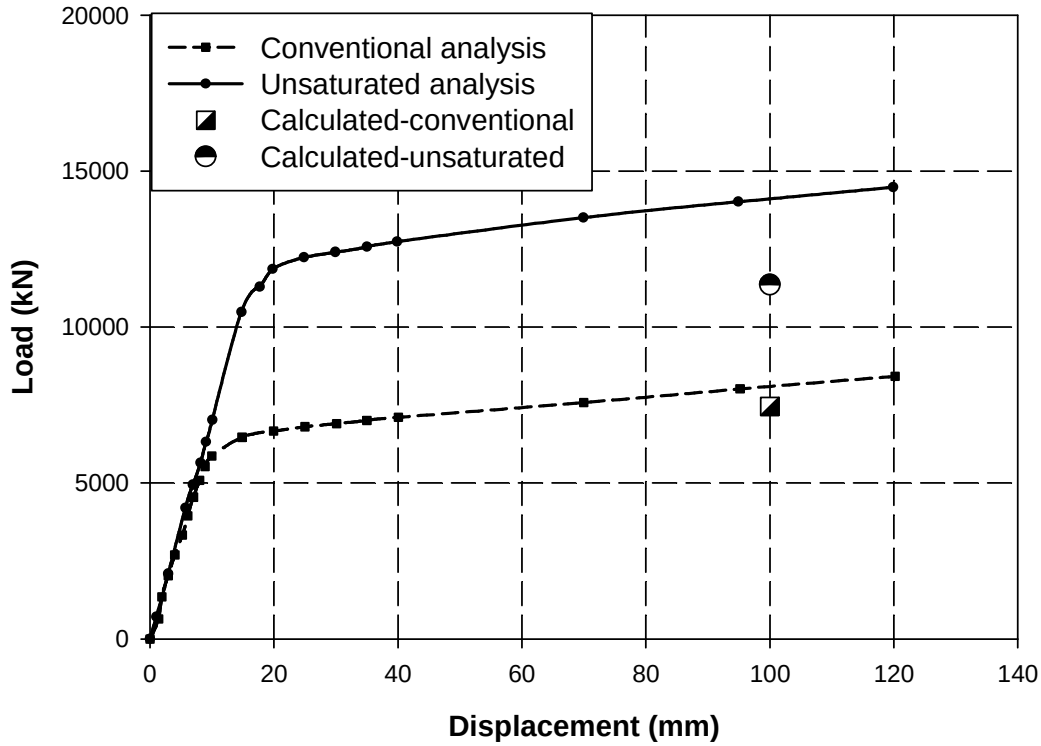

Figure 8.18 : Load-displacement curves and Analytical calculation results using the modified β method for conventional and unsaturated analysis for GWT = 25m.

8.6 Summary

The load-displacement (i.e. *p*-δ) behavior of pile foundations is conventionally estimated assuming saturated soil properties using theoretical, empirical or numerical analysis methods. The same methods are also conventionally used by practicing engineers for piles that are placed in an unsaturated soil state and the contribution of soil suction towards bearing capacity is ignored. However, experimental studies presented in this thesis show that there is a significant contribution of matric suction towards shaft resistance of single piles embedded in coarse and fine-grained compacted soils.

Georgiadis et al. (2003) proposed a constitutive model for unsaturated soils extending the critical state concepts and incorporated into the Imperial College Finite Element Program *(ICFEP).* The *ICFEP* was used to estimate *p*-δ behavior of a single pile of 20 m length and 1 m diameter in a glacial till considering different scenarios of saturated and unsaturated soil conditions. In this chapter, an elastic-plastic Mohr-Coulomb model is extended to estimate the same series of results reported by Georgiadis et al. (2003) by using the commercially available *FEA* software program

(SIGMA/W). The theoretical background and the numerical modeling technique associated with this extended model are presented. The model requires the conventional shear strength parameters (i.e. saturated shear strength parameters as, c' and ϕ'), the soil-water characteristic curve (*SWCC*), the elastic modulus for saturated condition (i.e. E_{sat}) and the *SWCC* data. The *SIGMA/W* analyses were compared with the *ICFEP* analysis results. There is a good agreement between the p-δ behaviors for axial loading of the single pile under saturated and unsaturated conditions using both the numerical modeling techniques. The studies presented in this chapter suggest that the elastic-plastic Mohr-Coulomb model provided by the commercial software (i.e. *SIGMA/W*) can be used as a tool to estimate the load-displacement (i.e. p-δ) behavior of pile foundations for both the saturated and unsaturated soil conditions.

Also in this chapter, the analytical calculation of ultimate bearing capacity for conventional and unsaturated analysis was performed using the conventional and modified β methods, respectively. Comparisons show that there is a good agreement between the conventional and modified β method calculation results and the numerical modeling results. The performed analysis reported in this study provide additional credence to the modified β method for implementation in engineering practice.

9. SUMMARY AND CONCLUSIONS

9.1 Introduction

Several recent studies have shown that the bearing capacities of shallow foundations in both coarse and fine-grained soils are significantly influenced due to the contribution of matric suction (Costa et al., 2003; Mohamed and Vanapalli, 2006; Vanapalli, 2009; Vanapalli and Oh, 2010). There are however limited studies reported in the literature that discuss the design of pile foundations taking account of the influence of matric suction in unsaturated soils (Georgiadis et al., 2002). Two key objectives form the research focus of this thesis. The first objective was directed towards developing reliable techniques to interpret the contribution of matric suction towards the shaft bearing capacity of single piles and also for proposing semi-emprical models to estimate the variation of load carrying capacity of single piles with respect to matric suction under both drained and undrained loading conditions. The second objective of the research was directed towards developing numerical modelling technique using an elastic-plastic Mohr-Coulomb model to estimate the *p*-δ behavior of single piles in unsaturated soils considering the influence of matric suction in-situ and model piles both in coarse and fine-grained unsaturated soils.

The summary and conclusions from the studies undertaken in this thesis are summarized in the following sections.

9.2 Estimation of the Shaft Bearing Capacity of Test Piles in Non-plastic Unsaturated Soils

1. Comprehensive experimental program was undertaken in a geotechnical test pit to determine the contribution of matric suction towards the total shaft resistance of piles embedded in two coarse-grained soils. These test results were used to propose an interpretation technique to estimate the shaft resistance considering the contribution of matric suction.

The shaft bearing capacity of a steel pipe pile which had been jacked hydraulically into two different types of sandy soils (i.e. Soil #1: silty sand and Soil #2: clean concrete sand) and tested under saturated and unsaturated conditions.

2. The test results have shown that the contribution of matric suction to be between 45 to 50% of the total shaft capacity of the test piles for silty sand; however, the influence of matric suction was negligible for clean sands. Thus, it can be concluded that in unsaturated coarse-grained soils, with the exception of clean sands and granular soils, the contribution of matric suction to the total shaft capacity of piles should be taken into account for the rational design of piles.

3. The conventional β-method was modified for interpreting the contribution of shaft resistance of single model piles. In addition, a semi-empirical model has been proposed which is consistent with the modified β-method to predict the variation of the shaft resistance with respect to matric suction using the Soil-Water Characteristic Curve (*SWCC*) and the effective shear strength parameters. The results of this study are promising to predict the contribution of matric suction towards shaft resistance using the modified β-method for sandy soils.

9.3 Shaft Bearing Capacity of Test Piles in Fine-grained Unsaturated Soils

1. Test equipment was specially designed to study the shaft bearing capacity of test piles in compacted fine-grained unsaturated soils. Stainless solid steel cylindrical rods with different diameters and circular high strength plastic tank were used as model piles and as testing chamber, respectively. Several series of single model pile tests were succesfully performed in a laboratory environment to study the influence of matric suction due to the pile shaft resistance. Two different unsaturated compacted fine-grained soils (i.e. Indian Head till and Loam soil) were used in this study. The shaft resistance of the model piles embedded in statically compacted soils prepared at predetermined constant initial water contents from dry of optimum to optimum conditions to achieve matric suction values in the range of 50 kPa to 200 kPa. A constant initial water content assures the uniform matric suction value over the entire depth. Tests were conducted under both saturated and unsaturated conditions using different drainage conditions succesfully using the specially designed equipment.

2. The total shaft resistance of piles in unsaturated conditions is significantly higher in comparison to saturated conditions for both drained and undrained loading conditions. (between 400-450%). These experimental results clearly demonstrate that ignoring the contribution of matric suction in the carrying capacity of single piles in fine-grained unsaturated soils is conservative.

3. The conventional α, β and λ methods were modified to interpret the contribution of matric suction on the shaft resistance capacity of single piles. In addition, semi-empirical models were developed to predict the variation of the shaft resistance of single piles with respect to matric suction using the *SWCC* and the shear strength parameters taking account of different drainage conditions (drained and undrained loading conditions).

4. The studies show that there was a reasonably good comparison was observed between the measured shaft capacity of single piles in unsaturated compacted fine-grained soils and estimated values using the modified α, β and λ methods.

The present research shows that the proposed methods and models are of considerable promise. The proposed approaches are consistent with the conventional engineering practice methods and also are simple. The research presented in this thesis therefore is of significant interest both to the researchers and the practitioners.

9.4 Modelling the *p*-δ Behaviors of a Single pile in Unsaturated Fine Grained Soils

The contribution of matric suction to the bearing capacity behavior of a full-scale single pile of 20 m in length and 1 m in diameter, placed in glacial till (i.e. Lower Cromer till-a low plastic sandy clay), was investigated by Georgiadis et al. (2002) considering the influence of capillary stresses above the ground water table for different groundwater table level conditions (i.e. depth of *GWT* from the surface: 0 m; 2 m; 6 m; 10 m and 25 m). The conventional and unsaturated analyses have been performed assuming drained loading conditions. The contribution of matric suction to the ultimate bearing capacity of a single pile for shallow *GWT* depths of 0-10 m in comparison to saturated soil conditions is not significant. In other words, the difference between the ultimate loads calculated using the mechanics of saturated (i.e. conventional) and unsaturated soils is relatively small in the range of 2-10%.

However, for greater depths of *GWT* (i.e. more than 25 m) the conventional approach significantly underestimated the ultimate pile load bearing capacity approximately by 45%. The analysis results also show that an increase in the bearing capacity for unsaturated analyses is mostly due to the contribution of matric suction to the shaft resistance. The end bearing capacity is not significantly influenced by the unsaturated zone.

A simple numerical model is developed using the elastic-plastic Mohr-Coulomb model to simulate load versus displacement *(p-δ)* behavior of a single pile placed in unsaturated soils considering the influence of matric suction. The conventional shear strength parameters (i.e. *c'* and ϕ') and the *SWCC* are required for performing the analyses using finite element analysis program *SIGMA/W* (Geostudio 2007) software.

Comparisons were provided between the p-δ behavior of a single pile placed in a glacial deposit under saturated and unsaturated soil conditions using the proposed elastic-plastic model and the comprehensive constitutive model based on critical state soil mechanics concepts for unsaturated soils (Georgiadis et al., 2003). There is a good comparison between the simulated results using both these approaches. In addition, predictions of using the conventional finite element analyses are also in good agreement with the modified β-method for the drained loading condition.

Two key conclusions can be derived from the numerical modelling studies. Firstly, the conventional calculation methods for estimating the p-δ behavior of pile foundations are conservative when they are extended for unsaturated fine-grained soils. Secondly, the elastic-plastic Mohr-Coulomb model supported by the commercial software (i.e. *SIGMA/W*) can be used as a tool to estimate the p-δ behavior of pile foundations for both the saturated and unsaturated soil conditions.

9.5 Recommendations and Suggestions for Future Studies

The recommendations and suggestions for the future studies with respect to; (1) Equipment and measurement techniques used, (2) Need for studying more soils to better understand the limitations of the proposed interpretation techniques, (3) Need for conducting in-situ pile load tests in unsaturated soils and perform numerical modeling studies, (4) Need for proposing interpretation methods for better

understanding the contribution of matric suction due to end resistance of piles. This section summarizes these details.

1. Equipment and measurement techniques: Equipment designed and used in the present research was satisfactory. Based on the experience of undertaking several tests, it is suggested to use a different technique of testing to alleviate some experimental problems encountered in the present research study. Instead of drilling a hole into the initially compacted soil, it is suggested to compact the soil around the pile using a specially designed compactor. Such a technique would reduce disturbance during pile installation for tests and likely provide better correlation results as it eliminates the problems associated with the soil disturbance. In addition, this technique also provides better contact between the pile and the soil. Additional measurements of lateral earth pressure using soil pressure gauges close to the vicinity of the pile-soil interface during pile installation and loading should also be considered for future studies to evaluate its effect on the measured shaft capacity.

2. Need for studying more soils to better understand the limitations of interpretation techniques: The results of this study are promising to predict the contribution of matric suction towards shaft resistance using the modified α, β and λ methods in the literature. However, the results summarized in this thesis study and the proposed techniques are based on the studies undertaken using limited number of compacted soils and analyzing few case studies. More experimental and numerical studies need to be performed and evaluated on both saturated and unsaturated soil conditions to better understand the contribution of matric suction on different coarse and fine-grained soils.

3. Need for conducting in-situ pile load tests in unsaturated soils and perform numerical modeling studies: The conventional α, β and λ methods are commonly used in engineering practice for estimating the ultimate shaft bearing capacity of single piles in saturated soils. In the present research, these methods were modified such that they can be used to estimate the shaft bearing capacity of single piles using the *SWCC* and the conventional shear strength parameters. The proposed semi-empirical models are also useful for estimating the variation of total shaft resistance of single piles with respect to

matric suction. There is a smooth transition from the modified methods to the conventional α, β and λ methods. However, the validity of the proposed techniques and models should be tested by conducting in-situ pile load tests, model tests and numerical analyses in order to check the validity of the proposed modified approaches for estimating the shaft bearing capacity.

4. Need for proposing interpretation methods for better understanding the contribution of matric suction due to end resistance of piles: The focus of the studies presented in thesis were directed towards interpreting and predicting the shaft resistance, Q_s of single piles. These studies are more valuable for fine-grained soils as the contribution from the base resistance, Q_b is rather low. However, the contribution of matric suction towards the end bearing capacity is significant in sandy soils and in sandy clays or soils with large percentage of sands. There are several soils in which the contributions arising from both end and shaft resistance is significant. In other words, there is a need to develop a better understanding of the contribution of end bearing capacity such that the total carrying capacity of a single pile, Q_p can be reliably determined by summation of the contributions from base (i.e. end) resistance, Q_b and shaft resistance, Q_s.

REFERENCES

Aitchison, G. D. (1965). Soil properties, shear strength, and consolidation. *Proc. of the 6th Int. Conf. On Soil Mechanics and Foundation Engineering*, Vol. *3*, pp. 318-321.

Al-Mhaidib, A. I. (2001). Loading rate effect on piles in clay from laboratory pile tests. *J. King Saud Univ.*, Vol.*13*, Eng. Sci. (1), 39-55.

Alonso, E. E., Gens, A. and Josa, A. (1990). A constitutive model for partially saturated soils. *Géotechnique. 40* (3), 405-430.

American Petroleum Institute (API) (1975). *Recommended practice for planning, designing, and constructing fixed offshore platforms,* API RP2A, 6th edn. American Petroleum Institute, Washington

American Petroleum Institute (API) (1984). *Recommended practice for planning, designing and constructing fixed offshore platforms,* API RP2A, 15th ed., American Petroleum Institute.

American Petroleum Institute (API) (1987). *Recommended practice for planning, designing, and constructing fixed offshore platforms,* API RP2A, 17th edn. American Petroleum Institute, Washington

American Petroleum Institute (API) (2000). *Recommended Practice for Planning, Designing and Constructing Fixed Offshore Platforms-Working Stress Design,* 2A-WSD (RP 2A-WSD) 21st edn., American Petroleum Institute, Washington.

ASTM D2325-68 (2000). *Standard test method for capillary-moisture relationships for coarse and medium textured soils by pressure plate apparatus*. ASTM Standards.

Azzouz, A. S. (1986). Shaft behavior of a model pile in plastic empire clays, J. *Geotech. Engrg. 112*, 389-406.

Barbour, S. L. (1998). Nineteenth Canadian Geotechnical Colloquium: The soil-water characteristic curve: a historical perspective, *Canadian Geotechnical Journal, 35*, 873-894.

Bea, R. G. (1975). Parameters affecting axial capacity of piles in clays, *7th Annual Offshore Technology Conference***,** Houston, Texas, USA., May 5-8.

Bell, F. G. (1991). A survey of the geotechnical properties of some till deposits on the north coast of Norfolk, *Engineering Geology Special Publications*. *7*, 103-110.

Bishop, A. W. (1959). The principle of effective stress, *Tecnisk Ukeblad, 39*, 859-863.

Bishop, A. W., Alpan, I., Blight, G. E. and Donald, I. B. (1960). Factors controlling the shear strength of partly saturated cohesive soils. *Proceedings of the ASCE Research Conference on Shear Strength of Cohesive Soils,* Boulder, (pp. 503-532). USA : University of Colorado.

Bishop, A. W. and Donald, I. B. (1961). The experimental study of partly saturated soil in triaxial apparatus. *Proceedings of the Fifth International Conference on Soil Mechanics and Foundation Engineering, 1,* (pp. 13–21). Paris.

Bishop, A. W. and Blight, G. E. (1963). Some aspects of effective stress in saturated and partly saturated soils. *Geotechnique, 13* (3), 177-197.

Blight, G. E. (1967). Effective stress evaluation for unsaturated soils, *Journal of Soil Mechanics and Foundation Div., ASCE. Proc. 193* (SM2), 125-148.

Bolzon, G., Schrefler, B. A. and Zienkiewicz, O. C. (1996). Elastoplastic soil constitutive laws generalized to partially saturated states, *Géotechnique, 46* (2), 279-289.

Briaud, J. L., Tucker, L. M. and Ng E. (1989). Axially Loaded 5 Pile Group and Single Pile in Sand, *Proceedings of the 12th ICSMFE, 2* (pp. 1121-1124). Brasil: Rio de Janeiro.

Brutsaert, W. (1966). Probability laws of pore-size distributions, *Soil Sci., 101,* 85–92.

Burland, J. B. (1964). Effective stresses in partly saturated soils, *Géotechnique, 14,* 65-68.

Burland, J. B. (1973). Shaft capacity of piles in clay- a simple fundamental approach, *Ground Engineering, 6* (2), 30-38.

Burland, J. P. (1993). Closing address. *In Proceedings of recent large-scale fully instrumented pile tests in clay,* (pp 590–595). London : Institute of Civil Engineers.

Catana, M. C. (2005). *Compaction and water retention characteristics of Champlain sea clay* (Master's thesis). University of Ottawa, Canada. Available from ProQuest Dissertations and Theses database.

Chandler R. J. (1968). The shaft friction of piles in cohesive soils in terms of effective stress, *Civil Engineering and Public Works Review, 63,* 48-51.

Chow F. C. (1996). *Investigations into Displacement Pile Behaviour for Offshore Foundations,* (Ph.D. thesis), University of London (Imperial College).

Chow, F. C., Jardine, R. J. and Nauroy, J. F. (1998). Effects of time on capacity of pipe piles in dense marine sand, J. *Geotech. Engrg, 124,* 254-264.

Jardine, R. J. and Chow, F. C. (1996). *New Design Methods for* Offshore Piles. *Marine Technology Directorate Ltd., Publication MTD 96/103,* London.

Clausen, C. J. F. and Aas, P. M. (2001). Capacity of driven piles in clays and sands on the basis of pile load tests, *11th International Journal of Offshore and Polar Engineering Conference*, (pp. 581-586). Norway, Stavanger.

Cooke, R.W. and Price, G. (1973). Strains and Displacements around Friction Piles, *Proceedings of the 8th International Conference on Soil Mechanics and Foundation Engineering, 2*, (pp. 53-60). Moscow.

Coop, M. R., Klotz E. U. and Clinton, L. (2005). The influence of the in situ state of sands on the load-deflection behavior of driven piles, *Géotechnique, 55* (10), 721-730.

Costa, Y. D., Cintra, J. C. and Zornberg, J. G. (2003). Influence of matric suction on the results of plate load tests performed on a leteritic soil deposit, *ASTM Geotechnical Testing Journal*, *26* (2), 219-227.

Dennis, N. D. and Olson, R . E. (1983a). Axial Capacity of Steel Pipe Piles in Clay, In *Proceedings of the Geotechnical Practice in Offshore Engineering*, Austin, Texas, pp. 370-388.

Dennis, N. D. and Olson, R.E. (1983b). Axial Capacity of Steel Pipe Piles in Sand, In *Proceedings of the Geotechnical Practice in Offshore Engineering*, (pp. 389-402). USA: Austin, Texas.

Douglas, D. J. (1989). Prediction study-driven piles, *Proceedings of the 5th Australian-New Zealand Conf. on Soil Mechanics*, (pp. 84-88). Special edition.

Doherty, P. and Gavin, K. (2011a). Shaft capacity of open-ended piles in clay, *Journal of Geotech. Geoenviron. Eng., 137*, 1090-1102. doi: 10.1061/(ASCE)GT.1943-5606.0000528

Doherty, P. and Gavin, K. (2011b). The shaft capacity of displacement piles in clay: A state of the art review, *Geotech. Geol. Eng., 29***,** 389-410. doi: 10.1007/s10706-010-9389-2.

Douthitt, B., Houston, W., Houston, S. and Walsh, K. (1998). Effect of wetting on pile friction, In *Proceedings of 2nd Int. Conf. on Unsaturated Soils*, China, Vol. **1**, pp. 219-224.

Escario, V. (1980). Suction controlled penetration and shear tests. *Proceedings of the 4th Int. Conf. Expansive Soils, ASCE*. Denver, *2*, 781-797.

Escario, V. and Saez, J. (1986). The shear strength of partly saturated soils, *Géotechnique, 36* (3), 453-456.

Fleming, W. G. K., Weltman, A. J., Randolph, M. F. and Elson, W. K. (1985). *Piling engineering.* New York: Surrey University Press, Halsted Press.

Fredlund, D. G. and Morgenstern, N. R. (1977). Stress state variables for unsaturated soils, *Journal of the Geotechnical Engineering Division, ASCE, **103*** (GT5), Proc. Paper 12919, 447-466.

Fredlund, D. G., Morgenstern, N. R. and Widger, R. A. (1978).The shear strength of unsaturated soils, *Canadian Geotechnical Journal, 15* (3), 313-321.

Fredlund, D. G. (1979). Second Canadian Geotechnical Colloquium: Appropriate concepts and technology for unsaturated soils, *Canadian Geotechnical Journal*, *16* (1), 121-139.

Fredlund, D. G., Rahardjo, H. and Gan, J. K. M. (1987). Non-linearity of strength envelope for unsaturated soils, *Proceedings of the 6th International Conference on Expansive Soils*, (pp. 49-54). India: New Delhi, December 1- 4.

Fredlund, D. G. and Rahardjo, H. (1993). *Soil Mechanics for Unsaturated Soils.* John Wiley & Sons, Inc.

Fredlund, D. G., Xing, A., Fredlund, M. D. and Barbour, S. L., (1996). The relationship of the unsaturated soil shear strength to the soil-water characteristic curve, *Canadian Geotechnical Journal*, *33* (3), 440-448.

Fredllund, M. D., Wilson, G. W. and Fredlund D. G. (2002). Use of the grain-size distribution for estimation of the soil-water characteristic curve, *Canadian Geotechnical Journal*, *39* (5), 1103-1117.

Fredlund, D. G. and Xing, A. (1994). Equations for the soil-water characteristic curve, *Canadian Geotechnical Journal*, *31* (4), 521-532.

Gan, J. K. M. (1986). *Direct shear testing of unsaturated soils* (Master's thesis). Dept. of Civil Eng., University of Saskatchewan, Saskatoon, Canada. Available from ProQuest Dissertations and Theses database.

Gan, J. K. M., Fredlund, D. G. and Rahardjo, H. (1988). Determination of the shear strength parameters of an unsaturated soil using the direct shear test, *Canadian Geotechnical Journal*, *25*, 500-510.

Gan, J. K. M. and Fredlund, D. G., (1988). Multistage direct shear testing of unsaturated soils, *ASTM Geotechnical Testing Journal*, *11* (2), 132-138.

Gavin, K. G. and Lehane, B. M. (2003). The shaft capacity of pile piles sand, *Canadian Geotechnical Journal, 40*, 36-45.

Gavin, K., Gallagher, D., Doherty, P. and McCabe, B. (2010). Field investigation of the effect of installation method on the shaft resistance of piles in clay, *Canadian Geotechnical Journal, 47*, 730-741.

Gens, A. (1982). *Stress-strain and strength characteristics of a low plasticity clay* (Ph.D thesis). University of London.

Georgiadis, K., Potts, D. M. and Zdravkovic, L. (2002). Behaviour of a footing on a partially saturated soil, *Proceeding of the 8th Int. Symp. Numer. Modelling Geomech., NUMOG VIII*, (pp. 451-456). Italy: Rome, April 10-12.

Georgiadis, K., Potts, D. M. and Zdravkovic, L. (2003). The influence of partial soil saturation pile behavior, *Géotechnique, 53* (1), 11-25.

Gurpersaud, N., Vanapalli, S. K. and Sivathayalan, S. (2013). A semi-empirical method for the estimation of pull-out capacity of grouted soil nails in saturated and unsaturated soil environments, *ASCE Journal of Geotechnical and Geoenvironmental Engineering, (*Accepted Manuscript-Not copyedited).

Hamid, T. B. and Miller, G. A. (2008). A constitutive model for unsaturated soil interfaces, *Int. J. Numer. Anal. Meth. Geomech. 32*, 1693–1714.

Hamid, T. and Miller G. A. (2009). Shear strength of unsaturated soil interfaces, *Canadian Geotechnical Journal, 46* (5), 595-606.

Hanke, R. (2001). *Shaft capacities of closed end piles under load reversals in sand* (Master's thesis). Faculty of Engineering and Applied Sciences, Memorial University of Newfoundland, St. John's, Newfoundland.

Hilf, J. W. (1956). *An investigation of pore water pressure in compacted cohesive soils* (Doctoral dissertation).Tech. Memo. No. 654, U.D. Dep. of the Interior, Bureau of Reclamation, Design and Construction Div. Denver, CO.

Ho, D. Y. F. and Fredlund, D. G. (1982). Increase in strength due to suction for two Hong Kong soils, *Proceedings of ASCE. Geotechnical Conference on Engineering and Construction in Tropical and Residual Soils,* (pp. 263-295). Hawaii, Honolulu.

Hossain, A. and Yin, J. H. (2010). Behavior of a compacted completely decomposed granite soil from suction controlled direct shear tests, *ASCE Journal of Geotechnical and Geoenvironmental Engineering, 136* (1), 189-198.

Igoe, D. J. P., Gavin, K. G. and O'Kelly, B. C. (2011). Shaft capacity of open-ended piles in sand. *J. Geotech. Geoenviron. Eng., 137*, 903-913.

Ismael, N. F. (1989). Skin friction of driven piles in calcareous sands, *J. Geotech. Engrg., 115*, 135-139.

Jardine, R., Chow F., Overy, R. and Standing, J. (2005). *ICP design methods for driven piles in sands and clays.* Imperial College, London, Thomas Telford.

Kerisel, J. (1965). Vertical and horizontal bearing capacity of deep foundation in clay, *Proceedings of Symposium on Bearing Capacity of Settlement of Foundations*, (pp. 45-52). Durham : Duke University.

Kohgo, Y., Nakano, M. and Miyazaki, T. (1993). Verification of the generalized elastoplastic model for unsaturated soils, *Soils and Foundations, 33* (4), 64-73.

Kolk, H. J. and van der Velde, E. (1996). A reliable method to determine friction capacity of piles driven into clays, *Offshore Technology Conference*, Houston, Texas, USA, May 6-9.

Kraft, L. M., Focht, J. A. and Amerasinghe, S. F. (1981). Friction capacity of piles driven into clay, *ASCE, J. Geotech. Engrg., 107* (GT11), 1521-1541.

Kraft, L. M. (1991). Performance of axially loaded pipe piles in sand, *J. Geotech. Engrg., 117*, 272-296.

Krahn, J. (2007). *Stress and deformation modeling with SIGMA/W (SIGMA/W manual).* Geo-Slope International Ltd.

Krishnapillai, H. and Ravichandran, N. (2012). New Soil-Water Characteristic Curve and Its Performance in the Finite Element Simulation of Unsaturated Soils, *ASCE International Journal of Geomechanics, 12* (3), 209-219.

Law, K. T. (1982). Numerical analysis of pile loading and pulling tests. In *Proceedings of the Forth International Conference on Numerical Methods in Geomechanics,* (pp. 825-833). Edmonton, Alberta,.

Lehane, B. M., Jardine, R. J., Bond, A. J. and Frank, R. (1993). Mechanisms of shaft friction in sand from instrumented pile tests, *Journal of Geotechnical Engineering. 119* (1), 19-35.

Lehane, B. M. and Jardine, R. J. (1994). Shaft capacity of driven piles in sand: A new design approach, *Proceedings of BOSS'94 Behavior of Offshore Structures*, (pp. 23-36). Boston, Massachussets, Pergamon Press Inc., Oxford U.K.,

Lehane, B. M., Ismail, M. A. and Fahey, M. (2004). Seasonal dependence of in-situ test parameters in sand above the water table, Technical Note, *Géotechnique, 54* (3), 215-218.

Lehane, B. M., Gaudin, C. and Schneider, J. A. (2005). Scale effects on tension capacity for rough piles buried in dense sand, *Géotechnique, 55* (10), 709-719.

Lehane, B. M. and White, D. J. (2005). Lateral stress changes and shaft friction for model displacement piles in sand**.** *Canadian Geotechnical Journal, 42*, 1039-1052.

Lehane, B. M., Li, Y. and Williams, R. (2013). Shaft capacity of displacement piles in clay using the Cone Penetration Test, *J. Geotech. Geoenviron. Eng., 139*, 253-266. doi: 10.1061/(ASCE)GT.1943-5606.0000749.

Lu, N. and Likos, W. J. (2004). *Unsaturated soil mechanics*. Wiley.

Maswoswe, J. (1985). *Stress path for a compacted soil during collapse due to wetting* (PhD thesis). Imperial College, London.

Mayoral, J. M., Pestana J. M. and Seed R. B. (2005). Determination of multidirectional p-y curves for soft clays, *Geotechnical Testing Journal, 28* (3), 1-11.

McClelland, B. (1974). Design of deep penetration piles for ocean structures, *J. Geotech Eng. Div. ASCE*, *100*(GT 7), 705-747.

Meyerhof, G. G. (1976). Bearing capacity and settlement of pile foundations, *Journal of the Geotechnical Engineering Division, 102* (GT3), 197-228.

Mirza, U. A. A. (1995). A simple approach for calculating pile skin friction in clays, *The 5th International Offshore and Polar Engineering Conference*, The Hague, The Netherlands, June 11-16.

Mirza, U. A. A. (1997). Pile skin friction in clays, *International Journal of Offshore and Polar Engineering*, ***7*** (1), 77-80.

Mochtar, I. B. and Edil, T. B. (1988). Shaft resistance of model pile in clay. *J. Geotech. Engrg., 114*, 1227-1244.

Mohamed, F. M. O. and Vanapalli, S. K. (2006). Laboratory investigations for the measurement of the bearing capacity of an unsaturated coarse-grained soils. In *Proceedings of the 59th Canadian Geotechnical Conf.,* (pp. 219-226), Vancouver.

Muraleetharan, K. K. and Ravichandran, N. (2009). Dynamics of Unsaturated Soils Using Various Finite Element Formulations, *International Journal for Numerical and Analytical Methods in Geomechanics*, *33*, 611-631.

Muraleetharan, K. K., Liu, C., Wei, C. F, Kibbey, T. C. G, Chen, L. (2008). An Elastoplastic Framework for Coupling Hydraulic and Mechanical Behavior of Unsaturated Soils, *International Journal of Plasticity*, *25*, 473-490.

Murff, J. D. (1985). Pile capacity in calcareous sands: state of art. J. *Geotech. Engrg., 113* (5), 490-507.

Nanda, S. and Patra, N. R. (2011). Shaft Resistance of Piles in Normally Consolidating Marine Clay Subjected to Compressive and Uplift Load, *ASCE Geo-Frontiers 2011*, pp. 263-272.

Oh, W. T. and Vanapalli, S. K. (2009). A simple method to estimate the bearing capacity of unsaturated fine-grained soils, *Proceedings of the 62nd Canadian Geotechnical Conf & 10th Joint CGS/IAH-CNC Groundwater Conf.,* (pp. 234-241).

Oh, W. T., Vanapalli, S. K. and Puppala A. J. (2009)**.** A semi-empirical model for the prediction of modulus of elasticity for unsaturated soils, *Canadian Geotechnical Journal*, *46* (8), 903-914.

Oh, W. T. and Vanapalli S. K. (2011). Modelling the applied vertical stress and settlement relationship of shallow foundations in saturated and unsaturated sands, *Canadian Geotechnical Journal*, *48*, 425-438.

Oloo, S. Y. (1994). *A bearing capacity approach to the design of low-volume traffics roads.* (Ph.D thesis). University of Saskatchewan, Saskatoon, Canada. Available from ProQuest Dissertations and Theses database.

Oloo, S. Y., Fredlund, D. G. and Gan J. K. M. (1997). Bearing capacity of unpaved roads, *Canadian Geotechnical Journal*, *34* (3), 398-407.

Peck, R. B. (1958). A study of the comparative behaviour of friction piles, Highway Research Board, Special Report 36.

Potts D. M. and Zdravkovic, L. (1999). *Finite element analysis in geotechnical engineering: theory*. Thomas Telford, London.

Potts D. M. and Zdravkovic, L. (2001). *Finite element analysis in geotechnical engineering: application*. Thomas Telford, London.

Poulos H. G. (1989). Pile behaviour-theory and application, *Géotechnique*, *39*, 365-413.

Power, K. and Vanapalli, S. K. (2011). Modified null pressure apparatus for measurement of matric suction, *ASTM Geotechnical Testing Journal*, 33 (4), 335-341.

Prakash, S. and Sharma, H. D. (1990). *Pile foundations in engineering practice*. Wiley, New York.

Randloph, M. F. and Wroth, C. P. (1978). Analysis of Deformation of Vertical Loaded Piles, *Journal of Geotechnical Engineering, ASCE, 104*, 1465-1488.

Randolph, M. F. and Murphy B. S. (1985). Shaft capacity of driven piles in clay; *Offshore Technology Conference*, (pp. 371-378). USA: Houston, Texas, May 6-9.

Randolph M. F., Dolwin, J. and Beck, R. (1994). Design of Driven Piles in Sand, *Géotechnique, 44* (3), 427-448.

Randolph, M. F. (2003). Science and empiricism in pile foundation design, *Géotechnique, 53* (10), 847-875.

Ravichandran, N. (2009). Fully Coupled Finite Element Model for Partially Saturated Soils, *Journal of Soil Dynamics and Earthquake Engineering, 29* (9), 1294-1304.

Robinsky, E. I. and Morrison, C. F. (1964). Sand Displacement and Compaction around Model Friction Piles, *Canadian Geotechnical Journal*, *1*, 81-93.

Rojas, J. C., Salinas, L. M. and Seja, C. (2007). Plate-load tests on an unsaturated lean clay, *Proceeding of the 2nd International Conference on Unsaturated Soils*, (pp. 445-452). Weimar.

Semple, R. M. and Rigden, W. J. (1984). Shaft capacity of driven pipe piles in clay, *Proceedings Symposium on Analysis and Design of Pile Foundations*, ASCE, (pp.59-79).

Shin, E. C., Das, B. M., Puri, V. K., Yen, S. C., Cook, E. E. (1993). Ultimate uplift capacity of model rigid metal piles in clay, *Geotech. Geologic. Eng.*, *11*, 203-215.

Skempton, A. W. (1959). Cast-in-situ bored piles in London clay, *Géotechnique*, *9*, 153-173.

Sladen, J. A. (1992). The adhesion factor: applications and limitations, *Canadian Geotechnical Journal*, *29*, 322-326.

Soilmoisture Equipment Corp. (2008). 1600 5-Bar Ceramic Plate Extractor. Operating instructions.

Soilmoisture Equipment Corp. (2009). 2100F Soilmoisture Probe. Operating instructions.

SoilVision (2000). Version 3.04. *Software Package for Modelling the Engineering Behavior of Unsaturated Soils.* Soil Vision Systems Ltd.

Sowers, G. B. and Sowers, G. G. (1970). *Introductory soil mechanics and foundations.* The Macmillan Company, New York.

Stannard, D. I. (1990). Tensiometers – theory, construction and use. *Groundwater and Vadose Zone Monitoring. D. M. Neilson and A. I. Johnson (eds), ASTM STP 1053*, 34-51.

Terzaghi, K. (1936). The shear resistance of saturated soils, *Proceedings of the 1st Int. Conf. On Soil Mechanics and Foundation Engineering, 1*, (pp. 54-56).

Terzaghi, K. (1939). Soil mechanics: a new chapter in engineering science, *J. Inst. Civ. Eng.*, *12*, 106-141.

Terzaghi, K. and Peck, R. B. (1967). *Soil mechanics in engineering practice* (2nd ed.). New York: Wiley.

Toolan, F. E., Lings, M. L. and Mirza, U. A. (1990). An Appraisal of API RP2A Recommendations for Determining Skin Friction of Piles in Sand, *OTC Paper 6422*, (pp. 33-42). Houston.

Toll, D. G. (1990). A framework for unsaturated soils behavior, *Géotechnique, 40* (1), 31-44.

Tomlinson M. J. (1957). The adhesion of piles driven in clay soils, *Proceedings of the 4th Int. Conf. on Soil Mech. and Foundation Eng.*, *2*, 66-71.

van Genuchten, M. T. (1980). A closed-form equation of predicting the hydraulic conductivity of unsaturated soils, *Soil Science Society of American Journal*, *44*, 892-898.

Vanapalli, S. K. (1994). *Simple test procedures and their interpretation in evaluating the shear strength of an unsaturated soil* (Ph.D Thesis). Dept. of Civil Eng., University of Saskatchewan, Saskatoon, Canada. Available from ProQuest Dissertations and Theses database.

Vanapalli, S. K., Fredlund, D. G., Pufahl, D. E. and Clifton, A. W. (1996). Model for the prediction of shear strength with respect to soil suction, *Canadian Geotechnical Journal*, *33*, 379-392.

Vanapalli, S. K., Sillers, W. S. and Fredlund, D. G. (1998). The meaning and relevance of residual water content to unsaturated soils, *51st Canadian Geotechnical Conference,* (pp. 101-108). Edmenton, Canada..

Vanapalli, S.K. and Fredlund, D.G. (2000). Comparison of different procedures to predict unsaturated soil shear strength, *Proceedings of the Geo-Denver Conference, ASCE Special Publication*, *99* (pp. 195-209). USA : Colorado, August 5-8.

Vanapalli, S. K., Salinas, L. M., Avila, D. and Karube, D. (2004). Suction and storage characteristics of unsaturated soils, *Proceedings of the Third International Conference on Unsaturated Soils, 3* (pp. 1045-1069). Brazil.

Vanapalli, S. K. and Catana, M. C. (2005). Estimation of the soil-water characteristic curve of coarse grained soils using one point measurement and simple properties, *International Symposium on Advanced Experimental Unsaturated Soil Mechanics*, (pp. 401-407). Trento.

Vanapalli, S. K. and Mohamed, F. M. O. (2007). Bearing capacity of model footings in unsaturated soils, *Proceedings of the 2nd International Conference on Unsaturated Soils*, (pp. 483-493). Weimar.

Vanapalli, S. K., Oh, W. T. and Puppala, A. J. (2007). Determination of the bearing capacity of unsaturated soils under undrained loading conditions, *Proceedings of the 60th Canadian Geotechnical Conf.,* (pp. 1002-1009).

Vanapalli, S. K. (2009). Shear strength of unsaturated soils and its application in geotechnical engineering practice, Keynote Address, *Proceedings. of the 4th Asia-Pacific Conference on Unsaturated Soils,* (pp. 579-598). Australia : November 23-25.

Vanapalli, S. K. and Oh, W. T. (2010). Interpretation of the bearing capacity of an unsaturated soils extending the effective and total stress approaches, *Proceedings of the 5th Int. Conf. on Unsaturated Soils, 2* (pp. 1223-1229). Spain: Barcelona, September 6-8.

Vanapalli, S. K. and Oh, W. T. (2011). Mechanics of unsaturated soils for the design of foundation structures, *Proceedings of EMESEG'10 of the 3rd WSEAS International conference on Engineering mechanics, structures, engineering geology*, (pp. 363-377).

Vesic, A. S. (1977). Design of Pile Foundation, *National Cooperative Highway Research Program, Synthesis of Highway Practice* No. *42,* Transportation Research Board, Washington, D.C.

Vijayvergiya, V. N. and Focht, J. A. (1972). A new way to predict capacity of piles in clay, *Proceedings of the 4th Annual Offshore technology Conf.,* (pp. 865-871). Houston, Texas, May 1-3.

Wheeler, S. J. and Sivakumar, V. (1995). An elasto-plastic critical state framework for unsaturated soil, *Géotechnique, 45* (1), 35-53.

Woodward, R. and Boitano, J. (1961). Pile loading tests in stiff clays. *Proceedings of 5th International Conference on Soil Mechanics and Foundation Engineering, 2*:177. Paris.

CURRICULUM VITAE

Name Surname:	Zehra Nil (TAYLAN) KUTLU
Place and Date of Birth:	ISTANBUL 1981
E-Mail:	taylanz@itu.edu.tr
B.Sc.:	ITU Geophysical Engineering
M.Sc. :	ITU Civil Engineering Faculty Soil Mechanics and Geotechnical Engineering

Professional Experience and Rewards:

Research Asisstant, ITU Civil Engineering Faculty, Geotechnical Engineering Division, (2005 – 2013)

List of Publications and Patents:

Journal Papers

- Özüdoğru, T.Y., Şenol, A., **Taylan, Z.N.,** 2009. *Pile Integrity Testing and Drivability Analysis*, Türkiye İnşaat Mühendisleri Odası Teknik Dergisi, Teknik Dergi, Cilt 20, No 3, Ankara, Türkiye.

PUBLICATIONS/PRESENTATIONS ON THE THESIS

Journal Papers

- Vanapalli, S.K., **Taylan Z. N**., 2012. *Design of Single Piles Using the Mechanics of Unsaturated Soils.* International Journal of GEOMATE. Geotec., Const. Mat. and Env. Mart, 2012, Vol. 2, No. 1 (Sl. No. 3), pp. 197-204, ISSN:2186-2982(P), 2186-2990(O), Japonya.

- Vanapalli, S.K., Eigenbrod, K.D, **Taylan Z.N**., review. *A Technique for Estimating the Shaft Resistance of Test Piles in Unsaturated Soils.* Canadian Geotechnical Journal. (Revised manuscript submitted to the CGJ for review and publication.)

Conference Papers

- Vanapalli, S.K, Eigenbrod, K. D., **Taylan, Z.N.;** Catana, C.; Oh, W.T.; Garven, E.; 2010. *A technique for estimating the shaft resistance of test piles in unsaturated soils.* Proceedings of the 5th International Conference Unsaturated Soils, September, 6-8 Eylül, 2010, Barselona, İspanya.
- Vanapalli, S.K., **Taylan Z.N.,** 2011. *Modeling the load carrying capacity of single piles in unsaturated soils using the modified α and the β methods.* Proceedings of the 13th International Conference of the International Association for Computer Methods and Advances in Geomechanics, 9-11 Mayıs 2011, Melbourne, Avusturalya.
- Vanapalli, S.K., **Taylan Z.N.,** 2011. *Model Piles Behaviour in a Compacted Fine-grained Unsaturated Soil.* XV European Conference on Soil Mechanics and Geotechnical Engineering.ECSMGE 2011, 12-15 Eylül 2011, Atina, Yunanistan.
- Vanapalli, S.K., **Taylan Z.N.,** 2011. Estimation of *Model Piles Behaviour in a Compacted Fine-grained Unsaturated Soil using the α, β and λ methods,* 14th Pan-American Conference on Soil Mechanics and Geotechnical Engineering & 64th Canadian Geotechnical Conference, 2011 Pan-Am CGS 2-6 Ekim 2011, Toronto, Kanada.
- Vanapalli, S.K., **Taylan Z.N.,** 2011.*Design of Single Pile Foundations Using the Mechanics of Unsaturated Soils*, Özel konulu bildiri (Keynote paper), 1st International Conference on Geotechnique, Construction Materials and Environment, 2011 GEOMAT Conference 21-23 Kasım 2011, Mie, Japonya. (Özel konulu bildiri ödülü kazandı)
- **Taylan Z.N.,** Vanapalli, S.K., 2012. *Estimation of the Shaft Capacity of Single Piles Using the Conventional and Modified β Method.* 2nd European Conf. On Unsaturated Soils, 20-22 Haziran 2012, Napoli, İtalya.
- **Taylan Z.N.,** Senol, A., Vanapalli, S.K. 2012. *Suya Doygun Olmayan Sıkıştırılmış Zeminlerde Modifiye a Metodu ile Kazık Taşıma Gücü Hesabı.* Zemin Mekaniği ve Temel Mühendisliği Ondördüncü Ulusal Kongresi 4-5 Ekim 2012, Süleyman Demirel Üniversitesi, Isparta.
- **Taylan Z.N.,** Senol, A., Vanapalli, S.K. 2012. *Comparisons between the estimations of the p-δ behavior of a single pile in a glacial till under saturated and unsaturated conditions using two different numerical techniques.* 10th International Congress on Advances in Civil Engineering, ACE 2012, 17-19 Ekim 2012, Ankara, Türkiye.